PHYSIOLOGY IN EXTREME CONDITIONS: ADAPTATIONS AND UNEXPECTED REACTIONS

EDITED BY: Maria Giovanna Trivella, Enrico Capobianco and Antonio L'Abbate
PUBLISHED IN: Frontiers in Physiology

frontiers Research Topics

frontiers

ISSN 1664-8714
ISBN 978-2-88945-338-2
DOI 10.3389/978-2-88945-338-2

About Frontiers

Frontiers is more than just an open-access publisher of scholarly articles: it is a pioneering approach to the world of academia, radically improving the way scholarly research is managed. The grand vision of Frontiers is a world where all people have an equal opportunity to seek, share and generate knowledge. Frontiers provides immediate and permanent online open access to all its publications, but this alone is not enough to realize our grand goals.

Frontiers Journal Series

The Frontiers Journal Series is a multi-tier and interdisciplinary set of open-access, online journals, promising a paradigm shift from the current review, selection and dissemination processes in academic publishing. All Frontiers journals are driven by researchers for researchers; therefore, they constitute a service to the scholarly community. At the same time, the Frontiers Journal Series operates on a revolutionary invention, the tiered publishing system, initially addressing specific communities of scholars, and gradually climbing up to broader public understanding, thus serving the interests of the lay society, too.

Dedication to Quality

Each Frontiers article is a landmark of the highest quality, thanks to genuinely collaborative interactions between authors and review editors, who include some of the world's best academicians. Research must be certified by peers before entering a stream of knowledge that may eventually reach the public - and shape society; therefore, Frontiers only applies the most rigorous and unbiased reviews.

Frontiers revolutionizes research publishing by freely delivering the most outstanding research, evaluated with no bias from both the academic and social point of view.

By applying the most advanced information technologies, Frontiers is catapulting scholarly publishing into a new generation.

What are Frontiers Research Topics?

Frontiers Research Topics are very popular trademarks of the Frontiers Journals Series: they are collections of at least ten articles, all centered on a particular subject. With their unique mix of varied contributions from Original Research to Review Articles, Frontiers Research Topics unify the most influential researchers, the latest key findings and historical advances in a hot research area! Find out more on how to host your own Frontiers Research Topic or contribute to one as an author by contacting the Frontiers Editorial Office: **researchtopics@frontiersin.org**

PHYSIOLOGY IN EXTREME CONDITIONS: ADAPTATIONS AND UNEXPECTED REACTIONS

Topic Editors:
Maria Giovanna Trivella, Istituto di Fisiologia Clinica, Consiglio Nazionale delle Ricerche, Italy
Enrico Capobianco, University of Miami, Center for Computational Science, United States
Antonio L'Abbate, Scuola Superiore Sant'Anna, Italy

Image: Dmitry Lityagin/Shutterstock.com

Physiology in extreme conditions can reveal important reactions of the human body, which help our assessment of limits emerging under healthy conditions and critical signals of transition toward disease.

While many mechanisms could simply be associated with adaptations, others refer to unexpected reactions in response to internal stimuli and/or external abrupt changes.

Citation: Trivella, M. G., Capobianco, E., L'Abbate, A., eds. (2017). Physiology in Extreme Conditions: Adaptations and Unexpected Reactions. Lausanne: Frontiers Media. doi: 10.3389/978-2-88945-338-2

Table of Contents

frontiers in Physiology

EDITORIAL
published: 29 September 2017
doi: 10.3389/fphys.2017.00748

Editorial: Physiology in Extreme Conditions: Adaptations and Unexpected Reactions

Maria G. Trivella[1]*, *Enrico Capobianco*[2] and *Antonio L'Abbate*[3]

[1] Consiglio Nazionale delle Ricerche, Istituto di Fisiologia Clinica, Pisa, Italy, [2] Center for Computational Science, University of Miami, Miami, FL, United States, [3] Scuola Superiore Sant'Anna, Pisa, Italy

Keywords: extreme environments, adaptation, homeostasis, space, underwater, sports

Editorial on the Research Topic

Physiology in Extreme Conditions: Adaptations and Unexpected Reactions

OUTREACH

"Physiology in extreme conditions" was concerned with two main issues:

(a) to increase knowledge about individual reactions and mechanisms of adaptations in specific extreme environmental conditions;

(b) to widen the analytical skills gap created by data generated in extremely severe conditions, and in response to pathological disorders.

A wide spectrum of topics was proposed by the included articles, which covered a wide variety of cases ranging from cellular systems to preclinical models. The focus was on healthy individuals experiencing extreme conditions induced by typically non-physiological environments. Studies of pathological relevance encompassing artificial organs were also comprised in the Research Topic.

LESSONS LEARNED

While many mechanisms could simply be associated with adaptations as evidenced by studies in sport, other mechanisms would rather refer to unexpected reactions in response to internal stimuli and/or external abrupt changes, as showed by the evaluation of psychostimulant abusers and/or unmedicated psychiatric patients.

In particular, the similarity noticeable in the behavioral symptoms shared by extremely agitated drug addicts and untreated psychiatric patients has been linked to a possible genetic disorder leading to a dysregulated central dopamine transporter function. This is the case with the biologically precipitating cause of acute delirium and sudden death (Mash).

The end-stage heart failure represents a condition where the cardiovascular system fails to maintain the blood supply to all organs and tissues and is generally a result of chronic disease in adults or of cardiac congenital abnormalities in children. This is a very serious condition with no optimal therapeutic treatments that can ultimately improve the situation to a point where mortality is avoided.

The development of durable ventricular assist devices (VADs) has reduced mortality rates and quality of life in patients with this critical condition. The mechanical support in smaller children is an effective strategy for bridging patients to heart transplantation (Di Molfetta et al.). The option of total artificial heart has been approved for humanitarian reasons both in pediatric surgery (Villa and Morales) and in adults (Cohn et al., 2015).

Edited and reviewed by:
Geoffrey A. Head, Baker IDI Heart and Diabetes Institute, Australia

***Correspondence:**
Maria G. Trivella
trivella@ifc.cnr.it

Specialty section:
This article was submitted to Integrative Physiology, a section of the journal Frontiers in Physiology

Received: *19 July 2017*
Accepted: *14 September 2017*
Published: *29 September 2017*

Citation:
Trivella MG, Capobianco E and L'Abbate A (2017) Editorial: Physiology in Extreme Conditions: Adaptations and Unexpected Reactions. Front. Physiol. 8:748. doi: 10.3389/fphys.2017.00748

Note that an artificial pump instead of the native heart could be considered as an abrupt interruption of the cardiovascular system continuity (endothelial lining, cell to cell communication signaling, neuro-humoral, and neuro-hormonal molecules production, sympathetic-parasympathetic balance as well as central perception of the substituted organ, i.e., not a simple pump). It is crucial to stress that the findings of cardiac support by VADs and artificial heart could clarify the physiological and the physio-pathological mechanisms of the cardiovascular system.

SPECIFIC ADDED VALUE OF STUDIES PERFORMED IN EXTREME CONDITIONS

We considered whether physiology in extreme conditions can reveal important reactions of the human body and can help the process of assessing the limits emerging under healthy conditions and critical signals of transition toward disease. Underwater environment is one in which many body functions are critically stressed (Pendergast and Lundgren, 2009).

Relevant answers were for instance found in the study on the effect of pre-dive whole body vibration on post-dive bubble formation: Balestra's paper referred that the whole body vibration with the diver laying on a vibrating mattress was much a better condition than preconditioning with oxygen for a reduction of decompression-induced vascular gas emboli (Balestra et al.). Evidence that intensive weight reduction regimens induce changes in female body composition and serum hormones was demonstrated by Hulmi et al.'s study, in which it was observed recovery in subsequent months owing to increased energy intake.

Space is another type of special environment that requires extreme changes and adaptations for living organisms (plants, animals, and human beings). Space flight imposes constraints on the body of highly selected, well-trained and healthy subjects (Aubert et al., 2016; Bergouignan et al., 2016). In particular, the pathophysiological adaptive changes resemble an accelerated aging process and relate with some disease processes (Fitts et al., 2000; Vernikos and Schneider, 2010). As such effects become manifest over a time span of weeks (i.e., cardiovascular deconditioning) to months (i.e., loss of bone density and muscle atrophy) of exposure to weightlessness, some kinds of corrections are possible during flight. Also note that, in due time, these effects are mostly reversible after landing (Demontis et al.).

Overall, a variety of stressors has been widely analyzed in preclinical models and in human studies. What is clear is that a pathway underlying such conditions is driven by inflammation, and this explains the multiple effects visible through multiple associated morbidities.

TRANSLATIONAL RELEVANCE

In the translational field, with reference to the study on the fluoxetine protection in decompression sickness in mice crosslinks molecular biology, pharmacological actions, and basic mechanisms of diseases like disseminated coagulation, inflammation, and ischemia induce neurological damage and death. These symptoms result from circulating bubbles generated by a pathogenic decompression: acute fluoxetine treatment increases the survival rate of mice subjected to an experimental dive, enhanced by TREK-1 inhibition (Vallée et al.).

Another adaptation in extreme acidic environment is analyzed by the study on hydrothermal vent organisms, which have evolved physiological adaptations to cope with extreme abiotic conditions including temperature and pH (Hu et al.). The considerable acid-base regulatory abilities in brachyuran crabs could suggest some basic mechanisms in support of both the understanding of the derangements in acid-base homeostasis and the design of mock systems addressing environmental safety.

We notice that the observations derived from animal behavior in terrestrial and marine environment are currently used for bioengineering studies and innovative research. Bio-robotic investigational areas could be linked to physiology in extreme conditions for foresight programs.

ETHICAL ASPECTS

By considering the ethical request of animal experiments reduction, an example of alternative methods is offered by the study of hepatic cells, prospecting a genetic therapeutic approach for prophylaxis and treatment of liver fibrosis by a double-knockdown interfering with the intracellular oxygen sensor-prolyl hydroxylase 1 (PHD1) and the intracellular oxidative stress sensor-kelch-like ECH associated protein 1 (Keap1). The findings pointed to increased cell viability and a down-regulated expression of pro-fibrogenic molecules (Liu et al.).

SPORT

A number of studies have been included in the research topic that have used sport as an example of extreme physiological processes. The recent advent of a widespread proliferation of ultra-long endurance races has consequently motivated the evaluation of factors such as the physiological response of the athletes, the cognitive and neurosensory pattern, the sleep deprivation effects (Tonacci et al.). These are all important elements to be considered for safety reasons.

Different types of activities can induce acute and chronic changes with or without recovery of homeostasis afterwards (Ujka et al.): monitoring during and after races physiological variables of different subjects seems to be essential in terms of human health.

Similarly to safety in competitions, and focusing at training, the analysis on the kinematics of the jump appears relevant in order to evaluate the adaptation of the motor cerebral programming to the jumper's physical characteristics, the control of the initial posture, and the jumper's perception of the position

of the body mass center, as underlined by some authors (Fargier et al.).

PHYSIOLOGY CHALLENGES, PEOPLE ENGAGEMENT, AND BIG DATA SUPPORT

Biomedical data have increased dramatically in both volume and variety with the emergence of people-integrated health data generating sources, typically referred as m-healh. Additional complexity is expected when tasks such as profiling or risk assessment are required. This calls for analytical improvements, not currently available from specialized rather than integrated disciplines, which in turn calls for a new generation of scientists and clinicians.

Conditio sine qua non remains the enhancement of communication skills, shared decision making and definition of disease reclassifications, but also a re-assessment of people engagement in the N-of-1 or individualized medicine era. While the Big Data realm of applications promises to be relevant and rich with opportunity, but benefits to people will come with harmonization among all specialized individuals operating with data (Beckmann and Lew, 2016).

CONCLUDING REMARKS

Other conditions beyond those presented in this research topic deserve future attention: namely, altitude (Grocott et al., 2007), consciousness abolished in anesthesia, sleep deprivation, and circadian rhythms, breakdown in sudden events, and catastrophes. Thinking ahead, all such studies belong to a novel, interdisciplinary and highly complex research field, which nevertheless could stimulate the curiosity of researchers and clinicians, hopefully inducing further interactions within joint scientific activities.

AUTHOR CONTRIBUTIONS

All authors listed have made a substantial, direct and intellectual contribution to the work, and approved it for publication.

REFERENCES

Aubert, A. E., Larina, I., Momken, I., Blanc, S., White, O., Kim Prisk, G., et al. (2016).Towards human exploration of space: the THESEUS review series on cardiovascular, respiratory, and renal research priorities. *npj Microgravity* 2:16031. doi: 10.1038/npjmgrav.2016.31

Beckmann, J. S., and Lew, D. (2016). Reconciling evidence-based medicine and precision medicine in the era of big data: challenges and opportunities. *Gen. Med.* 8, 134. doi: 10.1186/s13073-016-0388-7

Bergouignan, A., Stein, T. P., Habold, C., Coxam, V., O'Gorman, D., and Blanc, S. (2016). Towards human exploration of space: the THESEUS review series on nutrition and metabolism research priorities. *npj Microgravity* 2:16029. doi: 10.1038/npjmgrav.2016.29

Cohn, W. E., Timms, D. L., and Frazier, O. H. (2015). Total artificial hearts: past, present, and future. *Nat. Rev. Cardiol.* 12, 609–617. doi: 10.1038/nrcardio.2015.79

Fitts, R. H., Riley, D. R., and Widrick, J. J. (2000). Physiology of a microgravity environment invited review: microgravity and skeletal muscle. *J. Appl. Physiol.* 89, 823–839. Available online at: http://jap.physiology.org/content/89/2/823.abstract

Grocott, M., Montgomery, H., and Vercueil, A. (2007). High-altitude physiology and pathophysiology: implications and relevance for intensive care medicine. *Crit. Care* 11:203. doi: 10.1186/cc5142

Pendergast, D. R., and Lundgren, C. E. G. (2009). The underwater environment: cardiopulmonary, thermal, and energetic demands. *J. Appl. Physiol.* 106, 276–283. doi: 10.1152/japplphysiol.90984.2008

Vernikos, J., and Schneider, V. S. (2010). Space, gravity and the physiology of aging: parallel or convergent disciplines? A mini-review. *Gerontology* 56, 157–166. doi: 10.1159/000252852

Conflict of Interest Statement: The authors declare that the research was conducted in the absence of any commercial or financial relationships that could be construed as a potential conflict of interest.

frontiers in Physiology

MINI REVIEW
published: 13 October 2016
doi: 10.3389/fphys.2016.00435

Excited Delirium and Sudden Death: A Syndromal Disorder at the Extreme End of the Neuropsychiatric Continuum

Deborah C. Mash *

Department of Neurology and Molecular and Cellular Pharmacology, University of Miami Miller School of Medicine, Miami, FL, USA

Over the past decade, the excited delirium syndrome (ExDS) has raised continued controversy regarding the cause and manner of death of some highly agitated persons held in police custody, restrained or incapacitated by electrical devices. At autopsy, medical examiners have difficulty in identifying an anatomic cause of death, but frequently cite psychostimulant intoxication as a contributing factor. The characteristic symptoms of ExDS include bizarre and aggressive behavior, shouting, paranoia, panic, violence toward others, unexpected physical strength, and hyperthermia. Throughout the United States and Canada, these cases are most frequently associated with cocaine, methamphetamine, and designer cathinone abuse. Acute exhaustive mania and sudden death presents with behavioral symptoms that are identical to what is described for ExDS in psychostimulant abusers. Bell's mania or acute exhaustive mania was first described in the 1850's by American psychiatrist Luther Bell in institutionalized psychiatric patients. This rare disorder of violent mania, elevated body temperature and autonomic collapse continued to be described by others in the psychiatric literature, but with different names until the first cases of ExDS were seen at the beginning of the cocaine epidemic by medical examiners. The neurochemical pathology examination of brain tissues after death revealed a loss of dopamine transporter regulation together with increases in heat shock protein 70 (hsp70) expression as a biomarker of hyperthermia. The similarity in the behavioral symptoms between extremely agitated psychostimulant abusers and unmedicated psychiatric patients suggests that a genetic disorder that leads to dysregulated central dopamine transporter function could be a precipitating cause of the acute delirium and sudden death. While the precise cause and mechanism of lethality remains controversial, the likely whys and wherefores of sudden death of ExDS victims are seen to be "biological," since excessive dopamine in the brain triggers the manic excitement and delirium, which unabated, culminates in a loss of autonomic function that progresses to cardiorespiratory collapse.

Keywords: delirium, CNS, neurocardiac, dopamine, dopamine transporter, mania, cocaine

OPEN ACCESS

Edited by:
Maria Giovanna Trivella, National Research Council, Italy

Reviewed by:
Karie Scrogin, Loyola University Chicago, USA
Satoshi Eifuku, Fukushima Medical University, Japan

***Correspondence:**
Deborah C. Mash
dmash@med.miami.edu

Specialty section:
This article was submitted to Integrative Physiology, a section of the journal Frontiers in Physiology

Received: *01 April 2016*
Accepted: *13 September 2016*
Published: *13 October 2016*

Citation:
Mash DC (2016) Excited Delirium and Sudden Death: A Syndromal Disorder at the Extreme End of the Neuropsychiatric Continuum. Front. Physiol. 7:435. doi: 10.3389/fphys.2016.00435

INSET

Henry Maudsley MD described Acute Mania and Acute Maniacal Delirium in 1867 in his "Physiology and Pathology of the Mind," which best illustrates the view discussed in this article. He suggests that persons in an agitated state of acute mania benefit from "abundant exercise in the open air" while "such a practice would be most unscientific in acute delirium, and very likely to be followed by fatal consequences". He further states "it would be better to place a patient suffering from such acute degeneration of cerebral function entirely in seclusion" rather "than to aggravate his disorder by forced exercise and mischievous struggles with attendants". Medico-legal reports more than a hundred and fifty years after Maudsley and Luther Bell find the prognosis is never very favorable for individuals at risk for excited delirium.

HISTORICAL DESCRIPTIONS AND CASE REPORTS

Psychiatrists in the United Kingdom, France and America were the first to provide clinical descriptions and case reports of persons in states of acute exhaustive mania and delirium. In the 1800s, Dr. Luther Bell, psychiatrist at the McLean Asylum for the Insane in Massachusetts described a clinical condition with a 75 percent mortality rate. "Bell's mania" or acute exhaustive mania was characterized by delusions, hallucinations, hyperactivity, and frequent fevers. The descriptions although similar to the psychotic features of paranoid schizophrenics (e.g., hallucinations and delusions) revealed a more extreme condition of generalized severe disorganization of behavior, including hyperactive arousal, altered sleep-wake cycle, and elevated core body temperature. Calmeil's report of an uncommon, but life threating psychosis with extreme hyperactivity and mounting fear fading to stuperous exhaustion in 1832 was followed by Maudleys' description of the same disorder in 1867 (inset). Agitated delirium signs and symptoms were reported in hyperactive or mixed forms of the disorder throughout the pre-neuroleptic era of psychiatry (Kraines, 1934; Stauder, 1934; Larson, 1939).

In 1934, Stauder published detailed observations of 27 cases, which became the definitive description of a syndrome that he termed lethal catatonia (Stauder, 1934). The cases were mostly young people, in the age range of 18–26 years, who had no significant premorbid psychological or physical disturbances. Stauder observed the acute onset of a severe form of psychomotor agitation that he called "elementary catatonic excitement." Various degrees of clouding of consciousness and a strong tendency toward violent and self-destructive acts also were present. Although different nomenclature was used to describe a psychotic exhaustion syndrome, fatal cases of a life-threatening febrile neuropsychiatric disorder were widely recognized and reported by clinicians before modern psychiatric treatments became available (Shulack, 1946). The authors of these published reports found it remarkable that autopsies of these patients failed to reveal any clues to etiology or the cause of death, other than exhaustion.

Between 1954 and 1975, the advent of the neuroleptic drugs like Thorazine transformed psychiatric practice and reduced the incidence of exhaustive mania in institutionalized and unmedicated patients. However, the cocaine epidemic of the 1980's lead to a series of case reports describing sudden death in cocaine abusers with an extreme behavioral malady similar to what had been reported by Bell and others 150 years earlier. The agitated cocaine delirium deaths were associated with cocaine abuse and their appearance coincided with the introduction of cocaine into the United States (Fishbain and Wetli, 1981; Wetli, 1987). The trans-shipment of cocaine to South Florida through the Bahamian corridor and the increased incidence of cocaine-related medical emergency room admissions and drug related deaths placed Medical Examiners in Miami-Dade at the forefront of a new wave of cocaine-related excited delirium deaths.

Wetli and Fishbain (1985) described a case series of psychosis and sudden death in cocaine abusers, which was the first report of drug-related excited delirium (**Table 1**). The deaths occurred mostly in young cocaine intoxicated males, who exhibited extreme hyperactivity and violent behavior, hyperthermia and sudden cardiorespiratory collapse. Because these patients always presented with agitated and bizarre behavior, law enforcement was often called to the scene. The typical course was that after police restrained the individual, they died unexpectedly and suddenly following the use of various force methods, including maximal restraints, baton strikes, or use of noxious chemical "pepper" sprays (Wetli, 1987; Ross, 1998; Stratton et al., 2001). Medical examiner review of these cases did not reveal a definite anatomic cause of death, although drug overdose, trauma, and underlying cardiac disease were excluded (Wetli, 1987; Ruttenber et al., 1997; Stephens et al., 2004).

TABLE 1 | Historical descriptions and terminology of excited delirium syndrome.

Author and year	Nomenclature	Clinical description
Calmeil, 1832	Delirious mania	Rare, life-threatening psychosis extreme hyperactivity, mounting fear, stuporous exhaustion
Bell, 1849	Bell's mania	Sudden onset of hyperactive arousal, confusion, transient hallucinations, core body temperature dysregulation, 75% mortality rate
Maudsley, 1867	Acute maniacal delirium	Violent mania, rapid pulse, constant motion, elevated temperature of skin, complete exhaustion
Stauder, 1934	Lethal catatonia	Intense motor excitement, violent, suicide attempts, intermittent rigidity, incoherent speech, bizarre delusions; fever (43.3°C), cardiovascular collapse
Wetli and Fishbain, 1985	Excited delirium	Agitation motor excitement, super human strength, paranoia, mounting fear, hyperthermia, cardiorespiratory collapse, cocaine intoxication, no anatomic cause of death

FATAL COCAINE DELIRIUM AS A VARIANT OF THE NEUROLEPTIC MALIGNANT SYNDROME

Neuroleptic malignant syndrome (NMS) is a rare, life-threatening idiosyncratic reaction to antipsychotic drugs characterized by fever, altered mental status, muscle rigidity, and autonomic dysfunction (Levenson, 1985; Weinberger and Kelly, 1977; Berman, 2011). The hallmark symptoms of NMS include hyperpyrexia and muscular rigidity, while the cocaine-associated syndrome is atypical in having minimal rigidity. Based on these similarities, Kosten and Kleber (1988) proposed that cocaine-induced excited delirium should be considered a dopamine agonist variant of NMS. Wetli (2005) proposed that NMS might be an attenuated form of acute exhaustive mania/excited delirium. These observations lead him to hypothesize that there may be three related syndromes: (1) acute exhaustive mania, as described by Bell in psychiatric patients, (2), excited delirium, due to psychostimulants; and (3) the attenuated variant—NMS (for review, Wetli, 2005).

Delirious mania and malignant catatonia both have non-malignant and malignant clinical features with early, non-malignant symptoms responding to neuroleptics, while patients who pass over into the malignant phase require sedation by benzodiazepines (Mann et al., 2013). Although NMS is a rare, life-threatening idiosyncratic reaction associated with virtually all neuroleptics, including the newer atypical antipsychotics (e.g., dopamine blockers), the condition is linked also to the use of indirect and direct-acting dopamine agonists. The abrupt cessation or reduction in dose of dopaminergic agonists, such as levodopa, pergolide, and amantadine in Parkinson's disease may precipitate NMS in vulnerable patients (Ito et al., 2001; Reimer et al., 2002). Interestingly, the akinetic crisis of Parkinson's disease is associated with a severe loss of striatal dopamine transporter function (Kasssinen et al., 2014). This rare condition is a life-threatening complication of Parkinson's disease, with an estimated annual incidence of 0.3% and death rate of 15%, that is associated with hyperthermia, dysautonomia, and increased serum muscle enzymes (Takubo et al., 2003; Onofrj et al., 2009). The clinical picture is similar to that of NMS and has been termed as the malignant syndrome of parkinsonism-hyperpyrexia. The condition is not related to disease stage or medication dosage, but one of the main features is that, the akinetic crisis appears to be long lasting (on average 11 days) and the dopamine system is transiently blocked from treatments, which would usually give patients rapid motor benefit. To date, none of the theories put forth as the underlying cause of the NMS related syndrome in Parkinson's disease have been able to explain why only a small fraction of patients exposed to dopaminergic agonists develop the condition, although state (dopaminergic drugs) and trait (genetic) vulnerabilities are likely risk factors.

Hypothalamic dopamine antagonism leads to the elevated set point for thermoregulation and the myotoxicity associated with malignant hyperthermia. Sympathoadrenal hyperactivity and the loss of hierarchical integration and homeostatic control may constitute important risk factors for NMS and its associated variants. Gurrera (1999) advanced this hypothesis, suggesting that sympathetic nervous system hyperactivity should be viewed as primary in the etiology of NMS. The sympathetic nervous system mediates the hypothalamic coordination of thermoregulatory activity and is a regulator of muscle tone and thermogenesis. The sympathetic nervous system's latent capacity for autonomous activity is expressed when tonic inhibitory inputs from higher central nervous system dopaminergic centers are disrupted. The predominant sources of spinal dopamine are the descending fibers projecting from the dopaminergic A10 and A11 cell groups of the posterior hypothalamus (Skagerberg and Lindvall, 1985; Qu et al., 2006). These tonic inhibitory inputs relay to preganglionic sympathetic neurons by way of the dopaminergic hypothalamospinal tracts.

A predisposition to more extreme sympathetic nervous system activation and/or dysfunction in response to emotional or psychological stress may be an underlying state vulnerability for NMS, as well as, for the ExDS associated with psychostimulant abuse. State variables like the acute psychic stress reported originally in Bell's mania when coupled with a loss of presynaptic dopaminergic transporter function may lead to extremely elevated concentrations of synaptic dopamine, and the emergence of related clinical syndromes.

EXCITED DELIRIUM IS A SYNDROMAL DISORDER OF DYSREGULATED DOPAMINE

A syndrome is the association of several clinically recognizable features, signs, symptoms, or characteristics that often occur together, so that the presence of one feature alerts to the presence of the others. Most recognize that the condition of excited delirium represents a syndromal disorder rather than a specific disease. What has not been emphasized in the literature is that various organic brain disorders, as well as functional psychiatric conditions and psychostimulant abuse, contribute to the expression of a CNS disorder with high fatality rates that share a common underlying neurochemical dysregulation of central dopamine homeostasis.

Persons at risk for excited delirium are most likely at the extreme end of the neuropsychiatric continuum of several DSM-IV recognized disorders, including delirium induced by a drug, manic excitement, and psychomotor agitation (Vilke et al., 2012). Those at risk for excited delirium and sudden death include people who are withdrawing from or non-compliant with psychotropic drugs, substance abusers suffering from reward deficiency syndrome or alcoholics in withdrawal, and persons suffering from acute manic episodes that may be triggered or worsened by sleep deprivation.

The clinical description of excited delirium includes reports of increasing excitement with wild agitation and violent, often destructive behavior that can last for hours to days. The forensic pathology descriptions suggest that the disorder can wax and wane in severity over time with rigidity or stupor alternating

with excitement (Wetli, 2005; DiMaio and DiMaio, 2006). These progress to increasing and possible fluctuations of fever and persistent autonomic instability with rapid and weak pulse and hypotension. Cocaine delirium shares clinical similarity to the acute onset of excitement, grandiosity, emotional lability, delusions, and insomnia associated with emergence of mania, and the disorientation and altered consciousness characteristic of delirium. Psychostimulant intoxication, drug withdrawal states, and undiagnosed mania and bipolar affective disorder are the most commonly reported antecedents (Wetli, 2005; Mash et al., 2009; Vilke et al., 2012).

PATHOPHYSIOLOGY AND NEUROCHEMICAL TRIGGERS

Transmission of reward signals is a function of dopamine, a neurotransmitter known to be involved in the mechanism of psychosis. The symptoms of psychosis and mania are both related to dopaminergic hyperactivity in brain circuits implicated in neuropsychiatric disorders (Cipriani et al., 2011). In psychosis, post-synaptic receptor sensitization causes dysfunctional neural processing, leading to the development of delusional symptoms. This understanding fits well with the traditional hyperdopaminergic hypothesis of psychosis and schizophrenia. The hyperdopaminergia and disordered signaling in dopamine target regions of the brain also serves as a model for mania, since dopaminergic blocking drugs are effective in alleviating mania and psychosis.

Mania is the cardinal feature and a core symptom of bipolar disorder. PET scans in medicated, manic patients show abnormal brain activation in dorsal anterior cingulate, frontal polar, and right inferior frontal cortical regions (Rubinsztein et al., 2001). The increase in task-related anterior cingulate activation was positively correlated in this study with the severity of manic symptoms. Anterior cingulate cortex activation may be related to increased nucleus accumbens dopamine signaling, which leads to cortical and subcortical hyperactivity in mania (Perry et al., 2001). Genetic linkage studies have suggested an association of the dopamine transporter gene (Kelsoe et al., 1996; Greenwood et al., 2001, 2006) and lower levels of transporter protein expression in patients with bipolar affective disorder (Amsterdam and Newberg, 2007).

Cocaine and methamphetamine increase extracellular dopamine and produce behavioral effects similar to mania (Silverstone et al., 1983). Drug sensitization occurs in drug addiction, and is defined as an increased effect of a drug following repeated doses (the opposite of drug tolerance). Such sensitization involves increased brain mesolimbic dopamine transmission, as well as altered protein expression within mesolimbic dopamine neurons. Repeated treatment with psychostimulants leads to sensitization or reverse tolerance in animal models (Post and Rose, 1976; Hooks et al., 1994; Pierce and Kalivas, 1997; Zapata et al., 2003) and human cocaine abusers (Ujike and Sato, 2004; Seeman, 2011). Paranoia in the context of cocaine abuse is common and potentially dangerous and several lines of evidence suggest that this phenomenon may be related to loss of function of the dopamine transporter protein (Gelernter et al., 1994; van Dyck et al., 2005). These observations suggest that certain dopamine transporter genotypes might predispose to paranoia with chronic psychostimulant abuse.

The dopamine transporter undergoes neurobiological adaptations with chronic abuse of cocaine, depending on the duration, amount and pattern of use (e.g., binge vs. daily use). Intermittent cocaine self-administration in rodents produces sensitization of the stimulant effects of cocaine at the dopamine transporter (Calipari et al., 2014) and enhanced locomotor responsiveness or what is termed behavioral sensitization (Kalivas and Duffy, 1993; Robinson and Berridge, 1993; Kalivas et al., 1998). This phenomenon is not unique to cocaine; other psychomotor stimulants, some other classes of drugs, and mental stress induce the phenomenon of behavioral sensitization. Since cocaine directly inhibits dopamine reuptake by binding to the transporter, repeated cocaine administration may lead to a reduced potency of cocaine, which leads to an elevation in synaptic dopamine and the expression of behavioral sensitization (Zahniser et al., 1995, 1998).

The dopamine transporter expressed in presynaptic terminals of dopamine neurons regulates reuptake of dopamine from the synaptic cleft and keeps extracellular dopamine concentrations low (Amara and Kuhar, 1993; Giros and Caron, 1993; Mortensen and Amara, 2003). The dopamine transporter is critical in regulating the concentration of extracellular dopamine and overall dopaminergic tone (Mash and Staley, 1996; Drevits et al., 1999; Mash et al., 2002, 2009). By blocking the transporter protein, cocaine allows released dopamine to persist in the extracellular space, which prolongs dopamine receptor stimulation (**Figure 1**). A decrease in dopamine transporter numbers or function in response to cocaine leads to reduced dopamine reuptake, elevated synaptic dopamine, and increased dopamine signaling at postsynaptic receptors.

The syndrome of excited delirium in drug abusers demonstrates that cocaine is the most frequent reported illicit drug (Ruttenber et al., 1997; Mash et al., 2009; Vilke et al., 2012). Most drug-related excited delirium victims are chronic freebase cocaine ("crack") abusers, usually engaged in a "binge" pattern of drug use (Mash et al., 2002, 2009; Wetli, 2005). These persons use large amounts of "crack" cocaine or methamphetamine often for days, which interrupts normal sleep-wake cycles. Inhibition of dopamine transporter function is thought to be the primary mechanism underlying cocaine's addictive effects (Ritz et al., 1987). Although excited delirium is most frequently reported in cocaine abusers, psychostimulants including, methamphetamine, MDMA, alpha-PVP, methylome, and ephedrine have been associated with the syndrome (Mash et al., 2009; Penders et al., 2012). These psychostimulants directly interact with the dopamine transporter to cause a marked increase in the levels of synaptic dopamine.

Postmortem neurochemical studies of the human brain at autopsy demonstrate that chronic cocaine abuse leads to a compensatory upregulation of dopamine transporter number and function (Staley et al., 1994; Little et al., 1999; Mash et al., 2002). In contrast, there was no compensatory upregulation in dopamine transporter numbers in a case series of 90

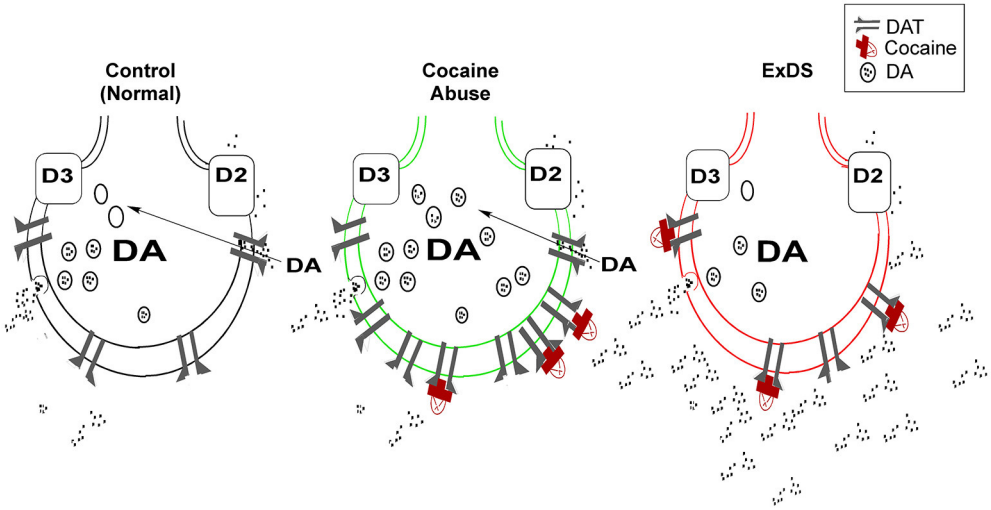

FIGURE 1 | Dysregulated dopamine transporter function in ExDS. Located on presynaptic dopamine nerve terminals, the dopamine transporter functions to regulate the duration and intensity of synaptic dopamine signaling (left). Cocaine (red) inhibits the reuptake of dopamine by blocking the transporter protein (center). With chronic cocaine abuse, the dopamine transporter is trafficked to the plasma membrane as a compensatory adaptation to increases in synaptic dopamine. In ExDS victims, there is a loss of dopamine transporter regulation, which causes dopamine overflow in the synapse (right). The elevated synaptic dopamine leads to a state of hyperdopaminergia, that is associated with the intense motor excitement, paranoia, bizarre, and often violent behavior. DAT, dopamine transporter; DA, dopamine; D2, D2 dopamine receptor; D3, D3 dopamine receptor.

cocaine-related excited delirium and exhaustive mania victims (Mash et al., 2009). The cocaine-related excited delirium cases occurred in persons who had reported histories of chronic cocaine abuse, consistent with the quantification of benzoylecgonine in blood and cocaine and benzoylecgonine measured in brain at autopsy (Mash et al., 2009). Mean core body temperature among the 90 victims was 40.7°C. Although the majority tested positive for cocaine, four had no licit or illicit drugs or alcohol measured in blood at autopsy. Forensic review of these four cases reported the cause of death as acute exhaustive mania, similar to the original description reported by Bell (1849).

All psychostimulants (e.g., cocaine, methamphetamine, and MDMA) increase the synaptic levels of dopamine (Amara and Kuhar, 1993; Giros and Caron, 1993), which may explain why chronic psychostimulant abusers are more at risk for exhibiting the behavioral symptoms associated with ExDS. A central role of dopamine is to mediate the "salience" of environmental events and internal representations in a dynamic process characterized by time and stimulus-dependent neural regulation (Kapur, 2003; Howes and Kapur, 2009). Dopamine can enhance both approach and avoidance behaviors and trigger extreme fear (Faure et al., 2008). In chronic cocaine abusers, there is a compensatory upregulation in dopamine transporter function, which is an adaptive increase to offset dopamine overflow in the synapse (**Figure 1**). When this homeostatic control of synaptic dopamine fails, it leads to a functional hyperdopaminergia, which triggers the acute onset of delirium and marked agitation in ExDS victims (Staley et al., 1996; Wetli et al., 1996; Mash et al., 2002, 2009).

Rhabdomyolysis secondary to mania and cocaine excited delirium is related to extreme physical exertion, although increased sympathetic tone during manic states and elevated epinephrine also play a role in its development (Manchip and Hurel, 1995; Ruttenber et al., 1999). Ruttenber et al. (1999) suggested that cocaine-associated rhabdomyolysis and excited delirium are components of the same syndrome and share the same initiating factors and pathophysiologic processes. Both hyperthermia and hyperactivity play important roles in the evolution of cocaine-associated rhabdomyolysis and excited delirium. Interestingly, in NMS, the elevated risk for hyperthermia results from disordered dopamine signaling precipitated by chronic administration of neuroleptic drugs (Strawn et al., 2007). The hyperthermia of neuroleptic malignant syndrome is associated with psychomotor agitation, and both syndromes have been related to increases in dopamine concentrations involved in thermoregulation and neuromuscular homeostasis (Keck et al., 1989).

Some undiagnosed psychiatric patients or those who are neuroleptic medication non-compliant may be at increased risk for excited delirium and sudden cardiac death. Dopamine transporter numbers fall below the normal homeostatic range for regulating dopamine in all cases of fatal excited delirium, including those with no known history of drug abuse and a negative toxicology screen at autopsy. These results suggest that the unabated conditions, which favor the development of excited delirium, are psychostimulant abuse, extreme mental stress or an underlying, or perhaps undiagnosed psychiatric condition.

A final common pathway for excited delirium related to chronic stimulant drug abuse, extreme environmental stress or acute mania of bipolar disorder might be a failure of the dopamine transporter to dynamically regulate synaptic dopamine. This failure of regulation leads to a hyperdopaminergic state, which triggers the violent behavior,

delirium, agitation, and motor excitement. Dopamine systems in the brain also play a role in temperature regulation (Mann and Boger, 1978). The rise in core body temperature is most likely induced by dopamine stimulation of D1 receptors in the human hypothalamus which occurs because of a downregulation in D2 mediated hypothermia (Mash, 2009). A dopamine transporter murine model of hyperdopaminergia displays a distinctive cardiorespiratory and thermal phenotype, providing further support for altered dopamine transporter regulation in excited delirium (Vincent et al., 2007). Dopamine also regulates sleep and arousal, suggesting that there might be an inter-relationship between thermal behavior and circadian rhythms mediated by disrupted CNS dopamine signaling in excited delirium.

WHEN NEUROCARDIAC SIGNALS TURN LETHAL

Mental and emotional stress is expressed in the brain as fluctuations in the activity of a subset of brain regions, including the insula, cingulate cortex, and amygdala (Critchley, 2009). These regions serve as an interface between emotional feeling states and visceral responses of the body. The insula and cingulate are viscerosensory cortices, which function to regulate attention and autonomic arousal. The amygdala is important in detecting and learning threat even in the absence of conscious awareness. The insula and cingulate cortices and subcortical regions of the limbic brain are heavily innervated by dopaminergic projections from the ventral tegmental nucleus (Gaspar, 1989). These closely connected brain regions together with the dorsal and ventral striatum are viewed as a "salience network," acting directly on hypothalamic and brainstem centers to increase our bodily arousal state through direct coupling with sympathetic and parasympathetic efferent nuclei and feedback control loops located in the brainstem.

The insular cortex and the infralimbic cortex are part of a network involved in the descending control of the cardiovascular system (for review, Cechetto, 2013). These forebrain regions are responsible for integrating emotional and cognitive aspects related to cardiovascular responses. Together with the autonomic nervous system nuclei of the brainstem, these forebrain regions regulate cardiac function and electrophysiology via direct neural influences. Taggart et al. (2011) suggest that the roles of mental stress and emotion in arrhythmogenesis and sudden cardiac death are no longer confined to the realm of anecdote, but should be viewed as contributors to the pathophysiology of cardiac sudden death. Sympathetic arousal magnifies the electrophysiological effects of ischemia (for review, Taggart et al., 2011) and abnormal brain activity during seizures is associated with abnormalities of cardiac repolarization, and peri-ictal VT/VF in the absence of any visible cardiovascular disease (Taggart, 2013). A centrally triggered arrhythmia is a likely cause of sudden unexpected death in epilepsy (Surges et al., 2010), and a similar neurocardiac mechanism could underlie the sudden cardiac collapse in ExDS.

An emerging theme from animal models of asphyxia and cardiac arrest supports the notion that the autonomic nervous system is under constant surveillance by the cerebral cortex to ensure functional integrity of vital organs (Borjigin et al., 2013). A life-threatening crisis of the heart, with a rapid and steep change in heart rate and cardiac output, markedly activates and recruits the cerebral cortex to form a hierarchical circuit of cardiac survival. When transient homeostatic feedback from the brain to the heart is insufficient to restore cardiac function, the brain may exhibit a sustained activation that causes a premature and rapid death of the heart (Li et al., 2015).

Dopamine (DA) is an immediate precursor of noradrenaline that has stimulatory or inhibitory effects on a variety of adrenergic receptors. Dopamine also suppresses responsiveness to hypoxia, both in the carotid bodies and in the CNS (Huey et al., 2000). Although the physiological relevance is not established, one possibility is that suppression of stimulatory responsiveness to hypoxia is a protective mechanism directed against excessive discharge activity in the CNS respiratory network, which can result in neuronal excitotoxicity (Richter et al., 2000, for review Lalley, 2008). In the rat asphyxia model of cardiac sudden death, at as early as time 0, a sevenfold elevation in dopamine levels is measured by microdialysis with increased 3-MT (3-methoxytyramine) and decreased DOPAC (3,4-dihydroxyphenylacetic acid) concentrations. Since hyperdopaminergia is a condition of ExDS, the increase in synaptic dopamine may account for the decreased respiratory rate caused by dysfunctional adaptations in respiratory network rhythm.

Victims of ExDS usually die from cardiopulmonary arrest (Takeuchi et al., 2011; Vilke et al., 2012). Sudden cardiac death induced by a life-threatening stressor results from a generalized sympathetic storm within the autonomic nervous system (Samuels, 2007). Consistent with this view, exposure to carbon dioxide leads to an immediate systemic surge of neurally released dopamine and norepinephrine in asphyxic rats (Li et al., 2015). Experimental brain stimulation of the left insula can induce QT prolongation, bradycardia, and pulse-less asystole (Oppenheimer et al., 1991; for review, Taggart, 2013), similar to the sudden loss of vital signs with asystole reported in ExDS victims (Vilke et al., 2012). Life-threatening stress can lead to sudden cardiac death in people with no previous history of abnormal heart and brain function (Samuels, 2007; Sharkey et al., 2011). These observations suggest that autonomic toxicity induced by central hyperdopaminergic activity in ExDS may hasten the demise of heart function (Samuels, 2007; Li et al., 2015).

CONCLUSIONS

Elevated synaptic dopamine when coupled with failed dopamine transporter function leads to agitation, paranoia and violent behaviors associated with ExDS. CNS dopamine also regulates heart rate, respiration, and core body temperature with chemical imbalance resulting in tachycardia, tachypnea, and hyperthermia. Hyperthermia is a hallmark of excited delirium and a harbinger

of death in this syndromal disorder. Victims of excited delirium are in an extremely heightened emotional state exhibiting marked paranoia and mounting irrational fear. Abnormal signaling in the brain-heart axis may be a precipitant of a sudden fatal arrhythmia, since hyperdopaminergic signaling in the limbic system can convert extreme emotional stress into autonomic toxicity. The connection between the hyperdopaminergia and chaotic signaling in higher brain autonomic regulatory centers may explain the abrupt loss of autonomic function that leads to sudden unexpected death in victims of the ExDS.

Excited delirium is a syndromal disorder, which is controversial and highly debated precisely because the mechanism of lethality is unknown. However, molecular studies of the brain of autopsy victims who died in states of excited delirium reveal a loss of dopamine transporter function as a possible trigger of a lethal cascade of neural activities that progress to asphyxia and sudden cardiac arrest. Both national and regional ExDS registries are needed with data about medical history, toxicology, gender, and race to improve outcomes and further translational molecular research studies of this highly disputed and often unrecognized psychopathological condition associated with central dopamine dysfunction.

AUTHOR CONTRIBUTIONS

The author confirms being the sole contributor of this work and approved it for publication.

FUNDING

The original studies were funded by grants from the National Institute on Drug Abuse (NIDA) (DA06227; DA033684).

REFERENCES

Amara, S. G., and Kuhar, M. J. (1993). Neurotransmitter transporters: recent progress. *Annu. Rev. Neurosci.* 16, 73–93. doi: 10.1146/annurev.ne.16.030193.000445

Amsterdam, J. D., and Newberg, A. B. (2007). Differences in dopamine transporter density in patients with bipolar type II and unipolar major depressive episode. *Neuropsychobiology* 55, 167–170. doi: 10.1159/000106476

Bell, L. V. (1849). On a form of disease resembling some advanced stages of mania and fever. *Am. J. Insanity* 6, 97–127.

Berman, B. D. (2011). Neuroleptic malignant syndrome: a review for neurohospitalists. *Neurohospitalist* 1, 41–47. doi: 10.1177/1941875210386491

Borjigin, J., UnCheol, L., Tiecheng, L., Dinesh, P., Huff, S., Klarr, D., et al. (2013). Surge of neurophysiological coherence and connectivity in the dying brain. *Proc. Natl. Acad. Sci. U.S.A.* 110, 14432–14437. doi: 10.1073/pnas.1308285110

Calipari, E. S., Ferris, M. J., Siciliano, C. A., Zimmer, A. B., and Jones, S. R. (2014). Intermittent cocaine self-admininstrationn produces sensitization of stimulant effects at the dopamine transporter. *J. Pharmacol. Exp. Ther.* 349, 192–198. doi: 10.1124/jpet.114.212993

Calmeil, L. F. (1832). *Dietionnaire de Medecine ou Repertoire General des Sciences*. Medicales sous Ie Rapport Theorique et Praetique, 2nd Edn. Bechet, Paris.

Cechetto, D. F. (2013). Cortical control of the autonomic nervous system. *Exp. Physiol.* 99, 326–331. doi: 10.1113/expphysiol.2013.075192

Cipriani, A., Barbui, C., Salanti, G., Rendell, J., Brown, R., Stockton, S., et al. (2011). Comparative efficacy and acceptability of antimanic drugs in acute mania: a multiple-treatments meta-analysis. *Lancet* 378, 1306–1315. doi: 10.1016/S0140-6736(11)60873-8

Critchley, H. D. (2009). Psychophysiology of neural, cognitive and affective integration: fMRIand autonomic indicants. *Int. J. Psychophysiol.* 73, 88–94. doi: 10.1016/j.ijpsycho.2009.01.012

DiMaio, T. G., and DiMaio, V. J. M. (2006). *Excited Delirium Syndrome: Cause of Death and Prevention*. New York, NY: Taylor and Francis.

Drevits, W. C., Price, J. C., Kupfer, D. J., Kinahan, P. E., Lopresti, B., Holt, D., et al. (1999). PET measures of amphetamine-induced release in ventral versus dorsal striatum. *Neuropsychopharmacology* 221, 694–709. doi: 10.1016/S0893-133X(99)00079-2

Faure, A., Reynolds, S. M., Richard, J. M., and Berridge, K. C. (2008). Mesolimbic dopamine in desire and dread: enabling motivation to be generated by localized glutamate disruptions in nucleus accumbens. *J. Neurosci.* 28, 7184–7192. doi: 10.1523/JNEUROSCI.4961-07.2008

Fishbain, D., and Wetli, C. V. (1981). Cocaine intoxication, delirium, and death in a body packer. *Ann. Emerg. Med.* 10, 531–532.

Gaspar, P. (1989). Catecholamine innervation of the human cerebral-cortex as revealed by comparative immunohistochemistry of tyrosine-hydroxylase and dopamine-β-hydroxylase. *J. Comp. Neurol.* 279, 249–271. doi: 10.1002/cne.902790208

Gelernter, J., Kranzler, H. R., Satel, S. L., and Rao, P. A. (1994). Genetic association between dopamine transporter protein alleles and cocaine-induced paranoia. *Neuropsychopharmacology* 11, 195–200. doi: 10.1038/sj.npp.1380106

Giros, B., and Caron, M. G. (1993). Molecular characterization of the dopamine transporter. *Trends Pharmacol. Sci.* 14, 43–49. doi: 10.1016/0165-6147(93)90029-J

Greenwood, T. A., Alexander, M., Keck, P. E., McElroy, S., Sadovnick, A. D., Remick, R. A., et al. (2001). Evidence for linkage disequilibrium between the dopamine transporter and bipolar disorder. *Am. J. Med. Genet.* 105, 145–151. doi: 10.1002/1096-8628(2001)9999:9999<::AID-AJMG1161>3.0.CO;2-8

Greenwood, T. A., Schork, N. J., Eskin, E., and Kelsoe, J. R. (2006). Identification of additional variants within the human dopamine transporter gene provides further evidence for an association with bipolar disorder in two independent samples. *Mol. Psychiatry* 11, 125–133. doi: 10.1038/sj.mp.4001764

Gurrera, R. J. (1999). Sympathoadrenal hyperactivity and the etiology of neuroleptic malignant syndrome. *Am. J. Psychiatry* 156, 169–180.

Hooks, M. S., Duffy, P., Striplin, C., and Kalivas, P. W. (1994). Behavioral and neurochemical sensitization following cocaine self-administration. *Psychopharmacology* 115, 265–272. doi: 10.1007/BF02244782

Howes, O. D., and Kapur, S. (2009). The dopamine hypothesis of schizophrenia: version III—the final common pathway. *Schizophr. Bull.* 35, 549–562. doi: 10.1093/schbul/sbp006

Huey, K. A., Brown, I. P., Jordan, M. C., and Powell, F. L. (2000). Changes in dopamine D2-receptor modulation of the hypoxic ventilatory response with chronic hypoxia. *Respir. Physiol.* 123, 177–187. doi: 10.1016/S0034-5687(00)00175-4

Ito, T., Shibata, K., Watanabe, A., and Akabane, J. (2001). Neuroleptic malignant syndrome following withdrawal of amantadine in a patient with influenza A encephalopathy. *Eur. J. Pediatr.* 160, 401. doi: 10.1007/s004310100743

Kalivas, P. W., and Duffy, P. (1993). Time course of extracellular dopamine and behavioral sensitization to cocaine. I. Dopamine axon terminals. *J. Neurosci.* 13, 266–275.

Kalivas, P. W., Pierce, R. C., Cornish, J., and Sorg, B. A. (1998). A role for sensitization in craving and relapse in cocaine addiction. *J. Psychopharmacol.* 12, 49–53. doi: 10.1177/026988119801200107

Kapur, S. (2003). Psychosis as a state of aberrant salience: a framework linking biology, phenomenology, and pharmacology in schizophrenia. *Am. J. Psychiatry* 160, 13–23. doi: 10.1176/appi.ajp.160.1.13

Kasssinen, V., Joutsa, J., Noponen, T., and Paivarinta, M. (2014). Akinetic crisis in Parkinson's disease is associated with a severe loss of striatal dopamine transporter function: a report of two cases. *Case Rep. Neurol.* 6, 275–280. doi: 10.1159/000369448

Keck, P. E. Jr., Pope, H. G. Jr., Cohen, B. M., McElroy, S. L., and Nierenberg, A. A. (1989). Risk factors for neuroleptic malignant syndrome. A case-control study.

Arch. Gen. Psychiatry 46, 914–918. doi: 10.1001/archpsyc.1989.01810100056011

Kelsoe, J. R., Sadovnick, A. D., Kristbjarnarson, H., Bergesch, P., Mroczkowski-Parker, Z., Drennan, M., et al. (1996). Possible locus for bipolar disorder near the dopamine transporter on chromosome 5. *Am. J. Med. Genet.* 67, 533–540.

Kosten, T. R., and Kleber, H. D. (1988). Rapid death during cocaine abuse: a variant of the neuroleptic malignant syndrome? *Am. J. Drug Alcohol Abuse* 14, 335–346. doi: 10.3109/00952998809001555

Kraines, S. H. (1934). Bell's mania (acute delirium). *Am. J. Psychiatry* 91, 29–40. doi: 10.1176/ajp.91.1.29

Lalley, P. M. (2008). Opioidergic and dopaminergic modulation of respiration. *Respir. Physiol. Neurobiol.* 164, 160–167. doi: 10.1016/j.resp.2008.02.004

Larson, C. P. (1939). Fatal cases of acute manic-depressive psychosis. *Am. J. Psychiatry* 95, 971–982. doi: 10.1176/ajp.95.4.971

Levenson, J. L. (1985). Neuroleptic malignant syndrome. *Am. J. Psychiatry* 142, 1137–1145. doi: 10.1176/ajp.142.10.1137

Li, D., Mabrouk, O. S., Liu, T., Tian, F., Xu, G., Rengifo, S., et al. (2015). Asphyxia-activated corticocardiac signaling accelerates onset of cardiac arrest. *Proc. Natl. Acad. Sci. U.S.A.* 112, E2073–E2082. doi: 10.1073/pnas.1423936112

Little, K. Y., Zhang, L., Desmond, T., Frey, K. A., Dalack, G. W., and Cassin, B. J. (1999). Striatal dopaminergic abnormalities in human cocaine users. *Am. J. Psychiatry* 156, 238–245.

Manchip, S. M., and Hurel, S. J. (1995). Rhabdomyolysis due to mania. *Br. J. Psychiatry* 167, 118–119.

Mann, S. C., and Boger, W. P. (1978). Psychotropic drugs, summer heat and humidity, and hyperpyrexia: a danger restated. *Am. J. Psychiatry* 135, 1097–1100. doi: 10.1176/ajp.135.9.1097

Mann, S. C., Caroff, S. N., Gabor, S., Ungavari, S., and Campbell, E. C. (2013). Catatonia and malignant catatonia, and neuroleptic malignant syndrome. *Curr. Psychiatr. Rev.* 9, 1111–1119. doi: 10.2174/1573400511309020005

Mash, D. C. (2009). "Biochemical brain markers in excited delirium deaths," in *TASER® Conducted Electrical Weapons: Physiology and Pathology, and Law (chapter 29)*, eds M. Kroll and J. Ho (New York, NY: Springer Kluwer), 365–378.

Mash, D. C., Duque, L., Pablo, J., Qin, Y., Adi, N., Hearn, W. L., et al. (2009). Brain biomarkers for identifying excited delirium as a cause of sudden death. *Forensic Sci. Int.* 190, e13–e19. doi: 10.1016/j.forsciint.2009.05.012

Mash, D. C., Pablo, J., Ouyang, Q., Hearn, W. L., and Izenwasser, S. (2002). Dopamine transport function is elevated in cocaine users. *J. Neurochem.* 81, 292–300. doi: 10.1046/j.1471-4159.2002.00820.x

Mash, D. C., and Staley, J. K. (1996). "Cocaine recognition sites on the human dopamine transporter in drug overdose victims," in *Neurotransmitter Transporters. Structure and Function,* ed M. E. A. Reith (New York, NY: Humana), 56–67.

Maudsley, H. (1867). Acute mania and acute maniacal delirium. *Br. J. Psychiatry* 13, 59–65. doi: 10.1192/bjp.13.61.59

Mortensen, O. V., and Amara, S. G. (2003). Dynamic regulation of the dopamine transporter. *Eur. J. Pharmacol.* 479, 159–170. doi: 10.1016/j.ejphar.2003.08.066

Onofrj, M., Bonanni, L., Cossu, G., Manca, D., Stocchi, F., and Thomas, A. (2009). Emergencies in parkinsonism: akinetic crisis, life-threatening dyskinesias, and polyneuropathy during L-Dopa gel treatment. *Parkinsonism Relat. Disord.* 15, S233–S236. doi: 10.1016/S1353-8020(09)70821-1

Oppenheimer, S. M., Wilson, J. X., Guiraudon, C., and Cechetto, D. F. (1991). Insular cortex stimulation produces lethal cardiac arrhythmias: a mechanism of sudden death? *Brain Res.* 550, 115–121.

Penders, T. M., Gestring, R. E., and Vilensky, D. E. (2012). Intoxication delirium following use of synthetic cathinone derivatives. *Am. J. Drug Alcohol Abuse* 38, 616–617. doi: 10.3109/00952990.2012.694535

Perry, W., Minassian, A., Feifel, D., and Braff, D. L. (2001). Sensorimotor gating deficits in bipolar disorder patients with acute psychotic mania. *Biol. Psychiatry* 50, 418–424. doi: 10.1016/S0006-3223(01)01184-2

Pierce, R. C., and Kalivas, P. W. (1997). A circuitry model of the expression of behavioral sensitization to amphetamine-like psychostimulants. *Brain Res. Brain Res. Rev.* 25, 192–216. doi: 10.1016/S0165-0173(97)00021-0

Post, R. M., and Rose, H. (1976). Increasing effects of repetitive cocaine administration in the rat. *Nature* 260, 731–732. doi: 10.1038/260731a0

Qu, S., Ondo, W. G., Zhang, X., Xie, W. J., Pan, T. H., and Le, W. D. (2006). Projections of diencephalic dopamine neurons into the spinal cord in mice. *Exp. Brain Res.* 168, 152–156. doi: 10.1007/s00221-005-0075-1

Reimer, J., Kuhlmann, A., and Müller, T. (2002). Neuroleptic malignant-like syndrome after rapid switch from bromocriptine to pergolide. *Parkinsonism Relat. Disord.* 9, 115–116. doi: 10.1016/S1353-8020(01)00045-1

Richter, D. W., Mironov, S. L., Büsselberg, D., Lalley, P. M., Bischoff, A. M., and Wilken, B. (2000). Respiratory rhythm generation: plasticity of a neuronal network. *Neuroscientist* 6, 181–198. doi: 10.1177/107385840000600309

Ritz, M. C., Lamb, R. J., Goldberg, S. R., and Kuhar, M. J. (1987). Cocaine receptors on dopamine transporters are related to self-administration of cocaine. *Science* 237, 1219–1223. doi: 10.1126/science.2820058

Robinson, T. E., and Berridge, K. C. (1993). The neural basis of drug craving: an incentive-sensitization theory of addiction. *Brain Res. Brain Res. Rev.* 18, 247–291. doi: 10.1016/0165-0173(93)90013-P

Ross, D. L. (1998). Factors associated with excited delirium deaths in police custody. *Mod. Pathol.* 11, 1127–1137.

Rubinsztein, J. S., Fletcher, P. C., Rogers, R. D., Ho, L. W., Aigbirhio, F. I., Paykel, E. S., et al. (2001). Decision making in mania: a PET study. *Brain* 124, 2550–2563. doi: 10.1093/brain/124.12.2550

Ruttenber, A. J., Lawler-Heavner, J., Yin, M., Wetli, C. V., Hearn, W. L., and Mash, D. C. (1997). Fatal excited delirium following cocaine use: epidemiologic findings provide new evidence for mechanisms of cocaine toxicity. *J. Forensic Sci.* 42, 25–31. doi: 10.1520/JFS14064J

Ruttenber, A. J., McAnally, H. B., and Wetli, C. V. (1999). Cocaine-associated rhabdomyolysis and excited delirium: different stages of the same syndrome. *Am. J. Forensic Med. Pathol.* 20, 120–127. doi: 10.1097/00000433-199906000-00003

Samuels, M. A. (2007). The brain-heart connection. *Circulation* 116, 77–84. doi: 10.1161/CIRCULATIONAHA.106.678995

Seeman, P. (2011). All roads to schizophrenia lead to dopamine supersensitivity and elevated dopamine D2 receptors. *CNS Neurosci. Ther.* 17, 118–132. doi: 10.1111/j.1755-5949.2010.00162.x

Sharkey, S. W., Lesser, J. R., and Maron, B. J. (2011). Cardiology patient page. Takotsubo (stress) cardiomyopathy. *Circulation* 124, e460–e462.

Shulack, N. R. (1946). Exhaustion syndrome in excited psychotic patients. *Am. J. Psychiatry* 102, 466–475. doi: 10.1176/ajp.102.4.466

Silverstone, T., Wells, B., and Trenchard, E. (1983). Differential dose–response effects of dexamphetamine sulphate on hunger, arousal and mood in human volunteers. *Psychopharmacology* 79, 242–245. doi: 10.1007/BF00427820

Skagerberg, G., and Lindvall, O. (1985). Organization of diencephalic dopamine neurones projecting to the spinal cord in the rat. *Brain Res.* 342, 340–351. doi: 10.1016/0006-8993(85)91134-5

Staley, J. K., Hearn, W. L., Ruttenber, A. J., Wetli, C. V., and Mash, D. C. (1994). High affinity cocaine recognition sites on the dopamine transporter are elevated in fatal cocaine overdose victims. *J. Pharmacol. Exp. Ther.* 271, 1678–1685.

Staley, J. K., Wetli, C. V., Ruttenber, A. J., Hearn, W. L., and Mash, D. C. (1996). Altered dopaminergic synaptic markers in cocaine psychosis and sudden death. *NIDA Res. Monogr. Ser.* 153, 491.

Stauder, K. H. (1934). Die todliche Katatonie. *Arch. Psychiatr. Nervenkr.* 102, 614–634.

Stephens, B. G., Jentzen, J. M., Karch, S., Wetli, C. V., and Mash, D. C. (2004). National association of medical examiners position paper on the certification of cocaine-related deaths. *Am. J. Forensic Med. Pathol.* 25, 11–13. doi: 10.1097/01.paf.0000114041.70865.24

Stratton, S. J., Rogers, C., Brickett, K., and Gruzinski, G. (2001). Factors associated with sudden death of individuals requiring restraint for excited delirium. *Am. J. Emerg. Med.* 19, 187–191. doi: 10.1053/ajem.2001.22665

Strawn, J. R., Keck, P. E. Jr., and Caroff, S. N. (2007). Neuroleptic malignant syndrome. *Am. J. Psychiatry* 164, 870–876. doi: 10.1176/ajp.2007.164.6.870

Surges, R., Taggart, P., Sander, J. W., and Walker, M. C. (2010). Too long or too short? New insights into abnormal cardiac repolarization in people with chronic epilepsy and its potential role in sudden unexpected death. *Epilepsia* 51, 738–744. doi: 10.1111/j.1528-1167.2010.02571.x

Taggart, P. (2013). Brain-heart interactions and cardiac ventricular arrhythmias. *Neth. Hear. J.* 21, 78–81. doi: 10.1007/s12471-012-0365-8

Taggart, P., Critchley, H., and Lambiase, P. D. (2011). Heart-brain interactions in cardiac arrhythmia. *Heart* 97, 698–708. doi: 10.1136/hrt.2010.209304

Takeuchi, A., Ahern, T. L., and Henderson, S. O. (2011). Excited delirium. *West J. Emerg. Med.* 12, 77–83. Available online at: http://escholarship.org/uc/item/8n55r1kj

Takubo, H., Harada, T., Hashimoto, T., Inaba, Y., Kanazawa, I., Kuno, S., et al. (2003). A collaborative study on the malignant syndrome in Parkinson's disease and related disorders. *Parkinsonism Relat. Disord.* 9(Suppl. 1), S31–S41. doi: 10.1016/S1353-8020(02)00122-0

Ujike, H., and Sato, M. (2004). Clinical features of sensitization to methamphetamine observed inpatients with methamphetamine dependence and psychosis. *Ann. N. Y. Acad. Sci.* 1025, 279–287. doi: 10.1196/annals.1316.035

van Dyck, C. H., Malison, R. T., Jacobsen, L. K., Seibyl, J. P., Staley, J. K., Laruelle, M., et al. (2005). Increased dopamine transporter availability associated with the 9-repeat allele of the SLC6A3 gene. *J. Nucl. Med.* 46, 745–751.

Vilke, G. M., DeBard, M. L., Chan, T. C., Ho, J. D., Dawes, D. M., Hall, C., et al. (2012). Excited Delirium Syndrome (ExDS): defining based on a review of the literature. *J. Emerg. Med.* 43, 897–905. doi: 10.1016/j.jemermed.2011.02.017

Vincent, S. G., Waddell, A. E., Caron, M. G., Walker, J. K. L., and Fisher, J. T. (2007). A murine model of hyperdopaminergic state displays altered respiratory control. *FASEB J.* 21, 1463–1471. doi: 10.1096/fj.06-7248com

Weinberger, D. R., and Kelly, M. J. (1977). Catatonia and malignant syndrome: a possible complication of neuroleptic administration. Report of a case involving haloperidol. *J. Nerv. Ment. Dis.* 165, 263–268. doi: 10.1097/00005053-197710000-00006

Wetli, C. V. (1987). Fatal cocaine intoxication. A review. *Am. J. Forensic Med. Pathol.* 8, 1–2.

Wetli, C. V. (2005). "Excited delirium," in *Encyclopedia of Forensic and Legal Medicine*, Vol. 2, eds R. Byard and J. Payne-James (Glasgow: Elsevier), 276–281.

Wetli, C. V., and Fishbain, D. A. (1985). Cocaine-induced psychosis and sudden death in recreational cocaine users. *J. Forensic Sci.* 30, 873–880. doi: 10.1520/JFS11020J

Wetli, C. V., Mash, D., and Karch, S. B. (1996). Cocaine-associated agitated delirium and the neuroleptic malignant syndrome. *Am. J. Emerg. Med.* 14, 425–428. doi: 10.1016/S0735-6757(96)90066-2

Zahniser, N. R., Gerhardt, G. A., and Cass, W. A. (1995). "Chronic cocaine action on the dopamine transporter," in *The Neurobiology of Cocaine: Cellular and Molecular Mechanisms*, ed R. L. Jr. Hammer (Boca Raton, FL: CRC Press), 181–197.

Zahniser, N. R., Gerhardt, G. A., Hoffman, A. F., and Lupica, C. R. (1998). "Voltage-dependency of the dopamine transporter in rat brain," in *Advances in Pharmacology*, Vol. 42. eds D. Goldstein, G.Eisenhofer, and R. McCarty (San Diego, CA: Academic Press), 195–198

Zapata, A., Chefer, V. I., Ator, R., Shippenberg, T. S., and Rocha, B. A. (2003). Behavioural sensitization and enhanced dopamine response in the nucleus accumbens after intravenous cocaine self-administration in mice. *Eur. J. Neurosci.* 17, 590–596. doi: 10.1046/j.1460-9568.2003.02491.x

Conflict of Interest Statement: The author declares that the research was conducted in the absence of any commercial or financial relationships that could be construed as a potential conflict of interest.

frontiers in Physiology

ORIGINAL RESEARCH
published: 06 December 2016
doi: 10.3389/fphys.2016.00614

The Use of Berlin Heart EXCOR VAD in Children Less than 10 kg: A Single Center Experience

*Arianna Di Molfetta, Fabrizio Gandolfo, Sergio Filippelli, Gianluigi Perri, Luca Di Chiara, Roberta Iacobelli, Rachele Adorisio, Isabella Favia, Alessandra Rizza, Giuseppina Testa, Matteo Di Nardo and Antonio Amodeo **

Department of Pediatric Cardiology and Cardiac Surgery, Pediatric Hospital Bambino Gesù, Rome, Italy

Objective: Despite the improvement in ventricular assist device (VAD) therapy in adults and in adolescents, in infant population only Berlin Heart EXCOR (BHE) is licensed as long term VAD to bridge children to Heart Transplantation (HTx). Particularly demanding in terms of morbidity and mortality are smallest patients namely the ones implanted in the first year of life or with a lower body surface area. This work aims at retrospective reviewing a single center experience in using BHE in children with a body weight under 10 kg.

Methods: Data of all pediatric patients under 10 kg undergoing BHE implantation in our institution from March 2002 to March 2016 were retrospectively reviewed.

Results: Of the 30 patients enrolled in the study, 53% were male, 87% were affected by a dilated cardiomyopathy with an average weight and age at the implantation of 6.75 ± 2.16 Kg and 11.57 ± 10.12 months, respectively. Three patients (10%) required a BIVAD implantation. After the implantation, 7 patients (23%) required re-intervention for bleeding and 9 patients (30%) experienced BHE cannulas infection. A total of 56 BHE pump were changed for thrombus formation (1.86 BHE pump for patient). The average duration of VAD support was 132.8 ± 94.4 days. Twenty patients (67%) were successfully transplanted and 10 patients (33%) died: 7 for major neurological complication and 3 for sepsis.

Conclusion: Mechanical support in smaller children with end stage heart failure is an effective strategy for bridging patients to HTx. The need for BIVAD was relegated, in the last years, only to restrictive cardiomiopathy. Further efforts are required in small infants to improve anticoagulation strategy to reduce neurological events and BHE pump changes.

Keywords: pediatric VAD, low weight LVAD, Berlin Heart

OPEN ACCESS

Edited by:
Antonio L'Abbate, Sant'Anna School of Advanced Studies, Italy

Reviewed by:
Valter Luis Pereira Junior, Universidade Camilo Castelo Branco, Brazil
Gabriela Fischer, Universidade Federal de Santa Catarina, Brazil

****Correspondence:***
Antonio Amodeo
antonio.amodeo@opbg.net

Specialty section:
This article was submitted to Integrative Physiology, a section of the journal Frontiers in Physiology

Received: *28 August 2016*
Accepted: *24 November 2016*
Published: *06 December 2016*

Citation:
Di Molfetta A, Gandolfo F, Filippelli S, Perri G, Di Chiara L, Iacobelli R, Adorisio R, Favia I, Rizza A, Testa G, Di Nardo M and Amodeo A (2016) The Use of Berlin Heart EXCOR VAD in Children Less than 10 kg: A Single Center Experience. Front. Physiol. 7:614. doi: 10.3389/fphys.2016.00614

INTRODUCTION

The definitive treatment for the end stage pediatric heart failure is the orthotopic heart transplantation (OHTx). However, because of the lack of organ donors, especially in very small children, the use of ventricular assist device (VAD) is a validated therapy to bridge patients to the OHTx with a success rate up to 84% (Ibrahim et al., 2000; Reinhartz et al., 2003; Chang and McKenzie, 2005; Stiller et al., 2005; Hetzer et al., 2006; Gandhi et al., 2008; Brancaccio et al., 2010,

2013; Potapov et al., 2011; Almond et al., 2013; Miera et al., 2014; Kirklin, 2015; Mascio, 2015; Sandica et al., 2016).

The use of left VADs (LVAD) could successfully support patients till the OHTx, increasing the cardiac output (CO), unloading the left ventricle (LV) and decreasing the left atrial pressure and the pulmonary arterial pressure. The LVAD decrease the LV volumes and the LV work because of the flow distribution between the native LV and the LVAD (Barbone et al., 2001). In fact, in the presence of the LVAD, the total cardiac output is the sum of the LV output and the LVAD output. Increasing the LVAD cardiac output (increasing the LVAD speed in the continuous flow LVAD or increasing the pump rate in pulsatility flow LVAD) it is possible to obtain an increment of the total cardiac output (untill a determined plateau) and a higher unloading of the LV with lower LV volumes, lower left atrial pressure, lower pulmonary pressure and lower LV output. In the case of total support, all the cardiac output is totally provided by the LVAD and the aortic valve remains closed. This condition is usually avoided to permit to the LV at least a slight ejection and to the aortic valve to open at least every three cardiac cycle.

The effects of the LVAD on the right ventricular function is controversial. In fact, one of the major complications in LVAD patients is the right ventricular (RV) failure with an incidence among 13–44% in adults and an incidence of 42% in children (Chen et al., 1996; Kukucka et al., 2011; Saraiva Santos et al., 2012; Karimova et al., 2014). Different explanations about the increased risk of the RV failure in LVAD patients were proposed:

- RV work increase due to RV venous return increase thanks to the LVAD because the RV and the LV work are in series. The RV overload is proportional to the LVAD contribution (Mandarino et al., 1992; Omoto et al., 2002),
- the leftward shift of the interventricular septum after the LVAD implantation could decrease the support given by the septum to the RV contraction and the leftward shift is proportional to the LVAD contribution (Hendry et al., 1994; Omoto et al., 2002).

On the contrary, it has been considered that the LVAD could decrease the RV afterload, decreasing the pulmonary arterial pressure, possibly leading to a better RV pump functioning (**?**). In literature, there are different opinions and several authors performed also animal experiments to study the interventricular interaction during LVAD assistance (Kawai et al., 1992; Mandarino et al., 1992; Morita et al., 1992; Hendry et al., 1994; Chen et al., 1996; Barbone et al., 2001; Omoto et al., 2002; de Jonge et al., 2005; Kukucka et al., 2011; Saraiva Santos et al., 2012; Umeki et al., 2012; Arakawa et al., 2014; Karimova et al., 2014).

Di Molfetta et al. (2016) summarized with a simulation the effects of the LVAD implantation and the effects of the increased LVAD contribution using a lumped parameter model (**Figure 1**). Increasing the LVAD contribution a decrement of the LV preload and volumes and an increment of the arterial systemic mean pressure can be obtained together with an increment of the RV preload and RV volumes and a decrement of the pulmonary mean pressure. Finally, a decrement of the LV work and an increment of RV work are obtained increasing the pump contribution.

Analyzing the infant population, only the Berlin Heart EXCOR (BHE; Berlin Heart, Berlin Heart AG, Berlin, Germany) is licensed as long term VAD to bridge children to OHTx (Ibrahim et al., 2000; Reinhartz et al., 2003; Chang and McKenzie, 2005; Stiller et al., 2005; Hetzer et al., 2006; Gandhi et al., 2008; Brancaccio et al., 2010, 2013; Potapov et al., 2011; Almond et al., 2013; Miera et al., 2014). The smallest patients are particularly demanding in terms of morbidity and mortality (Ibrahim et al., 2000; Reinhartz et al., 2003; Chang and McKenzie, 2005; Stiller et al., 2005; Hetzer et al., 2006; Gandhi et al., 2008; Brancaccio et al., 2010, 2013; Potapov et al., 2011; Almond et al., 2013; Miera et al., 2014) especially now that the LVAD staying is increasing over time. In particular, small body surface area, BHE size mismatch and younger age seems to be associated with an increased risk of thromboembolic complications (Almond et al., 2013; Miera et al., 2014).

In a recent study, Conway et al. reported about the outcome of a multicenter study on 97 pediatric patients under 10 kg undergoing Berlin Heart EXCOR VAD. In their study, the median LVAD stay was 26 days with a survival to heart transplantation less than 60% (Conway et al., 2015).

On the basis of these considerations, the aim of this study is to retrospectively review our single-center experience on the use of BHE in children under 10 Kg.

MATERIALS AND METHODS

Patients' Data Collection

Data of all pediatric patients under 10 kg undergoing BHE implantation in our institution from March 2002 to March 2016 were retrospectively reviewed including:

- *Before the implantation*: gender, diagnosis, age at the implantation, weight at the implantation, previous surgery, comorbidities, requirement of ECMO;
- *During the implantation*: concomitant surgical procedure, requirement of biventricular assistance using two BHE, neurological complication, bleeding, cannulas infections, sepsis; BHE pump changes, length of VAD staying, clinical outcome (OHTx, death, heart recovery, still on VAD), and cause of death during the assistance;

Informed consent for the BHE implantation and the divulgation of clinical data was obtained by all patients' parents. The protocol was approved by the ethical board of our hospital. The protocol adheres to the principle expressed in the Declaration of Helsinki.

Surgical Procedure

All patients underwent BHE VAD implantation. The BHE consists of a paracorporeal, pneumatically driven, polyurethane blood pump with a multilayer flexible membrane separating the blood from the air chamber. Silicon cannulae connect the blood pump to the patient, and tri-leaflets inflow and outflow valves prevent blood reflux. All surface in contact with blood are heparin-coated. Each pump is driven by a pulsatile electro-pneumatic system. All BHE implantation were

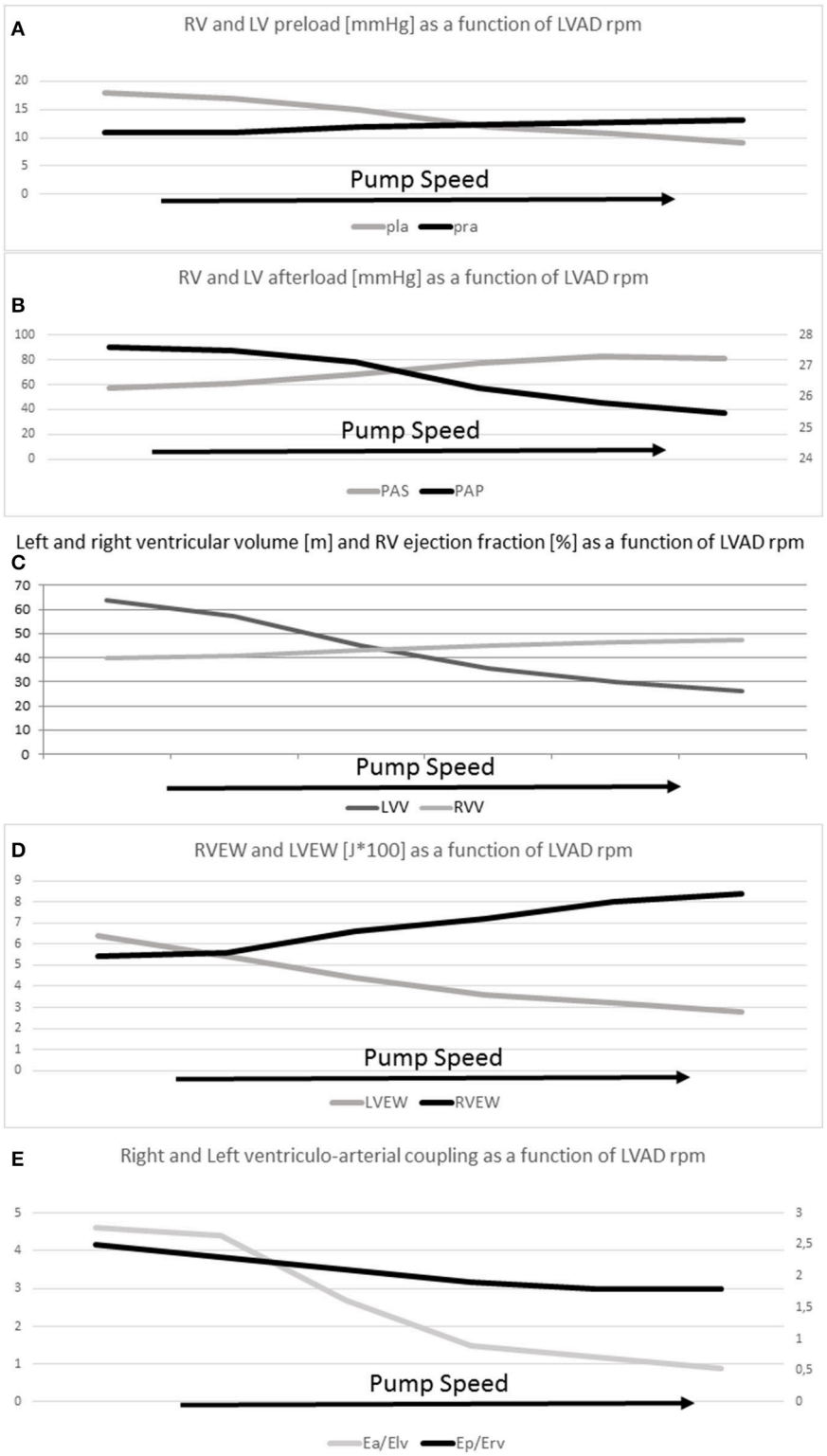

FIGURE 1 | (A) RV (pra) and LV (pla) preload (mmHg), **(B)** RV (Pap) and LV (Pas) afterload (mmHg), **(C)** RV (RVV) and LV (LVV) average volumes (ml), **(D)** RV (RVEW) and LV (LVEW) external work (J*100), **(E)** RV (Ep/Erv) and LV (Ea/Elv) ventriculo-arterial coupling as a function of LVAD rate.

performed in a full median sternotomy and mild hypothermic cardiopulmonary bypass. The heart was kept beating throughout the procedure except in patients requiring the interatrial communication closure where ventricular fibrillation was used. Inflow cannulation for the left ventricular assist device (LVAD) was preferentially achieved through the left ventricular apex or, alternatively, through the left atrium (before 2007). The pump size was chosen according to the BHE indications (Miera et al., 2014). The VAD rate was set to assure an adequate perfusion ranging from 100 ml/kg/min to 200 ml/kg/min. All the other VAD parameters were set with the aim of assuring a full-empty full-fill operating modality and with the aim of assuring the aortic valve opening at least every three cardiac cycle.

Anticoagulation Strategy and Patients Monitoring

All patients were routinely evaluated performing one echocardiography every week. Concerning the anticoagulation strategy, in the first post-operative day, the unfractioned heparin was started at initial dose of 15 IU/Kg/h every 12 h and increased after 6 hours at therapeutic dose of 28 IU/Kg/h to obtain a PTTs between 1.5 and 2.5 times the basal value with a correspective anti Xa between 0.35 and 0.5. After 1 week, if the active bleeding was absent, the hemodynamic status was stable and renal function was normal, low molecular weight heparin (LMWH) was introduced at a starting dose of 150 IU/kg with a target anti Xa of 0.6–1.2 IU/ml. The anti-aggregation therapy was modulated by platelet mapping, between 2nd and 4th POD if bleeding was stopped. Dypiridamole was started at 1 mg/kg/day at the POD 4 while the aspirin was started at 1 mg/kg/day divided in 2 doses at the POD 7, when chest drain are removed. Oral anticoagulant drugs (warfarin) was considered in children older than 12 months when oral or enteral feeding is optimized. Initial loading dose was 0.2 mg/Kg/die (maximum dose of 5 mg/die) and target INR was between 2.7 and 3.5.

Statistical Analysis

Continuous variables are expressed as mean values and standard deviation or as median values, where appropiate. Survival analysis is performed by Kaplan-Meyer curves and log rank test (Mentel-Cox). Hazard ratio is estimated by Mentel-Haenszel test. Statistical analysis was performed using the commercial software MedCalc.

RESULTS

Baseline Data

A total of 30 patients under 10 kg were implanted from 2002 to 2016 in our institution. Sixteen children were male (53%) with a mean weight at the implantation of 6.75 ± 2.16 Kg and an average age at the implantation of 11.57 ± 10.12 months. Most of the patients (25/30, 87%) were affected by a dilated cardiomyopathy (secondary to myocarditis in 4 cases and with left ventricular non compaction in 3 cases), 2 (6.5%) patients were affected by a restrictive cardiomyopathy, 1 patient developed heart failure post cardiotomy and 2 (6.5%) patients had a failing univentricular heart physiology (Reinhartz et al., 2003). Before the VAD implantation, one patient underwent surgery for a supravalvular mitral ring and developed heart failure post cardiotomy and two patients underwent Glenn procedure. Before the BHE implantation, 8 patients (27%) were mechanically ventilated and 3 patients (10%) were receiving ECMO for cardiorespiratory failure (**Table 1**).

VAD Implantation

Inflow cannulation for the LVAD was achieved through the left ventricular apex in the 27 (90%) children and through the left atrium in three. From August 2007, left atrial cannulation was dismissed in favor of left ventricular apical cannulation. An isolated LVAD was used in 27 (90%) patients and a BiVAD in three. All the BiVAD were implanted before 2007. Eight patients (27%) underwent concomitant atrial septal defect closure, while in one patient a ductus arteriosus was closed during the VAD implantation.

Postoperative

Before 2007, two patients underwent percutaneous atrial septal defect closure with an Amplatzer device after the LVAD implantation for severe desaturation (Brancaccio et al., 2010). Seven patients (23%) required re-intervention for bleeding after the LVAD implantation and 9 patients (30%) experienced BHE cannulas infection. A total of 56 BHE pumps were changed along all the studied period for thrombus formation (1.86 BHE pumps for patient). Two LVAD patients underwent BHE pump upgrading from 10 ml to 15 ml because of patients weight increment after April 2013, when the 15 ml BHE became available.

Outcome

The average duration of VAD support was 132.8 ± 94.4 days. Then, 20 patients (67%) were successfully transplanted and 10 patients (33%) died. Of these 10 patients, 7 died for major neurological complication and 3 for sepsis (**Table 2**).

TABLE 1 | Patients Demographics.

Variables	Data
Male/Female	16/14
Age at implant [months]	11.57 ± 10.12
Weight [Kg]	6.75 ± 2.16
DIAGNOSIS	
DCM	25 (83%)
RCM	2 (7%)
Failing UVH physiology	2 (7%)
After cardiotomy	1 (3%)

DCM, Dilatative Cardiomyopathy; RCM, Restrictive Cardiomyopathy; UVH, Univentricular Heart; VAD, Ventricular Assist Device.

TABLE 2 | Outcomes on VAD.

Outcome	No. (%) Tot No 30 patients
Days of assistance	132.8 ± 94.4
OHTx	20 (67%)
Death on VAD	10 (33%)
Fatal neurological complications	7 (23%)
Fatal sepsis	3 (10%)
Cannulae infection	9 (30%)
Overall no of pump change	56 (1.86/pts)
Bleeding requiring surgery	7 (23%)

DISCUSSION

The use of BHE could successfully bridge pediatric patients till the OHTx, but the management of small patients is especially challenging. In fact, small body surface area seems to be associated with an increased risk of thromboembolic complications during VAD assistance and increased mortality as reported by Almond et al. (2013). In accordance with this consideration, Reinhartz et al. (2003) evidenced that an oversized device, which is simpler in smaller patients, could lead to an increased risk of thromboembolisms because of the stasis into the devices or systemic hypertension due to large stroke work. Similarly, Miera et al. (2014) demonstrated the influence of the BHE size in relation to patients weight on the clinical outcome. In fact, in their study Miera et al. evidenced that a large pump size in relation to body surface area is an independent risk factor for the occurrence of thromboembolic events (Miera et al., 2014). Moreover, they evidenced that younger age and smaller body surface area patients showed a trend of increased risk of thromboembolic events. In their work, Stiller et al. (2005) reported about the BHE implantation in 18 children less than 1 year underlying that the small children could be successfully bridged to OHTx, but the intensive care management and the anticoagulation strategy should be optimized to improve the outcome in terms of mobility and mortality. Gandhi et al. (2008) reported their experience on the use of BIVAD in 9 small children with an average weight of 9.4 kg (3 to 38 kg). Patients were supported for 35 days (1 to 77) and then 8 patients were successfully transplanted. It should be underlined that, as reported by Hetzer et al. (Potapov et al., 2011), the length of VAD staying is increasing over time and the management of small patients to achive long term event free VAD support is still challenging (Potapov et al., 2011). Finally, Conway et al reported about the outcome of a multicenter study on 97 pediatric patients under 10 kg undergoing Berlin Heart EXCOR VAD. In their study, the median LVAD stay was 26 days with a survival to heart transplantation less than 60% (Conway et al., 2015).

In our study, we reported our experience on the use of BHE in 30 patients under 10 kg. Patients were assisted for a median time of 132.8 ± 94.4 days that is a significantly longer time compared to the experiences reported in literature (Almond et al., 2013; Conway et al., 2015). Despite a longer period of support the complications and the outcomes of our population are comparable to the complications and the outcomes reported in literature. Sixty seven percentage of patients were successfully transplanted, 23% of patients required re-intervention for bleeding, 23% of patients experienced major neurological complication and 30% experienced BHE cannulas infection.

In conclusion, the use of BHE in small children is becoming of common use in recent years. Longer support time of several months requires a careful management of these fragile patients especially in terms of coagulation and infections. Good results in short and long term are possible, encouraging the use of this strategy as bridge to OHTx.

AUTHOR CONTRIBUTIONS

FG, Clinical data; AD, Statistical analysis and clinical data; SF, Surgical procedure analysis; LD, Post operative data analysis; RI, Pre-op Echo analysis; RA, Preoperative analysis data; GP, Post-op Echo analysis; MD, Post-op Intensice care analysis; IF, Anticoagulation protocol; AR, Anticoagulant data analysis; GT, Post operative data analysis; AA, Paper Overview.

REFERENCES

Almond, C. S., Morales, D. L., and Blackstone, E. H. (2013). Berlin Heart EXCOR pediatric ventricular assist device for bridge to heart transplantation in US children. *Circulation* 127, 1702–1711. doi: 10.1161/CIRCULATIONAHA.112.000685

Arakawa, M., Nishimura, T., Takewa, Y., Umeki, A., Ando, M., Kishimoto, Y., et al. (2014). Novel control system to prevent right ventricular failure induced by rotary blood pump. *J. Artif. Organs* 17, 135–141. doi: 10.1007/s10047-014-0757-1

Barbone, A., Holmes, J. W., Heerdt, M., The, A. H. S., Naka, Y., Joshi, N., et al. (2001). Comparison of right and left ventricular responses to left ventricular assist device support in patients with severe heart failure. A primary role of mechanical unloading underlying reverse remodeling. *Circulation* 104, 670–675. doi: 10.1161/hc3101.093903

Brancaccio, G., Amodeo, A., Ricci, Z., Morelli, S., Gagliardi, M. G., Iacobelli, R., et al. (2010). Mechanical assist device as a bridge to heart transplantation in children less than 10 kilograms. *Ann. Thorac. Surg.* 90, 58–62. doi: 10.1016/j.athoracsur.2010.03.056

Brancaccio, G., Gandolfo, G., Carotti, A., and Amodeo, A. (2013). Ventricular assist device in univentricular heart physiology. *Interact Cardiovasc. Thorac. Surg.* 16, 568–569. doi: 10.1093/icvts/ivs559

Chang, A. C., and McKenzie, E. D. (2005). Mechanical cardiopulmonary support in children and young adults: extracorporeal membrane oxygenation, ventricular assist devices, and long-term support devices. *Pediatr. Cardiol.* 26, 2–28. doi: 10.1007/s00246-004-0715-4

Chen, J. M., Levin, H. R., Rose, E. A., Addonizio, L. J., Landry, D. W., Sistino, J. J., et al. (1996). Experience with right ventricular assist devices for perioperative right-sided circulatory failure. *Ann. Thorac. Surg.* 61, 305–310. doi: 10.1016/0003-4975(95)01010-6

Conway, J., St Louis, J., Morales, D. L., Law, S., Tjossem, C., and Humpl, T. (2015). Delineating survival outcomes in children <10 kg bridged to transplant or recovery with the Berlin Heart EXCOR ventricular assist device. *JACC Heart Fail.* 3, 70–77. doi: 10.1016/j.jchf.2014.07.011

de Jonge, N., Lahpor, J. R., van Wichen, D. F., Kirkels, H., Gmelig-Meyling, F. H., van den Tweel, J. G., et al. (2005). Similar left and right ventricular sarcomere structure after support with a left ventricular assist device suggests the utility of right ventricular biopsies to monitor left ventricular reverse remodeling. *Int. J. Cardiol.* 98, 465–470. doi: 10.1016/j.ijcard.2003.12.020

Di Molfetta, A., Ferrari, G., Iacobelli, R., Fresiello, L., Pilati, M., Toscano, A., et al. (2016). Acute biventricular interaction in pediatric patients with continuous or pulsatile flow LVAD: a simulation study. *ASAIO J.* 62, 591–599. doi: 10.1097/mat.0000000000000396

Gandhi, S. K., Huddleston, C. B., Balzer, D. T., Epstein, D. J., Boschert, T. A., and Canter, C. E. (2008). Biventricular assist devices as a bridge to heart transplantation in small children. *Circulation* 118(14 Suppl.), S89–S93. doi: 10.1161/CIRCULATIONAHA.107.754002

Hendry, P. J., Ascah, K. J., Rajagopalan, K., and Calvin, J. E. (1994). Does septal position affect right ventricular function during left ventricular assist in an experimental porcine model? *Circulation* 90(5 Pt 2), II353–II358.

Hetzer, R., Potapov, E. V., Stiller, B., Weng, Y., Hübler, M., Lemmer, J., et al. (2006). Improvement in survival after mechanical circulatory support with pneumatic pulsatile ventricular assist devices in pediatric patients. *Ann. Thorac. Surg.* 82, 917–924; discussion 924–5. doi: 10.1016/j.athoracsur.2006.03.065

Ibrahim, A. E., Duncan, B. W., Blume, E. D., and Jonas, R. A. (2000). Long-term follow-up of pediatric cardiac patients requiring mechanical circulatory support. *Ann. Thorac. Surg.* 69, 186–192. doi: 10.1016/S0003-4975(99)01194-7

Karimova, A., Pockett, C. R., Lasuen, N., Dedieu, N., Rutledge, J., Fenton, M., et al. (2014). Right ventricular dysfunction in children supported with pulsatile ventricular assist devices. *J. Thorac. Cardiovasc. Surg.* 147, 1691–1697. doi: 10.1016/j.jtcvs.2013.11.012

Kawai, A., Kormos, R. L., Mandarino, W. A., Morita, S., Deneault, L. G., Gasior, T. A., et al. (1992). Differential regional function of the right ventricle during the use of a left ventricular assist device. *ASAIO J.* 38, M676–M678. doi: 10.1097/00002480-199207000-00123

Kirklin, J. K. (2015). Advances in mechanical assist devices and artificial hearts for children. *Curr. Opin. Pediatr.* 27, 597–603. doi: 10.1097/MOP.0000000000000273

Kukucka, M., Stepanenko, A., Potapov, E., Krabatsch, T., Redlin, M., Mladenow, A., et al. (2011). Right-to-left ventricular end-diastolic diameter ratio and prediction of right ventricular failure with continuous-flow left ventricular assist devices. *J. Heart Lung Transplant.* 30, 64–69. doi: 10.1016/j.healun.2010.09.006

Mandarino, W. A., Morita, S., Kormos, R. L., Kawai, A., Deneaut, L. G., Gasior, T. A., et al. (1992). Quantitation of right ventricular shape changes after left ventricular assist device implantation. *ASAIO J.* 38, M228–M231 doi: 10.1097/00002480-199207000-00026

Mascio, C. E. (2015). The use of ventricular assist device support in children: the state of the art. *Artif. Organs* 39, 14–20. doi: 10.1111/aor.12439

Miera, O., Schmitt, K. R., Delmo-Walter, E., Ovroutski, S., Hetzer, R., and Berger, F. (2014). Pump size of Berlin Heart EXCOR pediatric device influences clinical outcome in children. *J. Heart Lung Transplant.* 33, 816–821. doi: 10.1016/j.healun.2014.03.007

Morita, S., Kormos, R. L., Mandarino, W. A., Eishi, K., Kawai, A., Gasior, T. A., et al. (1992). Right ventricular/arterial coupling in the patient with left ventricular assistance. *Circulation* 86(5SI), II316–II3125

Omoto, T., Tanabe, H., LaRia, P. J., Guerrero, J., and Vlahakes, G. J. (2002). Right ventricular performance during left ventricular unloading conditions: the contribution of the right ventricular free wall. *Thorac. Cardiovasc. Surg.* 50, 16–20. doi: 10.1055/s-2002-20158

Potapov, E., Stepanenko, A., Krabatsch, T., and Hetzer, R. (2011). Managing long term complication of left ventricular assist device therapy. *Curr. Opin. Cardiol.* 26, 237–244. doi: 10.1097/HCO.0b013e328345af80

Reinhartz, O., Coopeland, J. G., and Farrar, D. J. (2003). Thoratec ventricular assist device in children less than 1.3m^2 body surface area. *ASAIO J.* 49, 727–730. doi: 10.1097/01.MAT.0000093965.33300.83

Sandica, E., Blanz, U., Mime, L. B., Schultz-Kaizler, U., Kececioglu, D., Haas, N., et al. (2016). Long-term mechanical circulatory support in pediatric patients. *Artif. Organs* 40, 225–232. doi: 10.1111/aor.12552

Saraiva Santos, L. A., Benicio, A., de Mattos Ewaldo, J., Benvenutti, L. A., Cestari, I. A., Groppo Stolf, N. A., et al. (2012). Cavo-pulmonary anastomosis associated with left ventricular in comparison with biventricular circulatory support in acute heart failure. *Rev. Bras. Cir. Cardiovasc.* 27, 552–561. doi: 10.5935/1678-9741.20120097

Stiller, B., Weng, Y., Hubler, M., Lemmer, J., Nagdyman, N., Redlin, M., et al. (2005). Pneumatic pulsatile ventricular assist devices in children under 1 year of age. *Eur. J. Cardiothorac. Surg.* 28, 234–239. doi: 10.1016/j.ejcts.2005.04.023

Umeki, A., Nishimura, T., Ando, M., Takewa, Y. Yamazaki, K., Kyo, S., et al. (2012). Alteration of LV end diastolic volume by controlling the power of the continuous flow LVAD, so it synchronized with cardiac beat: development of a native heart load control system. *J. Artif. Organs* 15, 128–133. doi: 10.1007/s10047-011-0615-3

Conflict of Interest Statement: The authors declare that the research was conducted in the absence of any commercial or financial relationships that could be construed as a potential conflict of interest.

frontiers in Physiology

REVIEW
published: 09 May 2017
doi: 10.3389/fphys.2017.00131

The Total Artificial Heart in End-Stage Congenital Heart Disease

Chet R. Villa and David L. S. Morales*

Cincinnati Children's Hospital Medical Center, Heart Institute, Cincinnati, OH, USA

The development of durable ventricular assist devices (VADs) has improved mortality rates and quality of life in patients with end stage heart failure. While the use of VADs has increased dramatically in recent years, there is limited experience with VAD implantation in patients with complex congenital heart disease (CHD), despite the fact that the number of patients with end stage CHD has grown due to improvements in surgical and medical care. VAD use has been limited in patients with CHD and end stage heart failure due to anatomic (systemic right ventricle, single ventricle, surgically altered anatomy, valve dysfunction, etc.) and physiologic constraints (diastolic dysfunction). The total artificial heart (TAH), which has right and left sided pumps that can be arranged in a variety of orientations, can accommodate the anatomic variation present in CHD patients. This review provides an overview of the potential use of the TAH in patients with CHD.

Keywords: total artificial heart, congenital heart disease, mechanical circulatory support, pediatrics, bridge to transplantation

OPEN ACCESS

Edited by:
Maria Giovanna Trivella, Consiglio Nazionale Delle Ricerche (CNR), Italy

Reviewed by:
Georges Nemer, American University of Beirut, Lebanon
Juan Del Cañizo, Universidad Complutense de Madrid, Spain

****Correspondence:***
Chet R. Villa
chet.villa@cchmc.org

Specialty section:
This article was submitted to Integrative Physiology, a section of the journal Frontiers in Physiology

Received: *28 February 2016*
Accepted: *21 February 2017*
Published: *09 May 2017*

Citation:
Villa CR and Morales DLS (2017) The Total Artificial Heart in End-Stage Congenital Heart Disease. Front. Physiol. 8:131. doi: 10.3389/fphys.2017.00131

BACKGROUND

Ventricular assist devices (VADs) have been shown to improve mortality and quality of life in adults with refractory heart failure. This has led to a dramatic increase in VAD use among adults over the last decade (Kirklin et al., 2014). Recent reports have shown a dramatic increase in VAD use in children as well (Almond et al., 2013; Villa et al., 2017) as ∼20% of pediatric patients are bridged to transplant with a VAD in the current era (Dipchand et al., 2014). These trends in VAD utilization have in turn driven improvements in waitlist mortality for both children (Zafar et al., 2015a) and adults (Emin et al., 2013). Despite the improvement in survival and quality of life brought about by improvements in VAD technology, patients with congenital heart disease (CHD) are less likely to receive a VAD while on the waitlist and are more likely to die while awaiting transplantation (Gelow et al., 2013; Zafar et al., 2015a). The need for improved support options for patients with CHD is significant as ∼45% of pediatric heart transplant recipients have CHD (Dipchand et al., 2014) and the number of adults with CHD who experience heart failure (Khairy et al., 2010) or require transplant (Lund et al., 2014) is continuing to grow. Historically, VAD use has not been extended to patients with congenital disease due to multiple factors including patient size, anatomic complexity, multi-organ dysfunction (Kiesewetter et al., 2007; Dimopoulos et al., 2008; Ridderbos et al., 2015) and complex physiology including both systolic (Piran et al., 2002) and diastolic dysfunction (Gewillig et al., 1992). Data is starting to be collected regarding the use of VADs in patients with CHD, however, the current literature is limited to single center case series/case reports. This review will discuss the physiology underlying end stage heart disease with a focus on the potential use of the total artificial heart (TAH).

A few proprietary artificial heart devices have been developed including the Syncardia TAH (Syncardia, Tucson, AZ, USA), AbioCor (Abiomed, Danvers, Massachusetts, USA), and CARMAT (Carmat, Velizy, France). The history of these devices and their clinical use has recently been reviewed (Gerosa et al., 2014). Among the devices listed, the Syncardia (TAH) is the only device currently in use. The CARMAT is currently undergoing feasibility studies, however, data has been limited to a handful of patients thus far (Carpentier et al., 2015). There is also no data on the use of the AbioCor (Dowling et al., 2004) or CARMAT in patients with CHD. Given the paucity of data regarding the use of the AbioCor and CARMAT devices, this review will focus on the use of the Syncardia TAH.

The (TAH) was developed for use in adults with end-stage heart failure who had a contraindication to LVAD or biventricular VAD (BiVAD) (Copeland et al., 2004) including valve insufficiency, intractable arrhythmias and ventricular clot. Device use has subsequently been expanded to younger patients (Leprince et al., 2005; Ryan et al., 2015) and patients with CHD (Morales et al., 2012; Kirsch et al., 2013; Rossano et al., 2014; Ryan et al., 2015). The use of the TAH for complex CHD is potentially paradigm shifting for selected patients. Congenital heart patients with end-stage heart failure who have residual lesions (i.e., VSD, severe semilunar valve insufficiency, stenotic right ventricular to pulmonary artery conduit) that would have to be addressed in order to place a VAD or BiVAD clearly have a different mortality and morbidity profile when compared to patients with cardiomyopathy alone (Zafar et al., 2015b). It is in these patients that the TAH may simplify and optimize support rather than placing a VAD or BiVAD with concurrent cardiac procedures (i.e., VSD closure, conduit revision, aortic valve replacement). The current published experience with the TAH in CHD is listed in **Table 1**. The range of physiologies (single ventricle, two ventricle) and anatomic abnormalities represented shows the potential for the TAH to address multiple anatomic considerations with implantation alone. The TAH also has the ability to markedly improve patient symptoms and end organ dysfunction in anatomies/physiologies where medical management has shown limited or no benefit (i.e., diastolic dysfunction, CHD (Kouatli et al., 1997; Shaddy et al., 2007; van der Bom et al., 2013, etc.) and VAD options are limited (**Table 2**).

CONGENITAL HEART DISEASE IN THE TWO VENTRICLE CIRCULATION

Patients with a systemic right ventricle due to transposition of the great arteries (TGA) or congenitally corrected transposition of the great arteries (ccTGA) carry a life-long risk of systemic right ventricular dysfunction (Graham et al., 2000; Vejlstrup et al., 2015) and heart failure. The development of systemic ventricular dysfunction is reflected in the growing number of case series describing the outcome of VAD support for these patients (Joyce et al., 2010; Peng et al., 2014; Maly et al., 2015). While most centers have described morphologic right (systemic) ventricular support alone, the majority of patients will have coincident morphologic left ventricular (sub-pulmonic) dysfunction at time of surgery (Peng et al., 2014) suggesting these patients may be at risk for left (sub-pulmonic) ventricular failure and the need for possible ventricular mechanical support (Maly et al., 2015). The complexity of VAD support in these patients is further increased by the potential for cannula obstruction due to right ventricular trabeculations/moderator band (Agusala et al., 2010; Joyce et al., 2010) and the frequency of clinically significant tricuspid regurgitation in these patients (Graham et al., 2000; Peng et al., 2014).

The use of a TAH would alleviate the concerns mentioned above and also provide configuration flexibility, which is important to accommodate the variety of anatomic considerations in these patients. This was demonstrated by Morales et al. (2012) in a patient with ccTGA who presented with multi-system organ failure in the setting of severe biventricular dysfunction, severe aortic insufficiency and obstruction of a left-ventricle to pulmonary artery conduit. A TAH was implanted due to the multiple anatomic considerations noted above. He was discharged home within a month and was bridged to transplant during his sixth months of support. A recent report also described the use of a TAH in a patient with dextrocardia and ccTGA with ventricular septal defect, pulmonary stenosis and Ebsteinoid tricuspid valve who had recently undergone a Senning-Rastelli procedure due to pulmonary hypertension (Si et al., 2015). The patient had severe biventricular diastolic dysfunction and required extracorporeal membrane oxygenation (ECMO) support on post-operative day (POD) 1. The patient

TABLE 1 | Clinical experience with the total artificial heart (TAH) in patients in congenital heart disease.

References	Anatomy	Duration of support	Surgical considerations with TAH implantation	Outcome
Morales et al., 2012	Dextrocardia, {S,L,L} ccTGA status post Rastelli with severe aortic insufficiency and obstruction of left ventricle-pulmonary artery conduit	160 days	Separation of right and left pumps with parallel orientation	Bridged to transplantation
Rossano et al., 2014	Pulmonary atresia with intact ventricular septum status post Fontan	61 days	Creation of "neo-right atrium"	Bridged to transplantation
Si et al., 2015	Dextrocardia, {S,L,L} ccTGA, ventricular septal defect, pulmonary stenosis and Ebsteinoid tricuspid valve status post Senning-Rastelli with severe tricuspid regurgitation	8 days	Reversal of Senning	Bridged to transplantation

ccTGA, congenitally corrected transposition of the great arteries.

TABLE 2 | Potential indications for total artificial heart (TAH).

Failing congenital heart disease
Residual anatomic lesions with coexisting cardiac dysfunction
Fontan (Rossano et al., 2014)
Systemic right ventricular failure (Morales et al., 2012)
Transposition of the great arteries (TGA), status post Mustard or Senning
Congenitally corrected transposition of the great arteries (ccTGA)
Alternate clinical scenarios (Copeland et al., 2004)
Allograft failure
Biventricular heart failure
Cardiac tumor
Chronic right ventricular failure with existing left ventricular assist device
Intractable arrhythmias
Active malignancy receiving cardiotoxic therapies
Restrictive cardiomyopathy
Ventricular clot

could not be weaned from ECMO and underwent TAH with Senning pathway reversal. He tolerated the procedure well and underwent heart transplant on POD day 8, followed by hospital discharge within a month.

FAILING FONTAN

Much has been written about the long term outcomes of the Fontan circulation including end-organ dysfunction, and its eventual morbidity and mortality. Generally, there is an obligate increase in central venous pressure with passive flow into the lungs and decreased ventricular preload. This is driven by the initial anatomic considerations as well as inefficient flow dynamics (Whitehead et al., 2007), atrial arhrythmias (Khairy et al., 2008; d'Udekem et al., 2014; Quinton et al., 2015), thromboembolism (Khairy et al., 2008), abnormal pulmonary vascular remodeling (Ridderbos et al., 2015) atrioventricular valve dysfunction, relaxation abnormalities and systolic dysfunction (Piran et al., 2002; Eicken et al., 2003). The culmination of these abnormalities leads to a significant burden of end organ dysfunction (Dimopoulos et al., 2008; Rychik et al., 2012; Schumacher et al., 2014) and mortality (Khairy et al., 2008).

The multiple levels of organ and cardiovascular dysfunction that contribute to Fontan failure (Frazier et al., 2005; Morales et al., 2011; d'Udekem et al., 2014) complicate the discussion regarding the choice and potential benefits of mechanical circulatory support in these patients. For example, while a systemic VAD will improve Fontan physiology when the primary abnormality is systemic ventricular dysfunction the situation is more complex when failure is multifactorial, which is more often the case (Khairy et al., 2008). Pulmonary vascular remodeling (Khambadkone et al., 2003; Ridderbos et al., 2015) and diastolic abnormalities (Anderson et al., 2008) often conspire to limit pulmonary blood flow and assessing the contributions of each is difficult at best. One process may also exacerbate the other as cavopulmonary associated power loss may lead to chronic underfilling (Haggerty et al., 2015) and worsening diastolic dysfunction. The degree of diastolic dysfunction may also be underappreciated by testing at rest as Fontan patients may have limited inotropic reserve (Senzaki et al., 2006). A recent report from the Pediatric Heart Network Investigators suggests that while desaturation and inotropic reserve may limit exercise function, impaired stroke volume reserve (Paridon et al., 2008) may be the primary driver of Fontan dysfunction as the inability to increase trans-pulmonary blood flow drives impaired systemic ventricular preload. This is in keeping with data suggesting power loss within the Fontan worsens with activity (Khiabani et al., 2015). Thus, augmenting systemic ventricular output with a VAD alone may not improve the overall physiology and may lead to further increases in central venous pressure as trans-pulmonary blood flow remains the limiting factor.

In addition, the failing Fontan circulation is often addressed as a single state to which different therapies are applied. However, this is a misconception as early Fontan failure is very different than late Fontan failure. Each of these stages of Fontan failure probably require different therapies and applying one therapy to all of the stages will result in inconsistent results. Early failure of the Fontan Circulation is commonly noted by the development of re-entrant tachycardia or mild clinical symptoms. For those patients with an atrial-pulmonary Fontan or anatomic obstruction, this may be successfully addressed with a Fontan conversion. Those patients who start to develop atrial fibrillation and early signs of renal or hepatic dysfunction are in moderate failure and can still be successfully treated with cardiac transplantation (Kanter et al., 2011). There is growing evidence that VAD support can be successful in a subset of these patients (Halaweish et al., 2015; Jabbar et al., 2015), however, it remains unclear when VAD implantation should be considered and what percentage of patients will benefit from systemic VAD alone. Patients with isolated, or predominant ventricular failure, are likely to benefit from VAD alone, however, Fontan failure is commonly multifactorial. A VAD will surely not help the clinical situation if the end-diastolic pressure of the systemic ventricle is not high (at least above 12 mmHG). Some centers have utilized a sub-pulmonary assist device either alone (Prêtre et al., 2008) or as part of a "biventricular" support strategy (Nathan et al., 2006; Valeske et al., 2014) in circumstances where the pulmonary vascular bed remained a limiting factor and CVP remained elevated, however, the results are mixed and the medium to long term outcome of this approach remains unclear. The addition of a sub-pulmonary assist device to force blood through an abnormal pulmonary vascular bed and into an often restricted systemic ventricle in the setting of heart failure is unlikely to be a successful long-term support strategy. On the other hand, the application of a sub-pulmonary support system very early in the clinical course, prior to the development of multi-organ dysfunction, may be able to avoid many of these concerns and is the topic of ongoing research (Di Molfetta et al., 2015). Those patients presenting with severe failure of their Fontan circulation, who have developed marked end-organ dysfunction, protein losing enteropathy, and/or plastic bronchitis are not good transplant candidates. It is these patients who may benefit from the TAH as it not only provides a supra-physiological cardiac index (often over 4 L/min/m^2) but does so with a low CVP, something rarely

seen with VADs or even early after transplantation. It is this immediate improvement in cardiac output in the environment of a decongested venous system that may allow recovery of renal (Ryan et al., 2015) and liver disease previously thought not to be reversible and thus improve transplant candidacy/mortality (as has been demonstrated in VAD use in adults with end-stage heart failure Russell et al., 2009).

The feasibility of using a TAH in the failing Fontan has been demonstrated in a recent case report by Rossano et al. (2014). The team placed a TAH in a 13 year old with pulmonary atresia with intact ventricular septum who presented *in extremis* with respiratory failure, hepatic dysfunction, and plastic bronchitis. A 70-cc TAH was placed after creating a "neo-right atrium." The patient recovered end organ function and was able to ambulate prior to transplantation on POD 61. This case was also significant because it demonstrated the possibility of constructing a capacitance chamber in patients without two adequate AV valves. This is possible because the TAH does not generate significant "suction" which would collapse the capacitance chamber. That said, the mass of the device compressing the neo-atrium is a significant concern and may complicate this support strategy. It remains to be seen if a reproducible and efficient TAH implantation method can be developed that will function for the vast majority of Fontan anatomies.

VIRTUAL FIT

The TAH presents a number of potential advantages to VAD support in patients with congenital abnormalities and with complex hemodynamics, anatomic abnormalities or previous palliations for the reasons mentioned above; however, the implantation is technically more challenging than implantation of a VAD. Assessing thoracic anatomy and device fit has been a concern since the early development of artificial hearts (Jacobs et al., 1978). This issue is particularly relevant in small adults (i.e., women) and adolescents. Historically, the 70 cc TAH was limited to adults or adolescents with a minimum 10 cm distance from the anterior surface of the T10 vertebral body to the sternum in order to ensure device alignment and to prevent kinking or obstruction of venous structures and the outflow grafts. Size based fit recommendations were subsequently developed (Copeland et al., 2004). Population based size and anatomic assumptions regarding chest shape/size, heart size and arterial relationship have given rise to patient specific virtual implantation based on cross sectional imaging (Chatel et al., 1993; Zhang et al., 1999; Dowling et al., 2004; Moore et al., 2014). Understanding patient specific anatomy and device fit is likely to be even more significant in patients with CHD given the range of chamber, valve and great vessel anomalies across the disease spectrum.

SYNCARDIA® 50 CC CLINICAL TRIAL

While virtual fit may expand the number of patients who may benefit from a TAH, there was a clear need for a smaller device to accommodate small adults (especially women) and adolescents who are too small for the 70 cc TAH. Syncardia® has now developed a 50 cc pump which is 30% smaller by volume and is now enrolling children and adults in a bridge to transplant clinical study (**Figure 1**). The study will have both pediatric (age 10–18 years) and adult (19–75 years) arms. There are also secondary study arms for patients who would not qualify for study inclusion due to ECMO (either V-A or V-V) support >3 days or only 1 functioning AV valve (both of which are relevant to patients with CHD). Importantly, inclusion in the study is not based solely on patient BSA or thoracic measurement in a single plane. Patients can enroll in the study if virtual implantation suggests device implantation is feasible. Preoperative virtual implantation may alter device selection in up to ∼33% of patients and may help to identify patients with a BSA <1.2 m^2 who are candidates for implantation (Moore et al., 2016).

FIGURE 1 | Syncardia TAH 70 cc (left) and 50 cc (right) devices.

CONCLUSIONS

The last few decades have seen a dramatic improvement in clinical outcomes among patients with CHD. These improvements are most pronounced in young children and those with severe CHD (Moons et al., 1970; Nieminen et al., 2007; Khairy et al., 2010) which were historically almost uniformly fatal. While early survival and improved quality of life are now the rule, many of the surgical interventions employed for repairing CHD are palliative rather than curative. This has shifted the burden of heart failure and cardiac mortality to the teenage and early adult years (Zomer et al., 2013; Diller et al., 2015). While the availability of VAD technology has improved overall heart failure outcomes, the proportion of patients with CHD who are supported by a VAD noticeably trails the proportion of patients with cardiomyopathy who are supported by a VAD (Davies et al., 2011). This is especially concerning given children (Almond et al., 2009; Jeewa et al., 2014; Zafar et al., 2015a) and adults (Davies et al., 2011) with CHD have higher waitlist mortality. The differences in waitlist mortality are multifactorial, but have been attributed to both limited access to VAD technology (Gelow et al., 2013) and sub-optimal outcomes once a VAD has been implanted in patients with

CHD (Davies et al., 2011; Everitt et al., 2011). Recent use of the TAH (Morales et al., 2012; Rossano et al., 2014) has highlighted how the TAH may be able to overcome some of the historical limitations to VAD use in CHD, although long-term data is needed. The TAH has the ability to improve end-organ function by simultaneously increasing cardiac output and lowering CVP, to address restrictive heart failure, and to provide a reliable, pulsatile pump that can address the multiple levels of failure that lead to Fontan failure. The TAH pumps may also be placed in a variety of orientations (criss-cross, parallel, other) which allows surgical flexibility and innovation to account for the anatomic variation associated with CHD. Ultimately, these characteristics may make the TAH the most effective bridge to normal physiology for patients with complex CHD who have been only partially medically or surgically palliated since birth.

AUTHOR CONTRIBUTIONS

CV provided conception/design of the review, contributed to critical drafting and revision of the manuscript and provided final approval for the manuscript. DM provided conception/design of the review, contributed to critical drafting and revision of the manuscript and provided final approval for the manuscript.

REFERENCES

Agusala, K., Bogaev, R., Frazier, O. H., and Franklin, W. J. (2010). Ventricular assist device placement in an adult with D-transposition of the great arteries with prior Mustard operation. *Congenit. Heart Dis.* 5, 635–637. doi: 10.1111/j.1747-0803.2010.00408.x

Almond, C. S., Morales, D. L., Blackstone, E. H., Turrentine, M. W., Imamura, M., and Massicotte, M. P. (2013). Berlin heart EXCOR pediatric ventricular assist device for bridge to heart transplantation in US children. *Circulation* 127, 1702–1711. doi: 10.1161/CIRCULATIONAHA.112.000685

Almond, C. S., Thiagarajan, R. R., Piercey, G. E., Gauvreau, K., Blume, E. D., Bastardi, H. J., et al. (2009). Waiting list mortality among children listed for heart transplantation in the United States. *Circulation* 119, 717–727. doi: 10.1161/CIRCULATIONAHA.108.815712

Anderson, P. A., Sleeper, L. A., Mahony, L., Colan, S. D., Atz, A. M., Breitbart, R. E., et al. (2008). Contemporary outcomes after the Fontan procedure: a Pediatric Heart Network multicenter study. *J. Am. Coll. Cardiol.* 52, 85–98. doi: 10.1016/j.jacc.2008.01.074

Carpentier, A., Latrémouille, C., Cholley, B., Smadja, D. M., Roussel, J. C., Boissier, E., et al. (2015). First clinical use of a bioprosthetic total artificial heart: report of two cases. *Lancet* 386, 1556–1563. doi: 10.1016/S0140-6736(15)60511-6

Chatel, D., Martin-Bouyer, Y., Vicaut, E., Bouchoucha, H., Achard, F., Sablayrolles, J. L., et al. (1993). Criteria for anatomical compatibility of the total artificial heart: computerized three-dimensional modeling of the cardiovascular anatomy. *Artif. Organs* 17, 1022–1035. doi: 10.1111/j.1525-1594.1993.tb03185.x

Copeland, J. G., Smith, R. G., Arabia, F. A., Nolan, P. E., Sethi, G. K., Tsau, P. H., et al. (2004). Cardiac replacement with a total artificial heart as a bridge to transplantation. *N. Engl. J. Med.* 351, 859–867. doi: 10.1056/NEJMoa040186

Davies, R. R., Russo, M. J., Yang, J., Quaegebeur, J. M., Mosca, R. S., and Chen, J. M. (2011). Listing and transplanting adults with congenital heart disease. *Circulation* 123, 759–767. doi: 10.1161/CIRCULATIONAHA.110.960260

Diller, G. P., Kempny, A., Alonso-Gonzalez, R., Swan, L., Uebing, A., Li, W., et al. (2015). Survival prospects and circumstances of death in contemporary adult congenital heart disease patients under follow-up at a large tertiary centre. *Circulation* 132, 2118–2125. doi: 10.1161/CIRCULATIONAHA.115.017202

Di Molfetta, A., Amodeo, A., Fresiello, L., Trivella, M. G., Iacobelli, R., Pilati, M., et al. (2015). Simulation of ventricular, cavo-pulmonary, and biventricular ventricular assist devices in failing fontan. *Artif. Organs* 39, 550–558. doi: 10.1111/aor.12434

Dimopoulos, K., Diller, G. P., Koltsida, E., Pijuan-Domenech, A., Papadopoulou, S. A., Babu-Narayan, S. V., et al. (2008). Prevalence, predictors, and prognostic value of renal dysfunction in adults with congenital heart disease. *Circulation* 117, 2320–2328. doi: 10.1161/CIRCULATIONAHA.107.734921

Dipchand, A. I., Edwards, L. B., Kucheryavaya, A. Y., Benden, C., Dobbels, F., Levvey, B. J., et al. (2014). The registry of the international society for heart and lung transplantation: seventeenth official pediatric heart transplantation report—2014; focus theme: retransplantation. *J. Heart Lung Transplant.* 33, 985–995. doi: 10.1016/j.healun.2014.08.002

Dowling, R. D., Gray, L. A. Jr., Etoch, S. W., Laks, H., Marelli, D., Samuels, L., et al. (2004). Initial experience with the AbioCor implantable replacement heart system. *J. Thorac. Cardiovasc. Surg.* 127, 131–141. doi: 10.1016/j.jtcvs.2003.07.023

d'Udekem, Y., Iyengar, A. J., Galati, J. C., Forsdick, V., Weintraub, R. G., Wheaton, G. R., et al. (2014). Redefining expectations of long-term survival after the Fontan procedure: twenty-five years of follow-up from the entire population of Australia and New Zealand. *Circulation* 130, S32–S38. doi: 10.1161/CIRCULATIONAHA.113.007764

Eicken, A., Fratz, S., Gutfried, C., Balling, G., Schwaiger, M., Lange, R., et al. (2003). Hearts late after fontan operation have normal mass, normal volume, and reduced systolic function: a magnetic resonance imaging study. *J. Am. Coll. Cardiol.* 42, 1061–1065. doi: 10.1016/S0735-1097(03)00986-0

Emin, A., Rogers, C. A., Parameshwar, J., Macgowan, G., Taylor, R., Yonan, N., et al. (2013). Trends in long-term mechanical circulatory support for advanced heart failure in the UK. *Eur. J. Heart Fail.* 15, 1185–1193. doi: 10.1093/eurjhf/hft127

Everitt, M. D., Donaldson, A. E., Stehlik, J., Kaza, A. K., Budge, D., Alharethi, R., et al. (2011). Would access to device therapies improve transplant outcomes for adults with congenital heart disease? Analysis of the United Network for Organ Sharing (UNOS). *J. Heart Lung Transplant.* 30, 395–401. doi: 10.1016/j.healun.2010.09.008

Frazier, O. H., Gregoric, I. D., and Messner, G. N. (2005). Total circulatory support with an LVAD in an adolescent with a previous Fontan procedure. *Tex. Heart Inst. J.* 32, 402–404.

Gelow, J. M., Song, H. K., Weiss, J. B., Mudd, J. O., and Broberg, C. S. (2013). Organ allocation in adults with congenital heart disease listed for heart transplant: impact of ventricular assist devices. *J. Heart Lung Transplant.* 32, 1059–1064. doi: 10.1016/j.healun.2013.06.024

Gerosa, G., Scuri, S., Iop, L., and Torregrossa, G. (2014). Present and future perspectives on total artificial hearts. *Ann. Cardiothorac. Surg.* 3, 595–602. doi: 10.3978/j.issn.2225-319X.2014.09.05

Gewillig, M., Daenen, W., Aubert, A., and Van der Hauwaert, L. (1992). Abolishment of chronic volume overload. Implications for diastolic function of the systemic ventricle immediately after Fontan repair. *Circulation* 86, II93–II99.

Graham, T. P. Jr., Bernard, Y. D., Mellen, B. G., Celermajer, D., Baumgartner, H., Cetta, F., et al. (2000). Long-term outcome in congenitally corrected transposition of the great arteries: a multi-institutional study. *J. Am. Coll. Cardiol.* 36, 255–261. doi: 10.1016/S0735-1097(00)00682-3

Haggerty, C. M., Whitehead, K. K., Bethel, J., Fogel, M. A., and Yoganathan, A. P. (2015). Relationship of single ventricle filling and preload to total cavopulmonary connection hemodynamics. *Ann. Thorac. Surg.* 99, 911–917. doi: 10.1016/j.athoracsur.2014.10.043

Halaweish, I., Ohye, R. G., and Si, M. S. (2015). Berlin heart ventricular assist device as a long-term bridge to transplantation in a Fontan patient with failing single ventricle. *Pediatr. Transplant.* 19, E193–E195. doi: 10.1111/petr.12607

Jabbar, A. A., Franklin, W. J., Simpson, L., Civitello, A. B., Delgado, R. M. III., and Frazier, O. H. (2015). Improved systemic saturation after ventricular assist device implantation in a patient with decompensated dextro-transposition of the great arteries after the fontan procedure. *Tex. Heart Inst. J.* 42, 40–43. doi: 10.14503/THIJ-13-3374

Jacobs, G. B., Agishi, T., Ecker, R., Meaney, T., Kiraly, R. J., and Nose, Y. (1978). Human thoracic anatomy relevant to implantable artificial hearts. *Artif. Organs* 2, 64–82. doi: 10.1111/j.1525-1594.1978.tb01005.x

Jeewa, A., Manlhiot, C., Kantor, P. F., Mital, S., McCrindle, B. W., and Dipchand, A. I. (2014). Risk factors for mortality or delisting of patients from the pediatric heart transplant waiting list. *J. Thorac. Cardiovasc. Surg.* 147, 462–468. doi: 10.1016/j.jtcvs.2013.09.018

Joyce, D. L., Crow, S. S., John, R., St Louis, J. D., Braunlin, E. A., Pyles, L. A., et al. (2010). Mechanical circulatory support in patients with heart failure secondary to transposition of the great arteries. *J. Heart Lung Transplant.* 29, 1302–1305. doi: 10.1016/j.healun.2010.05.030

Kanter, K. R., Mahle, W. T., Vincent, R. N., Berg, A. M., Kogon, B. E., and Kirshbom, P. M. (2011). Heart transplantation in children with a Fontan procedure. *Ann. Thorac. Surg.* 91, 823–829. doi: 10.1016/j.athoracsur.2010.11.031

Khairy, P., Fernandes, S. M., Mayer, J. E., Triedman, J. K., Walsh, E. P., Lock, J. E., et al. (2008). Long-term survival, modes of death, and predictors of mortality in patients with Fontan surgery. *Circulation* 117, 85–92. doi: 10.1161/CIRCULATIONAHA.107.738559

Khairy, P., Ionescu-Ittu, R., Mackie, A. S., Abrahamowicz, M., Pilote, L., and Marelli, A. J. (2010). Changing mortality in congenital heart disease. *J. Am. Coll. Cardiol.* 56, 1149–1157. doi: 10.1016/j.jacc.2010.03.085

Khambadkone, S., Li, J., de Leval, M. R., Cullen, S., Deanfield, J. E., and Redington, A. N. (2003). Basal pulmonary vascular resistance and nitric oxide responsiveness late after Fontan-type operation. *Circulation* 107, 3204–3208. doi: 10.1161/01.CIR.0000074210.49434.40

Khiabani, R. H., Whitehead, K. K., Han, D., Restrepo, M., Tang, E., Bethel, J., et al. (2015). Exercise capacity in single-ventricle patients after Fontan correlates with haemodynamic energy loss in TCPC. *Heart* 101, 139–143. doi: 10.1136/heartjnl-2014-306337

Kiesewetter, C. H., Sheron, N., Vettukattill, J. J., Hacking, N., Stedman, B., Millward-Sadler, H., et al. (2007). Hepatic changes in the failing Fontan circulation. *Heart* 93, 579–584. doi: 10.1136/hrt.2006.094516

Kirklin, J. K., Naftel, D. C., Pagani, F. D., Kormos, R. L., Stevenson, L. W., Blume, E. D., et al. (2014). Sixth INTERMACS annual report: a 10,000-patient database. *J. Heart Lung Transplant.* 33, 555–564. doi: 10.1016/j.healun.2014.04.010

Kirsch, M. E., Nguyen, A., Mastroianni, C., Pozzi, M., Leger, P., Nicolescu, M., et al. (2013). SynCardia temporary total artificial heart as bridge to transplantation: current results at la pitie hospital. *Ann. Thorac. Surg.* 95, 1640–1646. doi: 10.1016/j.athoracsur.2013.02.036

Kouatli, A. A., Garcia, J. A., Zellers, T. M., Weinstein, E. M., and Mahony, L. (1997). Enalapril does not enhance exercise capacity in patients after Fontan procedure. *Circulation* 96, 1507–1512. doi: 10.1161/01.CIR.96.5.1507

Leprince, P., Bonnet, N., Varnous, S., Rama, A., Leger, P., Ouattara, A., et al. (2005). Patients with a body surface area less than 1.7 m2 have a good outcome with the CardioWest Total Artificial Heart. *J. Heart Lung Transplant.* 24, 1501–1505. doi: 10.1016/j.healun.2005.01.016

Lund, L. H., Edwards, L. B., Kucheryavaya, A. Y., Benden, C., Christie, J. D., Dipchand, A. I., et al. (2014). The registry of the International Society for Heart and Lung Transplantation: thirty-first official adult heart transplant report—2014; focus theme: retransplantation. *J. Heart Lung Transplant.* 33, 996–1008. doi: 10.1016/j.healun.2014.08.003

Maly, J., Netuka, I., Besik, J., Dorazilova, Z., Pirk, J., and Szarszoi, O. (2015). Bridge to transplantation with long-term mechanical assist device in adults after the Mustard procedure. *J. Heart Lung Transplant.* 34, 1177–1181. doi: 10.1016/j.healun.2015.03.025

Moons, P., Bovijn, L., Budts, W., Belmans, A., and Gewillig, M. (1970). Temporal trends in survival to adulthood among patients born with congenital heart disease from to 1992 in Belgium. *Circulation* 2010, 2264–2272.

Moore, R. A., Lorts, A., Madueme, P. C., Taylor, M. D., and Morales, D. L. (2016). Virtual implantation of the 50cc SynCardia total artificial heart. *J. Heart Lung Transplant.* 35, 824–827. doi: 10.1016/j.healun.2015.12.026

Moore, R. A., Madueme, P. C., Lorts, A., Morales, D. L., and Taylor, M. D. (2014). Virtual implantation evaluation of the total artificial heart and compatibility: beyond standard fit criteria. *J. Heart Lung Transplant.* 33, 1180–1183. doi: 10.1016/j.healun.2014.08.010

Morales, D. L., Adachi, I., Heinle, J. S., and Fraser, C. D. Jr. (2011). A new era: use of an intracorporeal systemic ventricular assist device to support a patient with a failing Fontan circulation. *J. Thorac. Cardiovasc. Surg.* 142, e138–e140. doi: 10.1016/j.jtcvs.2011.05.018

Morales, D. L., Khan, M. S., Gottlieb, E. A., Krishnamurthy, R., Dreyer, W. J., and Adachi, I. (2012). Implantation of total artificial heart in congenital heart disease. *Semin. Thorac. Cardiovasc. Surg.* 24, 142–143. doi: 10.1053/j.semtcvs.2012.04.006

Nathan, M., Baird, C., Fynn-Thompson, F., Almond, C., Thiagarajan, R., Laussen, P., et al. (2006). Successful implantation of a Berlin heart biventricular assist device in a failing single ventricle. *J. Thorac. Cardiovasc. Surg.* 131, 1407–1408. doi: 10.1016/j.jtcvs.2006.02.015

Nieminen, H. P., Jokinen, E. V., and Sairanen, H. I. (2007). Causes of late deaths after pediatric cardiac surgery: a population-based study. *J. Am. Coll. Cardiol.* 50, 1263–1271. doi: 10.1016/j.jacc.2007.05.040

Paridon, S. M., Mitchell, P. D., Colan, S. D., Williams, R. V., Blaufox, A., Li, J. S., et al. (2008). A cross-sectional study of exercise performance during the first 2 decades of life after the fontan operation. *J. Am. Coll. Cardiol.* 52, 99–107. doi: 10.1016/j.jacc.2008.02.081

Peng, E., O'Sullivan, J. J., Griselli, M., Roysam, C., Crossland, D., Chaudhari, M., et al. (2014). Durable ventricular assist device support for failing systemic morphologic right ventricle: early results. *Ann. Thorac. Surg.* 98, 2122–2129. doi: 10.1016/j.athoracsur.2014.06.054

Piran, S., Veldtman, G., Siu, S., Webb, G. D., and Liu, P. P. (2002). Heart failure and ventricular dysfunction in patients with single or systemic right ventricles. *Circulation* 105, 1189–1194. doi: 10.1161/hc1002.105182

Prêtre, R., Häussler, A., Bettex, D., and Genoni, M. (2008). Right-sided univentricular cardiac assistance in a failing Fontan circulation. *Ann. Thorac. Surg.* 86, 1018–1020. doi: 10.1016/j.athoracsur.2008.03.003

Quinton, E., Nightingale, P., Hudsmith, L., Thorne, S., Marshall, H., Clift, P., et al. (2015). Prevalence of atrial tachyarrhythmia in adults after Fontan operation. *Heart* 101, 1672–1677. doi: 10.1136/heartjnl-2015-307514

Ridderbos, F. J., Wolff, D., Timmer, A., van Melle, J. P., Ebels, T., Dickinson, M. G., et al. (2015). Adverse pulmonary vascular remodeling in the Fontan circulation. *J. Heart Lung Transplant.* 34, 404–413. doi: 10.1016/j.healun.2015.01.005

Rossano, J. W., Goldberg, D. J., Fuller, S., Ravishankar, C., Montenegro, L. M., and Gaynor, J. W. (2014). Successful use of the total artificial heart in the failing Fontan circulation. *Ann. Thorac. Surg.* 97, 1438–1440. doi: 10.1016/j.athoracsur.2013.06.120

Russell, S. D., Rogers, J. G., Milano, C. A., Dyke, D. B., Pagani, F. D., Aranda, J. M., et al. (2009). Renal and hepatic function improve in advanced heart failure patients during continuous-flow support with the HeartMate II left ventricular assist device. *Circulation* 120, 2352–2357. doi: 10.1161/CIRCULATIONAHA.108.814863

Ryan, T. D., Jefferies, J. L., Zafar, F., Lorts, A., and Morales, D. L. (2015). The evolving role of the total artificial heart in the management of end-stage congenital heart disease and adolescents. *ASAIO J.* 61, 8–14. doi: 10.1097/MAT.0000000000000156

Rychik, J., Veldtman, G., Rand, E., Russo, P., Rome, J. J., Krok, K., et al. (2012). The precarious state of the liver after a Fontan operation: summary of a multidisciplinary symposium. *Pediatr. Cardiol.* 33, 1001–1012. doi: 10.1007/s00246-012-0315-7

Schumacher, K. R., Singh, T. P., Kuebler, J., Aprile, K., O'Brien, M., and Blume, E. D. (2014). Risk factors and outcome of Fontan-associated plastic bronchitis: a case-control study. *J. Am. Heart Assoc.* 3:e000865. doi: 10.1161/JAHA.114.000865

Senzaki, H., Masutani, S., Ishido, H., Taketazu, M., Kobayashi, T., Sasaki, N., et al. (2006). Cardiac rest and reserve function in patients with Fontan circulation. *J. Am. Coll. Cardiol.* 47, 2528–2535. doi: 10.1016/j.jacc.2006.03.022

Shaddy, R. E., Boucek, M. M., Hsu, D. T., Boucek, R. J., Canter, C. E., Mahony, L., et al. (2007). Carvedilol for children and adolescents with heart failure: a randomized controlled trial. *JAMA* 298, 1171–1179. doi: 10.1001/jama.298.10.1171

Si, M. S., Pagani, F. D., and Haft, J. W. (2015). Use of the total artificial heart as a bridge to transplant in a 13-year-old with congenitally corrected transposition of the great arteries. *J. Thorac. Cardiovasc. Surg.* 151, e71–e73. doi: 10.1016/j.jtcvs.2015.11.049

Valeske, K., Yerebakan, C., Mueller, M., and Akintuerk, H. (2014). Urgent implantation of the Berlin Heart Excor biventricular assist device as a

total artificial heart in a patient with single ventricle circulation. *J. Thorac. Cardiovasc. Surg.* 147, 1712–1714. doi: 10.1016/j.jtcvs.2014.01.012

van der Bom, T., Winter, M. M., Bouma, B. J., Groenink, M., Vliegen, H. W., Pieper, P. G., et al. (2013). Effect of valsartan on systemic right ventricular function: a double-blind, randomized, placebo-controlled pilot trial. *Circulation* 127, 322–330. doi: 10.1161/CIRCULATIONAHA.112.135392

Vejlstrup, N., Sørensen, K., Mattsson, E., Thilen, U., Kvidal, P., Johansson, B., et al. (2015). Long-term outcome of mustard/senning correction for transposition of the great arteries in sweden and denmark. *Circulation* 132, 633–638. doi: 10.1161/CIRCULATIONAHA.114.010770

Villa, C. R., Khan, M. S., Zafar, F., Morales, D. L., and Lorts, A. (2017). United states trends in pediatric ventricular assist implantation as bridge to transplantation. *ASAIO J.* doi: 10.1097/MAT.0000000000000524. [Epub ahead of print].

Whitehead, K. K., Pekkan, K., Kitajima, H. D., Paridon, S. M., Yoganathan, A. P., and Fogel, M. A. (2007). Nonlinear power loss during exercise in single-ventricle patients after the Fontan: insights from computational fluid dynamics. *Circulation* 116, I165–I171. doi: 10.1161/CIRCULATIONAHA.106.680827

Zafar, F., Castleberry, C., Khan, M. S., Mehta, V., Bryant, R., Lorts, A., et al. (2015a). Pediatric heart transplant waiting list mortality in the era of ventricular assist devices. *J. Heart Lung Transplant.* 34, 82–88. doi: 10.1016/j.healun.2014.09.018

Zafar, F., Jefferies, J. L., Tjossem, C. J., Bryant, R. III., Jaquiss, R. D., Wearden, P. D., et al. (2015b). Biventricular Berlin heart EXCOR pediatric use across the united states. *Ann. Thorac. Surg.* 99, 1328–1334. doi: 10.1016/j.athoracsur.2014.09.078

Zhang, B., Masuzawa, T., Tatsumi, E., Taenaka, Y., Uyama, C., Takano, H., et al. (1999). Three-dimensional thoracic modeling for an anatomical compatibility study of the implantable total artificial heart. *Artif. Organs* 23, 229–234. doi: 10.1046/j.1525-1594.1999.06313.x

Zomer, A. C., Vaartjes, I., van der Velde, E. T., de Jong, H. M., Konings, T. C., Wagenaar, L. J., et al. (2013). Heart failure admissions in adults with congenital heart disease; risk factors and prognosis. *Int. J. Cardiol.* 168, 2487–2493. doi: 10.1016/j.ijcard.2013.03.003

Disclosure: DM has served as a consultant for Syncardia. DM is also a consultant for HeartWare and Berlin Heart.

Conflict of Interest Statement: The authors declare that the research was conducted in the absence of any commercial or financial relationships that could be construed as a potential conflict of interest.

frontiers in Physiology

ORIGINAL RESEARCH
published: 30 November 2016
doi: 10.3389/fphys.2016.00586

Pre-dive Whole-Body Vibration Better Reduces Decompression-Induced Vascular Gas Emboli than Oxygenation or a Combination of Both

Costantino Balestra[1, 2, 3, 4, 5, 6], *Sigrid Theunissen*[1, 2, 3], *Virginie Papadopoulou*[7], *Cedric Le Mener*[1], *Peter Germonpré*[2, 3, 8], *François Guerrero*[2, 3, 9] *and Pierre Lafère*[2, 3, 9]*

[1] *Environmental, Occupational, Ageing (Integrative) Physiology Laboratory, Haute Ecole Bruxelles-Brabant - HE2B, Brussels, Belgium,* [2] *DAN Europe Research Division, Roseto, Italy,* [3] *DAN Europe Research Division, Brussels, Belgium,* [4] *Anatomical Research and Clinical Studies (ARCS), Vrije Universiteit Brussel, Brussels, Belgium,* [5] *Anatomical Research Training and Education (ARTE), Vrije Universiteit Brussel, Brussels, Belgium,* [6] *Motor Sciences, Université Libre de Bruxelles, Brussels, Belgium,* [7] *Dayton Lab, Department of Biomedical Engineering, University of North Carolina, Chapel Hill, NC, USA,* [8] *Center for Hyperbaric Oxygen Therapy, Military Hospital "Queen Astrid", Brussels, Belgium,* [9] *ORPHY Laboratory, EA 4324, Université de Bretagne Occidentale, Brest, France*

OPEN ACCESS

Edited by:
Antonio L'Abbate, Sant'Anna School of Advanced Studies, Italy

Reviewed by:
Jacek Kot, Gdańsk Medical University, Poland
Jie Liu, Fourth Military Medical University

***Correspondence:**
Pierre Lafère
pierre.lafere@chu-brest.fr

Specialty section:
This article was submitted to Integrative Physiology, a section of the journal Frontiers in Physiology

Received: *03 September 2016*
Accepted: *14 November 2016*
Published: *30 November 2016*

Citation:
Balestra C, Theunissen S, Papadopoulou V, Le Mener C, Germonpré P, Guerrero F and Lafère P (2016) Pre-dive Whole-Body Vibration Better Reduces Decompression-Induced Vascular Gas Emboli than Oxygenation or a Combination of Both. Front. Physiol. 7:586. doi: 10.3389/fphys.2016.00586

Purpose: Since non-provocative dive profiles are no guarantor of protection against decompression sickness, novel means including pre-dive "preconditioning" interventions, are proposed for its prevention. This study investigated and compared the effect of pre-dive oxygenation, pre-dive whole body vibration or a combination of both on post-dive bubble formation.

Methods: Six healthy volunteers performed 6 no-decompression dives each, to a depth of 33 mfw for 20 min (3 control dives without preconditioning and 1 of each preconditioning protocol) with a minimum interval of 1 week between each dive. Post-dive bubbles were counted in the precordium by two-dimensional echocardiography, 30 and 90 min after the dive, with and without knee flexing. Each diver served as his own control.

Results: Vascular gas emboli (VGE) were systematically observed before and after knee flexing at each post-dive measurement. Compared to the control dives, we observed a decrease in VGE count of 23.8 ± 7.4% after oxygen breathing ($p < 0.05$), 84.1 ± 5.6% after vibration ($p < 0.001$), and 55.1 ± 9.6% after vibration combined with oxygen ($p < 0.001$). The difference between all preconditioning methods was statistically significant.

Conclusions: The precise mechanism that induces the decrease in post-dive VGE and thus makes the diver more resistant to decompression stress is still not known. However, it seems that a pre-dive mechanical reduction of existing gas nuclei might best explain the beneficial effects of this strategy. The apparent non-synergic effect of oxygen and vibration has probably to be understood because of different mechanisms involved.

Keywords: decompression sickness/*etiology/metabolism, diving/*adverse effects, risk assessment, risk factors, preconditioning

INTRODUCTION

Scuba diving is a sport with exhilaration, beauty, and fascination. This is probably why there are an estimated 10 million active recreational scuba divers worldwide (Trout et al., 2015). Additionally, diving is also key for environmental and scientific monitoring, construction and maintenance work, offshore oil exploitation, forensic, rescue, military, and filming purposes. However, the risks involved are often not advertised. Indeed, the overall rate of diving-related injury is 3.02 per 100 dives (Ranapurwala et al., 2014).

One of these injuries is decompression illness (DCI), a pathology affecting divers, astronauts, pilots and compressed air workers. Although DCI occurrence is relatively rare, with rates of 0.01–0.1% per dive (the higher end of the spectrum reflecting rates for commercial diving and the lower rates for scientific and recreational diving), the consequences can be dramatic (Ladd et al., 2002; Vann, 2004; Buzzacott, 2012). Indeed, DCI severity can vary from skin itching and marbled appearance to excruciating pain, convulsions, paralysis, coma and death. Over 60% of symptoms present in the first 3 h post dive, with some presenting as late as 48 h post-dive (Levett and Millar, 2008), and can be localized (joint pain in a particular articulation) or involve multiple systems. Therefore, divers should understand their limitations and how to prevent adverse outcomes.

Except for the more dramatic instance of arterial gas embolism by pulmonary overpressure, DCI is caused by bubble formation from dissolved inert gas in the tissues during decompression, vascular gas emboli (VGE). VGE can cause problems through direct mechanical effects (by blocking or distorting blood vessels) but also from the associated inflammatory response they trigger (Blatteau et al., 2014). Therefore, since decompression sickness (DCS) risk is inherently dependent on the dive profile and most importantly on the ascent profile (Marroni et al., 2004), it is managed by adhering to decompression schedules dictated by tables or dive computers, which are based on a decompression model or algorithm. Current algorithms include multi-tissue, diffusion, split phase gradient, linear-exponential, asymmetric tissue, thermodynamic, varying permeability, reduced gradient bubble, tissue bubble diffusion, and linear-exponential phase models. All of these models aim to limit bubble formation and growth during the decompression phase. Indeed, if VGE load is high, so is the risk of DCI. Moreover, VGE can cross from the central venous to the arterial circulation via a pulmonary shunt or a Patent Foramen Ovale. The more VGE are present after the dive, the higher this risk (Nishi, 1972; Blogg et al., 2014; Pollock and Nishi, 2014). However, all models can only partly describe reality and are by essence incomplete; they merely serve to "organize our ignorance" of the phenomenon. Therefore, the past 15 years or so, have witnessed changes and additions to diving protocols and table procedures, such as shorter nonstop time limits, slower ascent rates, shallow safety stops, ascending repetitive profiles, deep decompression stops, helium-based breathing mixtures, permissible reverse profiles, multilevel techniques, both faster, and slower controlling repetitive tissue halftimes, smaller critical tensions, longer flying-after-diving surface intervals, and others (Wienke, 2009). Nonetheless, VGE are still known to form in the body after many dives, even those done well within the limits of the accepted decompression model. Understanding these processes physiologically has been a challenge for decades and there are a number of questions still unanswered such as the exact primer for bubble formation, theories to account for micronuclei stability (hydrophobicity of surfaces or tissue elasticity), or the relevance of predisposing factors (dehydration for instance) (Papadopoulou et al., 2013).

Since non-provocative dive profiles are no guarantor of protection against DCS, novel means are required for its prevention including pre-dive procedures that could induce more resistance to decompression stress. This idea has prompted a change in research paradigm. Indeed, since several years, field research focuses on "preconditioning" methods that might attenuate bubble formation post-dive. Several practical, simple and feasible pre-dive measures have been studied such as endurance exercise (Blatteau et al., 2005; Castagna et al., 2011), pre-dive exposition to a warm environment (Blatteau et al., 2008), oral hydration (Gempp et al., 2009) or ingestion of dark chocolate (Theunissen et al., 2015). Others have tested the benefit of pre-dive oxygenation (Castagna et al., 2009; Bosco et al., 2010), or whole-body vibration (Germonpré et al., 2009). All of these studies show a positive effect with a significant decrease of post-dive VGE. Several hypotheses have been advocated to explain the possible protective effect: rheological changes affecting tissue perfusion, endothelial adaptation with nitric oxide pathway, up-regulation of cytoprotective proteins, and reduction of pre-existing gas nuclei from which bubbles originate (Gempp and Blatteau, 2010).

From a physiological point of view, comparing the effectiveness of preconditioning is interesting because it would allow to identify critical factors in the physiopathology of DCS. Similarly, it would be of practical interest to examine the possible synergy or antagonism of preconditioning methods when combined. Therefore, the aim of this study is to compare the effect on post-dive VGE of different types and combination of preconditioning methods: oxygenation, whole-body vibration and vibration associated with oxygenation.

MATERIALS AND METHODS

All experimental procedures were conducted in accordance with the Declaration of Helsinki (World Medical Association, 2013) and were approved by the Academic Ethical Committee of Brussels (B200-2009-039). All methods and potential risks were explained in detail to the participants.

Study Population

After written informed consent, 6 healthy male divers (Minimum certification "Autonomous Diver" according to European Norm EN 14153-2 or ISO 24801-2, with at least 50 logged dives) volunteered for this study. They were selected from a large sports diver population in order to obtain a group of comparable age [30–40 years, 34.8 $\pm$ 5.3 (mean $\pm$ SD)], body composition (BMI between 20 and 25, 23.7 $\pm$ 1.1) and comparable health status: non-smokers with regular but not excessive physical activity

(aerobic exercise one to three times a week). The divers that participated in this protocol have already participated in some of our experiments and are known as being consistent "bubblers" (Theunissen et al., 2015). Prior to entry into the study, they were assessed fit to dive. None of the subjects had a previous history of decompression sickness and none of them were on any cardio-active medication.

Participants were instructed not to dive 72 h prior to the experimental dive. They were also were asked to refrain from strenuous exercise and nitrate-rich food for 48 h before the tests (Blatteau et al., 2005).

Dive Protocol

Each diver performed 6 standardized dives with a minimum interval of 1 week between then. This standard dive profile (see below) was performed at least three times under normal conditions i.e., without preconditioning ("control"), and several times under experimental conditions, when the effects of several methods of preconditioning were measured, making each diver his own control. The order of the experimental dives was randomized. Preconditioned dives were preceded either by a 100% normobaric oxygen breathing session (O_2) through a non-rebreather facemask (Teleflex medical BVBA, Vianen, Nederland), a whole-body vibration session (Vib) using a commercially available vibration mattress (VM 9100 RM, HHP Products, Karlsruhe, Germany), or a combination of both simultaneously ($VibO_2$). Vibration frequencies ranged from 35 to 40 Hz along the whole body thanks to 11 motors embedded in the mattress. The subject lay motionless on the mattress during the entire vibration session, or a non-vibrating mattress while only breathing oxygen. All preconditioning had duration of 30 min and ended 1 h before the start of the dive.

Dives were performed to a depth of 33 mfw (0.4 MPa) for 20 min in a pool environment (Nemo33, Brussels, Belgium) with a water and air temperature of 33 and 29°C respectively, thus needing no thermal protection suit.

The descent was done at 20 $m.min^{-1}$. At depth, subjects were asked to swim slowly without effort, then came back to the surface with an ascent speed of 10 $m.min^{-1}$. Since this depth-time profile falls within accepted "no-decompression limits" (NAVSEA, 2008), no decompression stop was added to the profile.

Participant safety was guaranteed through the buddy system, a procedure in which two divers, "the buddies," operate together as a single unit so that they are able to monitor and help each other. Moreover, a safety diver was ready to intervene at 20 m depth.

Measurements

Bubbles which form as a consequence of decompression can be detected as VGE by ultrasonic methods (Møllerløkken et al., 2016). Using a two-dimensional echocardiography technique (Vivid 7, GE Healthcare, Pollards Wood, UK), a frame-based counting method as described by Germonpré et al. (2014) was used to quantify VGE.

In this method, in the left lateral supine position, a cardiac four-chamber view is obtained by placing the probe at the level of the left fifth intercostal space. It is necessary to modify the standard four-chamber view by rotating the probe slightly ventrally (in the direction of the xyphoid process) so the right atrium and ventricle can be fully visualized. A series of at least 15 cardiac cycles are recorded while keeping the probe immobile. Each diver was evaluated at three time points: before the dive, at 30 min and at 90 min after surfacing. They were made at the end of a period during which subjects remain at rest (without flexion) and following active provocation by two deep knee bends (with flexion). In total, 5 videos of 15 cardiac cycles were recorded for each dive.

At a later stage, these recordings are reviewed using the MPEGVue software (GE Healthcare, Pollards Wood, UK). First, the pre-dive echography loops are reviewed in order to identify intra-cardiac structures that may mimic VGE (e.g., papillary muscles, valve leaflets, Chiari network, Valsalva sinus). Then, the post-dive echography is reviewed and played in a loop at real-time speed in order to rapidly assess the presence or not of circulating bubbles.

In cases where bubbles are seen, a formal bubble counting procedure is performed. Using the pause button, the loop is frozen at the start, and then with the forwards and backwards buttons, an image frame is selected in end-diastolic/proto-systolic position and bubbles are counted in both the right atrium and ventricle. Ten consecutive frames are analyzed and the bubble count is averaged over these 10 frames.

The counting was performed independently twice by two trained scientists acquainted with the method used (CB, PG) the numbers of VGE considered for calculation were those that reached consensus (**Figure 1**).

Statistical Analysis

Since all data passed the Kolmogorov-Smirnov and Shapiro-Wilk tests, allowing us to assume a Gaussian distribution, they were analyzed with repeated-measures ANOVA with Bonferroni *post-hoc* test.

Taking the mean bubble count of the control dives (without preconditioning) as 100%, percentage changes were calculated for each preconditioning protocol, allowing an appreciation of the magnitude of change rather than the absolute values.

All statistical tests were performed using a standard computer statistical package, GraphPad Prism version 5.00 for Windows (GraphPad Software, San Diego California USA). A threshold of $P < 0.05$ was considered statistically significant. All data are presented as mean ± standard error on mean (SEM).

RESULTS

None of the dives resulted in decompression sickness symptoms.

After the control dives, the absolute VGE counts ranged from 15.2 ± 4.3 VGE per cardiac cycle at rest to 18.9 ± 4.3 after knee flexion. After the experimental dives, absolute maximal bubble counts were 4.9 ± 3.2 and 5.6 ± 1.9 (Vib); 8.1 ± 2.9 and 9.8 ± 2.9 ($Vib+O_2$) and 10.9 ± 4.9 VGE and 14.4 ± 2.3 (O_2), VGE per cardiac cycle respectively without and with knee flexion. Maximal bubble counts were systematically used to evaluate the magnitude of the change independently of the bubble peak kinetics. However, it can be seen on **Figure 2** that it was

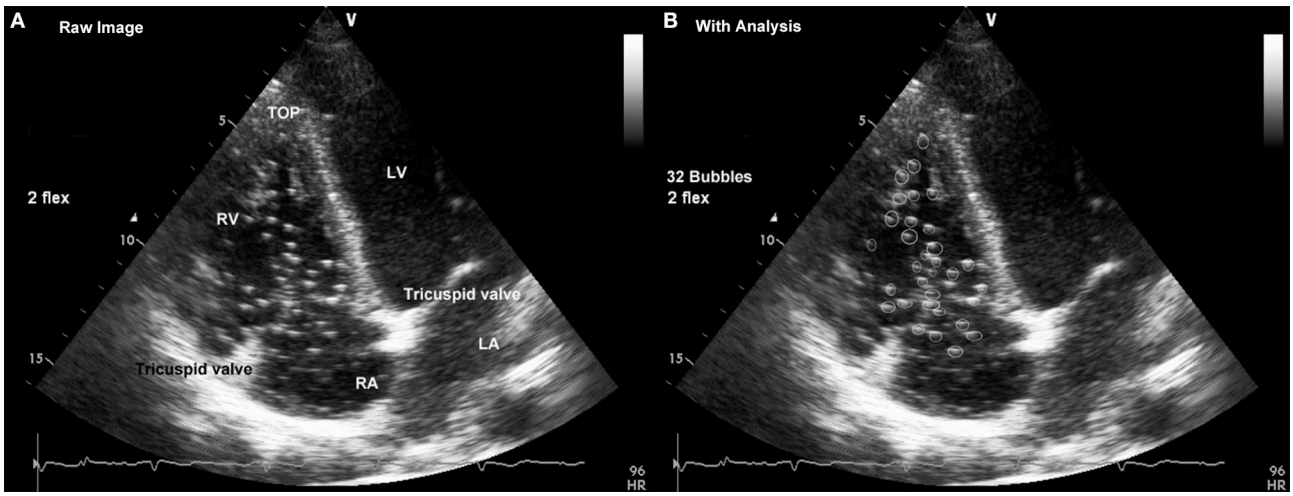

FIGURE 1 | Cardiac four-chamber view obtained by placing the probe at the level of the left fifth intercostal space. (A) Raw Image: Landmark structures in the right heart are easily identified with the "top" of the right ventricle (RV) and the tricuspid annulus on either side of the right atrium that constitute the "upper" border of the right atrium (RA). **(B)** With Analysis: Bubble signals are identified as bright spots and counted individually; tricuspid valve leaflets and other fixed structures (e.g., papillary muscles in the top of the right ventricle) are not counted. (LA: Left Atrium; LV: Left Ventricle).

preferentially obtained after active provocation (knee flexion) at the 30 min post-dive measurement.

The effect of the different preconditioning protocols on bubble formation after the dive is illustrated in **Figure 3**. Each pre-dive procedure induced a significant post-dive VGE change (ANOVA, $p < 0.0001$, df $= 23$). Compared to baseline, this variation is characterized by a decrease in VGE count of $23.8 \pm 7.4\%$ after oxygen breathing (O_2, $p < 0.05$), $84.1 \pm 5.6\%$ after vibration (Vib, $p < 0.001$), and $55.1 \pm 9.6\%$ after vibration combined with oxygen (Vib+O_2, $p < 0.001$). The effectiveness of the various protocols was also statistically significantly different when they were compared to each other, whole-body vibration (Vib) being the most effective ($p < 0.001$).

DISCUSSION

The origin and formation of VGE is still incompletely understood. Bubble formation after hyperbaric exposure is not simply the consequence of inert gas supersaturation during decompression. Experimental data have shown that supersaturation by itself will not produce bubbles in a homogenous fluid unless the pressure reduction is about 1400 ATA for air (Zheng et al., 1991)! These "homogenous nucleation" limits have been studied for several gases and may vary according to their solubility: 120 ATA for methane, 190 ATA for nitrogen and 350 ATA for helium (Finkelstein and Tamir, 1985). It seems thus that homogenous nucleation cannot be held responsible for (diving decompression) VGE generation. Indeed, numerous experiments indicate that bubbles originate as pre-existing gas nuclei (Yount et al., 1979; Vann et al., 1980; Christman et al., 1986; Lee et al., 1993). Nitrogen, diffusing out of the tissues during decompression, would preferably fill these gas nuclei rather than transfer as molecular nitrogen to blood. This causes the gas nuclei to grow and spill out nitrogen gas bubble into the bloodstream. Here, they either grow or shrink depending on surface tension and free gas tension (Blatteau et al., 2006). Although we only have indirect evidence of the presence of these gas nuclei, if this hypothesis is correct, eliminating gas nuclei before the dive would result in lower bubble production after the dive.

The aim of our study was to compare the effect of three different preconditioning methods on post-dive VGE. All three methods have already been shown to significantly decrease the number of VGE compared to controls dives in a way that is consistent with data in the literature (Castagna et al., 2009; Germonpré et al., 2009). The observation of a bubble peak after active provocation (knee flexing) at the 30 min post-dive measurement is also coherent with the literature (Blogg and Gennser, 2011).

The role of oxygen breathing (O_2) in the reduction of DCS risk has been extensively investigated before altitude decompression (Webb and Pilmanis, 2011; Foster et al., 2013; Webb et al., 2016). Several studies have shown that a single hyperbaric oxygen exposure before diving appeared to be beneficial for preventing the occurrence of DCS in animals (Butler et al., 2006; Arieli et al., 2007; Katsenelson et al., 2007) and reducing bubble generation in humans (Landolfi et al., 2006). This approach did not seem as effective when normobaric oxygen was used as pretreatment before a simulated dive in rats (Butler et al., 2006). Nonetheless, Castagna et al. found that oxygen prebreathing provides a significant reduction in decompression-induced bubble formation, regardless of the experimental conditions (Castagna et al., 2009). This is confirmed by the work of Bosco et al. although hyperbaric oxygen seems more effective (Bosco et al., 2010).

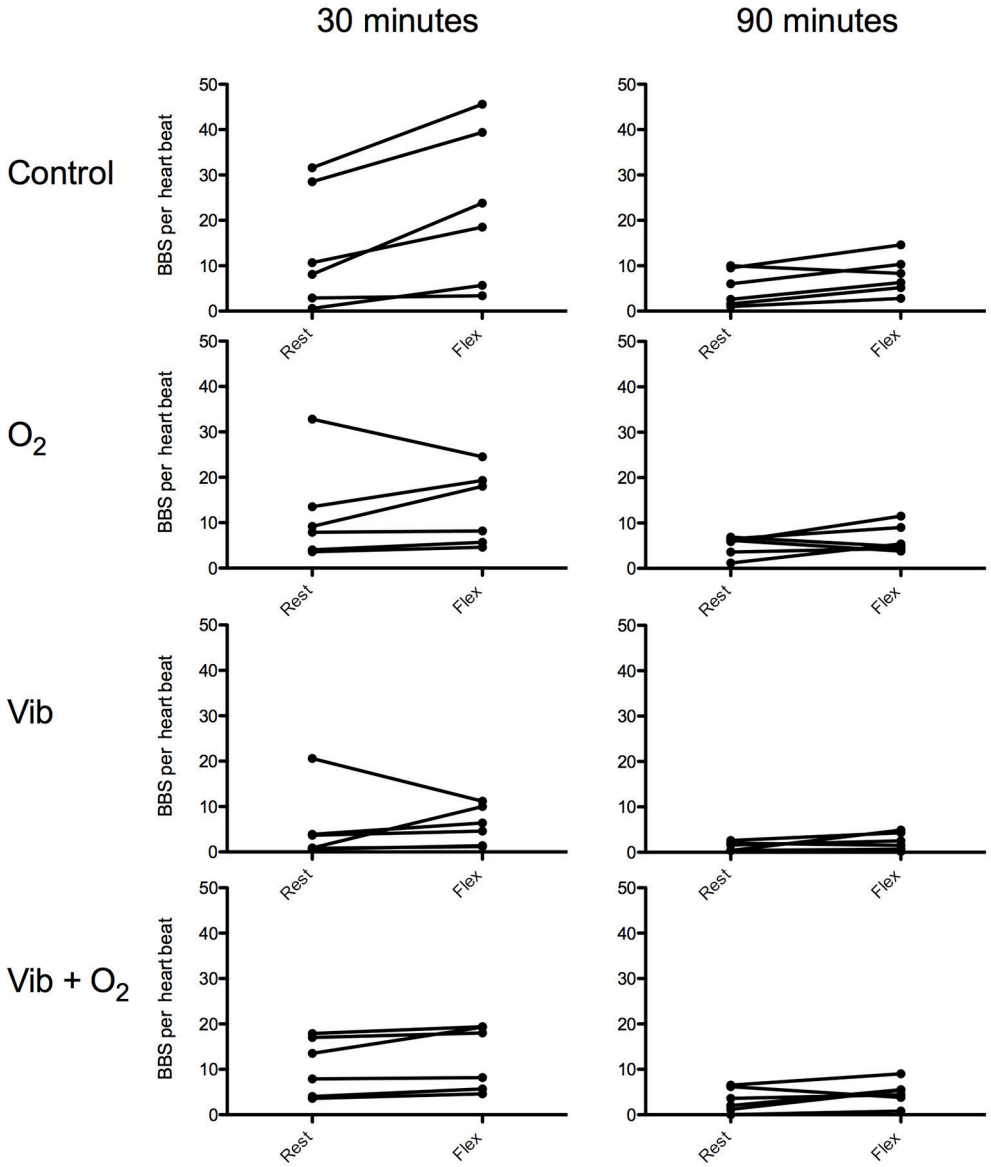

FIGURE 2 | Individual VGE count after a 33 mfw dive without (control) and with preconditioning for 30 min ending 1 h before the dive [oxygenation (O_2), whole body vibration (Vib) or a combination of both (Vib+O_2)]. VGE counts are shown at 30 and 90 min post-dive, before and after knee flex.

Denitrogenation *per-se* does not seem preponderant in the effectiveness of oxygen prebreathing (Gempp and Blatteau, 2010). On the contrary, the proposed mechanism is based on the ability of oxygen to replace nitrogen in the gas nuclei by diffusion. Reduction of tissue oxygen pressure after switching from oxygen to air would then enhance the consumption of oxygen from the gas nuclei, thus eliminating it completely (Arieli et al., 2002). Another possibility is that oxygen administration induces prolonged hemodynamic effects such as decrease in heart rate, cardiac output, and increase in systemic vascular resistance (Waring et al., 2003; Thomson et al., 2006), leading to a reduction in inert gas load in peripheral tissues during diving—which would subsequently reduce post-dive inert gas bubble formation.

Whilst exposure to vibration is traditionally regarded as perilous, recent research has focused on potential benefits. Indeed, it was demonstrated that 30 min of whole-body vibration before a wet dive had preventive effects on post-dive VGE (Germonpré et al., 2009).

Vibration is a mechanical oscillation, i.e., a periodic alteration of force, acceleration and displacement over time. Vibration exercise, in a physical sense, is a forced oscillation, where energy is transferred from an actuator (i.e., the vibration device) to a resonator (i.e., the human body). As a consequence acute physiological responses can be observed.

As in this study there was no observed change in FMD after vibration, the authors did not believe an NO mediated

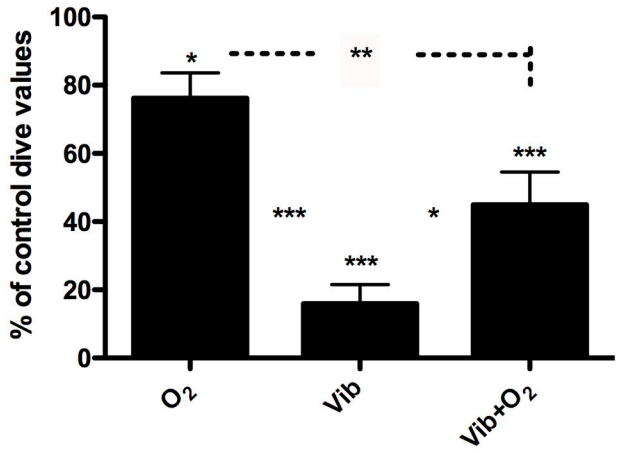

FIGURE 3 | Percentage variation of post-dive VGE count (mean ± SEM) after a 20 min dive to 33 mfw after different preconditioning measures: oxygen prebreathing (O_2), whole-body vibration (Vib), or a combination of both (Vib+O_2). Control dive value is taken as 100%. Each subject is compared to his own control dive value. (***$p < 0.001$; **$p < 0.01$; *$p < 0.05$) ($n = 6$).

mechanism was involved; rather, a mechanical dislodgement of VGE precursors (located in microcrevices between endothelial cells). This is illustrated by the prompt increase of post-dive VGE after a few seconds of exposure on the vibration mattress (Germonpré et al., 2009) or by the knee flexion maneuver, which by increasing the shear stress on the vessel wall, increases the liberation of any existing, adherent gas bubbles (Møllerløkken et al., 2016). Another regional effect may be involved. Vibrations applied to a limb have been shown to increase the rate of lymphatic drainage. Since evacuation of gas bubbles (and nuclei) is possibly happening in part by means of lymphatic fluid (Leduc et al., 1981; Madhavan et al., 2006), it cannot be excluded that an increased lymphatic flow during the whole-body vibration session is partly responsible for the observed effect. Indeed, vibrations could induce, by force transmission, a modification of endothelial spatial conformation. Secondly, the increase in lymphatic circulation induced by vibration (Leduc et al., 1981; Balestra, 2014) would allow the elimination of inter-cellular tissue-located micronuclei.

Therefore, although the exact mechanism by which gas nuclei are eliminated from the vessel by mechanical vibration remains to be clarified, the benefits of whole-body vibration (Vib) are best explained by the mechanical action of vibration on endovascular and tissue localization of the micronuclei.

As stated above, bubbles either grow or shrink depending on surface tension and free gas tension. This also applies to gas nuclei (Papadopoulou et al., 2013), which are thought to be stabilized by trapping in intercellular cervices (Tikuisis, 1986) or by coating with surface-active molecules like surfactant, platelets or proteins (Letho and Laitinen, 1979; Thorsen et al., 1987, 1993). It is thus reasonable to assume a synergistic effect of oxygen and vibration in VibO_2 preconditioning. Yet it is the opposite that we observed, Vib+O_2 being superior to O_2 but inferior to Vib in decreasing post-dive VGE counts.

This absence of synergy could be explained by the fact that the two modes of preconditioning, mechanical or diffusion, could act on the same nuclei and thus be in direct competition.

Oxygen breathing will produce a higher level of reactive oxygen species (ROS), which lead to oxidative stress. Increased production of ROS favors vascular dysfunction (Kuznetsova et al., 2014), inducing a decrease in endovascular NO production, altered vascular permeability and inflammation, accompanied by the loss of vascular modulatory function, the imbalance between vasorelaxation and vasoconstriction, and the aberrant expression of inflammatory adhesion molecules (Bielli et al., 2015). All these mechanisms could then counteract the influence of vibration. However, in the study by Germonpre et al. vibration sessions did not result in a significant modification of endothelial reactivity, as indicated by the FMD measurements (Germonpré et al., 2009). Therefore, the probability that NO production or vessel wall reactivity was significantly altered in the present study (that uses the same experimental setting) is low. It is also possible that since oxygen administration induced prolonged hemodynamic effects such as decrease in heart rate, cardiac output, and increase in systemic vascular resistance (Waring et al., 2003; Thomson et al., 2006), blood flow was sufficiently reduced to diminish the necessary shear forces induced by vibration reducing the capacity of the mechanical intervention to dislodge gas nuclei.

However, the most likely hypothesis explaining this lack of potentiation is that mechanical denucleation is the preponderant mechanism.

CONCLUSIONS

The precise mechanism that induces the decrease in post-dive VGE and thus makes the diver more resistant to decompression stress is still not known. Different preconditioning methods based on oxygen prebreathing or whole-body vibration produce significant results. However, it seems that a pre-dive mechanical reduction of existing gas nuclei might best explain the beneficial effects observed. The apparent non-synergic effect of oxygen and vibration has probably to be understood because of different mechanisms involved.

AUTHOR CONTRIBUTIONS

All authors gave substantial contributions to the conception or design of the work; the acquisition, analysis, and interpretation of data for the work. PG, CB, FG, and PL were responsible for drafting the work or revising it critically for important intellectual content. Final approval of the version to be published was made by CB, FG, and PL.

FUNDING

This study is part of the Phypode Project, financed by the European Union under a Marie Curie Initial Training Network Program FRP/2007-2013/ under REA grant agreement n° 264816.

ACKNOWLEDGMENTS

The authors thank Ing. J. Beernaerts for accepting us in his diving pool, Nemo 33; also, GE Belgium for the generous loan and technical support for the Vivid-i portable echocardiograph and probes, and of course all volunteers (divers and supporting staff) for participating in this study.

REFERENCES

Arieli, Y., Arieli, R., and Marx, A. (2002). Hyperbaric oxygen may reduce gas bubbles in decompressed prawns by eliminating gas nuclei. *J. Appl. Physiol.* 92, 2596–2599. doi: 10.1152/japplphysiol.01059.2001

Arieli, Y., Katsenelson, K., and Arieli, R. (2007). Bubble reduction after decompression in the prawn *Palaemon elegans* by pretreatment with hyperbaric oxygen. *Undersea Hyperb. Med.* 34, 369–378.

Balestra, C. (2014). The lymphatic pathway for microbubbles. *Diving Hyperb. Med.* 44:1.

Bielli, A., Scioli, M. G., Mazzaglia, D., Doldo, E., and Orlandi, A. (2015). Antioxidants and vascular health. *Life Sci.* 143, 209–216. doi: 10.1016/j.lfs.2015.11.012

Blatteau, J. E., David, H. N., Valleé, N., Meckler, C., Demaistre, S., Risso, J. J., et al. (2014). Cost-efficient method and device for the study of stationary tissular gas bubble formation in the mechanisms of decompression sickness. *J. Neurosci. Methods* 236, 40–43. doi: 10.1016/j.jneumeth.2014.07.010

Blatteau, J. E., Gempp, E., Balestra, C., Mets, T., and Germonpre, P. (2008). Predive sauna and venous gas bubbles upon decompression from 400 kPa. *Aviat. Space Environ. Med.* 79, 1100–1105. doi: 10.3357/ASEM.2377.2008

Blatteau, J. E., Gempp, E., Galland, F. M., Pontier, J. M., Sainty, J. M., and Robinet, C. (2005). Aerobic exercise 2 hours before a dive to 30 msw decreases bubble formation after decompression. *Aviat. Space Environ. Med.* 76, 666–669.

Blatteau, J. E., Souraud, J. B., Gempp, E., and Boussugues, A. (2006). Gas nuclei, their origin, and their role in bubble formation. *Aviat. Space Environ. Med.* 76, 666–669.

Blogg, S. L., and Gennser, M. (2011). The need for optimisation of post-dive ultrasound monitoring to properly evaluate the evolution of venous gas emboli. *Diving Hyperb. Med.* 41, 139–146.

Blogg, S. L., Gennser, M., Møllerløkken, A., and Brubakk, A. O. (2014). Ultrasound detection of vascular decompression bubbles: the influence of new technology and considerations on bubble load. *Diving Hyperb. Med.* 44, 35–44.

Bosco, G., Yang, Z. J., Di Tano, G., Camporesi, E. M., Faralli, F., Savini, F., et al. (2010). Effect of in-water oxygen prebreathing at different depths on decompression-induced bubble formation and platelet activation. *J. Appl. Physiol.* 108, 1077–1083. doi: 10.1152/japplphysiol.01058.2009

Butler, B. D., Little, T., Cogan, V., and Powell, M. (2006). Hyperbaric oxygen prebreathe modifies the outcome of decompression sickness. *Undersea Hyperb. Med.* 33, 407–417.

Buzzacott, P. L. (2012). The epidemiology of injury in scuba diving. *Med. Sport Sci.* 58, 57–79. doi: 10.1159/000338582

Castagna, O., Brisswalter, J., Vallee, N., and Blatteau, J. E. (2011). Endurance exercise immediately before sea diving reduces bubble formation in scuba divers. *Eur. J. Appl. Physiol.* 111, 1047–1054. doi: 10.1007/s00421-010-1723-0

Castagna, O., Gempp, E., and Blatteau, J. E. (2009). Pre-dive normobaric oxygen reduces bubble formation in scuba divers. *Eur. J. Appl. Physiol.* 106, 167–172. doi: 10.1007/s00421-009-1003-z

Christman, C. L., Catron, P. W., Flynn, E. T., and Wheathersby, P. K. (1986). *In vivo* microbubble detection in decompression sickness using a second harmonic resonant bubble detector. *Undersea Biomed. Res.* 13, 1–18.

Finkelstein, Y., and Tamir, A. (1985). Formation of gas bubbles in supersaturated solutions of gases in water. *AIChE J.* 31, 1409–1418. doi: 10.1002/aic.690310902

Foster, P. P., Pollock, N. W., Conkin, J., Dervay, J. P., Caillot, N., Chhikara, R. S., et al. (2013). Protective mechanisms in hypobaric decompression. *Aviat. Space Environ. Med.* 84, 212–225. doi: 10.3357/ASEM.3314.2013

Gempp, E., and Blatteau, J. E. (2010). Preconditioning methods and mechanisms for preventing the risk of decompression sickness in scuba divers: a review. *Res. Sports Med.* 18, 205–218. doi: 10.1080/15438627.2010.490189

Gempp, E., Blatteau, J. E., Pontier, J. M., Balestra, C., and Louge, P. (2009). Preventive effect of pre-dive hydration on bubble formation in divers. *Br. J. Sports Med.* 43, 224–228. doi: 10.1136/bjsm.2007.043240

Germonpré, P., Papadopoulou, V., Hemelryck, W., Obeid, G., Lafère, P., Eckersley, R. J., et al. (2014). The use of portable 2D echocardiography and 'frame-based' bubble counting as a tool to evaluate diving decompression stress. *Diving Hyperb. Med.* 44, 5–13.

Germonpré, P., Pontier, J. M., Gempp, E., Blatteau, J. E., Deneweth, S., Lafère, P., et al. (2009). Pre-dive vibration effect on bubble formation after a 30-m dive requiring a decompression stop. *Aviat. Space Environ. Med.* 80, 1044–1048. doi: 10.3357/ASEM.2588.2010

Katsenelson, K., Arieli, Y., Abramovich, A., Feinsod, M., and Arieli, R. (2007). Hyperbaric oxygen pretreatment reduces the incidence of decompression sickness in rats. *Eur. J. Appl. Physiol.* 101, 571–576. doi: 10.1007/s00421-007-0528-2

Kuznetsova, T., Van Vlierberghe, E., Knez, J., Szczesny, G., Thijs, L., Jozeau, D., et al. (2014). Association of digital vascular function with cardiovascular risk factors: a population study. *BMJ Open* 4:e004399. doi: 10.1136/bmjopen-2013-004399

Ladd, G., Stepan, V., and Stevens, L. (2002). The Abacus project: establishing the risk of recreational scuba death and decompression illness. *J. South Pacific Underw. Med. Soc.* 32, 124–128.

Landolfi, A., Yang, Z. J., Savini, F., Camporesi, E. M., Faralli, F., and Bosco, G. (2006). Pre-treatment with hyperbaric oxygenation reduces bubbles formation and platelet activation. *Sport Sci. Health* 1, 122–128. doi: 10.1007/s11332-006-0022-y

Leduc, A., Lievens, P., and Dewald, J. (1981). The influence of multidirectional vibrations on wound healing and on regeneration of blood- and lymph vessels vessel. *Lymphology* 14, 179–185.

Lee, Y. C., Wu, Y. C., Gerth, W. A., and Vann, R. D. (1993). Absence of intravascular bubble nucleation in dead rats. *Undersea Hyperb. Med.* 20, 289–296.

Letho, V. P., and Laitinen, L. A. (1979). Scanning and transmission electron microscopy of the blood-bubble interface in decompressed rats. *Aviat. Space Environ. Med.* 50, 803–807.

Levett, D. Z., and Millar, I. L. (2008). Bubble trouble: a review of diving physiology and disease. *Postgrad. Med. J.* 84, 571–578. doi: 10.1136/pgmj.2008.068320

Madhavan, G., Cole, J. P., Pierce, C. S., and McLeod, K. J. (2006). Reversal of lower limb venous and lymphatic pooling by passive non-invasive calf muscle pump stimulation. *Conf. Proc. IEEE Enf. Med. Biol. Soc.* 1, 2875–2877. doi: 10.1109/iembs.2006.260364

Marroni, A., Bennett, P. B., Cronje, F. J., Cali-Corleo, R., Germonpre, P., Pieri, M., et al. (2004). A deep stop during decompression from 82 fsw (25 m) significantly reduces bubbles and fast tissue gas tensions. *Undersea Hyperb. Med.* 31, 233–243

World Medical Association (2013). World Medical Association Declaration of Helsinki: ethical principles for medical research involving human subjects. *JAMA* 310, 2191–2194. doi: 10.1001/jama.2013.281053

Møllerløkken, A., Blogg, S. L., Doolette, D. J., Nishi, R. Y., and Pollock, N. W. (2016). Consensus guidelines for the use of ultrasound for diving research. *Diving Hyperb. Med.* 46, 26–32.

NAVSEA (ed.). (2008) "Air decompression," in *US Navy Diving Manual* (Revision 6): *SS521-AG-PRO-010/0910- LP-106-0957*, Vol 2. Washington, DC: U.S. Government Printing Office, 1–84.

Nishi, R. Y. (1972). Ultrasonic detection of bubbles with doppler flow transducers. *Ultrasonics* 10, 173–179. doi: 10.1016/0041-624X(72)90359-9

Papadopoulou, V., Eckersley, R. J., Balestra, C., Karapantsios, T. D., and Tang, M. X. (2013). A critical review of physiological bubble formation in hyperbaric decompression. *Adv. Colloid Interface Sci.* 191–192, 22–30. doi: 10.1016/j.cis.2013.02.002

Pollock, N. W., and Nishi, R. Y. (2014). Ultrasonic detection of decompression-induced bubbles. *Diving Hyperb. Med.* 44, 2–3.

Ranapurwala, S. I., Bird, N., Vaithiyanathan, P., and Denoble, P. J. (2014). Scuba diving injuries among Divers Alert Network members 2010–2011. *Diving Hyperb. Med.* 44, 79–85.

Theunissen, S., Balestra, C., Boutros, A., De Bels, D., Guerrero, F., and Germonpré, P. (2015). The effect of pre-dive ingestion of dark chocolate on endothelial function after a scuba dive. *Diving Hyperb. Med.* 45, 4–9.

Thomson, A. J., Drummond, G. B., Waring, W. S., Webb, D. J., and Maxwell, S. R. (2006). Effects of short-term isocapnic hyperoxia and hypoxia on cardiovascular function. *J. Appl. Physiol.* 101, 809–816. doi: 10.1152/japplphysiol.01185.2005

Thorsen, T., Dalen, H., Bjerkvig, R., and Holmsen, H. (1987). Transmission and scanning electron microscopy of N2 micro-bubble activated human platelets *in vitro*. *Undersea Biomed. Res.* 14, 45–58.

Thorsen, T., Klausen, H., Lie, R. T., and Holmsen, H. (1993). Bubble-induced aggregation of patelets: effects of gas species, proteins and decompression. *Undersea Hyperb. Med.* 20, 101–119.

Tikuisis, P. (1986). Moding the observations of *in vivo* bubble formation with hydrophobic crevices. *Undersea Biomed. Res.* 13, 165–180.

Trout, B. M., Caruso, J. L., Nelson, C., Denoble, P. J., Nord, D. A., Chimiak, J., et al. (2015). *DAN Annual Diving Report 2012–2015 Edition: A Report on 2010-2013 Data on Diving Fatalities, Injuries, and Incidents*. Durham, NC.

Vann, R. D. (2004). "Mechanisms and risks of decompression," in *Bove and Davis' Diving Medicine. Saunders,* ed A. A. Bove (Philadelphia, PA: Saunders), 127–164. doi: 10.1016/b978-0-7216-9424-5.x5001-1

Vann, R., D. Grimstad J, Nielsen C., H. (1980). Evidence for gas nuclei in decompressed rats. *Undersea Biomed. Res.* 7, 107–112.

Waring, W. S., Thomson, A. J., Adwani, S. H., Rosseel, A. J., Potter, J. F., Webb, D. J., et al. (2003). Cardiovascular effects of acute oxygen administration in healthy adults. *J. Cardiovasc. Pharmacol.* 42, 245–250. doi: 10.1097/00005344-200308000-00014

Webb, J. T., Morgan, T. R., and Sarsfield, S. D. (2016). Altitude Decompression sickness risk and physical activity during exposure. *Aerosp. Med. Hum. Perform.* 87, 516–520. doi: 10.3357/AMHP.4390.2016

Webb, J. T., and Pilmanis, A. A. (2011). Fifty years of decompression sickness research at Brooks AFB, TX: 1960-2010. *Aviat. Space Environ. Med.* 82(Suppl. 5), A1–A25. doi: 10.3357/ASEM.2576.2011

Wienke, B. R. (2009). Diving decompression models and bubble metrics: modern computer syntheses. *Comput. Biol. Med.* 39, 309–331. doi: 10.1016/j.compbiomed.2008.12.013

Yount, D. E., Yeung, C. M., and Ingle, F. W. (1979). Determination of the radii of gas cavitation nuclei by filtering gelatin. *J. Acoust. Soc. Am.* 65, 1440–1450. doi: 10.1121/1.382905

Zheng, Q., Durben, D. J., Wolf, G. H., and Angell, C. A. (1991). Liquids at large negative pressures: water at the homogenous nucleation limit. *Science* 254, 829–832. doi: 10.1126/science.254.5033.829

Conflict of Interest Statement: The authors declare that the research was conducted in the absence of any commercial or financial relationships that could be construed as a potential conflict of interest.

frontiers in Physiology

ORIGINAL RESEARCH
published: 10 January 2017
doi: 10.3389/fphys.2016.00689

The Effects of Intensive Weight Reduction on Body Composition and Serum Hormones in Female Fitness Competitors

Juha J. Hulmi[1,2], Ville Isola[1], Marianna Suonpää[3], Neea J. Järvinen[1], Marja Kokkonen[4], Annika Wennerström[5,6], Kai Nyman[7], Markus Perola[5,6,8], Juha P. Ahtiainen[1] and Keijo Häkkinen[1]*

[1] Department of Biology of Physical Activity, Neuromuscular Research Center, University of Jyväskylä, Jyväskylä, Finland, [2] Department of Physiology, Faculty of Medicine, University of Helsinki, Helsinki, Finland, [3] Department of Health Sciences, University of Jyväskylä, Jyväskylä, Finland, [4] Department of Physical Education, University of Jyväskylä, Jyväskylä, Finland, [5] Genomics and Biomarkers Unit, Department of Health, National Institute for Health and Welfare, Helsinki, Finland, [6] Institute for Molecular Medicine Finland and Diabetes and Obesity Research Program, University of Helsinki, Helsinki, Finland, [7] Central Hospital of Central Finland, Jyväskylä, Finland, [8] The Estonian Genome Center of the University of Tartu, Tartu, Estonia

OPEN ACCESS

Edited by:
Antonio L'Abbate, Sant'Anna School of Advanced Studies, Italy

Reviewed by:
Matteo Maria Pecchiari, University of Milan, Italy
Eric Helms, Auckland University of Technology, New Zealand

***Correspondence:**
Juha J. Hulmi
juha.hulmi@jyu.fi

Specialty section:
This article was submitted to Integrative Physiology, a section of the journal Frontiers in Physiology

Received: *17 November 2016*
Accepted: *23 December 2016*
Published: *10 January 2017*

Citation:
Hulmi JJ, Isola V, Suonpää M, Järvinen NJ, Kokkonen M, Wennerström A, Nyman K, Perola M, Ahtiainen JP and Häkkinen K (2017) The Effects of Intensive Weight Reduction on Body Composition and Serum Hormones in Female Fitness Competitors. Front. Physiol. 7:689. doi: 10.3389/fphys.2016.00689

Worries about the potential negative consequences of popular fat loss regimens for aesthetic purposes in normal weight females have been surfacing in the media. However, longitudinal studies investigating these kinds of diets are lacking. The purpose of the present study was to investigate the effects of a 4-month fat-loss diet in normal weight females competing in fitness-sport. In total 50 participants finished the study with 27 females (27.2 ± 4.1 years) dieting for a competition and 23 (27.7 ± 3.7 years) acting as weight-stable controls. The energy deficit of the diet group was achieved by reducing carbohydrate intake and increasing aerobic exercise while maintaining a high level of protein intake and resistance training in addition to moderate fat intake. The diet led to a ∼12% decrease in body weight ($P < 0.001$) and a ∼35–50% decrease in fat mass (DXA, bioimpedance, skinfolds, $P < 0.001$) whereas the control group maintained their body and fat mass (diet × group interaction $P < 0.001$). A small decrease in lean mass (bioimpedance and skinfolds) and in vastus lateralis muscle cross-sectional area (ultrasound) were observed in diet ($P < 0.05$), whereas other results were unaltered (DXA: lean mass, ultrasound: triceps brachii thickness). The hormonal system was altered during the diet with decreased serum concentrations of leptin, triiodothyronine (T3), testosterone ($P < 0.001$), and estradiol ($P < 0.01$) coinciding with an increased incidence of menstrual irregularities ($P < 0.05$). Body weight and all hormones except T3 and testosterone returned to baseline during a 3–4 month recovery period including increased energy intake and decreased levels aerobic exercise. This study shows for the first time that most of the hormonal changes after a 35–50% decrease in body fat in previously normal-weight females can recover within 3–4 months of increased energy intake.

Keywords: fat loss, exercise, nutrition, fitness, body composition, sex hormones, thyroid hormones

INTRODUCTION

Many persons lead an active lifestyle aiming to lose body fat with minimal muscle loss for aesthetic or performance purposes. An extreme example of these individuals are competitors in different aesthetic and/or weight class sports (Sundgot-Borgen et al., 2013). These fat loss regimens are very popular and are shown regularly in the media in a similar way as diets for the obese are (Fothergill et al., 2016). Although, worries have arisen about the negative consequences of these diets on, for example, the female hormonal system, comprehensive longitudinal weight-loss studies investigating these diets are lacking on this area, especially in normal-weight females. This lack of studies is probably due to ethical reasons and practical constraints as it is not ethical to conduct a randomized controlled trial (RCT) with normal weight individuals so that the participants would diet as heavily as needed in these kinds of situations.

A classic Minnesota starvation study in the 1940s investigated the effects of prolonged and extreme dieting in young previously normal weights males (Keys et al., 1950; Dulloo et al., 1996). This type of a long-term semi-starvation experiment would no longer be possible in civilized countries and thus only much shorter semi-starvation studies have been conducted, mainly in males (Alemany et al., 2008; Henning et al., 2014; Müller et al., 2015). Nevertheless, cross-sectional and longitudinal refeeding studies have been conducted in females with low energy availability such as anorexia nervosa or with the female athlete triad. These studies have shown that prolonged undernutrition is often associated with low fat and lean mass, decreased bone mineral content, and other physiological and psychological changes from which recovery can be very slow and difficult (Sundgot-Borgen et al., 2013). It is not known how well a normal weight female body can recover from an energy deficit.

There is a lack of studies in females even though they often take part in weight reduction ending up in a rather large energy deficit. For this research question, female fitness competitors are important as they voluntarily conduct a prolonged heavy diet concurrent to participating in a large amount of exercise. The aim of these competitors is to achieve an aesthetic appearance with symmetry, balance, and muscle "definition" that is accomplished by low fat mass. These competitors usually compete and thus diet once per year. Their routine includes a 2–5 month progressive diet ending up in a state of low energy intake, which is usually achieved mainly by decreasing carbohydrate and/or fat intake with maintenance of high protein. Furthermore, exercise volume is increased to reduce fat mass effectively while maintaining muscle mass (Helms et al., 2014, 2015). The diet is typically followed by a recovery period, during which the competitors increase their energy intake back to baseline. This is quite a contrast to overweight individuals, who try to maintain their weight loss, although only rarely that goal is achieved (Fothergill et al., 2016). Previous weight loss studies with fitness athletes or bodybuilders have often been case studies using male bodybuilders (Rossow et al., 2013; Kistler et al., 2014; Robinson et al., 2015) or they have focused only on body composition, muscle strength (Sandoval et al., 1989; Bamman et al., 1993; van der Ploeg et al., 2001), or psychology (Newton et al., 1993). Thus, physiology, including the hormonal system, has not yet been comprehensively investigated in a larger group of individuals following a diet that aims to achieve very low levels of fat mass.

In the present study voluntary fitness-competitors and their controls are used in a unique research model to investigate the physiological effects of a demanding 3–4 month period of dietary energy restriction concurrent with a large amount of exercise aiming to achieve prolonged negative energy balance. It is also asked whether a similar 3–4 month period of increased energy intake is enough to restore endocrine function and body composition. We hypothesized that (1) fitness-competitors are able to decrease their body mass mainly by decreasing fat mass and that (2) the endocrine system is altered, approaching levels that are typically considered unhealthy if maintained for longer periods of time, and that (3) the hormonal levels are increased back to the baseline together with body weight during the recovery period.

METHODS

Participants

A total of 184 healthy, physically active young females, recruited by web page and social media advertisements and who claimed to meet the inclusion criteria volunteered for the study. Out of the females who fulfilled the preliminary criteria, 63 participants were planning on competing under the International Federation of Bodybuilding and Fitness (IFBB) in the year of the study and, thus, would diet accordingly. In addition, a total of 121 volunteers were aiming not to diet now, but would probably diet later in their life or at least try to maintain a fitness lifestyle. An online pre-study questionnaire was sent to the available 44 diet- and 70 randomly chosen control group candidates that fulfilled the preliminary requirements for the study (see below). Females, who were diagnosed with chronic diseases or prescribed medications such as thyroxine, but excluding contraception, and who were younger than 20 or older than 38 years old, whose BMI was below 20 or above 27, or who did not have at least 2 years of resistance training experience were excluded from the study. As a result, the diet group competing in the autumn of 2015 consisted of 30 volunteers. We chose these exclusion criteria because our aim was to investigate normal-weight healthy previously trained females. An equal number of control participants were quasi-randomized by matching based on their age, height, weight, and training experience reported on the pre-study questionnaire. The participants selected for the study filled in an additional questionnaire that was subsequently reviewed by the physician of our study to confirm that they did not meet the exclusion criteria relating to health.

All of the diet participants were IFBB amateur fitness competitors aiming to lose fat, but maintain their muscle mass in a sport that is tested for prohibited performance enhancing drugs. Out of these participants, 17 were bikini fitness and 9 body fitness competitors and 1 was a fitness competitor. These groups were very similar at the baseline and with regard to the changes during diet (body composition and hormones, data not shown).

The subjects were given comprehensive explanations regarding the study design, protocols, and possible risks. This

study was carried out in accordance with the recommendations of Ethical Committee at the University of Jyväskylä with written informed consent from all subjects. All subjects gave written informed consent in accordance with the Declaration of Helsinki. The protocol was approved by the Ethical Committee at the University of Jyväskylä.

Study Design

The study included 3 test days at the laboratory: baseline testing before the diet or the control period started (Pre), after the diet (Mid), and after a refeed recovery period (Post) during which the participants were advised to continue their training regimen, but to stop dieting. The control participants were advised to maintain their activity levels and nutrient intake throughout the study. The participants were given identification numbers and the measurement team was blinded so that they did not know into which group participants belonged to.

Out of the 30+30 participants eventually 30 volunteers that would follow the diet (referred to as "diet group" from here on) and 29 controls arrived to our baseline testing. During the study, nine females (3 from the diet group and 6 controls) dropped out. All three drop-outs in the diet group stopped dieting due to failing to follow the diet program whereas controls either were not able to follow the control period or for some unknown reason finished the study. This resulted in 50 participants (27 dieters and 23 controls) overall finishing the whole study. The diet group ($n = 27$) was on average 27.2 ± 4.1 years old and the controls 27.7 ± 3.7 years old. The length of the diet-period for the diet group was 19.8 ± 3.6 weeks while the recovery period was 17.5 ± 2.6 weeks. The length of the respective control periods were 22.4 ±5.0 and 19.2 ± 5.3 weeks, respectively. **Figure 1A** depicts the study design and two females from each group.

For 15 of the competitors, this was their first competition diet and the rest of the diet group ($n = 12$) had been dieting for competitions between 1 and 4 times. Three of the 27 of the diet group participants were competing at the world championship level, while the rest competed in the Finnish National championships or in the qualification rounds.

Three Test Days

The participants came to the laboratory from all over the Finland. If they traveled >50 km to our laboratory, they were provided with a hotel room for the night prior to testing. **Figure 1B** depicts the measurement day of the participant in the laboratory. The participants came to the tests after 8 h of fasting and the first measurements (blood sampling, DXA, bioimpedance) were conducted before a quick standardized low-fat breakfast (a protein-drink, a protein bar and a medium-sized apple/banana: in total ∼47–48 g proteins, ∼72–80 g carbohydrates, ∼6 g fat). Thereafter, ultrasound, skinfolds, blood pressure, and muscle strength measurements were conducted. The breakfast was especially important in the measurements after the diet since some of the participants were in a large energy deficit and potentially not able to perform, for example, muscle strength testing in a reliable and safe manner. The mid measurement day after the diet was conducted the morning after the competition.

All the measurements were conducted at the same time (always within max ±1 h) due to the importance of standardizing the time of the day of measurements. The control group participants were measured on the same days as the competitors. The same researcher/research assistant was always responsible for conducting the measurements and analysis to avoid interobserver/-analyzer variability. The participants were asked to sleep for at least 8 h during the preceding night and were required to refrain from strenuous physical activity for at least 24 h.

Resistance and Aerobic Training

The resistance training background of the participants was 3.5 ± 1.4 years in the diet group and 3.1 ± 1.1 years in the control group. The participants trained with their own training programs and they were asked to provide their training diaries throughout the study period. The training frequency, intensity and volume were calculated from the diaries. Total exercise metabolic equivalents in hours (MET-hours) were calculated based on recommendations (Ainsworth et al., 2000).

Split routines were used for resistance training by all competitors in the diet group meaning that they focused on single muscle groups per session as is often the case also in bodybuilders (Hackett et al., 2013). The main muscle groups trained included thighs, hamstrings, buttocks, chest, shoulders, arms, upper and lower back, calves, and abdominals. Dividing training into separate body parts per session did not differ significantly throughout the training. At baseline the 3-, 4-, 5-, and 6-split training was used by 3, 10, 13, and 1 of the 27 participants, respectively, while the same numbers were during the diet on average 5, 8, 14, and 0 and during the recovery period 7, 8, 12, and 0. In addition, the competitors also practiced their posing routines. Training sessions lasted between 40 and 90 min.

Aerobic training for the participants was almost uniquely either high-intensity interval training (HIT) with bicycle, crosstrainer, or other gym equipment or both HIT and steady-state low to medium intensity aerobics (usually walking/running or with crosstrainer). During the competition week the participants did not report doing HIT, but instead lower intensity aerobics. Typical HIT-exercise was 10–25 min in total including high intensity 15–45 s intervals with 30–60 s of recovery between the sets. Steady state lower intensity aerobics was typically 30–60 min in duration. Part of the females completed their aerobic training mainly together with their resistance exercise workouts while most of the participants completed also separate aerobic workouts, especially during the diet.

At the last week of a typical fitness or bodybuilding diet there is a tapering period during which total training load is typically slightly decreased and carbohydrate and total energy intakes are increased toward the baseline levels. This is conducted to replenish muscle glycogen stores and, thus, prevent an artificial decrease in muscle size that occurs with low carbohydrate diets as ∼2.7 g of water per each gram of glycogen is stored in skeletal muscle.

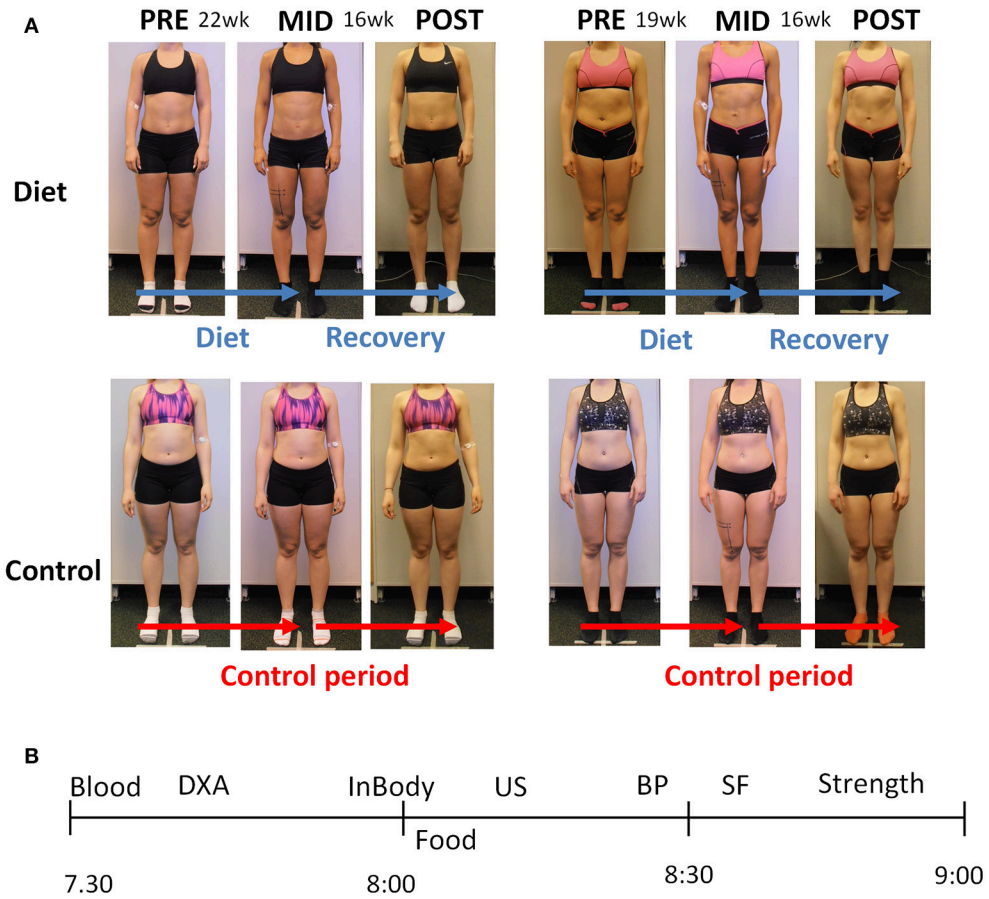

FIGURE 1 | (A) The experimental design of the study. Two representative participants are shown from each group. The pre to mid time period lasted ~20 weeks during which the participants decreased their energy intake and the amount of exercise (see the Results Section), whereas the controls maintained their activity levels and nutrient intake. The mid to post period lasting ~18 weeks was a recovery period with increased energy intake back toward the baseline levels in the diet participants, whereas the controls maintained their energy intake and exercise levels (see the Results Section). **(B)** The measurement day example for each participant. The x-axis depicts AM-time (morning). Blood, blood sample; DXA, Dual-energy X-ray absorptiometry; InBody, bioelectrical impedance; Food, breakfast; US, ultrasound; BP, blood pressure; SF, skinfolds; Strength, muscle strength measurements.

Nutrient Intake

The participants maintained their diet during the diet phase. About 50% percent of the participants reported all their meals to the investigators. The rest of the participants had a more flexible diet or did not share all the details of their diet, but, instead reported representative days throughout the diet. The controls kept their dietary diary over 3 weekdays and 1 weekend day at the baseline, in the middle of the study and during the last part of the study. Nutrients provided by nutritional supplements were included in the analysis. The food diaries were analyzed by nutrient analysis software (Aivodiet, Flow-team Oy, Oulu, Finland).

Body Composition

DXA

Body composition was estimated by Dual-energy X-ray absorptiometry (DXA, Lunar Prodigy Advance, GE Medical Systems—Lunar, Madison WI USA) using methods similar to Hulmi et al. (2015) in a fasted state. Participants were tested on their back in a supine position on the DXA table with their arms at their sides and feet together with minimal clothing (i.e., a pair of shorts). The legs were secured by non-elastic straps at the knee and ankles, and the arms were aligned along the trunk with the palms facing the thighs. All metal objects were removed from the participant before the scan. Analysis (using enCORE 2005, version 9.30 and Advance 12.30) provided total, lean (bone-free), bone, and fat masses. The android region is the area between the ribs and the pelvis within the trunk region (the upper part of the trunk) and correlates with visceral fat measures (Hill et al., 2007; Miazgowski et al., 2014). High levels of visceral fat mass are strongly associated with metabolic abnormalities (Kang et al., 2011). The gynoid area defined by the software is a region including the sex organs and lower-part of the hips (Miazgowski et al., 2014). In a previous study in our laboratory the intraclass correlation coefficient (ICC) for the body composition measures were 0.786–0.975 (Schumann et al., 2014).

Bioimpedance

After an overnight fast, body fat percentage, fat, and lean masses were measured by bioelectrical impedance using an InBody720 machine with a multifrequency current (Seoul, Korea).

Skinfolds

Skinfold thicknesses were analyzed with Harpender calibers from four sites: biceps, triceps, subscapular, and suprailiac and replicated at least three times. Fat percentage was calculated with a formula (Durnin and Womersley, 1974) while total fat mass and fat-free masses were calculated by subtraction from body mass.

Ultrasound for Muscle Cross-Sectional Area and Thickness and Subcutaneous Fat Thickness

Cross-sectional area (CSA) of the vastus lateralis muscle was examined at the mid-thigh by extended field of view mode using a B-mode axial plane ultrasound (model SSD-α10, Aloka, Tokyo, Japan) using a 10 MHz linear-array probe (60 mm width) with the extended-field-of-view mode (23 Hz sampling frequency). The CSA of the vastus lateralis muscle was determined from two levels: the first was exactly 40% from the superior point of patella toward anterior superior spina iliaca and the second 2 cm distally from the first level. The thickness of subcutaneous fat in the thigh was examined from the 40% line mentioned above, but at the medial-lateral axis at the border of vastus lateralis and rectus femoris. The thickness of triceps brachii muscle and subcutaneous fat were measured at exactly the midpoint between medial epicondyle and acromion. A customized convex-shaped probe support coated with water-soluble transmission gel was used to assure a perpendicular measurement and to constantly distribute pressure on the tissue. For CSA, the transducer was moved manually from medial to lateral along a marked line on the skin. Three images were scanned from each lines (CSA) and measurement point (thicknesses). CSA and thicknesses were analyzed manually using ImageJ software (version 1.44p; National Institutes of Health, Bethesda, MD). The average values were used for the statistical analyses. The panoramic ultrasound method has been shown by us to be very reliable and valid against magnetic resonance imaging (MRI) to detect resistance training-induced change in muscle CSA in our laboratory, e.g., ICC $>$ 0.9 and high limits of agreement by Bland Altman method (Ahtiainen et al., 2010). Also for subcutaneous fat thickness intra-assay CV and reliability for this method are high (Müller et al., 2016).

Maximal and Explosive Strength

In the beginning of the actual measurements, the participants were carefully familiarized with the test procedures and techniques. The participants had a general warm up (body-weight 1- and 2-legged squats and hand rotations) after which several warm-up trials were performed on each test device. A horizontal leg press extension dynamometer (custom built: Department of Biology of Physical Activity, University of Jyväskylä, Jyväskylä, Finland) was used to determine maximal isometric bilateral leg press force (maximal voluntary contraction, MVC). In the leg press, the participants were seated with a hip and knee angle of 110° and 107°, respectively. Maximal leg extension force was analyzed by a customized script (Signal 4.04, Cambridge Electronic Design, UK). Maximal isometric bilateral bench press for the upper-body strength (MVC) was measured in a smith-machine and the bar was locked to the position with the elbow angle of 90° (Ojasto and Häkkinen, 2009). The subject was in a supine position on the bench and pushed against the fixed bar. The test position including the wideness of the grip was standardized throughout the study. The maximum force was measured by the force plates under the bench using a customized script (Signal 4.04, Cambridge Electronic Design, UK). In these isometric tests, the participants were instructed to produce maximal force on verbal command and to maintain their maximal force plateau for 3–4 s while being verbally encouraged. Maximal explosive strength of the hip and knee extensors was measured using a vertical counter movement jump (Komi and Bosco, 1978) on a custom-built infrared contact mat (Department of Biology of Physical activity, University of Jyväskylä). The height of rise of the center of gravity was calculated from the flight time. The subjects were instructed to perform a quick and explosive countermovement and to jump as high as possible while their hands were on the hips throughout the action. In each strength test 3 maximal trials were conducted with recovery periods of 1 min in the isometric tests and 0.5 min in the jump test. Up to two additional trials were performed if the result during the last trial was greater by 5% compared with that during the previous attempt. The trial with the highest result was used for statistical analysis.

Blood Pressure and Heart Rate

The participants were seated in a quiet room and after resting their blood pressure and heart rate (pulse) was measured using calibrated Omron M6 automatic blood pressure monitor with appropriate cuff size (Omron R6, Omron Healthcare, Kyoto, Japan). The measurements were conducted three times and the average was selected as the final result.

Venous Blood Sampling and Analysis

Venous blood samples were taken from the antecubital vein into serum tubes (Venosafe; Terumo Medical Co., Leuven, Hanau, Belgium) using standard laboratory procedures. Whole blood was immediately analyzed (Sysmex XP 300 analyzator Sysmex Inc, Kobe, Japan) for hemoglobin and hematocrit. Blood samples for hormone analysis were stored in room temperature for 30 min, after which they were centrifuged at 3500 rpm for 10 min (Megafure 1.0 R Heraeus; DJB Lab Care, Germany). Free thyroxine (T_4), free triiodothyronine (T_3), thyroid-stimulating hormone (TSH), cortisol, testosterone, estradiol were analyzed from serum by Immulite 2000 XPi immunoassay system (Siemens Healthineers, Erlangen, Germany). Serum leptin was analyzed by Dynex Ds 2 ELISA prosessing System (DYNEX Technologies, Chantilly, VA, USA) using a commercial kit (Human leptin ELISA, BioVendor, Heidelberg, Germany). These hormones are routinely analyzed in our laboratory and day-to day reliability (CV%) for all of these hormones in our laboratory is <8%.

Profile of Moods (POMS) and Reproductive Function Questionnaires

Mood and menstrual bleeding was asked by the questionnaires at pre time-point, in the middle of the pre and mid timepoints and the week before the mid- and post measurements. The participant's mood was examined using the Finnish version (Vuoskoski and Eerola, 2011) of the Profile of Mood States-Adolescents questionnaire (POMS-A; Terry et al., 1999). The 24 items of the POMS, designed to measure six moods of Vigor, Confusion, Anger, Fatigue, Depression, and Tension, were rated on a 5-point Likert scale ranging from 1 = not at all to 5 = extremely.

Menstrual/reproductive function questionnaire involves yes or no answers to the following questions: Have you had some of these menstrual irregularities within the last 2 months: 1: menstrual cycle has become irregular, 2: menstrual bleeding has decreased, 3: menstrual bleeding has increased, and 4: no menstrual bleeding.

Statistical Analysis

All data are expressed as means ± SD, except where designated. Normality, skewness and possible outliers were checked with the Shapiro–Wilk test and several plots. Data was analyzed with the repeated ANOVA (time × group) with contrasts. Logarithm transformations were applied when needed to normalize variables or to homogenize group variances. If assumptions for parametric tests were not met even with transformations, nonparametric tests (Friedman's test, Sign test and Mann–Whitney test) were utilized, and variables were RANK-transformed for the estimation of interaction term (time × group in parametric ANOVA). Average percentage changes between groups were tested with the nonparametric Mann–Whitney test due to deviations from normality and outliers. Holm–Bonferroni was used to manually correct for the multi-tests between individual time-points between the groups and within the groups. IBM SPSS for Windows 22.0 (Armonk NY, 2013) was utilized for statistical analyses. Significance level was set as 0.05.

RESULTS

Nutrition

The energy intake during the diet was on average 22.9 ± 13.8% ($p < 0.001$) lower than before the diet, while the energy intake of the control group remained unaltered (**Table 1**). The decreased energy intake in the diet group was mainly explained by reduced carbohydrate ingestion. Although, absolute protein and fat intake slightly decreased, these values were explained by decreased weight and, thus, per kg of body mass only very slight decrease in fat and no changes in protein intake was noticed (**Table 1**). Actually, the relative protein intake (% of total energy) increased ($p < 0.001$) and relative CHO intake decreased ($p < 0.01$), while relative fat intake remained unaltered (Supplementary Table 1). During the recovery energy intake of the participants returned to baseline levels.

Exercise

The training frequencies and MET-hours of the participants are shown in **Table 2**. The participants resistance trained 4.7 ± 0.7 (diet group) and 3.9 ± 1.9 (controls) times per week at the time of the pre-measurements. The diet group maintained their resistance training frequency during the diet, during the competition week and during the recovery period. However, when taking into account the reported length and intensity of their resistance exercise bouts, the MET-hours of the participants decreased during the competition week ($p < 0.001$), probably due to the tapering period fitness-competitors have before the competition. The controls maintained their resistance training frequencies and MET-hours throughout the study period. Lower body muscles were trained during the diet 1.4 ± 0.5 times per week and specific upper body muscle groups 1.1 ± 0.3 times per week in a split design. Unlike resistance training, the diet group increased their aerobic training during the diet (4.9 ± 2.9 times per week) when compared to pre-state (3.6 ± 2.8; $P < 0.05$ and diet × group interaction $p = 0.013$). This was due to the increased amount of steady state aerobics in several subjects, while part of the participants also started to conduct or increased the amount of HIT-exercises. The level of aerobic training decreased during the recovery period in these participants down to 2.3 ± 1.9 times per week while the controls maintained their levels of aerobic training.

Body Composition

Body composition was examined with many indirect measurements [DXA, bioimpedance (InBody) and skinfolds] as well as direct measures (ultrasound) as the diet itself may distort some of the assumptions of individual body composition measurements or their formulas used. There was group × time interaction ($p < 0.001$) in body mass and fat mass independent of the method used (DXA, skinfolds, bioimpedance; **Table 3**) as well as in fat thickness (**Figures 2A,B**; ultrasound). These were explained by the fact that the body and fat mass of the diet group participants decreased during the diet and returned almost completely (body mass) or partially (fat mass and thickness) to the baseline after the recovery period. No change of these parameters was observed in the control group (**Table 3**). This resulted in a decrease in fat % by diet on average from 23.1 ± 5.6 to 12.7 ± 4.0% (DXA), from 19.7 ± 4.2 to 11.6 ± 3.9% (bioimpedance), and from 25.2 ± 3.0 to 18.3 ± 2.7% (skinfolds). From these values, fat % increased during the recovery period to 20.1 ± 5.4%, 18.0 ± 4.5%, and 25.9 ± 4.1% based on DXA, bioimpedance, and skinfold measurements, respectively. Regarding individual areas, the android region in DXA reflecting visceral fat decreased ∼68% in the diet group ($p < 0.001$) and then recovered toward baseline and controls (**Table 3**). Similarly, fat in the gynoid area decreased by diet 44.2 ± 12.8% ($p < 0.001$) followed by an increase close to the pre-values during the recovery period (post–pre: −9.4 ± 19.5%, $p < 0.05$) while remaining unaltered in the controls (diet × group interaction $p < 0.001$).

Unlike body mass and fat mass, diet or the recovery period did not significantly alter lean mass measured by DXA. There

TABLE 1 | Macronutrient consumption.

	Pre	Mid-diet	Diet average	Competition-week	Recovery	Group × time (p)
ENERGY (kJ)						
Diet	9903.7 ± 1785.8	7887.6 ± 1440.9***	7524.2 ± 1556.2***	9789.7 ± 2553.8	9273.4 ± 2186.6	< 0.01
Cont	10446.1 ± 2307.5			9795.0 ± 1774.0	10425.5 ± 1549.8	
ENERGY (kJ/kg bw)						
Diet	155.0 ± 27.8	131.4 ± 24.4***	125.4 ± 26.2***	166.0 ± 61.1	158.8 ± 41.4	0.067
Cont	162.6 ± 34.7			151.9 ± 24.7	163.6 ± 24.5	
PROTEINS (g)						
Diet	202.5 ± 44.1	189.7 ± 39.5*	184.7 ± 40.5*	160.6 ± 32.5**	195.4 ± 41.5	< 0.05
Cont	172.3 ± 37.6			181.9 ± 37.9	184.7 ± 39.5	
PROTEINS (g/kg bw)						
Diet	3.16 ± 0.61	3.14 ± 0.63	3.07 ± 0.64	2.84 ± 0.52	3.34 ± 0.81	0.282
Cont	2.68 ± 0.53			2.81 ± 0.48	2.87 ± 0.85	
CHO (g)						
Diet	215.6 ± 67.7	126.1 ± 49.1***	127.8 ± 39.7***	229.9 ± 199.0	188.5 ± 72.5	< 0.01
Cont	218.8 ± 50.3			216.7 ± 41.4	224.0 ± 49.8	
CHO (g/kg bw)						
Diet	3.35 ± 0.99	2.10 ± 0.84***	2.12 ± 0.66***	4.10 ± 1.65	3.24 ± 1.34	< 0.01
Cont	3.40 ± 0.72			3.37 ± 0.63	3.52 ± 1.05	
FAT (g)						
Diet	64.4 ± 16.2	56.8 ± 16.4*	52.8 ± 16.4***	63.9 ± 25.3	59.7 ± 13.0	0.184
Cont	82.2 ± 23.3			73.8 ± 28.8	84.9 ± 29.4	
FAT (g/kg bw)						
Diet	1.02 ± 0.29	0.95 ± 0.29	0.88 ± 0.29*	1.07 ± 0.49	1.02 ± 0.23	0.692
Cont	1.29 ± 0.38			1.14 ± 0.44	1.34 ± 0.51	

*The results are averaged daily values. *, **, and *** $p < 0.05$–0.001 change vs. pre. bw, body weight; CHO, carbohydrates. Diet × group interaction includes pre and diet average time-points. Data is n = 27 diet and n = 18 control participants at pre and mid/average, n = 21 for the competition week and n = 18 and n = 16 for the diet- and control participants at the recovery. Recovery nutrition diaries were collected from the middle of the recovery period.*

TABLE 2 | Exercise levels.

	Pre	Mid-diet	Second-last week	Competition-week	Recovery	Group × time (p)
RE x/wk						
Diet	4.7 ± 0.7	4.7 ± 0.6	4.7 ± 0.7	4.2 ± 1.1	4.6 ± 0.8	0.961
Cont	3.9 ± 1.9		3.8 ± 1.7		3.8 ± 1.7	
RE METh/wk						
Diet	44.9 ± 8.6	46.0 ± 8.5	45.6 ± 9.7	19.5 ± 10.9***	42.4 ± 8.3	0.186
Cont	31.9 ± 19.5		27.8 ± 14.9		32.2 ± 17.2	
AE x/wk						
Diet	3.6 ± 2.8	4.4 ± 2.9	4.9 ± 2.9*	4.4 ± 2.5	2.3 ± 1.9##	0.013
Cont	2.6 ± 2.6		2.9 ± 2.4		3.3 ± 3.5	
AE METh/wk						
Diet	13.3 ± 10.4	19.1 ± 15.6	22.0 ± 17.1	13.2 ± 8.4	9.7 ± 7.8#	0.015
Cont	17.9 ± 23.7		14.9 ± 14.9		18.3 ± 24.8	

, **, and * is significant $p < 0.05$–0.001 change vs. pre and #–## is significant ($p < 0.05$–< 0.01) difference between the groups in the change. RE, resistance exercise; AE, aerobic exercise. Of the RE-results, n = 24–26 for the diet participants and n = 18 for the controls. Regarding the AE, n = 21–26 and n = 19 for the diet and control participants, respectively.*

was, however, a small, but statistically significant decrease in lean mass, fat-free mass (**Table 3**), and VL-muscle CSA (**Figure 2C**) measured by bioimpedance, skinfolds, and ultrasonography, respectively. These small changes, when existing, were fully recovered during the recovery period (**Table 3**, **Figure 2C**). No significant change was observed in the triceps brachii muscle thickness due to diet or the recovery period (**Figure 2D**). When individual values were looked at more closely, all the females had medium to large decrease in fat mass after diet, but some females of the diet group had a small increase in their lean mass (average of DXA and bioimpedance) while most of them had a decrease or no change (**Figure 2E**).

TABLE 3 | Body composition of the subjects.

	Pre	Mid	Post	ΔMid-Pre	ΔPost-Mid	ΔPost-Pre	Group × time (p)
HEIGHT (cm)							
Diet	165.3 ± 4.3						
Cont	165.9 ± 5.7						
BODY MASS (kg)							
Diet	64.3 ± 6.9	56.5 ± 5.3	62.6 ± 6.9	−11.9 ± 3.8%***	10.9 ± 5.3%***	−2.4 ± 5.6%*	< 0.001
Cont	64.3 ± 5.3	64.5 ± 5.5	64.4 ± 5.5	0.3 ± 3.1%###	−0.1 ± 3.4###	0.1 ± 3.7%	
FAT MASS (DXA: kg)							
Diet	14.6 ± 4.6	7.1 ± 2.7	12.7 ± 4.2	−50.4 ± 12.4%***	84.7 ± 50.7%***	−10.1 ± 25.6%*	< 0.001
Cont	14.9 ± 3.7	15.5 ± 3.9	15.1 ± 4.4	5.1 ± 12.9%###	−2.6 ± 13.2%###	2.1 ± 16.8%	
FAT MASS (InBody: kg)							
Diet	12.8 ± 3.4	6.6 ± 2.5	11.2 ± 3.3	−47.4 ± 17.9%***	91.5 ± 74.0%***	−6.1 ± 29.3%	< 0.001
Cont	13.0 ± 3.1	13.2 ± 3.5	13.0 ± 4.0	2.1 ± 16.2%###	−1.5 ± 15.6%###	−0.1 ± 17.8%	
FAT MASS (SKINFOLDS: kg)							
Diet	16.3 ± 3.3	10.4 ± 2.2	16.4 ± 4.0	−35.2 ± 11.2%#***	57.9 ± 26.7%***	1.3 ± 18.8%	< 0.001
Cont	15.5 ± 9.4	16.2 ± 9.7	16.3 ± 9.9	9.5 ± 29.6%	−4.5 ± 43.6%	9.5 ± 52.4%	
ANDROID FAT (DXA: kg)							
Diet	0.92 ± 0.34	0.25 ± 0.14	0.82 ± 0.30	−68.1 ± 19.8%***	276 ± 204.2%***	2.4 ± 53.6%	< 0.001
Cont	0.98 ± 0.38	1.05 ± 0.43	0.98 ± 0.48	7.8 ± 17.7%###	−6.2 ± 23.4%###	1.2 ± 29.2%	
LEAN MASS (DXA: kg)							
Diet	47.6 ± 4.1	48.0 ± 3.9	48.3 ± 4.3	1.1 ± 3.1%	0.6 ± 3.8%	1.7 ± 4.4%	0.272
Cont	47.3 ± 4.7	47.2 ± 4.7	47.4 ± 5.0	−0.2 ± 2.4%	0.5 ± 2.7%	0.3 ± 3.1%	
LEAN MASS (InBody: kg)							
Diet	48.6 ± 4.9	47.1 ± 4.3	47.9 ± 5.0	−3.0 ± 4.4%**	2.1 ± 3.2%**	−1.1 ± 4.7%	0.341
Cont	49.2 ± 4.9	48.4 ± 4.8	48.5 ± 4.6	−1.6 ± 5.8%	0.2 ± 2.9%	−1.3 ± 6.1%	
FFM (SKINFOLDS: kg)							
Diet	48.0 ± 4.3	46.1 ± 3.9	46.3 ± 4.1	−3.9 ± 2.7%#***	0.4 ± 2.4%	−3.5 ± 3.1%***	< 0.05
Cont	48.8 ± 6.8	48.2 ± 7.0	48.0 ± 7.1	−1.2 ± 3.1%	−0.4 ± 4.0%	−1.6 ± 4.5%	
TOTAL BONE (DXA: kg)							
Diet	2.56 ± 0.28	2.53 ± 0.29	2.56 ± 0.31	−1.3 ± 1.8%***	1.5 ± 3.6%	0.1 ± 3.6%	0.104
Cont	2.57 ± 0.28	2.58 ± 0.29	2.61 ± 0.29	0.3 ± 1.3%##	1.3 ± 2.7%	1.6 ± 2.5% #*	

*Δ are %-changes. *–*** is significant (p < 0.05–< 0.001) difference to Pre and #–### is significant (p < 0.05–< 0.001) difference between the groups in the change. Group × time = ANOVA interaction effect p-value. n = 27 diet and 23 control participants for the variables except InBody in which n = 25 for diet subjects for the post-measurement. FFM = fat-free mass.*

Total bone mass tended to have group × time interaction ($p = 0.10$), which was explained by a decrease in bone mass during diet ($p < 0.001$) while no change was observed in the controls ($p > 0.3$; **Table 3**).

Maximal and Explosive Strength

Isometric maximal strength and explosive strength of leg extensors remained unchanged during diet and there was no difference compared to controls (group × time interaction $p > 0.1$; **Table 4**). However, isometric bench press decreased during the diet when compared to control participants ($p < 0.05$; **Table 4**).

Hormones

There was group × time interaction in serum concentrations of leptin, testosterone, T_3 ($p < 0.001$), and estradiol ($p < 0.01$; **Figures 3A–D**). This was shown as decreases in these hormones due to the diet when compared to the control group. Leptin and estradiol (**Figures 3A,C**) increased back to baseline while T_3 (**Figures 3D**, **4**) and testosterone (**Figure 3B**) remained slightly, but significantly below the baseline even after the recovery period. No changes to the controls at the post timepoints were, however observed. T_4 showed an increase due to diet and a reduction back to baseline during the recovery period, but these changes were small and non-significant in comparison to controls (**Figure 3E**). No treatment × time interaction was observed in TSH and cortisol ($p > 0.19$, **Figures 3F,G**).

Blood Pressure, Heart Rate, Hemoglobin, and Hematocrit

Systolic blood pressure showed a group × time interaction ($p < 0.001$), whereas no effect was observed on diastolic blood pressure ($p = 0.177$) (**Table 5**). The *post-hoc* analysis showed that diet led to decreased systolic blood pressure ($p < 0.001$), which remained decreased after the recovery period, when compared

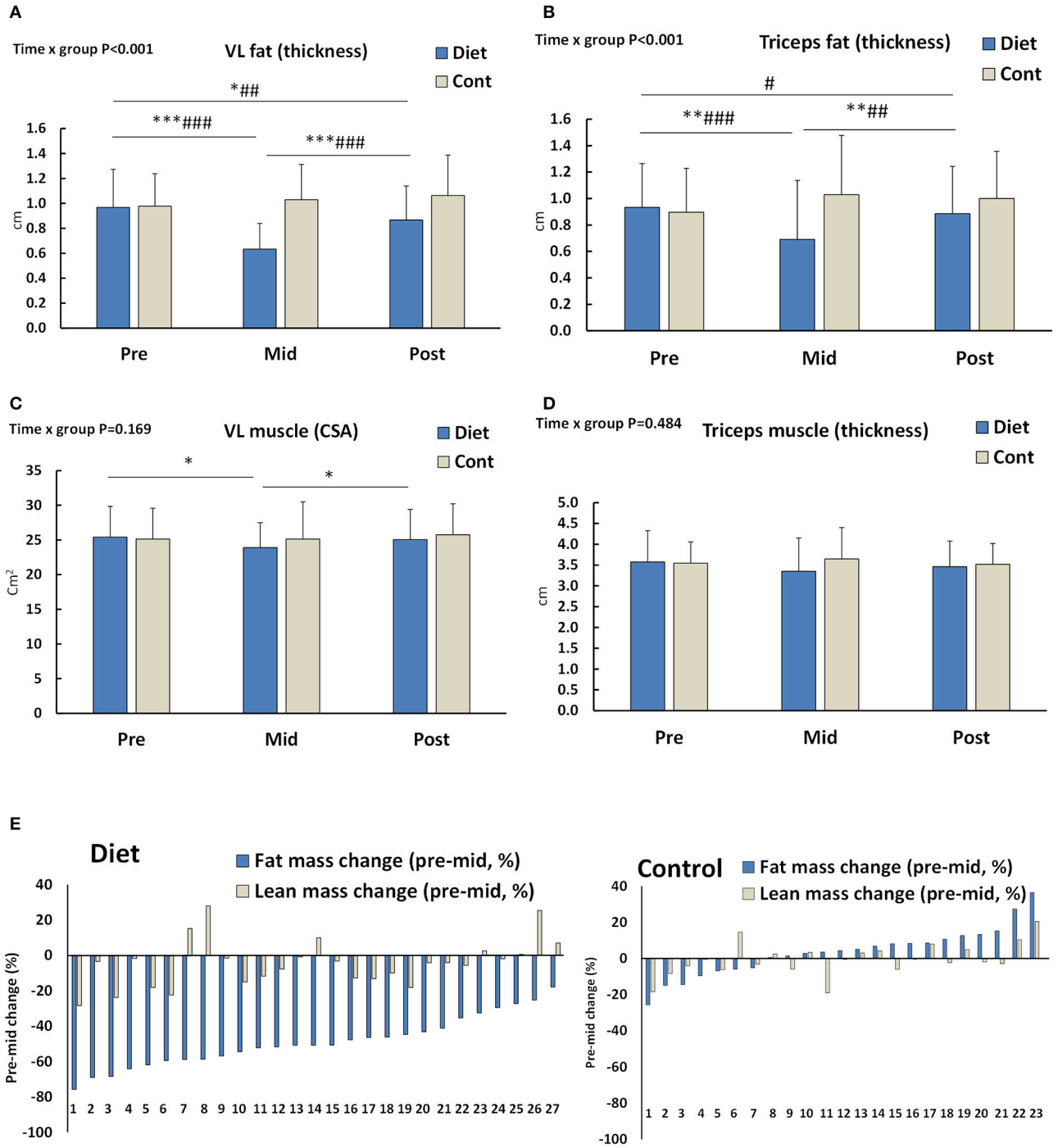

FIGURE 2 | (A,B) Subcutaneous fat thickness around Vastus lateralis (VL) and triceps brachii muscles (n = 25–27 diet and 19–20 control participants). **(C,D)** VL muscle cross-sectional area (CSA) and triceps brachii muscle thickness (n = 27 diet and 20 control participants). **(E)** Individual fat and lean mass percentage changes during the diet or pre to mid control period. Number at the x-axis depicts participant numbers ordered based on the amount of fat loss. DXA and bioimpedance values are averaged (n = 27 diet and 23 control participants). *–*** is significant (p < 0.05–< 0.001) difference to Pre and #–### is significant (p < 0.05–< 0.001) difference between the groups in the change. Group × time = ANOVA interaction effect p-value.

to baseline ($p < 0.01$) and to the controls ($p < 0.05$). Similarly, heart rate showed a group × time interaction ($p < 0.007$) with a decrease-effect found with the diet ($p < 0.001$) that was sustained still after the recovery period ($p < 0.01$; **Table 5**). Blood hemoglobin showed a group × time interaction ($p < 0.017$), while a trend existed with hematocrit ($p = 0.076$; **Table 5**). The

TABLE 4 | Muscle force of the subjects.

	Pre	Mid	Post	ΔMid-Pre	ΔPost-Mid	ΔPost-Pre	Group × time (p)
LEG PRESS (N)							
Diet	2855 ± 430	2855 ± 656	3059 ± 538**	−0.5 ± 9.5%	8.9 ± 12.2%	6.8 ± 9.7%	0.316
Cont	2908 ± 315	2893 ± 388	3021 ± 454	−0.5 ± 6.3%	4.2 ± 8.1%	2.5 ± 8.1%	
BENCH PRESS (N)							
Diet	620.0 ± 104.1	581.1 ± 104.4	598.9 ± 104.4	−3.4 ± 7.5%#	−0.2 ± 8.0%###	−3.7 ± 8.2%	< 0.001
Cont	645.6 ± 91.4	662.6 ± 82.3	602.8 ± 84.5***	2.1 ± 5.8%	−8.7 ± 3.8%	−6.9 ± 5.4%	
VERTICAL JUMP (cm)							
Diet	26.1 ± 4.2	25.2 ± 4.5	26.3 ± 4.7	−3.4 ± 9.1%	4.7 ± 8.9%	0.9 ± 9.6%	0.107
Cont	28.1 ± 5.5	28.4 ± 5.0	28.2 ± 5.1	1.6 ± 10.4%	−0.4 ± 7.7%	0.8 ± 9.2%	

*Δ are %-changes. *–*** is significant (p < 0.05–< 0.001) difference to Pre and #–### is significant (p < 0.05–< 0.001) difference between the groups in the change. Group × time = ANOVA interaction effect p-value. n = 27 diet and 23 control participants for the vertical jump and for isometric leg press and bench press n = 25 and 26 for the diet participants and n = 20 and n = 23 for the controls, respectively.*

post-hoc analysis showed that diet decreased hemoglobin ($p < 0.01$), but an increase back to baseline was observed after the recovery period.

Menstrual Irregularities

The baseline values for the missing menses in the diet-participants was 11.1% (3/27) and for irregularities in menstrual bleeding 37.0% (10/27) while in the controls the same values were and 4.3% (1/23) and 30.4% (7/23) without differences between the groups ($p > 0.6$). Fisher's exact test revealed that the diet group had more (63%) irregular menstrual bleeding than controls (30%; $p < 0.05$) and tended to have more missing menses (44 vs. 22%, $p = 0.082$) during the diet than the controls during their weight-maintenance period (measurement-points in the middle of the diet or after the diet before the competition). After the recovery period at post, in the diet group 28% (7/25) females had no menstrual bleeding and in the controls the respective value was 14.0% (3/22; $p = 0.297$). For those competitors using estrogen containing contraception ($n = 19$) there were irregularities in menstrual bleeding during the diet in 10/19 participants and/or lack of menstruation in 8/19 participants (at baseline 8/19 and 2/19, respectively). On the other hand, those subjects not using estrogen containing contraception ($n = 5$), 5/5 demonstrated irregular menstrual bleeding during the diet and/or lack of menstruation in 3/5 participants (at baseline 2/5 and 1/5, respectively). Three subjects did not report whether they used contraception medication or not.

Mood

There was no statistically significant changes in the mood of the participants within the diet group or between the diet and control groups at any of the time-points (Supplementary Table 2). The only statistical trend was a slight decrease in the vigor of the competitors ($p = 0.066$) in the middle of the diet when compared to the changes in the control group participants.

DISCUSSION

The present study showed that a diet to achieve very low levels of body fat can be completed with very small losses of lean mass/muscle size and muscle function in normal weight females with high levels of protein intake and resistance exercise. Moreover, the endocrine system is altered during the diet, but is recovered in most of the females following a recovery period of 3–4 months that includes increased energy intake together with the recovery of body weight.

Previous studies with energy deficits in otherwise normal weight individuals have shown various results in body composition. In the classic Minnesota starvation study body mass decreased in males on average by 25% with lean mass representing 6–28% (mean ∼15%), and the rest being fat (Keys et al., 1950; Dulloo et al., 1996). On the other hand, fat-free mass showed only a small decrease during a diet in female bodybuilders (van der Ploeg et al., 2001). There are a few possible explanations why lean mass and muscle size were maintained in the present study. First, the proportion of lean mass loss during diet has been larger the smaller the initial body fat% was (Dulloo et al., 1996; Huovinen et al., 2015). In the present study, females had an average 19–25% of fat (depending on whether DXA, bioimpedance, or skinfolds was used) at baseline, which is relatively high in comparison to e.g., ∼14% of fat in the male participants of the Minnesota study (Keys et al., 1950; Dulloo et al., 1996). Second, studies have shown that during energy deficit lean mass can be better maintained with ≥1.7–2 g/kg body weight per day protein ingestion in males and females (Mettler et al., 2010; Josse et al., 2011; Arciero et al., 2013; Churchward-Venne et al., 2013; Pasiakos et al., 2013; Longland et al., 2016). In our study cohort of fitness-competitors the protein content remained high, on average 3 g/kg even during the energy deficit. Third, resistance and aerobic training have been shown to attenuate the loss of lean mass during energy deficit when compared to energy restriction alone (Kraemer et al., 1999; Miller et al., 2013), which were both also used during the diet by the present fitness competitors. Moreover, the changes in body weight of the diet group were rather slow, on average ∼0.4 g/kg per week, which is actually pretty close to the level that was previously observed to maintain lean mass in normal-weight females on a diet (Mero et al., 2010) and what has been recommended for fat loss in fitness diets (Helms et al., 2014). The average participant, while resistance trained, had not

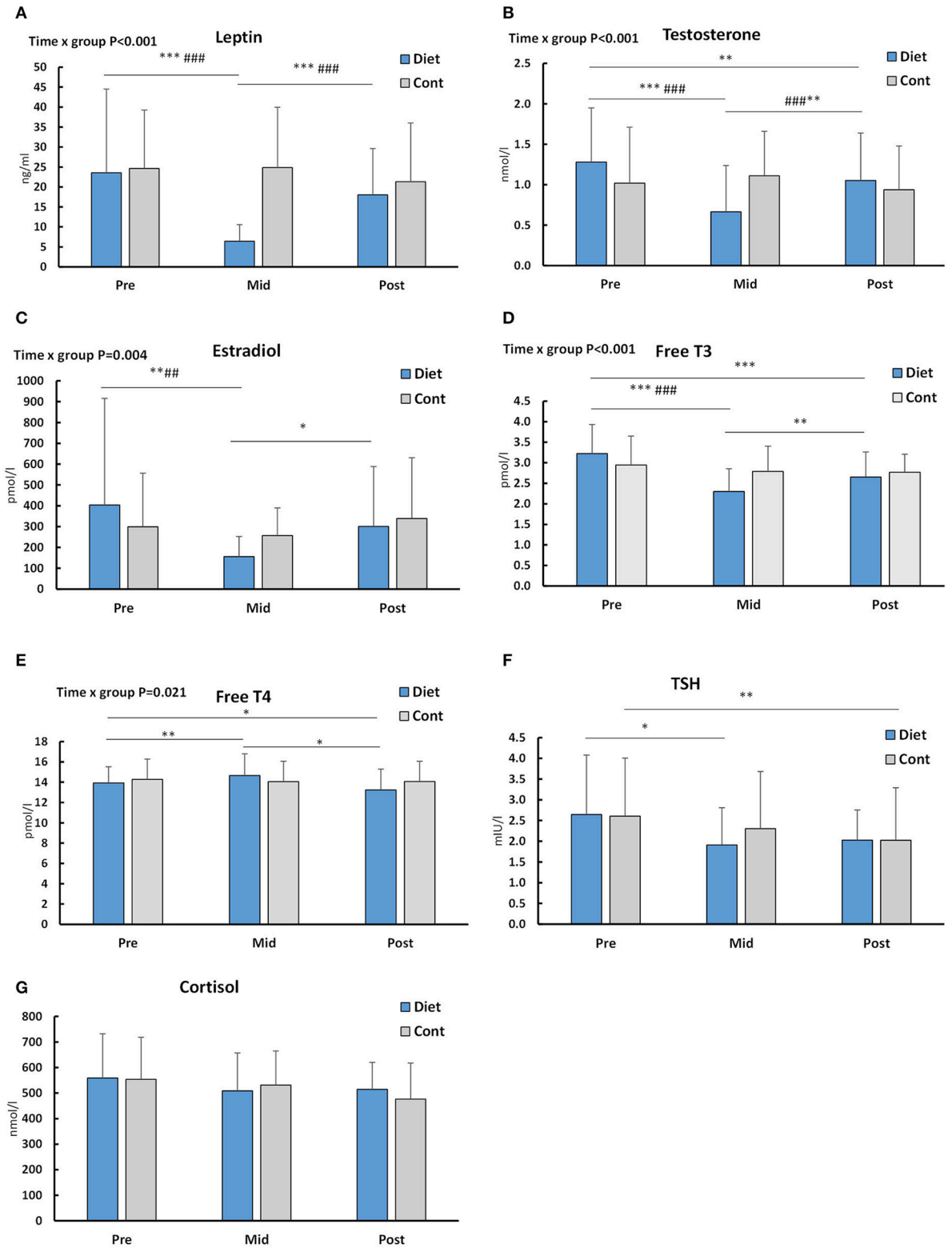

FIGURE 3 | Serum hormone concentrations at baseline (Pre), after the diet/control period (Mid) and after that during the recovery period (Post). Out of individual panels, **(A)** depicts leptin, **(B)** testosterone, **(C)** estradiol, **(D)** free T_3, **(E)** free T_4, **(F)** TSH, and **(G)** cortisol. $n = 27$ diet and 23 control participants for all hormones except TSH and testosterone data, which is obtained from 22 controls. *–*** is significant ($p < 0.05$–< 0.001) difference to Pre and #–### is significant ($p < 0.05$–< 0.001) difference between the groups in the change. Significant ($p < 0.05$) group × time = ANOVA interaction effect p-values are shown. For TSH and cortisol there were no significant interaction effects ($p = 0.198$ and $p = 0.332$, respectively).

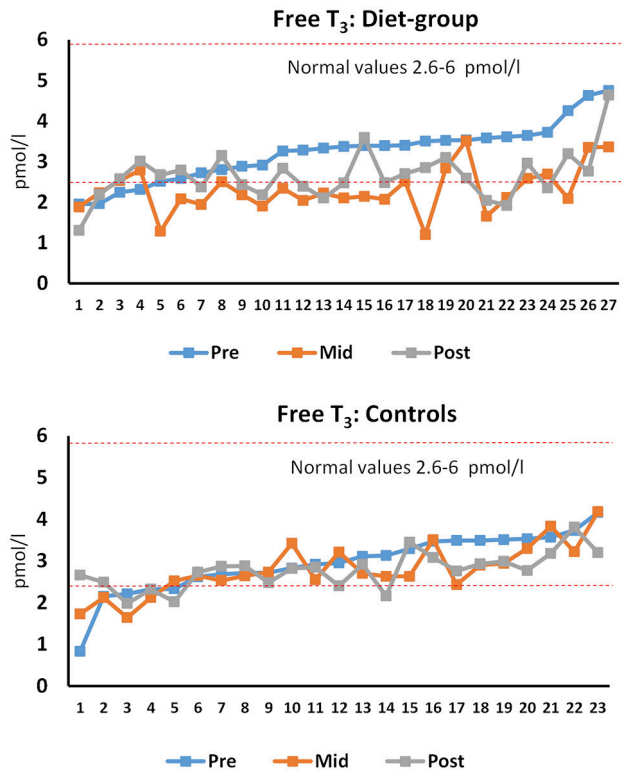

FIGURE 4 | Individual free T_3 at pre, mid, and post time-points for diet and control participants. Number at the x-axis depicts participant numbers ordered based on the pre-value. The red dotted lines limit the reference values in normal-weight healthy females. $n = 27$ diet and 23 control participants.

had many years of training experience (average 3.5 ± 1.4 years in the diet group and 3.1 ± 1.2 years in the controls), which makes it possible for some to even gain some muscle mass on a diet when regularly conducting resistance training combined with high protein intake (Josse et al., 2011; Longland et al., 2016). It is also important to recognize that the last week of a typical fitness or bodybuilding diet includes tapering of training, which was observed as decreased MET-hours of resistance training and similar to baseline carbohydrate eating. This makes lean mass and muscle sizes after diet more comparable when compared to baseline. When this is not taken into account in diet studies in which carbohydrates are restricted, small 1–3 kg losses in lean mass may just be glycogen and water losses instead of an actual decrease in protein mass.

Out of the present serum hormones investigated the concentration of leptin robustly decreased but recovered close to baseline levels after the recovery period following energy intake and fat mass as expected (Kelesidis et al., 2010). Decreased leptin after diet has orexigenic effects in response to energy deficiency and in decreased fat mass (Kelesidis et al., 2010) and may be one of the reasons why maintaining low energy intake and energy deficit for a long time has been shown to be psychologically very difficult (Keys et al., 1950). In our study, only a few of the females had leptin levels <3 ng/ml (6 of 27 diet-participants) after the diet, a level thought to be a low-limit for many physiological changes in females such as decreased immune function (Chan et al., 2006). This state was reversed by the recovery period as serum leptin levels did recover to ≥3 ng/ml levels in all females. This is important as recovery of leptin can in itself restore, for instance, ovulatory menstrual cycles and improve levels of reproductive and thyroid hormones as well as bone markers in amenorrhea (Rosenbaum et al., 2002; Kelesidis et al., 2010).

Weight reduction in obese or overweight individuals typically decreases T_3 while T_4 and TSH usually remain unaltered (Fothergill et al., 2016). We now showed that also in normal weight to thin individuals, weight loss from mainly fat stores decreases only T_3 and not T_4 and TSH. This is also supported by data from individuals with anorexia nervosa who have lowered serum leptin and T_3, together with low fat mass (Tolle et al., 2003). These hormones are usually at least partially recovered toward the values of normal-weight individuals after weight gain (Tolle et al., 2003). Individual T_3 levels were also compared to the reference values. For T_3, in dieters, 5/27 were below the reference values (2.6–6 pmol/L) at pre, 20/27 after the diet and 13/27 at recovery while in controls the number of participants was 5/23, 8/23, and 7/23, respectively (**Figure 3**). Statistically significantly lowered T_3 at the post time-point suggests that 3–4 months of recovery may not be enough in some individuals after heavy energy deficit. These females should probably continue the recovery period of increased energy intake before dieting again for the competition to avoid longer term changes in their hormonal balance. This is because in addition to possible health risks, decreased T_3 can lead to decreased metabolic rate (Kim, 2008). The decrease and only a partial recovery of T_3 was accompanied by the decreased heart rate and systolic blood pressure. Similarly as T_3, heart rate also remained decreased after the recovery period. Together with decreased fat mass, decreased blood pressure and heart rate are typical responses after a diet, even for normotensive and non-overweight individuals (Keys et al., 1950; Awazu et al., 2000; Rossow et al., 2013) showing that the autonomic nervous system also adapts to an energy deficit as expected and, thus, may not be a health risk at these levels of heart rate of ≥49 bpm in all females. However, when the heart rate is more substantially decreased and long lasting such as in anorectic individuals without supervised and controlled refeeding, this can lead to a long QT in ECG and an increased risk for arrhytmia (Sachs et al., 2016).

Anorectic females have very low serum estradiol (Tolle et al., 2003) and testosterone (Miller et al., 2007). Not surprisingly, in the present study, serum sex-hormones estradiol and testosterone both decreased during the diet. In addition, estradiol, but not testosterone, recovered at or close to baseline levels within 3–4 months of recovery. This suggests that recovery of serum testosterone in females takes longer time and/or larger energy intake and/or fat mass when compared to estradiol. It is unknown whether the levels observed in the present study are physiologically meaningful as the mean values are within normal values of serum testosterone in most of the participants (Haring et al., 2012) and the measured loss of muscle size was very small. However, higher serum testosterone levels in females have been associated with larger lean mass to fat mass ratio (Rickenlund et al., 2003) and occasionally correlation between gains in muscle

TABLE 5 | Blood pressure and hemoglobin/hematocrit of the subjects.

	Pre	Mid	Post	ΔMid-Pre	ΔPost-Mid	ΔPost-Pre	Group × time (p)
SYSTOLIC BLOOD PRESSURE (mmHg)							
Diet	118.3 ± 9.3	111.1 ± 7.6	113.9 ± 7.2	−5.9 ± 5.9%***	2.6 ± 5.3%*	−3.5 ± 5.4%**	< 0.001
Cont	119.3 ± 6.3	121.7 ± 7.7	119.2 ± 11.0	2.0 ± 2.1%***###	−2.1 ± 7.3%#	−0.1 ± 7.5%#	
DIASTOLIC BLOOD PRESSURE (mmHg)							
Diet	67.4 ± 8.0	64.1 ± 6.4	65.3 ± 6.4	−4.0 ± 10.2%	2.1 ± 8.3%	−2.5 ± 8.1%	0.177
Cont	69.1 ± 7.1	70.1 ± 13.3	67.7 ± 7.4	1.7 ± 18.1%	−1.0 ± 16.1%	−1.9 ± 5.6%	
HEART RATE (bpm)							
Diet	68.9 ± 12.1	62.4 ± 9.0	64.6 ± 10.1	−8.4 ± 10.6%***	4.0 ± 11.5%	−5.5 ± 8.9%**	0.007
Cont	69.6 ± 8.5	70.1 ± 13.3	68.8 ± 9.8	0.2 ± 10.5%#	−0.4 ± 12.3%	−1.1 ± 8.1%	
HEMOGLOBIN (g/L)							
Diet	138.8 ± 8.1	134.7 ± 7.8	137.7 ± 7.7	−2.9 ± 4.1%**	2.4 ± 4.3%*	−0.7 ± 3.4%	0.017
Cont	135.5 ± 6.1	135.3 ± 5.7	134.9 ± 7.2	0.0 ± 3.6%	−0.3 ± 3.6%	−0.4 ± 4.0%	
HEMATOCRIT (%)							
Diet	40.8 ± 2.3	39.8 ± 2.4	40.8 ± 2.2	−2.3 ± 4.4%	2.6 ± 4.4%	0.2 ± 3.6	0.076
Cont	40.3 ± 1.5	40.0 ± 1.6	40.1 ± 1.8	−0.6 ± 3.0%	0.1 ± 3.5%	−0.5 ± 3.8%	

*Δ are %-changes. *–*** is significant ($p < 0.05$–< 0.001) difference to Pre and #–### is significant ($p < 0.05$–< 0.001) difference between the groups in the change. Group × time = ANOVA interaction effect p-value. n = 27 diet and 23 control participants for all the result.*

cross-sectional area and/or strength during resistance training have also been observed (Häkkinen et al., 1992). Interestingly, a slightly decreased bone mass by DXA was observed in diet, increasing back to baseline after the recovery period. The result may be due to the direct effects of decreased body and muscle mass on mechanical forces (Goodman et al., 2015), decreased energy availability (Ihle and Loucks, 2004) and/or lowered estradiol and testosterone that are both anabolic to bone based on some (Davis et al., 1995), but not all studies (Muñoz et al., 2002).

Some studies have suggested that for optimal health, minimum body fat for females would be within the range of 12–14% (Meyer et al., 2013), but this depends on the individual and the body composition assessment method. BMI decreased from 23.5 ± 1.8 to 20.6 ± 1.4 recovering to 22.9 ± 2.0 while the lowest BMI's after the diet were 18.7–19.0 in four females. On the other hand, 6/27 females had <10% body fat after the diet in both DXA and in bioimpedance. In many sports such as in distance running, figure skating and gymnastics fat % in females can be as low as 10–15% and in some females even below 10% almost year round (Wilmore et al., 1977). Instead, in fitness-competitors, fat percentage is usually kept at low levels only for a rather short period of time. Indeed, none of the participants had <10% levels after the recovery period, while levels of 15–20% were frequent. This may, in theory, offer a health protection. Weight cycling, i.e., repeated cycles of weight loss and regain that are observed in those who frequently compete and thus diet may, however, predispose to some health risks such as obesity in some groups of people (Saarni et al., 2006), although the total weight of evidence is very weak (Mehta et al., 2014). Nevertheless, females need a higher fat percentage than males because of the endocrine function that is necessary for ovulation and maintenance of bone mass. Indeed, in the present study, more dieting females reported changes in their menstrual function during their diet than controls in their control period. The values reported are not unexpected as menstrual dysfunction is very common among many thin female athletes (Melin et al., 2015). These results are probably related, in part, to changes in fat mass around visceral and genital areas. In the present study the estimation of visceral fat measured as an android region mass by DXA showed a substantial ∼68% decrease followed by an increase back to the pre-values after the recovery period. A recent meta-analysis suggests that in negative energy balance, both exercise and diet reduce fat mass, but exercise may be more important to reduce visceral adipose tissue (Verheggen et al., 2016). The decrease in fat in these areas combined with energy deficit can, in theory, signal the hypothalamus-pituitary axis to decrease secretion of hormones relating to ovulation such as estradiol and eventually, to transiently stop ovulation and menstrual bleeding.

Even though muscle strength is not essential for fitness competition performance *per se*, it may be, in theory, important to maintain muscle strength for the purposes of resistance training adaptations. In the present study, the participants maintained their maximal isometric muscle strength and explosive strength of leg extensors during the diet. This can be explained, in part by maintenance of muscle size in the important knee extensor muscles investigated and by frequent heavy intensity resistance training that was maintained throughout the study, which can sustain or improve voluntary activation of muscles even in strength trained female athletes (Häkkinen and Kallinen, 1994). However, a measure of upper-body strength, isometric bench press, decreased during diet when compared to controls suggesting that during the diet especially the upper-body strength may be difficult to maintain due to energy/carbohydrate deficit with a typical training program of fitness athletes. This was observed even though the thickness of triceps brachii muscle, which is one of the

main muscles responsible for the bench press strength, remained unaltered during the diet. Previously, Bamman et al. (1993) noticed a decrease in isometric strength after a bodybuilding diet in males while Rossow et al. (2013) reported decreased absolute, but not relative levels of muscle strength and Robinson et al. (2015) reported no changes in most of the isokinetic measures of maximal strength in a male bodybuilder after the diet.

Mentally, maintaining rather a large energy deficit can be hard, possibly especially for those who are dieting toward very low body fat levels as observed previously in bodybuilders on a competition diet (Newton et al., 1993). Perhaps surprisingly, the present fitness-diet did not markedly affect the mood state of the participants. Supporting the mood results, serum cortisol did not increase following the diet. This was also a bit surprising considering that in stressful situations such as energy restriction and monitoring calories, serum cortisol level often increase (Tomiyama et al., 2010). However, a slight decrease in the vigor of the participants ($P = 0.066$) was observed in the middle of the diet when compared to the changes in the control group participants. This suggest that some individuals on the diet may have felt less active, lively, and/or energetic when compared to their baseline levels than individuals in the control group. This supports the earlier case-study with male drug-free bodybuilder (Rossow et al., 2013). The reason why the results were not very consistent may be explained, in part, by the fact that the participants were voluntarily taking part in the diet, which makes the situation different compared to a full randomized trial without a clear "reward" (competition) at the end.

The present study had several strengths. The n-size of the study was rather large and a control group was included, which is quite rare in energy deficit—refeeding studies. In addition, the comprehensive analysis of body composition with direct measures of muscle and fat size can be regarded as a strength. On the other hand, the study was limited in the experimental design that it was not randomized. However, we think that a similar background of the groups enables us to compare the changes in the diet group to almost an identical group of the controls not changing their nutrition or exercise during the experimental period. The physiology and body composition measurements were taken after a competition and not a week before the "peak" week. This is, however, in our view also an advantage as mentioned above at least regarding the body composition measurements. Contraceptive medication use did not result in exclusion from the study. In the present study the majority (19) of the competitors reported using estrogen-containing contraception and five not. While we acknowledge that in addition to the variation in the phase of the menstrual cycle, also oral contraception use can have effects and thus add extra variation on the measured variables. We analyzed the changes in serum estradiol from pre to mid and from mid to post and those remained significant in the estrogen containing contraception users and in non-users ($p < 0.05$) similarly as shown with all the subjects pooled (data not shown). Unfortunately the n-size is too small to conduct a valid statistical analysis for the menstrual irregularities, but our data tends to suggests that those who do not use estrogen containing medication may be slightly more vulnerable to menstrual irregularities during the diet than those who use them. However, this question needs to be addressed with studies using larger n-size in the future.

In conclusion, a fitness diet in healthy young females accomplished by restricting carbohydrate ingestion and increasing aerobic exercise while maintaining high levels of protein intake and resistance exercise can be carried out without major decreases in lean mass/muscle size. Therefore, the diet almost exclusively decreased body fat and altered serum hormones, but most of those values recovered within 3–4 months with the increase in energy intake and decrease in high level of aerobic exercise. However, in some females this time period may not have been long enough for a full recovery (e.g., free T_3 and testosterone hormones). Future studies should investigate the time-course of the changes during the diet and in the recovery period and whether repeating heavy diets for many times has any long-lasting negative effects.

AUTHOR CONTRIBUTIONS

JH, VI, JA, and KH conceived and designed the experiments with the help from MP and AW. VI, MS, and NJ carried out the experiments with the help from students and laboratory technicians. KN acted as a physician of the project. JH drafted the manuscript. Analysis was conducted by VI, MS, NJ, JH, and MK together with students and technicians. All authors critically read/revised and approved the final manuscript.

FUNDING

This work was financially supported by the Academy of Finland (grant No. 275922 to JH and No. 269517 to MP), Finnish Fitness Sports Association and Department of Biology of Physical Activity.

ACKNOWLEDGMENTS

The authors thank Risto Puurtinen, Aila Ollikainen, Johanna Ihalainen, and many students and research assistants (Inga Luotonen, Heli-Maija Koukkari, Jaakko Forssell, Tuija Toivola, and Esa Hukkanen) for their help in the data collection and analysis. We also thank the very dedicated participants who made this project possible. The statistician Elina Vaara is thanked for valuable statistical work, Pertti Matilainen for converting the paper questionnaires into digital, the web-based questionnaires and Ritva Taipale for critically reviewing the manuscript.

SUPPLEMENTARY MATERIAL

The Supplementary Material for this article can be found online at: http://journal.frontiersin.org/article/10.3389/fphys.2016.00689/full#supplementary-material

REFERENCES

Ahtiainen, J. P., Hoffren, M., Hulmi, J. J., Pietikäinen, M., Mero, A. A., Avela, J., et al. (2010). Panoramic ultrasonography is a valid method to measure changes in skeletal muscle cross-sectional area. *Eur. J. Appl. Physiol.* 108, 273–279. doi: 10.1007/s00421-009-1211-6

Ainsworth, B. E., Haskell, W. L., Whitt, M. C., Irwin, M. L., Swartz, A. M., Strath, S. J., et al. (2000). Compendium of physical activities: an update of activity codes and MET intensities. *Med. Sci. Sports Exerc.* 32, S498–S504. doi: 10.1097/00005768-200009001-00009

Alemany, J. A., Nindl, B. C., Kellogg, M. D., Tharion, W. J., Young, A. J., and Montain, S. J. (2008). Effects of dietary protein content on IGF-I, testosterone, and body composition during 8 days of severe energy deficit and arduous physical activity. *J. Appl. Physiol.* (1985) 105, 58–64. doi: 10.1152/japplphysiol.00005.2008

Arciero, P. J., Ormsbee, M. J., Gentile, C. L., Nindl, B. C., Brestoff, J. R., and Ruby, M. (2013). Increased protein intake and meal frequency reduces abdominal fat during energy balance and energy deficit. *Obesity (Silver Spring)* 21, 1357–1366. doi: 10.1002/oby.20296

Awazu, M., Matsuoka, S., Kamimaki, T., Watanabe, H., and Matsuo, N. (2000). Absent circadian variation of blood pressure in patients with anorexia nervosa. *J. Pediatr.* 136, 524–527. doi: 10.1016/S0022-3476(00)90017-9

Bamman, M. M., Hunter, G. R., Newton, L. E., Roney, R. K., and Khaled, M. A. (1993). Changes in body composition, diet, and strength of bodybuilders during the 12 weeks prior to competition. *J. Sports Med. Phys. Fitness* 33, 383–391.

Chan, J. L., Matarese, G., Shetty, G. K., Raciti, P., Kelesidis, I., Aufiero, D., et al. (2006). Differential regulation of metabolic, neuroendocrine, and immune function by leptin in humans. *Proc. Natl. Acad. Sci. U.S.A.* 103, 8481–8486. doi: 10.1073/pnas.0505429103

Churchward-Venne, T. A., Murphy, C. H., Longland, T. M., and Phillips, S. M. (2013). Role of protein and amino acids in promoting lean mass accretion with resistance exercise and attenuating lean mass loss during energy deficit in humans. *Amino Acids* 45, 231–240. doi: 10.1007/s00726-013-1506-0

Davis, S. R., McCloud, P., Strauss, B. J., and Burger, H. (1995). Testosterone enhances estradiol's effects on postmenopausal bone density and sexuality. *Maturitas* 21, 227–236. doi: 10.1016/0378-5122(94)00898-H

Dulloo, A. G., Jacquet, J., and Girardier, L. (1996). Autoregulation of body composition during weight recovery in human: the Minnesota Experiment revisited. *Int. J. Obes. Relat. Metab. Disord.* 20, 393–405.

Durnin, J. V., and Womersley, J. (1974). Body fat assessed from total body density and its estimation from skinfold thickness: measurements on 481 men and women aged from 16 to 72 years. *Br. J. Nutr.* 32, 77–97. doi: 10.1079/BJN19740060

Fothergill, E., Guo, J., Howard, L., Kerns, J. C., Knuth, N. D., Brychta, R., et al. (2016). Persistent metabolic adaptation 6 years after "The Biggest Loser" competition. *Obesity (Silver Spring)* 24, 1612–1619. doi: 10.1002/oby.21538

Goodman, C. A., Hornberger, T. A., and Robling, A. G. (2015). Bone and skeletal muscle: key players in mechanotransduction and potential overlapping mechanisms. *Bone* 80, 24–36. doi: 10.1016/j.bone.2015.04.014

Hackett, D. A., Johnson, N. A., and Chow, C. M. (2013). Training practices and ergogenic aids used by male bodybuilders. *J. Strength Cond. Res.* 27, 1609–1617. doi: 10.1519/JSC.0b013e318271272a

Häkkinen, K., and Kallinen, M. (1994). Distribution of strength training volume into one or two daily sessions and neuromuscular adaptations in female athletes. *Electromyogr. Clin. Neurophysiol.* 34, 117–124.

Häkkinen, K., Pakarinen, A., and Kallinen, M. (1992). Neuromuscular adaptations and serum hormones in women during short-term intensive strength training. *Eur. J. Appl. Physiol. Occup. Physiol.* 64, 106–111. doi: 10.1007/BF00717946

Haring, R., Hannemann, A., John, U., Radke, D., Nauck, M., Wallaschofski, H., et al. (2012). Age-specific reference ranges for serum testosterone and androstenedione concentrations in women measured by liquid chromatography-tandem mass spectrometry. *J. Clin. Endocrinol. Metab.* 97, 408–415. doi: 10.1210/jc.2011-2134

Helms, E. R., Aragon, A. A., and Fitschen, P. J. (2014). Evidence-based recommendations for natural bodybuilding contest preparation: nutrition and supplementation. *J. Int. Soc. Sports Nutr.* 11:20. doi: 10.1186/1550-2783-11-20

Helms, E. R., Fitschen, P. J., Aragon, A. A., Cronin, J., and Schoenfeld, B. J. (2015). Recommendations for natural bodybuilding contest preparation: resistance and cardiovascular training. *J. Sports Med. Phys. Fitness* 55, 164–178.

Henning, P. C., Scofield, D. E., Spiering, B. A., Staab, J. S., Matheny, R. W. Jr., Smith, M. A., et al. (2014). Recovery of endocrine and inflammatory mediators following an extended energy deficit. *J. Clin. Endocrinol. Metab.* 99, 956–964. doi: 10.1210/jc.2013-3046

Hill, A. M., LaForgia, J., Coates, A. M., Buckley, J. D., and Howe, P. R. (2007). Estimating abdominal adipose tissue with DXA and anthropometry. *Obesity (Silver Spring)* 15, 504–510. doi: 10.1038/oby.2007.629

Hulmi, J. J., Laakso, M., Mero, A. A., Häkkinen, K., Ahtiainen, J. P., and Peltonen, H. (2015). The effects of whey protein with or without carbohydrates on resistance training adaptations. *J. Int. Soc. Sports Nutr.* 12:48. doi: 10.1186/s12970-015-0109-4

Huovinen, H. T., Hulmi, J. J., Isolehto, J., Kyröläinen, H., Puurtinen, R., Karila, T., et al. (2015). Body composition and power performance improved after weight reduction in male athletes without hampering hormonal balance. *J. Strength Cond. Res.* 29, 29–36. doi: 10.1519/JSC.0000000000000619

Ihle, R., and Loucks, A. B. (2004). Dose-response relationships between energy availability and bone turnover in young exercising women. *J. Bone Miner. Res.* 19, 1231–1240. doi: 10.1359/JBMR.040410

Josse, A. R., Atkinson, S. A., Tarnopolsky, M. A., and Phillips, S. M. (2011). Increased consumption of dairy foods and protein during diet- and exercise-induced weight loss promotes fat mass loss and lean mass gain in overweight and obese premenopausal women. *J. Nutr.* 141, 1626–1634. doi: 10.3945/jn.111.141028

Kang, S. M., Yoon, J. W., Ahn, H. Y., Kim, S. Y., Lee, K. H., Shin, H., et al. (2011). Android fat depot is more closely associated with metabolic syndrome than abdominal visceral fat in elderly people. *PLoS ONE* 6:e27694. doi: 10.1371/journal.pone.0027694

Kelesidis, T., Kelesidis, I., Chou, S., and Mantzoros, C. S. (2010). Narrative review: the role of leptin in human physiology: emerging clinical applications. *Ann. Intern. Med.* 152, 93–100. doi: 10.7326/0003-4819-152-2-201001190-00008

Keys, A., Brozek, J., Henschel, A., Mickelsen, O., and Taylor, H. (1950). *The Biology of Human Starvation*. Minneapolis, MN: The University of Minnesota Press.

Kim, B. (2008). Thyroid hormone as a determinant of energy expenditure and the basal metabolic rate. *Thyroid* 18, 141–144. doi: 10.1089/thy.2007.0266

Kistler, B. M., Fitschen, P. J., Ranadive, S. M., Fernhall, B., and Wilund, K. R. (2014). Case study: natural bodybuilding contest preparation. *Int. J. Sport Nutr. Exerc. Metab.* 24, 694–700. doi: 10.1123/ijsnem.2014-0016

Komi, P. V., and Bosco, C. (1978). Utilization of stored elastic energy in leg extensor muscles by men and women. *Med. Sci. Sports* 10, 261–265.

Kraemer, W. J., Volek, J. S., Clark, K. L., Gordon, S. E., Puhl, S. M., Koziris, L. P., et al. (1999). Influence of exercise training on physiological and performance changes with weight loss in men. *Med. Sci. Sports Exerc.* 31, 1320–1329. doi: 10.1097/00005768-199909000-00014

Longland, T. M., Oikawa, S. Y., Mitchell, C. J., Devries, M. C., and Phillips, S. M. (2016). Higher compared with lower dietary protein during an energy deficit combined with intense exercise promotes greater lean mass gain and fat mass loss: a randomized trial. *Am. J. Clin. Nutr.* 103, 738–746. doi: 10.3945/ajcn.115.119339

Mehta, T., Smith, D. L. Jr., Muhammad, J., and Casazza, K. (2014). Impact of weight cycling on risk of morbidity and mortality. *Obes. Rev.* 15, 870–881. doi: 10.1111/obr.12222

Melin, A., Tornberg, Å. B., Skouby, S., Møller, S. S., Sundgot-Borgen, J., Faber, J., et al. (2015). Energy availability and the female athlete triad in elite endurance athletes. *Scand. J. Med. Sci. Sports* 25, 610–622. doi: 10.1111/sms.12261

Mero, A. A., Huovinen, H., Matintupa, O., Hulmi, J. J., Puurtinen, R., Hohtari, H., et al. (2010). Moderate energy restriction with high protein diet results in healthier outcome in women. *J. Int. Soc. Sports Nutr.* 7:4. doi: 10.1186/1550-2783-7-4

Mettler, S., Mitchell, N., and Tipton, K. D. (2010). Increased protein intake reduces lean body mass loss during weight loss in athletes. *Med. Sci. Sports Exerc.* 42, 326–337. doi: 10.1249/MSS.0b013e3181b2ef8e

Meyer, N. L., Sundgot-Borgen, J., Lohman, T. G., Ackland, T. R., Stewart, A. D., Maughan, R. J., et al. (2013). Body composition for health and performance: a survey of body composition assessment practice carried out by the *Ad Hoc* Research Working Group on Body Composition, Health and Performance

under the auspices of the IOC Medical Commission. *Br. J. Sports Med.* 47, 1044–1053. doi: 10.1136/bjsports-2013-092561

Miazgowski, T., Krzyzanowska-Swiniarska, B., Dziwura-Ogonowska, J., and Widecka, K. (2014). The associations between cardiometabolic risk factors and visceral fat measured by a new dual-energy X-ray absorptiometry-derived method in lean healthy Caucasian women. *Endocrine* 47, 500–505. doi: 10.1007/s12020-014-0180-7

Miller, C. T., Fraser, S. F., Levinger, I., Straznicky, N. E., Dixon, J. B., Reynolds, J., et al. (2013). The effects of exercise training in addition to energy restriction on functional capacities and body composition in obese adults during weight loss: a systematic review. *PLoS ONE* 8:e81692. doi: 10.1371/journal.pone.0081692

Miller, K. K., Lawson, E. A., Mathur, V., Wexler, T. L., Meenaghan, E., Misra, M., et al. (2007). Androgens in women with anorexia nervosa and normal-weight women with hypothalamic amenorrhea. *J. Clin. Endocrinol. Metab.* 92, 1334–1339. doi: 10.1210/jc.2006-2501

Müller, M. J., Enderle, J., Pourhassan, M., Braun, W., Eggeling, B., Lagerpusch, M., et al. (2015). Metabolic adaptation to caloric restriction and subsequent refeeding: the Minnesota Starvation Experiment revisited. *Am. J. Clin. Nutr.* 102, 807–819. doi: 10.3945/ajcn.115.109173

Müller, W., Lohman, T. G., Stewart, A. D., Maughan, R. J., Meyer, N. L., Sardinha, L. B., et al. (2016). Subcutaneous fat patterning in athletes: selection of appropriate sites and standardisation of a novel ultrasound measurement technique: *ad hoc* working group on body composition, health and performance, under the auspices of the IOC Medical Commission. *Br. J. Sports Med.* 50, 45–54. doi: 10.1136/bjsports-2015-095641

Muñoz, M. T., Morandé, G., García-Centenera, J. A., Hervás, F., Pozo, J., and Argente, J. (2002). The effects of estrogen administration on bone mineral density in adolescents with anorexia nervosa. *Eur. J. Endocrinol.* 146, 45–50. doi: 10.1530/eje.0.1460045

Newton, L., Hunter, G., Bammon, M., and Roney, R. (1993). Changes in psychological state and self-reported diet during various phases of training in competitive bodybuilders. *J. Strength Cond. Res.* 7, 153–158. doi: 10.1519/00124278-199308000-00005

Ojasto, T., and Häkkinen, K. (2009). Effects of different accentuated eccentric load levels in eccentric-concentric actions on acute neuromuscular, maximal force, and power responses. *J. Strength Cond. Res.* 23, 996–1004. doi: 10.1519/JSC.0b013e3181a2b28e

Pasiakos, S. M., Cao, J. J., Margolis, L. M., Sauter, E. R., Whigham, L. D., McClung, J. P., et al. (2013). Effects of high-protein diets on fat-free mass and muscle protein synthesis following weight loss: a randomized controlled trial. *FASEB J.* 27, 3837–3847. doi: 10.1096/fj.13-230227

Rickenlund, A., Carlström, K., Ekblom, B., Brismar, T. B., von Schoultz, B., and Hirschberg, A. L. (2003). Hyperandrogenicity is an alternative mechanism underlying oligomenorrhea or amenorrhea in female athletes and may improve physical performance. *Fertil. Steril.* 79, 947–955. doi: 10.1016/S0015-0282(02)04850-1

Robinson, S. L., Lambeth-Mansell, A., Gillibrand, G., Smith-Ryan, A., and Bannock, L. (2015). A nutrition and conditioning intervention for natural bodybuilding contest preparation: case study. *J. Int. Soc. Sports Nutr.* 12:20. doi: 10.1186/s12970-015-0083-x

Rosenbaum, M., Murphy, E. M., Heymsfield, S. B., Matthews, D. E., and Leibel, R. L. (2002). Low dose leptin administration reverses effects of sustained weight-reduction on energy expenditure and circulating concentrations of thyroid hormones. *J. Clin. Endocrinol. Metab.* 87, 2391–2394. doi: 10.1210/jcem.87.5.8628

Rossow, L. M., Fukuda, D. H., Fahs, C. A., Loenneke, J. P., and Stout, J. R. (2013). Natural bodybuilding competition preparation and recovery: a 12-month case study. *Int. J. Sports Physiol. Perform.* 8, 582–592. doi: 10.1123/ijspp.8.5.582

Saarni, S. E., Rissanen, A., Sarna, S., Koskenvuo, M., and Kaprio, J. (2006). Weight cycling of athletes and subsequent weight gain in middleage. *Int. J. Obes. (Lond).* 30, 1639–1644. doi: 10.1038/sj.ijo.0803325

Sachs, K. V., Harnke, B., Mehler, P. S., and Krantz, M. J. (2016). Cardiovascular complications of anorexia nervosa: a systematic review. *Int. J. Eat. Disord.* 49, 238–248. doi: 10.1002/eat.22481

Sandoval, W. M., Heyward, V. H., and Lyons, T. M. (1989). Comparison of body composition, exercise and nutritional profiles of female and male body builders at competition. *J. Sports Med. Phys. Fitness* 29, 63–70.

Schumann, M., Küüsmaa, M., Newton, R. U., Sirparanta, A. I., Syväoja, H., Häkkinen, A., et al. (2014). Fitness and lean mass increases during combined training independent of loading order. *Med. Sci. Sports Exerc.* 46, 1758–1768. doi: 10.1249/MSS.0000000000000303

Sundgot-Borgen, J., Meyer, N. L., Lohman, T. G., Ackland, T. R., Maughan, R. J., Stewart, A. D., et al. (2013). How to minimise the health risks to athletes who compete in weight-sensitive sports review and position statement on behalf of the *Ad Hoc* Research Working Group on Body Composition, Health and Performance, under the auspices of the IOC Medical Commission. *Br. J. Sports Med.* 47, 1012–1022. doi: 10.1136/bjsports-2013-092966

Terry, P. C., Lane, A. M., Lane, H. J., and Keohane, L. (1999). Development and validation of a mood measure for adolescents. *J. Sports Sci.* 17, 861–872. doi: 10.1080/026404199365425

Tolle, V., Kadem, M., Bluet-Pajot, M. T., Frere, D., Foulon, C., Bossu, C., et al. (2003). Balance in ghrelin and leptin plasma levels in anorexia nervosa patients and constitutionally thin women. *J. Clin. Endocrinol. Metab.* 88, 109–116. doi: 10.1210/jc.2002-020645

Tomiyama, A. J., Mann, T., Vinas, D., Hunger, J. M., Dejager, J., and Taylor, S. E. (2010). Low calorie dieting increases cortisol. *Psychosom. Med.* 72, 357–364. doi: 10.1097/PSY.0b013e3181d9523c

van der Ploeg, G. E., Brooks, A. G., Withers, R. T., Dollman, J., Leaney, F., and Chatterton, B. E. (2001). Body composition changes in female bodybuilders during preparation for competition. *Eur. J. Clin. Nutr.* 55, 268–277. doi: 10.1038/sj.ejcn.1601154

Verheggen, R. J., Maessen, M. F., Green, D. J., Hermus, A. R., Hopman, M. T., and Thijssen, D. H. (2016). A systematic review and meta-analysis on the effects of exercise training versus hypocaloric diet: distinct effects on body weight and visceral adipose tissue. *Obes. Rev.* 17, 664–690. doi: 10.1111/obr.12406

Vuoskoski, J. K., and Eerola, T. (2011). The role of mood and personality in the perception of emotions represented by music. *Cortex* 47, 1099–1106. doi: 10.1016/j.cortex.2011.04.011

Wilmore, J. H., Brown, C. H., and Davis, J. A. (1977). Body physique and composition of the female distance runner. *Ann. N.Y. Acad. Sci.* 301, 764–776. doi: 10.1111/j.1749-6632.1977.tb38245.x

Conflict of Interest Statement: The authors declare that the research was conducted in the absence of any commercial or financial relationships that could be construed as a potential conflict of interest.

frontiers in Physiology

REVIEW
published: 02 August 2017
doi: 10.3389/fphys.2017.00547

Human Pathophysiological Adaptations to the Space Environment

*Gian C. Demontis[1], Marco M. Germani[2], Enrico G. Caiani[3], Ivana Barravecchia[1,2], Claudio Passino[2,4] and Debora Angeloni[2]**

[1] Department of Pharmacy, University of Pisa, Pisa, Italy, [2] MedLab, Institute of Life Sciences, Scuola Superiore Sant'Anna, Pisa, Italy, [3] Department of Electronics, Information and Biomedical Engineering, Politecnico di Milano, Milan, Italy, [4] Fondazione Toscana G. Monasterio, Pisa, Italy

Space is an extreme environment for the human body, where during long-term missions microgravity and high radiation levels represent major threats to crew health. Intriguingly, space flight (SF) imposes on the body of highly selected, well-trained, and healthy individuals (astronauts and cosmonauts) pathophysiological adaptive changes akin to an accelerated aging process and to some diseases. Such effects, becoming manifest over a time span of weeks (i.e., cardiovascular deconditioning) to months (i.e., loss of bone density and muscle atrophy) of exposure to weightlessness, can be reduced through proper countermeasures during SF and in due time are mostly reversible after landing. Based on these considerations, it is increasingly accepted that SF might provide a mechanistic insight into certain pathophysiological processes, a concept of interest to pre-nosological medicine. In this article, we will review the main stress factors encountered in space and their impact on the human body and will also discuss the possible lessons learned with space exploration in reference to human health on Earth. In fact, this is a productive, cross-fertilized, endeavor in which studies performed on Earth yield countermeasures for protection of space crew health, and space research is translated into health measures for Earth-bound population.

Keywords: microgravity, space radiation, endothelium, stress response, aging, pre-nosological medicine, bed rest, visual acuity

OPEN ACCESS

Edited by:
Ovidiu Constantin Baltatu, Anhembi Morumbi University, Brazil

Reviewed by:
Christopher S. Fry, University of Texas Medical Branch, United States
Joyce McClendon Evans, University of Kentucky, United States

****Correspondence:***
Debora Angeloni
angeloni@santannapisa.it

Specialty section:
This article was submitted to Integrative Physiology, a section of the journal Frontiers in Physiology

Received: *18 March 2016*
Accepted: *14 July 2017*
Published: *02 August 2017*

Citation:
Demontis GC, Germani MM, Caiani EG, Barravecchia I, Passino C and Angeloni D (2017) Human Pathophysiological Adaptations to the Space Environment. Front. Physiol. 8:547. doi: 10.3389/fphys.2017.00547

Abbreviations: ARED, Advanced Resistive Exercise Device; ADH, antidiuretic hormone; ANS, autonomic nervous systems; BP, blood pressure; bALP, bone alkaline phosphatase; BMD, bone mineral density; BBI, Bowman-Birk Inhibitor; BBIC, Bowman-Birk Inhibitor Concentrate; CTX, c-terminal telopeptide; CO, cardiac output; CEC, circulating ECs; EMG, electromyography; ECs, endothelial cells; eNOS, endothelial NOSl; FVC, forced vitality capacity; FRC, functional reserve capacity; GCR, galactic cosmic radiations; GCSF, granulocyte colony stimulating factor; HDBR, head-down tilt BR; HR, heart rate; HZE, high atomic number and energy nuclei; HMEC-1, human microvascular EC; iNOS, inducible nitric oxide synthase; iRED, Interim Resistive Exercise Device; IL, interleukin; ISS, International Space Station; IVD, intervertebral disc; IOP, intraocular pressure; SeM, L-Selenomethionine; LVETi, left ventricular ejection time index; LF, light flashes; LBNP, low body negative pressure; LEO, low Earth orbit; VImax, maximal shortening velocity index; MEP, maximum expiratory pressure; MIP, maximum respiratory pressure; MVC, maximum voluntary contraction; MAP, mean arterial pressure; SIMT, musculotendinous stiffness index; NTX, n-terminal telopeptide; nNOS, neuronal nitric oxide synthase; NE, norepinephrine; OCT, optical coherence tomography; PTH, parathyroid hormone; PP, perfusion pressure; PUFA, polyunsaturated fatty acids; PAEC, porcine aortic endothelial cells; PINP, procollagen type I N-terminal propeptide; RPM, random positioning machine; ROS, reactive oxygen species; RAAS, renin-angiotensin-aldosterone system; RV, residual volume; RVE, Resistive Vibration Exercise; REID, risk of exposure-induced death; RWV, rotating wall vessel; SWT, Si-Wu-Tang; SPE, solar particle events; SAS, space activity suits; SF, space flight; SVR, systemic vascular resistance; TAS, total antioxidant status; VEGF, Vascular Endothelial Growth Factor; VC, vital capacity.

INTRODUCTION

Physiology under extreme conditions uncovers reactions of the human body that may advance our understanding of limits for a healthy organism and may also shed light on premonitory signs of disease. Spaceflight (SF) physiology is no exception. During the last 50 years of manned space exploration studies have shown that humans can adapt to space and can remain productive for up to 1 year and possibly longer.

Many of the basic problems of space medicine—hypoxia, dysbarism, thermal support, acceleration, and response to great altitudes—have been studied by aviation and diving medicine long before the first human SF. In fact, flight, diving, and space traveling all involve pressure changes, forced changes in body position, controlled breathing sources, and dependence on life support equipment (Barratt, 2008). However, space flight poses unique medical problems due to prolonged exposure to a combination of stressful stimuli, such as acceleration forces, radiation, and weightlessness. In particular, the latter condition is a critical feature of SF and has effects on human physiology which were quite unexpected at the beginning of space exploration.

To appreciate the uniqueness of SF conditions, one should consider that a static gravitational field of 9.81 m/s^2 and a protective atmosphere are major factors that have made Earth amenable to life. The gravity force, always present with a fixed direction, has influenced the development of all organisms since the dawn of life (Anken and Rahmann, 2002). It was a major contributor to biological adaptations from water to land, by forcing ancestral organisms to develop complex systems for stability, fluid regulation, gravity sensing, and locomotion. In fact, every single cell may sense changes in gravity and convert mechanical stimuli into biochemical signals (Ingber, 1997). In Low Earth Orbit (LEO), astronauts are still exposed to about 90% of ground level gravity force. However, the spacecraft speed counterbalances the gravitational force and consequently astronauts are in a free-falling state resulting in an apparent weightlessness. In space, many physical and biological changes occur that highligth the importance of gravity in the evolutionary course, while coincidentally revealing unexpected links between microgravity, disease onset and aging. In fact, the adaptive response to microgravity by a healthy human has many features in common with aging, as both induce the decline of almost every body system.

In the 1970s, with three sequential Skylab missions of increasing duration (28, 56, and 84 days), each with three astronauts, enough data were collected to establish the foundation of space physiology (Dietlein, 1977; Buckey, 2006). From these preliminary results showing negative calcium balance with bone density loss, muscle atrophy, cardiovascular and hematic changes, metabolic, endocrine, and sleep disturbances, space physicians concluded that astronauts undergo rapid senescence in space. Their symptoms, in fact, were similar to those of the elderly (Vernikos and Schneider, 2010). However, this conclusion lost credit as soon as it was realized that astronauts could recover after returning to Earth. Systematic rehabilitation data are not always available and procedures are not standard, but the fact that anomalies subside in due time points to a significant difference from the normal aging process. Nevertheless, this coincidence of symptoms and the possibility that a longer stationing in space may have greater impact keeps the issue of accelerated aging at the fore front (Michel et al., 2007).

An additional issue is the possible impact of radiation exposure during SF. Outside the natural shield of the atmosphere and the Earth geomagnetic field, astronauts are exposed to heavy ions and proton fluxes, far higher than those experienced at most locations on Earth. Despite the limited number of crew members available for an analysis of space radiation effects, it is assumed that the perception of light flashes being reported by these individuals in a dark environment results from the action of heavy ions on the retina. Other long-term ocular damage may result from altered body fluid distribution in microgravity. The latter is of particular interest as it may provide insights on a possible combined impact of radiation exposure and microgravity.

WEIGHTLESSNESS AND FLUID REDISTRIBUTION AS STRESS FACTORS IN SPACE

Effects on the Cardiovascular System

The cardiovascular system holds the capacity to adapt to vastly different environmental and metabolic conditions. Physiological adaptation to postural changes relies on multiple, coordinated mechanisms such as the Starling-type and those operated by the endocrine and autonomic nervous systems (ANS). Gravity is a crucial factor in fluid distribution and has played an enormous role in shaping the evolution of the cardiovascular system. In upright posture, gravity determines a pattern of fluid distribution with higher arterial pressure in the feet (200 mmHg) and lower pressure in the head (70 mmHg) relative to the heart (100 mmHg). In space, this gradient is lost. Blood redistribution toward the head causes altered responses of baroreceptor, nervous and endocrine systems (Katkov and Chestukhin, 1980). As a result, within few minutes of microgravity exposure, astronauts suffer from a syndrome, known as "space motion sickness," which includes anorexia, vomiting, nausea, headache and malaise, gradually solved over 48–72 h. Dramatic physiological rearrangements due to headward body fluid shift occur under chronic microgravity exposure, from weeks to month, as well. However, the cause-effect relationship between fluid redistribution and space motion sickness remains not completely understood. An increase in cerebral spinal fluid and intracranial pressure has been theorized, but never demonstrated (Simanonok and Charles, 1994). Parasympathetic overstimulation, triggered by abnormal vestibular activity in microgravity, may play a crucial role, causing vomit, nausea, and baroreceptor desensitization. The interplay between vestibular and parasympathetic systems is currently under investigation (Clément et al., 1992).

Cardiovascular (mal)adaptation to microgravity is also responsible for acute orthostatic intolerance on returning to earth gravity, which represents an important problem encountered by

humans once they are adapted to microgravity: low vascular resistance and hypoadrenergic responses, related to a dysfunction of central integration of baroreflex afferent input as a result of SF, are considered the putative pathophysiological mechanisms of this phenomenon (Meck et al., 2004).

The best experimental setting for exploring acute and chronic cardiovascular adaptation in microgravity is represented by space missions. Nonetheless, precious experimental data and countermeasures against microgravity-dependent physiological adaptations have been collected from on-earth experiments. These include, for example, prolonged bed rest protocols and head-down tilt experiments for simulation of long-term microgravity exposure and free-fall parabolic flights (Limper et al., 2014), for acute simulation of microgravity.

Considering the complexity of the integrated neural and endocrine regulatory mechanisms that control the cardiovascular system, we will analyze the impact of SF on their operation in the following paragraphs.

Reflex Mechanisms

Blood redistribution early during microgravity produces engorgement of the central circulation, sensed by mechanoreceptors which activate autonomic offloading and volume regulating reflexes. As a result, there is a vasodilation and pooling of blood in the viscera and tissues and initial renal fluid and salt loss. Most adaptations occur within 6–10 h of SF.

Concerning heart rate (HR), values during SF have been reported as higher, lower, or unchanged from preflight values. Significantly, different authors have reported an evident fall in HR, in both short- and long-term missions (Fritsch-Yelle et al., 1996; Verheyden et al., 2009). Such reduction is consistent with a rise in arterial pressure being sensed by neck baroreceptors due to cephalic blood redistribution. A recent 14-day mission involving three Chinese astronauts failed to show changes in mean HR, but nevertheless HR excursions increased compared to pre-SF measurements (Liu et al., 2015).

Similarly, conflicting data exist on mean arterial pressure (MAP). Several authors have claimed that microgravity decreases MAP (Fritsch-Yelle et al., 1994; Baevsky et al., 2007; Verheyden et al., 2009), while others have reported the opposite, at least during short-term SFs (Hughson et al., 2012). This discrepancy is likely due to differences in the definition of the pre-flight baseline as well as in a variety of countermeasures and study protocols being adopted in-SF. Recently, thanks to a regular exercise program, six male astronauts being stationed for 2–6 months in the International Space Station (ISS) could redress any change in systolic and diastolic pressure, and presented normal MAP (Hughson et al., 2012).

The baroreflex acts in a coordinated way on both heart and blood vessels to control blood pressure (BP), with the effects on the heart occurring in parallel to those on systemic vascular resistance (SVR). Indeed, a decreased SVR may contribute to the increase in CO reported during SF. However, data from a long-term ISS mission showed a non-significant reduction in SVR (although this was possibly due to the high variability in the experimental group; Hughson et al., 2012). Shear blood stress in vessel remodeling might help interpreting the impact of SF on SVR, but the literature is rather elusive and contradictory on this issue. For years experimental observations were based on animal models exposed to simulated microgravity. The initial hypothesis was that vascular smooth muscle cells would suffer from deconditioning in space and undergo atrophy similar to that observed in skeletal muscles, thus resulting in loss of tone and hypotension (Trappe et al., 2009). However, several experiments performed on Earth on the hindlimb-unloaded rat model demonstrated that the outcome of vessel remodeling processes changes according to the anatomic region involved. At 1 g, vessel walls stressed by BP become hypertrophic, while low BP leads to wall atrophy. Furthermore, the lumen increases in the carotid and the basilar arteries, while becomes narrowed in the hindlimb rat vessels, like the femoral and the anterior tibial arteries (Zhang, 2001). Some studies have reported reduced vasoconstriction in hind limb and abdominal arteries (Ma et al., 1997; Zhang et al., 2001), while others have reported basilar artery and common carotid vasoconstriction (Purdy et al., 1998). In light of that, the attendant effect on SVR may be small and variable. Therefore, it is important to consider both vasoconstriction and vasodilation responses to microgravity when evaluating any change in SVR.

NO release may represent an additional factor impacting on SVR. In fact, 20-day tail suspension resulted in the up-regulation of inducible nitric oxide synthase (iNOS) in thoracic aorta and heart, and in the over-expression of neuronal nitric oxide synthase (nNOS) in the brain and kidney (Schrage et al., 2000).

Recently, it was shown that mice exhibit an impaired vasoconstrictive response of mesenteric arteries and veins to norepinephrine (NE), KCl, and caffeine during SF, due to a decreased response of the adrenergic receptors and a reduced influx of Ca^{++}. However, these results did not match with any macroscopic structural change of the arteries (such as lumen and wall thickness), nor did they show impairment in passive mechanical properties (Taylor et al., 2013). Collectively, these data indicate that both structural changes and molecular adaptations to microgravity may suppress the vasoconstrictive response to ANS, thus reducing SVR. Consequently, the arterial pressure control may become impaired and this causes orthostatic hypotension upon return on Earth.

Endocrine Mechanisms

Bearing in mind the key role of the kidney in BP regulation, in space the upward redistribution of blood volume with the concomitant decrease of a pressure gradient should reduce kidney perfusion. In turn, a lower than normal pressure within the renal artery should lead to a greater release of renin and, ultimately, to a more marked activation of the renin-angiotensin-aldosterone system (RAAS).

Still, kidney perfusion has been found normal in space, along with increased plasma filtration, diuresis, and natriuresis (Leach et al., 1975). One should note however that more recent studies show a marked reduction of diuresis and natriuresis in space with NE, RAAS, and antidiuretic hormone (ADH) increasing through unknown mechanisms (Grigoriev et al., 1994; Drummer et al., 2000; Christensen et al., 2001).

A drastic weight-loss of the astronauts proved to be unrelated to the increased diuresis and natriuresis (Christensen et al., 2005). Imbalanced fluid distribution and atrophy of the antigravitational muscles (e.g., postural muscles and lower limb muscles) may facilitate fluid and albumin accumulation within the muscle interstitial space. An increase of glomerular filtration and by extension of diuresis and natriuresis, is ascribed to reduced colloid osmotic pressure. Accordingly, long-term BP adjustment in space may be mainly sympathetic-dependent, since RAAS activation is not due to altered kidney perfusion but rather to higher NE plasma concentration. In space, the colloid osmotic pressure due to plasma proteins is the only factor that prevents fluid extravasation. Moreover, microgravity reduces interstitial fluid removal by the lymphatic system, since this drainage depends on tissue deformation and local hydrostatic pressure (Hargens et al., 2013). This situation leads to oedema formation, particularly evident as a facial congestion (Parazynski et al., 1991).

Recent work has investigated the actual role of barorereflex and endocrine mechanisms in long-term microgravity exposure. Data collected between May 2007 and December 2009, before, during and after a 6-month mission to the ISS, showed no change in the baroreflex response slope while adopting an accurate countermeasure program (Hughson et al., 2012). Indeed, these data (Hughson et al., 2012) differ from those collected in a 10-day mission (Drummer et al., 2000) and confirm some previous findings while disagreeing with other investigations (Eckberg et al., 2010; Verheyden et al., 2010). From this evidence, it seems possible that over an extended period other mechanisms, possibly hormone release, may progressively displace the baroreflex in the control of BP. However, the gradual adjustment of the human body to weightlessness may involve other mechanisms besides the baroreflex and endocrine systems that on Earth are the main players in the operation of the cardiovascular system.

In summary, despite some contradictory results from different groups employing diverse research protocols, a consensus may be reached over the fact that the circulation of blood becomes more efficient in microgravity. Specifically, a lower HR supports the body's energy and perfusion requirements and, notwithstanding the higher stroke volume, the heart works less since it does not operate against gravity. Although, microgravity *per-se* does not seem to be a stress factor, the rapid adaptive changes being triggered by fluid redistribution, while appropriate for space, cause a significant deconditioning and orthostatic hypotension upon return to Earth. These dynamic phenomena occurring during SF provide the opportunity to investigate pathophysiological mechanisms underlying deconditioning and orthostatic hypotension, regardless of its etiology.

Effects on the Endothelium: A Molecular View

The endothelium is a spatially diffuse organ, composed of a single layer of cells (the endothelial cells, ECs) that covers the inner surface of blood and lymphatic vessels (Fishman, 1982; Augustin et al., 1994). ECs function ensures vascular integrity and homeostasis and regulates a variety of essential physiological processes. Conversely, endothelial dysfunction is involved in a variety of vascular pathologies (e.g., atherosclerosis, hypertension, thrombosis) as well as in cardiovascular anomalies frequently found in a sedentary and elderly population (Cines et al., 1998). EC senescence is characterized by alterations in adherens junctions and leads to increased vascular permeability. This phenomenon mostly involves small blood vessels. Vascular permeability is central to the progression of different diseases linked to aging (Oakley and Tharakan, 2014), with pro-inflammatory (e.g., Tumor Necrosis Factor alpha, TNF-α, and TNF-Related Apoptosis-Inducing Ligand, TRAIL) and patently inflammatory (e.g., histamine, thrombin, Vascular Endothelial Growth Factor, VEGF) stimuli causing cytoskeleton disorganization (Kumar et al., 2009; Sawant et al., 2011).

Significantly, head down tilt bed rest (HDBR) studies have provided evidence of an increase in circulating ECs (CECs) in case of diffuse tissue damage (Demiot et al., 2007). ECs are most susceptible to variations in gravitational loading (Augustin et al., 1994; Cines et al., 1998), as exemplified by studies in an animal model (Xianyun et al., 1997) showing an increase in CECs in response to simulated microgravity.

ECs isolated from vessels of different size and location in the body are morphologically and functionally heterogeneous (Monahan-Earley et al., 2013). Since ECs from the microvasculature cover a surface 50 times larger than that of all large vessels lumped together, the endothelium of small blood vessels has a marked impact on systemic homeostasis. Its importance is evident from the modulation of inflammation to wound healing and tissue repair. A microvascular endothelial dysfunction is likely to play a significant role in osteoporosis, muscle atrophy and in the cardiovascular deconditioning being reported by astronauts. The same sequence of events may also occur in healthy volunteers during long-lasting HDBR (Demiot et al., 2007; Coupé et al., 2009; Morrison et al., 2014).

Several studies have reported the response of ECs to either simulated or real microgravity, although they mostly involve models of macrovascular ECs, HUVEC or their derivative EA.hy926 (Maier et al., 2015). Of note, several devices may simulate microgravity on Earth (including 2D clinostat, random positioning machine, RPM, rotating wall vessel, RWV, and diamagnetic levitation; Herranz et al., 2013), but the resulting gravity vector is averaged to near zero over time and is not neutralized (Herranz et al., 2013). On the other hand, microgravity can be obtained through sounding rockets, drop towers, or parabolic aircraft flights, albeit over very short periods, while aboard the ISS or other spacecraft samples are exposed to real microgravity (Herranz et al., 2013) for a considerable amount of time.

In simulated microgravity, HUVEC showed increased migration and proliferation (Carlsson et al., 2003), along with down-regulation of interleukin-1α (IL-1α), an antagonist of endothelial proliferation, and up-regulation of heat shock protein 70 (Hsp70). Conversely, up-regulation of apoptotic signals (e.g., Bax, Fas-L) occurs in porcine aortic endothelial cells (PAEC) cultured in RPM.

NO is an important effector for many signaling pathways and a potent vasodilator responsible for vascular homeostasis.

Increased NO synthesis following NOS up-regulation is a common trait of EC adaptation to microgravity (see also Reflex Mechanisms above). It might have a crucial role in the endothelial response to microgravity since its level increases in both microvascular ECs from murine (1G11; Cotrupi et al., 2005) and human (HMEC-1; Mariotti and Maier, 2008) source as well as in macrovascular HUVEC (Shi et al., 2012) and EAhy926 (Siamwala et al., 2010) cells of human origin.

Responses to simulated microgravity suggest substantial differences between microvascular and macrovascular ECs, but the interpretation of findings is made difficult by intrinsic variations in cell types and ground simulators among cell biology studies in microgravity. Indeed, the same experimental model may generate different responses when challenged in diverse devices or by space microgravity. Although not evident morphologically, these differences emerge at the molecular level (Grimm et al., 2002; Pietsch et al., 2013; Ma et al., 2014; Warnke et al., 2014).

In Summer 2015, we dispatched samples of human microvascular ECs HMEC-1 (a reductionist representation of human dermal microvascular endothelium) to the ISS (Balsamo et al., 2014). Still in progress, integrated analyses of their transcriptome, methylome, and morphology in real microgravity should shed light on the adaptive response to the space environment and, possibly, should also uncover differences with ECs of macrovascular origin.

A new type of EC, type H, mediates neo-angiogenesis, and osteogenesis in bone (Kusumbe et al., 2014). The decline of type H cells and the concomitant reduction of osteoprogenitor cells could offer a convincing explanation for the loss of bone mass during aging. If so, the activation of specific molecular pathways promoting type H vessel formation may pave the way to therapeutic osteogenesis. In this light, it would be of interest to characterize the response to microgravity by type H ECs and by extension to evaluate their possible role in the response of the human body to SF.

In sum, it is clear that gravity has shaped the physiological properties of different components of the cardiovascular system. However, the impact of SF on blood vessel functions and specific properties is far from being explained by the response of cells and tissues to just microgravity alone.

The Eye, Microgravity, and Vision

The eye is a small organ whose function relies on the coordinated operation of its optical, vascular, epithelial, and neural components. In space, the fluid redistribution caused by microgravity affects the blood supply to the eye with an impact that depends on specific facets of its vascularization. The evolution of initial fluid redistribution into long-lasting effects on eye anatomy and function depends on SF duration (Mader et al., 2011). Blood supply to the retina and the posterior pole of the eye is via the ciliary arteries and the central retinal artery branches of the ophthalmic artery, a branch of the internal carotid artery, although variations are frequent (Hayreh, 2006). The retina has an oxygen consumption rate per unit weight higher than the brain (Ye et al., 2010), consistent with the high metabolic rate of photoreceptors (Demontis et al., 1995, 1997). To support retinal oxidative metabolism (Wang et al., 2010), the choriocapillaris of the choroidal vascular bed have evolved as a system with large fenestrated capillaries (i.e., high flux and permeability) and low oxygen extraction (Linsenmeier and Padnick-Silver, 2000). Furthermore, the choroidal circulation may absorb the heat generated by the focusing of the infrared component of light on the posterior pole of the eye (Parver et al., 1980), a role of high relevance in the foveal region (Parver, 1991). Similarly, blood supply to the eye supports the secretion of the aqueous humor by the ciliary epithelium, thus generating an intraocular pressure (IOP) to set eye tonicity. This process likewise satisfies the metabolic needs of eye tissues lacking a vascular bed, such as the lens and the cornea. In turn, IOP affects the perfusion pressure (PP) of the choroidal circulation that depends on the difference between blood pressure in the ophthalmic artery and IOP. In humans, the occurrence of autoregulatory mechanisms (Riva et al., 1981, 1997a,b) prevents increases in IOP from translating into corresponding changes in choroidal blood flow, despite their influence on PP. PP regulations are also apparent in response to HDBR protocols, with a persistent increase in ophthalmic arterial pressure, IOP and PP in response to transient changes in the size of retinal arterioles and venules (Baer and Hill, 1990). Optical coherence tomography (OCT), paired with angiography using near infrared fluorescent probes poorly absorbed by pigment epithelium such as indocyanine green, has significantly enhanced the functional evaluation of the choroidal circulation, otherwise not accessible using visible light (recently reviewed; Ferrara et al., 2015). Similar to retinal vessels, HDBR tilting increased choroidal thickness and IOP in proportion to the tilt angle, as assessed by OCT and indocyanine green angiography, while retinal thickness was largely unaffected (Shinojima et al., 2012). These results indicate that an upward shift in blood distribution may quickly affect eye vasculature.

Blood redistribution toward the head induced by microgravity is expected to affect eye vasculature by reducing arterial blood supply and slowing venous flow from the eye. It is important to remind that venous blood return from the head, neck and upper trunk is typically assisted by gravity, as it occurs via veins that lack both valves and muscular contraction, as opposed to the lower half of the body, where this mechanism provides the propulsive force that opposes gravity. In microgravity, a reduced blood flow return from head and neck to the heart is expected to raise the venous pressure and increase filtration at the capillaries causing, in turn, an increase in both intracranial pressure and IOP, consistent with face swelling mentioned above (see Endocrine Mechanisms).

Several papers report the effects of microgravity on eye function. Short exposures to microgravity during parabolic flights (20 s-long) were found associated with a significant increase (58%) in IOP and a non-significant decrease (4%) of retinal arteries size, indicating that the effects of microgravity on IOP take place on a short time-scale (Mader et al., 1993). An important issue is whether these rapid changes in the eye vascular bed affect its function.

Exposure to microgravity on a time scale of a few days, such as during shuttle flights, was associated with reduced near sight in about 23% of astronauts (Mader et al., 2011). Furthermore,

48% of astronauts returning from ISS long-duration SFs reported near sight vision reduction (Mader et al., 2011). Detailed investigations in astronauts that reported visual problems upon returning from 6 month-long SFs indicate the occurrence of ocular damage. A hyperopic shift was found in 6/7 astronauts, with posterior eye pole flattening and choroidal folding in 5/7 (Mader et al., 2011).

MRI investigations of orbital and intracranial effects of microgravity were carried out in 27 astronauts at a variable time after their return from space, while pre-SF control data were not available (Kramer et al., 2012). However, in 8 of them, the analysis included measurements carried out between two consecutive SFs and in 7/27 (26%) globe flattening was present. This study also documented swollen and bent optic nerve sheath in 26/27 (96%) astronauts. Importantly, evidence of optic nerve protrusion in 4/27 (15%) and pituitary dome concavity in 3/27 (11%) astronauts support the hypothesis of an increase in intracranial pressure (Kramer et al., 2012).

Overall, these findings recall those found in patients affected by idiopathic intracranial hypertension (Jacobson, 1995). Specifically, the elevation of fluid pressure within the skull may lead to an increased volume of choroidal vessels, shifting the fovea along the anterior-posterior axis with ensuing shortsightedness, but this hypothesis awaits confirmation (Nelson et al., 2014). Swelling of choroidal vessels may also damage the papilla, the site of optic nerve emergence from the eye. However, despite the expected increase in intracranial pressure in all the flying astronauts (those exposed to microgravity, as opposed to those that trained but did not travel to space), globe flattening was found in at least one eye in only 7/27 astronauts. Moreover, changes in visual acuity were reported to occur after 3 weeks up to 3 months in microgravity (Mader et al., 2011), well beyond the initial increase in cranial pressure from blood redistribution (Tatebayashi et al., 2002), making problematic a straightforward link between the immediate increase in cranial pressure and late visual impairments. Furthermore, the persistence of these anatomical changes and visual problems several months after return to Earth, i.e., after removing the initial increase in intracranial pressure, suggests that the structural damage possibly results from additional events triggered by intracranial hypertension during long-term exposure to microgravity (Taibbi et al., 2013), rather than by hypertension *per-se*.

The finding that visual problems associated with prolonged exposure to space are present only in a fraction of astronauts suggests that genotype also plays a role in the frequency with which persistent functional and anatomical damage in response to microgravity may appear. Interestingly, those astronauts that developed eye and vision problems (Zwart et al., 2012) had reduced folate and increased homocysteine levels, despite similar nutrition before, during and after SFs. Genetic polymorphisms in methylene-tetrahydrofolate-reductase (MTHFR), the gene coding for a key step in folate synthesis, are frequent and associated with reduced enzymatic activity. Therefore, differences in folate levels based on genetic backgrounds may account for part of the variability in the propensity of astronauts to develop eye problems in microgravity. However, despite this clear association, we lack a mechanistic link between folate deficit and the probability of developing eye problems in microgravity.

Effects on the Musculoskeletal System

Prolonged exposure to microgravity affects the musculoskeletal system, with the loss of bone and muscle mass attributed to both reduced use and perfusion changes (Hargens et al., 2013). Skylab missions showed an increase in bone resorption markers (n-terminal telopeptide, NTX, and hydroxyproline) and a significant reduction in Ca^{++} balance. Bone mineral loss was higher in sites supporting the body weight in normal gravity, like lumbar spine, femoral neck, and trochanter, pelvis, calcaneus, and leg, whereas arm bones were not affected (LeBlanc et al., 2007).

Soyuz and Mir missions confirmed the Skylab results, adding novel insights into bone marker change in cosmonauts. Levels of osteocalcin, a structural protein of the bone, slightly but significantly increased in blood samples collected at day 14 in space, but significantly decreased after 110 days in space (LeBlanc et al., 2000). Osteocalcin drastically increased upon return to Earth. Data from long-lasting American and Russian missions ($n = 60$, between 4 and 6.5 months) demonstrated that 92% of crewmembers suffered 5% loss of bone mineral density (BMD) in at least one skeletal site (LeBlanc et al., 2000). For the sake of comparison, the rate of BMD loss occurring during a 6-month stay on ISS is similar on average to that occurring between the 5th and 6th decade of life on Earth.

Osteoclast activity increases and major bone resorption occurs in 14-day long, -6° HDBR studies, with control subjects showing increased level of resorption markers in blood and urine compared with subjects undergoing vibration training as countermeasure. The analyzed markers included urine levels of c-terminal telopeptide (CTX) and NTX, in addition to blood levels of bone alkaline phosphatase (bALP) and Procollagen type I N-terminal propeptide (PINP; Smith et al., 2005).

In reference to bone metabolism, the levels of vitamin D, bALP, osteocalcin, calcitonin, parathyroid hormone (PTH), and Ca^{++} have been investigated. Results from the Mir18 mission showed a significant decrease in $1,25(OH)_2$-vitamin D and its precursor 25(OH)-vitamin D. Calcitonin levels were not affected either in space or back on Earth. The observation that PTH values rapidly increase upon return to Earth (Smith et al., 1999) indicates detrimental mass bone restoration, as PTH promotes bone resorption and elevates blood Ca^{++} levels by activating osteoclasts. However, PTH acts on kidneys too, to increase Ca^{++} and decrease PO_4^{3-} reabsorption (Lee et al., 2009), suggesting that bone loss in microgravity may be due mainly to impaired kidney function and vitamin D production, rather than to a significant calcitonin and PTH imbalance. Therefore, reduced vitamin D level may decrease Ca^{++} fixation in bones and reabsorption in kidneys, causing increased Ca^{++} excretion despite normal levels of calcitonin and PTH (Smith et al., 1999). Vitamin D level increases later on, upon a prolonged re-exposure to gravity, to promote net bone fixation.

Perfusion remodeling during SF may affect bone mass, and unbalance the ratio between osteoblastic and osteoclastic activity. Data on perfusion-dependent effects on muscle mass

are only available from tail-suspended mice (a simulation of weightlessness). Tail suspension was performed for 10 min, 7 days, and 28 days. Femoral and tibial perfusion were reduced with 10 min of treatment, and blood flow to the femoral shaft and marrow were further diminished with 28 days of treatment. Correspondingly, the mass of femora and tibiae was lowered with 28 days of tail suspension. In this condition, the femur was hypoperfused both in acute and chronic simulated microgravity, while the tibia showed a perfusion increase at the distal bone region only, at least in acute treatment. However, the authors (Colleran et al., 2000) may not have considered that tibia fuses with fibula in mouse (Moss, 1977) and the vascular anastomosis of tibial and fibular arteries provides blood supply to the tibia. Interestingly, it was shown that blood flow to the skull, mandible, and humerus increases only acutely (i.e., upon acute perfusion). It is possible that in chronic conditions aortic pressure increases, due to the blood shift from the hindlimbs to the forelimbs and head, and adjusts within a longer period by vasoconstriction of the most perfused arteries (Colleran et al., 2000).

There is high variability in results regarding extension and grade of muscle atrophy, which may ensue from different durations of muscle unloading but also relate to pre-flight muscle size in a non-linear way (Belavý et al., 2009). For instance, when comparing the plantar flexors with the knee extensors, atrophy was more pronounced in the former, possibly because during locomotion on Earth a higher load stresses the plantar flexors than the knee extensors. Consequently, unloading in space causes more damage in plantar flexors than in the extensors. The damage does not derive from fiber loss, but rather from a reduction in their size and protein synthesis.

Exactly what type of muscle fiber suffers the most damage from exposure to microgravity is still unclear, due to controversial results from human and mouse models (Belavý et al., 2009). Even though type I fibers seem to be the most affected in both species, the underlying mechanism may be different. In humans exposed to 5-week HDBR, protein anabolism was severely affected, as shown by the decreased synthesis of myofibrillar proteins and collagen along with an unchanged catabolism, unlike the mouse model that showed considerable protein breakdown (de Boer et al., 2008).

To explore the mechanism underlying the loss of anti-gravitational muscle mass in response to prolonged disuse in humans, the fascicle length and pennation angle were analyzed in the gastrocnemius and in the vastus lateralis at the end of 5 weeks of horizontal BR. In both muscles, the reduction of the pennation angle was quite remarkable, and mirrored the loss of sarcomeres, both in parallel and in series. Interestingly, these parameters were not affected in biceps brachii, an upper limb muscle (de Boer et al., 2008). At the functional level, data on neuromuscular activity registered by electromyography (EMG) to investigate the plantar flexor activity showed a 35–40% reduction after 90–180 days in space (Lambertz et al., 2001). Of note, these data differ from those showing an increased EMG activity in the tibialis anterior and soleus, without changes in the gastrocnemius medialis (Edgerton et al., 2001).

High individual heterogeneity might partially account for such differences. The muscular parameters of cosmonauts were studied focusing on their maximal voluntary contraction (MVC), maximal shortening velocity index (VImax) and musculotendinous stiffness index (SIMT), collecting data pre- and post-SF. Despite a significant decrease in MVC and an increase in VImax and SIMT, the number of observations was small and there was high inter-individual variability (Edgerton et al., 2001).

In conclusion, it is not surprising that a varying degree of muscle loss results from different duration of microgravity exposure. These considerations may have a major impact on rehabilitation after injuries, especially in aging subjects, highlighting the need to focus on those muscle groups more prone to mass loss in response to unloading.

Effects on the Respiratory System

Microgravity-induced respiratory modifications have been studied for decades, focusing on several parameters that characterize respiration and ventilation (Baranov et al., 1992; Prisk, 2000; Prisk et al., 2006). Different studies are difficult to compare due to environmental bias (for example, during the Skylab missions in the 1970s, data were collected from astronauts exposed to the hypobaric and hyperoxic environment; Sawin et al., 1976) and to the variability of experimental protocols (which included pre-, in- and post-SF measurements; Baranov et al., 1992). Furthermore, indirect experimental procedures were used to estimated gas exchange and the ventilation-perfusion ratio.

Studies from Spacelab missions 1 and 2 on lung ventilation and perfusion showed that microgravity causes a slight increase in respiratory frequency and a reduced physiological dead space thanks to homogenous blood redistribution in lung vessels. Data from the same missions described a reduction in tidal volume (Donnelly et al., 2010), which was confirmed by other studies (Prisk et al., 2006). Data collected from a 6-month stay on ISS (where the environment is normoxic), failed to show significant modifications in gas exchange in space. However, there was a significant reduction in O_2 consumption and CO_2 production at 2 and 4 months (Prisk et al., 2006). The reason why this happens remains unknown (Prisk, 2014). A possible explanation needs to consider multiple concomitant factors. First, the reduction of muscle work due to reduced gravitational loading. Second, the difference in perfusion and ventilation between upper and lower lung regions, which decreases and may require less frequent and deep ventilation by the respiratory muscles. Altogether, these effects are expected to reduce the metabolic rate.

Changes in thorax wall and respiratory mechanics are among the first aspects to address when considering respiration in space. In microgravity, the contribution of the abdomen to the tidal volume increases, while rib cage expansion is reduced (Wantier et al., 1998). Studies in the 1990s suggested that microgravity decreased vital capacity (VC; Venturoli et al., 1998), forced vitality capacity (FVC), and peak inspiratory and expiratory flows (Baranov et al., 1992). The authors proposed that microgravity could weaken respiratory muscles, compromising the respiratory function. However, more recent data questioned these concepts: apart from a significant early increase during the mission's first 2 months, VC and FVC at 4 and 6 months were not statistically

different from pre-SF values (Prisk et al., 2006). Peak inspiratory and expiratory flows showed the same trends. Prisk et al. showed a significant reduction in maximum inspiratory pressure (MIP) at functional reserve capacity (FRC) and residual volume (RV) during the entire mission (Prisk, 2000). Maximum expiratory pressure (MEP) at total lung volume was significantly reduced at 2 and 4 months but showed a trend toward full recovery at 6 months. MEP at FRC was not affected. Notably, the same authors reported a significant reduction in tidal volume between in-SF respiration and steady respiration on-Earth (Prisk, 2000). As already mentioned, this may be due to different lung perfusion in space: since blood redistributes upward, lung vessels should receive more blood, resulting in more efficient gas exchange and therefore lead to a lower excursion between inspiration and expiration at rest.

Remarkably, FRC in space reduces significantly to around 500 ml (Elliott et al., 1994). This reduction is explained directly by microgravity: since FRC is a direct measure of the balance between lung collapse and the outward expansion of the thoracic chamber, in space the contribution of the abdominal content weight to thorax expansion becomes negligible, therefore FRC falls (Prisk, 2014). RV measured after forced expiration decreases significantly in space. In fact, on Earth alveoli at the bottom of the lungs deflate more easily than the alveoli at the top, causing the retention of a larger amount of air in the upper lung regions. In space, this does no longer occur and therefore RV is lower than on Earth (Elliott et al., 1994).

These results suggest that the respiratory system undergoes significant adaptation after prolonged exposure to blood redistribution in microgravity. These changes develop over several weeks, possibly indicating that adaptation occurs through anatomical rather than functional changes, a finding relevant to the impact of prolonged bed rest on elderly subjects or chronically ill patients.

RADIATION EFFECTS

In addition to weightlessness, a main environmental factor acting upon the human body in space is represented by cosmic radiation. Far from Earth, beyond the Van Allen radiation belt, the astronauts of long-term missions to Moon or Mars would be exposed to remarkable doses of radiations of two kinds: solar particle events (SPE) and galactic cosmic radiations (GCR), which cause acute and late morbidity respectively. SPE occur in space with different intensity according to periodic oscillations of solar activity and contribute to total irradiation for a maximum 5% (Cucinotta et al., 2013). GCR consist mainly of protons and high atomic number and energy nuclei (HZE, 1%), establishing a qualitative difference between cosmic and Earth radiation spectra, which consists of α-, β-, and γ-rays.

A 3% risk of exposure-induced death (REID) at the upper 95% confidence interval is considered the maximum acceptable risk for a space mission (Cucinotta and Durante, 2006). Future long-duration missions, including landing on Mars, need to take this limit into account because the estimated impact of radiations for a mission to the red planet lasting 460–780 days exceeds the REID limit (Cucinotta et al., 2013). However, these data lack accuracy since they are based on predictions for cardiovascular and ischemic heart disease computed from a meta-analysis of studies concerning atomic-bomb survivors and radio-exposed workers (Kennedy, 2014). In addition, while small animals and human cell cultures have been exposed to simulated GCR, the effect of HZE particles was not investigated, although this aspect is quite relevant indeed. In fact, HZE particles are qualitatively different from the protons of GCR and exert a stronger effect on biomolecules, resulting in complex DNA damage and higher amounts of reactive oxygen species (ROS) formation, which in turn leads to chronic oxidative stress and increases drastically genomic instability (Kennedy, 2014).

Radiation effects on the human body can be classified either as acute or long-term. The first may cause the astronauts to suffer from acute radiation sickness, including vomiting, nausea, and a falling blood count (Donnelly et al., 2010); the latter corresponds to cancer development. The risk of suffering from acute radiation poisoning is quite low during internal vehicle activity, also during long-term missions. Nonetheless, consequences of acute irradiation could decrease the white blood cell count, and break epithelial layers thus resulting, for example, in translocation of bacteria and their products in the intervillous district of the ileum. T-lymphocyte decrease, vomiting, and nausea, skin damage with loss of blood vessels density under the dermis could occur as well (Cucinotta et al., 2013; Kennedy, 2014). Disseminated intravascular coagulation is among the most serious acute effects of chronic exposure to cosmic radiations.

Concerning long-term effects, experiments conducted on mice proved that 0.5–3 Gy protons or 0.5 Gy ^{56}Fe exposures reduced overall survival and caused malignant lymphoma and Harderian gland tumors. In experimentally irradiated mice, pre-malignant and malignant lesions of myeloid origins were observed, with proton and γ-ray-induced accumulation of p53, along with increased ROS generation and deregulation of the extra-cellular matrix compartment (Barcellos-Hoff et al., 2015).

When exposed to radiation in microgravity, an organism may in principle suffer from a diminished capability of DNA repair systems, which physically consist of enzymes transported through the cell to exert their role in the nucleus whenever necessary. In fact, there is at the moment evidence of the combined effects of both microgravity and radiations on different organs and organ systems, such as the eye, the cardiovascular, and the immune systems. Although, we will not discuss here the latter (well-reviewed in Crucian et al., 2014), still we want to remark that several other factors such as isolation, confinement, and disrupted circadian rhythms in general add to microgravity and radiation to generate the complex phenotype of a space-exposed organism.

Radiation Effects on the Eye

During SF, cosmic radiations are expected to affect all organs to some extent. The eye is particularly susceptible to cosmic radiations, as it lacks the protections warranted to inner organs by the skin, with its layer of dead keratinocytes, or to the brain by the skull. Not surprisingly, the first evidence of the effects of cosmic radiation on the human body came from Apollo 11 lunar

module pilot Buzz Aldrin (Pinsky et al., 1974), who reported the occurrence of light flashes (LF) upon dark-adaptation. Most astronauts have later reported the occurrence of LF when dark-adapted. There is evidence that multiple components of cosmic radiation may cause LF (Casolino et al., 2003). Depending on the energy of impinging particles, LF may result from retina stimulation by photons generated via Cerenkov's effect by particles traversing the vitreous (Fazio et al., 1970) or the lens (McAulay, 1971). However, an additional mechanism may explain HZE-triggered LF. Hydroxyl radicals generated by HZE interaction with water (Yamaguchi et al., 2005) may cause the peroxidation of polyunsaturated fatty acids (PUFA) ensheathing rhodopsin molecules in the disk membrane of rod outer segments (reviewed in Catalá, 2006). Evidence for PUFA peroxidation induced by the exposure to high-energy carbon ions via reactive hydroxyl radicals has been gathered both *in vivo* and *in vitro*. Furthermore, the annihilation of two peroxy radicals leads to the emission of a photon, which may isomerize a rhodopsin molecule (Narici et al., 2012, 2013). Due to the high amplification of the phototransduction cascade in retinal rods, isomerization of a rhodopsin protein by a single photon is sufficient to lead an individual to LF perception (Baylor et al., 1979). According to this model, rod photoreceptors work as a sensitive probe to detect light emitted in response to a chain reaction triggered by cosmic radiation via the generation of highly reactive radical species, thus signaling the occurrence of nearby damaging molecules. However, the generation of reactive radical species by HZE may also take place in other retinal neurons, although it may go unnoticed due to the lack of light-sensitive probes for photons emitted during radical annihilation. In fact, the electrophysiological response of mice exposed to both light and ^{12}C ions suggest that charged particles do not simply mimic the light response at the rod level, but rather may interfere with the processing of light signals downstream of rods (Carozzo et al., 2015). Consistent with this notion, increased apoptosis along with ganglion and amacrine cell damage are indicators of inner retinal injury in space-flown mice. This damage correlated with increased accumulation of lipid peroxidation byproducts and up-regulated expression of genes involved in response to oxidative stress as well as in mitochondria-associated apoptotic pathways (Mao et al., 2013). The lack of damage at the site of origin of LF (outer retina) may result from the protection afforded to rods by rhythmic disk shedding, which removes the outer segment tip damaged by HZE-generated free radicals (recently reviewed in McMahon et al., 2014).

The notion that HZE may trigger lipid peroxidation and ultimately lead to the activation of the phototransduction cascade in rods and LF perception by astronauts is supported by multiple and independent evidence gathered both *in vitro* and *in vivo*. However, some discrepancies remain. In particular, it is unclear how to reconcile the role of HZE-triggered lipid peroxidation with the observation that LF frequency is about twice as much when traveling toward the Moon than on the way back. Although the sensitivity of astronauts to LF may decrease during the first few days in orbit, the underlying mechanisms and their link with lipid peroxidation are unclear. A second issue is the large inter-individual variability in sensitivity to LF (Pinsky et al., 1974). In fact, while some astronauts report the occurrence of LF as soon as they became dark-adapted (i.e., when the rod system takes over vision) and refer to LF as an annoying phenomenon that may interfere with their ability to rest (Fuglesang et al., 2006), others are far less sensitive. At the extreme, the Apollo 16 command module pilot Thomas K. Mattingly did not report LF at all, possibly because of his poor night vision (possibly confirming the role of rods in LF perception). However, the occurrence of intermediate sensitivities to LF in astronauts with normal rod-mediated vision may indicate a role of additional, as yet unknown, factors. By analogy with the eye damage caused by microgravity (see The Eye, Microgravity, and Vision), genetic polymorphisms may play a role in setting the sensitivity of astronauts to LF perception in response to HZE exposure.

LESSONS LEARNED FOR/FROM SPACE RESEARCH

Countermeasures for Space from Bed Rest Studies

Ground-based studies represent an essential opportunity to investigate human physiology in simulated microgravity, and thus to test the effectiveness of potential countermeasures for preventing or mitigating the undesired physiological changes associated with SF, mentioned in the above paragraphs.

At the beginning of the human SF era in 1961, head-out water immersion was used to simulate weightlessness on the ground, limited to short periods (6–12 h). In the early 1970s, head-out dry immersion (i.e., immersion with an impermeable elastic cloth barrier between subject and thermo-neutral water, thus providing an absence of mechanical support of specific zones during immersion—supportlessness), was proposed (Shulzhenko and Vil-Vilyams, 1975) and then widely used, in particular by Russian scientists (Navasiolava et al., 2011). Gradually, the model of HDBR became the method of choice for studying the effects of prolonged musculoskeletal unloading on the ground. Based on the sensation of astronauts after long-duration SF, HDBR was considered more appropriate for simulating physiological changes of SF than horizontal BR, and -6° HDBR was found to be the best compromise among possible bed inclinations (Atkov and Bednenko, 1992). Placing healthy volunteers in bed became the model of choice for inducing and studying the effects of prolonged SF and for testing potential countermeasures. While earlier studies were more focused on the role of inactivity resulting from HDBR and related exercise countermeasures to restore normal physiological function (Sandler and Vernikos, 1986), subsequent research aimed at exploring new approaches for developing comprehensive, more efficient countermeasures (Pavy-Le Traon et al., 2007). However, the lack of standardized measures from different HDBR campaigns, conducted in different locations and by different space agencies, precluded drawing an overall conclusion on the efficiency of the various tested countermeasures. To overcome these limitations, in the context of the Roadmap for European Countermeasure Research with Bed Rest, in 2006 the European Space Agency (ESA) took the lead in defining a standardized framework for future HDBR

studies. Fixed durations were defined for short-, medium-, and long-term HDBR, as well as the duration of ambulatory and post-HDBR period. In addition, a crossover design with one control and several treatment groups, with a washout period in between, was defined for short- and medium-term HDBR. To facilitate direct comparison among studies, a set of physiological measures (Bed Rest Core Data) and related times of examination was defined, thus providing standards for cardiovascular, nutrition, exercise, bone, and muscle, neuro-vestibular and psychology assessment, on top of other experimental variables proposed by different research groups. The application of this standardization started with the BR-AG1 study in 2010 (**Table 1**). In this study, +1 Gz artificial gravity (AG) at heart level elicited by short-arm centrifuge, was applied as daily countermeasure using two different protocols (30 min continuously, and 6 × 5 min intermittent) in 12 male volunteers enrolled in a cross-over design. The two protocols did not show differences in aerobic power (peak VO2) after HDBR compared with the control condition, while the 6 × 5 min protocol was more effective in preserving orthostatic tolerance after HDBR. However, neither protocol attenuated plasma volume loss (Linnarsson et al., 2015), nor prevented changes in left ventricular function (Caiani et al., 2014). Compared to the 30 min protocol, the intermittent AG protocol resulted in increased MVC capability in the knee extensor and plantar flexor muscles (Rittweger et al., 2015), lower adrenocortical stress responses (Choukèr et al., 2013), and fewer neurovestibular symptoms (Clément et al., 2015).

In the SAG 5-d HDBR, daily 25 min upright standing as a countermeasure, compared to 25 min locomotion-replacement training including a combination of heel raising, squatting, and hopping exercise, were studied (Mulder et al., 2014). However, cardiovascular, bone and metabolic deconditioning persisted despite the applied countermeasures (Feuerecker et al., 2013).

The following MEP 21-d HDBR study focused on the beneficial effects of a nutritional countermeasure, constituted by supplementing high protein intake (1.2 g/kg body weight/d plus 0.6 g/kg body weight/d whey protein) with alkaline salts (90 mMol potassium bicarbonate/day). The results were unclear. The countermeasure resulted in marginal changes in structural myofibril properties, with a possible delay in hybrid fiber transition in some but not all subjects, together with no major shifts in the major proteolysis markers in biopsy material. Altogether, data suggested little if any proteolysis to occur above constitutive protein turn-over in disused human skeletal muscles (Blottner et al., 2014). The same nutritional countermeasure was also studied in the MNX 21-d HDBR in conjunction with a resistive vibration exercise (RVE).

In the 60-d RSL study, the efficacy of a countermeasure system that allows reactive jumps independently of gravitational forces (i.e., used in the horizontal position) was tested to prevent muscle and bone loss during HDBR. Starting in January 2017, another 60-d HDBR will study the effects of a novel nutritional countermeasure, consisting of a cocktail of several substances (530 mg/day of polyphenols + 168 mg of vitamin E with 80 μg selenium + 2.1 g omega-3). The cocktail is supposed to have an effect on blood antioxidant capacity, lipid metabolism, and muscle cell metabolism.

Physical Exercise Programs to Protect the Musculoskeletal System

Physical exercise programs are the main countermeasure used pre-, in-, and post-SF to protect the musculoskeletal system. In the last decades, new solutions to mitigate the effects

TABLE 1 | Updated list of ESA-sponsored bed rest campaigns since 2000.

Name	Year	Place, subjects	PRE (d)	HDT (d)	POST (d)	Intervention	HDT angle
LTBR 01-02	2001/2002	Toulouse, 25 males	15	90	15	1) Flywheel exercise 2) Bisphosphonate	−6°
STBR 01-02	2001/2002	Cologne, 9 males. Cross-over	9	14	3	Caloric variations in nutrition, Amino acid infusion	−6°
BBR	2003/2004	Berlin, 20 males	3	56	6	Vibration exercise	0°
WISE	2005	Toulouse, 24 females	20	60	20	1) Combined resistive exercise, aerobic exercise, Lower Body Negative Pressure 2) Nutritional supplement	−6°
BBR2-2	2007/2008	Berlin, 24 males	9	60	7	1) High-load resistive exercise (RE) 2) RE+ whole-body vibration	−6°
BR-AG1	2010	Toulouse, 12 males Cross-over	5	5	5	1) Artificial gravity by daily short-arm centrifuge for: 30 min 2) Intermittent 6x 5 min	−6°
SAG	2010/2011	Cologne, 10 males Cross-over	5	5	5	1) Locomotion replacement training 2) Upright standing	−6°
MEP	2011/2012	Cologne, 10 males Cross-over	7	21	6	Combined supplementation of 0.6 g whey protein (WP)/kg body weight (BW) and 90 mmol potassium bicarbonate (KHCO3)	−6°
MNX	2012/2013	Toulouse, 12 males Cross-over	7		6	1) Resistive Vibration Exercise (RVE) 2) RVE + Nutritional Supplement	−6°
RSL	2015/2016	Cologne, 24 males	14	60	14	Reactive jump	−6°
TBD	2017/2018	Toulouse, 20 males	14	60	14	Cocktail	−6°

TBD, to be defined; d, duration (days) of the different bed rest phases (PRE, before; HDT, head-down tilt; POST, after HDBR). Cross-over, subjects repeated the study, first in the control group, then in the countermeasure one.

of microgravity on musculoskeletal atrophy were adopted. Remarkable progress from a rowing ergometer, used in the Skylab missions, to a much more complex motorized treadmill, used in the ISS, derived from a growing attention to this issue. Thanks to countermeasures, HR and the maximum O_2 consumption seem not to change in short- and long-term missions, with suboptimal levels reached for O_2 consumption.

Recovery on Earth appears to depend on the duration of a space mission. Moreover, post-SF responses and orthostatic tolerance change when exercises in an upright seated position are performed (Moore et al., 2010). However, despite these promising results regarding cardiac performance, other studies highlight that the current strategy is not sufficient to prevent severe loss of the anti-gravitational muscles like calf (Trappe et al., 2009). A program consisting of treadmill running/cycling and 3–6 days per week of moderate-intensity, resistive exercises was proposed (Caiozzo et al., 1996). Nonetheless, calf muscle showed serious damage: muscle volume, maximum voluntary contraction (MVC) and peak force declined after a 6-month stationing in space. Remarkably, the soleus was more affected than the gastrocnemius and the astronaut with the largest gastrocnemius experienced the more severe deterioration. Overall, the observed transition from slow MHC-I to fast MHC-IIa fibers was significant, despite individual variability. This phenomenon occurs both in animal (Caiozzo et al., 1996) and human models (Widrick et al., 1999). The reason for this transition is not clear, but might be linked to the upward redistribution of blood and the subsequent hypoperfusion and reduced oxygenation of the calf, a situation possibly causing reduced oxidative phosphorylation and eventually transition to oxidative/glycolytic metabolism typical of the fast MHC-IIa fibers.

The devices used by the crew were a bicycle ergometer, a treadmill, bungee cords, and an elastomer providing a resistance exercise, the Interim Resistive Exercise Device (iRED; Lamoreaux and Landeck, 2006). iRED is unsuitable for long-term weightless exercise programs (Lamoreaux and Landeck, 2006). Therefore, a new device called Advanced Resistive Exercise Device (ARED) was developed (Lamoreaux and Landeck, 2006). Experiments on the efficiency of ARED conducted on Earth gave positive results: there were not statistical differences between the ARED-trained and the free-weight exercise-trained groups regarding muscle strength, muscle volume, vertical jump height, and lumbar spine BMD gained in 16 weeks of exercises (Loehr et al., 2011). The machinery, now onboard the ISS, is expected to improve astronaut cardiovascular and musculoskeletal recovery.

Treadmill technology has recently made substantial progress too, aiming to overcome the limited weight load of the Subject Load Device (SLD) used in the old-model machinery through a novel Zero-Gravity Locomotion Simulator (ZLS). Simulations proved that this system can provide a ground resistance force (GRF) statistically comparable to the GRF provided by over-ground run (Genc et al., 2006).

Another suggestive solution to mitigate the adverse effects of microgravity is to simulate gravity itself. The best way to achieve this purpose is to exploit the centripetal force produced by a centrifuge. Applications are currently under investigations with interesting results. Recently, a study proved that 1 h per day of exposure to 2.5 Gz AG counteracts the adverse effects of a 21-day BR program on the muscle fibers of the vastus lateralis and gastrocnemius (Caiozzo et al., 2009). The torque-velocity of the knee extensor was better preserved after exposure to AG, compared to the HDBR control group, and the plantar flexor torque-velocity increased after the AG program, whereas parameters of the control group worsened. The muscle fiber cross-sectional area was preserved in the soleus, in opposition to the HDBR group. Investigations on the slow-to-fast fiber transition revealed the MHC-I fibers to be better preserved in the soleus of the AG group, but MHC-IIx fibers still increased in both the vastus lateralis and the gastrocnemius. However, centrifugation alone cannot revert the effects of microgravity in terms of oxygen uptake, HR, and pulmonary ventilation, despite cycle ergometer exercise (Greenleaf et al., 1999). An optimal solution could be represented by a combination of centrifugation with (i) intensive aerobic exercise for cardiovascular system protection and (ii) moderate exercise to prevent musculoskeletal system deterioration. However, the use of a small-radius centrifuge requires the rotation rate must increase to obtain a centripetal force comparable to the g-force. That may not be affordable by an astronaut exercising on the centrifuge. In addition, both the Coriolis Effect and the centrifugal force cause motion sickness, so further studies are required to determine the most appropriate exercise program integrated with AG exposure (Hargens et al., 2013).

Another tool to counteract the upward fluid shift in space might be represented by the Low Body Negative Pressure (LBNP) chamber. Exposure of the legs to a negative pressure causes interstitial fluid pressure fall in the legs and blood shift from the higher to the lower regions of the body. Results showed that −30 mmHg pressure increased transcapillary fluid transport by decreasing the interstitial fluid pressure and the plasma volume, without affecting the foot venous pressure. Moreover, after LBNP exposure, even though transcapillary fluid transport decreased again, the plasma volume remained lower. Although the plasma volume extracted from the blood flowing in the legs was not exactly quantified, the increased circumference of the leg during and after LBNP exposure suggested that the headward blood shift occurring in space had been effectively counteracted (Aratow et al., 1993). Thus, a crew might use the LBNP chamber during a resting period and alternate low-pressure exposure with aerobic exercise performed on a properly set centrifuge so as to maximize cardiovascular and musculoskeletal performance.

Space activity suits (SAS) or mechanical counter-pressure suits might represent another possible solution for the future. Those are spacesuits made to apply a steady pressure against the skin by means of skintight elastic garments. Several were designed and tested in the past. Recently, with the Soyuz TMA-18M 44S mission to the ISS, a new type of SkinSuit was tested in space (SkinSuit, 2015). It was developed over some years to provide simulated +Gz that increases gradually from the shoulders to the feet. SkinSuit aims to counteract the stretching of the spine in space, which causes the lower back pain experienced by 50% of astronauts early in their missions. The ability to control spinal elongation in space might also help reduce the risk of post-SF

injury to intervertebral discs (IVD), which astronauts are at greater danger of experiencing upon return to Earth. In terrestrial life, the SkinSuit technology has the potential to help the elderly and many people with lower-back problems, in addition to improving support garments currently used for conditions like cerebral palsy.

Further, studies on whole-body vibrations investigated how RVE can ameliorate musculoskeletal performance in volunteers undergoing prolonged HDBR. In a cohort of 20 male subjects immobilized for 8 weeks and monitored during a 6-month follow-up (Belavý et al., 2012), a significant amelioration of the activity ratio of the lumbopelvic muscles and a not significant improvement of the co-contraction of the lumbopelvic extensors and flexors were documented. Another interesting research revealed tail-suspended mice to be affected by IVD hypotrophy and glycosaminoglycan/collagen ratio imbalance. When exposed to a vertical platform oscillating with a 90 Hz frequency, disc deterioration was mitigated. In particular, the disc height, the glycosaminoglycan content in the whole disc and typical dimensions of the nucleus pulposus were restored (Kennedy, 1998). It must be noted that in humans exposed to microgravity a biochemical rearrangement of the IVDs leads to disc hypertrophy, just opposite of what happens in mice (Holguin et al., 2011). However, the finding that RVE of the vertebral column can ameliorate the anatomic and biochemical status of the IVDs is still valid and might be addressed to humans too.

The space crew diet is supplemented with calcium, vitamins D and K, and bisphosphonates, a common postmenopausal drug also successfully tested in HDBR study to reduce bone reabsorption to minimize bone demineralization (Smith et al., 1999). Potassium citrate and PTH were also evaluated (Buckey, 2006; LeBlanc et al., 2007; Stein, 2013).

Interestingly, technologies and some medicines developed for SF have found application on Earth. Examples include a drug to improve physical condition and cognition with low side effects (phenotropil; Zvejniece et al., 2011), or a powerful antiseptic (miramistin; Vasil'eva et al., 1993). The most recent one is a medicine developed against astronaut bone loss and now used for the treatment of osteoporosis caused by menopause and chemotherapy (antibody against sclerostin protein; Rodent Research, 2016).

Protection against Irradiation

Two approaches can be useful to mitigate the adverse effects of space radiations. One is pharmacological and based on the prescription of antioxidants and other protective substances. Another one is mechanical, based on a protective physical barrier provided by novel materials—yet to be developed—to reinforce the spaceship (that we will not examine here).

Antioxidants can neutralize ROS generated by GRC and SPE particles. However, different molecules exert different antioxidative reactions, which render the administration of a combination of various antioxidants more protective. Thus, combined doses of L-Selenomethionine (SeM), sodium ascorbate, N-acetylcysteine, α-lipoic acid, vitamin E succinate, and coenzyme Q10 were administered both to cell cultures and mice (Kennedy, 2014). The most interesting results came from the *in vivo* model: after exposure to ^{56}Fe ion (0.5 Gy), proton or γ-rays (both 3 Gy), the plasma total antioxidant status (TAS) decreased, but the administration of the previously cited antioxidant combination improved TAS. Moreover, use of the Bowman-Birk Inhibitor (BBI, a soybean-derived protease inhibitor) completely restored TAS. BBI mode of action is not clear yet, but it is used in chemotherapy to prevent cancer progression. BBI was also suggested to neutralize anti-inflammatory proteases, trypsin, and chymotrypsin (Kennedy, 1998). In another experiment, BBI, BBIC (Bowman-Birk Inhibitor Concentrate), SeM alone or in combination with ascorbic acid, coenzyme Q10, and vitamin E succinate protected HTori cells from transformation after HZE and proton radiation exposure (Kennedy et al., 2004). Hematopoietic tissue is most sensitive to irradiation, so the antioxidant activity was investigated in mice undergoing 1 and 8 Gy X-ray, γ-ray, and proton irradiation. Remarkably, antioxidants prolonged mouse life and improved the total count and neutrophil count in peripheral blood and partially prevented the degeneration of bone marrow cells even though the treatment could not rescue peripheral lymphopenia (Wambi et al., 2008). In addition to antioxidants, growth factors can be administered to stimulate granulocyte production and neutralize the lymphopenia reported after antioxidant treatment only.

Two forms of granulocyte colony stimulating factor (GCSF), filgrastim and pegfilgrastim, were given to mice exposed to SPE-like proton or γ-rays. Pegfilgrastim was found more effective for neutrophil protection (Romero-Weaver et al., 2013). On this basis, Pegfilgrastim, also known as Neulasta, was also administered to irradiated ferrets and pigs. Interestingly, the neutrophil count never decreased below the baseline level (i.e., before irradiation), suggesting that Neulasta can increase the number of circulating neutrophils in different animal models (Kennedy, 2014).

Chinese medicine inspired a suggestive solution for protecting lymphocytes from radiation-induced death. In China, the formula SWT (Si-Wu-Tang) was used in the past for treating patients suffering from radiation sickness after radiation accidents. The formula components were investigated and were found to be paeoniflorin, ferulic acid, tetramethylpyrazine, and fructose. The analysis of the physiological response induced by each of these compounds revealed that the only protective active principle for granulocytes and lymphocytes was, surprisingly, fructose. Irradiated mice treated with fructose showed higher levels of granulocytes and lymphocytes if compared to the irradiated untreated samples, and fructose supplementation of the diet before radiation exposure improved the outcomes (Romero-Weaver et al., 2014). Given that, these stimulating data need to be confirmed by further studies to better define the real impact on the immune system.

CONCLUSION

Humans adapt to the hostile environment of space, characterized by the absence of gravity and chronic radiation exposure, through cardiovascular adaptation and drastic changes in metabolism, respiration, body mass, bone density, and muscle integrity.

From the analysis of published data, it appears that a reductionist approach (assuming one or another main challenging factor) cannot easily explain the impact of long-term exposure to SF conditions. Indeed, this review shows that the independent actions of either body fluid redistribution or radiation exposure may not account for the organism response to long-term SF. In addition, the role of hormonal stress response to weightlessness may contribute to shaping the adaptation of the human body to space although this aspect has remained largely unexplored. Indeed, increased cortisol levels during SF are expected to affect kidney operation, bone resorption, immunity, muscle loss, glycaemic control, endothelial response and may contribute to the discrepancies observed between short- and long-term SF and to the inter-individual variability as well.

An important side of human body adaptation to SF conditions is its relevance to human health in general. Analysis of SF impact on health may benefit aging people on Earth. Aging is a progressive, time-dependent physiological deterioration of the homeostatic response and adaptation to the external environment that makes the individual fragile and more vulnerable to diseases. Several molecular-oriented studies shed light on the molecular pathways involved in aging (Weinert and Timiras, 2003). On Earth, aging affects the cardiovascular, musculoskeletal, nervous, gastrointestinal, urinary and neuroendocrine systems (Boss and Seegmiller, 1981), with immune system impairment and an enhanced inflammatory activity (Montecino-Rodriguez et al., 2013). Remarkably, these changes occur in space 10-fold faster than on Earth (Vernikos and Schneider, 2010), allowing scientists to speculate that the astronauts may be an appropriate model for exploring the mechanisms of aging. SF may allow researchers overcoming limitations of studying precocious aging, for example in progeroid syndromes, and physiological aging in healthy primates that would require 15–30 years to be properly characterized (Le Bourg, 1999).

Ground simulations, HDBR studies among them (Sandler and Vernikos, 1986; Pavy-Le Traon et al., 2007; Vernikos and Schneider, 2010), have been essential to investigate and analyze observations made on space crews, about the influence of contributing factors, mapping time course of physiological changes and exploring biological mechanisms under controlled conditions. In turn, insights gained from HDBR studies found application in the health care of chronically-ill people.

Obviously, there are significant differences among the effects of SF, HDBR, and physiological aging. A possible conceptual context to compare, differentiate and understand them is offered by considering them as disorders of mechanotransduction. Ingber's tensegrity theory and research (Ingber, 1997) provide the framework for understanding how external and internal mechanical forces influence the living organism at molecular and cellular levels. His work reveals that "molecules, cells, tissues, organs, and our entire bodies use tensegrity architecture to stabilize their shape mechanically, and seamlessly to integrate structure and function at all size scales." This theory could explain at a mechanistic level how intermittent mechanical forces applied externally, such as vibration (Rubin et al., 2002), movement, or exercise (Bachl et al., 1993), centrifugation (Vernikos et al., 2004), push/pull or intermittent tension (Pietramaggiori et al., 2007), can influence cell and tissue growth and function.

In this perspective, physiology of space and extreme environments might deepen our understanding of aging and/or medical disorders.

AUTHOR CONTRIBUTIONS

DA conceived and designed the article and coordinated the manuscript preparation. GD contributed the chapter devoted to "Eye, microgravity, and vision" and rewrote extensively several sections; EC wrote the chapter "Countermeasures for space from bed rest studies." CP contributed to the chapter "Weightlessness and fluid redistribution as stress factors in space." All other chapters were contributed by MG, IB, and DA. All authors read, discussed, edited, and approved the whole work.

ACKNOWLEDGMENTS

DA was recipient of contracts ILSRA-2009-1026 from the European Space Agency and 2013-066-R.0 (SFEF) from the Italian Space Agency. EC was the recipient of contracts 2013-032-R.0 (AEQUABED) and 2013-033-R.0 (QT-BED) from the Italian Space Agency. The authors are truly grateful to Antonio L'Abbate and Flavio Coceani for critical reading of the manuscript.

REFERENCES

Anken, R., and Rahmann, H. (2002). "Gravitational zoology: how animals use and cope with gravity," in *Astrobiology*, eds G. Horneck and C. Baumstark-Khan (Heidelberg: Springer), 315–333.

Aratow, M., Fortney, S. M., Watenpaugh, D. E., Crenshaw, A. G., and Hargens, A. R. (1993). Transcapillary fluid responses to lower body negative pressure. *J. Appl. Physiol.* 74, 2763–2770.

Atkov, O., and Bednenko, V. (1992). *Hypokinesia and Weightlessness: Clinical and Physiologic Aspects*. Madison: International University Press.

Augustin, H. G., Kozian, D. H., and Johnson, R. C. (1994). Differentiation of endothelial cells: analysis of the constitutive and activated endothelial cell phenotypes. *Bioessays* 16, 901–906. doi: 10.1002/bies.950161208

Bachl, N., Baron, R., Tschan, H., Mossaheb, M., Bumba, W., Hildebrand, F., et al. (1993). Principles of muscle efficiency in weightlessness. *Wien. Med. Wochenschr.* 143, 588–610.

Baer, R. M., and Hill, D. W. (1990). Retinal vessel responses to passive tilting. *Eye* 4 (Pt 5), 751–756. doi: 10.1038/eye.1990.107

Baevsky, R. M., Baranov, V. M., Funtova, I. I., Diedrich, A., Pashenko, A. V., Chernikova, A. G., et al. (2007). Autonomic cardiovascular and respiratory control during prolonged spaceflights aboard the International Space Station. *J. Appl. Physiol.* 103, 156–161. doi: 10.1152/japplphysiol.00137.2007

Balsamo, M., Barravecchia, I., Mariotti, S., Merenda, A., De Cesari, C., Vukich, M., et al. (2014). Molecular and cellular characterization of space flight effects on microvascular endothelial cell function – preparatorywork for the SFEF project. *Microgravity Sci. Technol.* 26, 351–363. doi: 10.1007/s12217-014-9399-4

Baranov, V. M., Tikhonov, M. A., and Kotov, A. N. (1992). The external respiration and gas exchange in space missions. *Acta Astronaut.* 27, 45–50. doi: 10.1016/0094-5765(92)90174-H

Barcellos-Hoff, M. H., Blakely, E. A., Burma, S., Fornace, A. J., Gerson, S., Hlatky, L., et al. (2015). Concepts and challenges in cancer risk prediction for the space radiation environment. *Life Sci. Space Res.* 6, 92–103. doi: 10.1016/j.lssr.2015.07.006

Barratt, M. R. (2008). "Chapter 1: Physical and bioenvironmental aspects of human space flight," in *Principles of Clinical Medicine for Space Flight*, ed L. Sam (Heidelberg: Springer), 3–26: "Chapter 2: Human response to space flight" 27–57.

Baylor, D. A., Lamb, T. D., and Yau, K. W. (1979). Responses of retinal rods to single photons. *J. Physiol.* 288, 613–634.

Belavý, D. L., Miokovic, T., Armbrecht, G., Richardson, C. A., Rittweger, J., and Felsenberg, D. (2009). Differential atrophy of the lower-limb musculature during prolonged bed-rest. *Eur. J. Appl. Physiol.* 107, 489–499. doi: 10.1007/s00421-009-1136-0

Belavý, D. L., Wilson, S. J., Armbrecht, G., Rittweger, J., Felsenberg, D., and Richardson, C. A. (2012). Resistive vibration exercise during bed-rest reduces motor control changes in the lumbo-pelvic musculature. *J. Electromyogr. Kinesiol.* 22, 21–30. doi: 10.1016/j.jelekin.2011.09.009

Blottner, D., Bosutti, A., Degens, H., Schiffl, G., Gutsmann, M., Buehlmeier, J., et al. (2014). Whey protein plus bicarbonate supplement has little effects on structural atrophy and proteolysis marker immunopatterns in skeletal muscle disuse during 21 days of bed rest. *J. Musculoskelet. Neuronal Interact.* 14, 432–444. doi: 10.1152/japplphysiol.00936.2015

Boss, G., and Seegmiller, J. (1981). Age-related physiological changes and their clinical significance. *West. J. Med.* 135, 434–440.

Buckey, J. (2006). *Space Physiology*. New York, NY: Oxford University Press.

Caiani, E. G., Massabuau, P., Weinert, L., Vaïda, P., and Lang, R. M. (2014). Effects of 5 days of head-down bed rest, with and without short-arm centrifugation as countermeasure, on cardiac function in males (BR-AG1 study). *J. Appl. Physiol.* 117, 624–632. doi: 10.1152/japplphysiol.00122.2014

Caiozzo, V. J., Haddad, F., Baker, M. J., Herrick, R. E., Prietto, N., and Baldwin, K. M. (1996). Microgravity-induced transformations of myosin isoforms and contractile properties of skeletal muscle. *J. Appl. Physiol.* 81, 123–132.

Caiozzo, V. J., Haddad, F., Lee, S., Baker, M., Paloski, W., and Baldwin, K. M. (2009). Artificial gravity as a countermeasure to microgravity: a pilot study examining the effects on knee extensor and plantar flexor muscle groups. *J. Appl. Physiol.* 107, 39–46. doi: 10.1152/japplphysiol.91130.2008

Carlsson, S. I. M., Bertilaccio, M. T. S., Ballabio, E., and Maier, J. A. M. (2003). Endothelial stress by gravitational unloading: effects on cell growth and cytoskeletal organization. *Biochim. Biophys. Acta* 1642, 173–179. doi: 10.1016/j.bbamcr.2003.08.003

Carozzo, S., Ball, S. L., Narici, L., Schardt, D., and Sannita, W. G. (2015). Interaction of (12)C ions with the mouse retinal response to light. *Neurosci. Lett.* 598, 36–40. doi: 10.1016/j.neulet.2015.04.048

Casolino, M., Bidoli, V., Morselli, A., Narici, L., De Pascale, M. P., Picozza, P., et al. (2003). Space travel: dual origins of light flashes seen in space. *Nature* 422:680. doi: 10.1038/422680a

Catalá, A. (2006). An overview of lipid peroxidation with emphasis in outer segments of photoreceptors and the chemiluminescence assay. *Int. J. Biochem. Cell Biol.* 38, 1482–1495. doi: 10.1016/j.biocel.2006.02.010

Choukèr, A., Feuerecker, B., Matzel, S., Kaufmann, I., Strewe, C., Hoerl, M., et al. (2013). Psychoneuroendocrine alterations during 5 days of head-down tilt bed rest and artificial gravity interventions. *Eur. J. Appl. Physiol.* 113, 2057–2065. doi: 10.1007/s00421-013-2640-9

Christensen, N. J., Drummer, C., and Norsk, P. (2001). Renal and sympathoadrenal responses in space. *Am. J. Kidney Dis.* 38, 679–683. doi: 10.1053/ajkd.2001.27758

Christensen, N. J., Heer, M., Ivanova, K., and Norsk, P. (2005). Sympathetic nervous activity decreases during head-down bed rest but not during microgravity. *J. Appl. Physiol.* 99, 1552–1557. doi: 10.1152/japplphysiol.00017.2005

Cines, D. B., Pollak, E. S., Buck, C. A., Loscalzo, J., Zimmerman, G. A., McEver, R. P., et al. (1998). Endothelial cells in physiology and in the pathophysiology of vascular disorders. *Blood* 91, 3527–3561.

Clément, G., Bareille, M. P., Goel, R., Linnarsson, D., Mulder, E., Paloski, W. H., et al. (2015). Effects of five days of bed rest with intermittent centrifugation on neurovestibular function. *J. Musculoskelet. Neuronal Interact.* 15, 60–68.

Clément, G., Wood, S. J., and Reschke, M. F. (1992). Effects of microgravity on the interaction of vestibular and optokinetic nystagmus in the vertical plane. *Aviat. Space Environ. Med.* 63, 778–784.

Colleran, P. N., Wilkerson, M. K., Bloomfield, S. A., Suva, L. J., Turner, R. T., and Delp, M. D. (2000). Alterations in skeletal perfusion with simulated microgravity: a possible mechanism for bone remodeling. *J. Appl. Physiol.* 89, 1046–1054.

Cotrupi, S., Ranzani, D., and Maier, J. A. M. (2005). Impact of modeled microgravity on microvascular endothelial cells. *Biochim. Biophys. Acta* 1746, 163–168. doi: 10.1016/j.bbamcr.2005.10.002

Coupé, M., Fortrat, J. O., Larina, I., Gauquelin-Koch, G., Gharib, C., and Custaud, M. A. (2009). Cardiovascular deconditioning: from autonomic nervous system to microvascular dysfunctions. *Respir. Physiol. Neurobiol.* 169 (Suppl.), S10–S12. doi: 10.1016/j.resp.2009.04.009

Crucian, B., Simpson, R. J., Mehta, S., Stowe, R., Chouker, A., Hwang, S.-A., et al. (2014). Terrestrial stress analogs for spaceflight associated immune system dysregulation. *Brain Behav. Immun.* 39, 23–32. doi: 10.1016/j.bbi.2014.01.011

Cucinotta, F. A., and Durante, M. (2006). Cancer risk from exposure to galactic cosmic rays: implications for space exploration by human beings. *Lancet Oncol.* 7, 431–435. doi: 10.1016/S1470-2045(06)70695-7

Cucinotta, F. A., Kim, M.-H. Y., Chappell, L. J., and Huff, J. L. (2013). How safe is safe enough? Radiation risk for a human mission to Mars. *PLoS ONE* 8:e74988. doi: 10.1371/journal.pone.0074988

de Boer, M. D., Seynnes, O. R., di Prampero, P. E., Pisot, R., Mekjavić, I. B., Biolo, G., et al. (2008). Effect of 5 weeks horizontal bed rest on human muscle thickness and architecture of weight bearing and non-weight bearing muscles. *Eur. J. Appl. Physiol.* 104, 401–407. doi: 10.1007/s00421-008-0703-0

Demiot, C., Dignat-George, F., Fortrat, J.-O., Sabatier, F., Gharib, C., Larina, I., et al. (2007). WISE 2005: chronic bed rest impairs microcirculatory endothelium in women. *Am. J. Physiol. Heart Circ. Physiol.* 293, H3159–H3164. doi: 10.1152/ajpheart.00591.2007

Demontis, G. C., Longoni, B., Gargini, C., and Cervetto, L. (1997). The energetic cost of photoreception in retinal rods of mammals. *Arch. Ital. Biol.* 135, 95–109.

Demontis, G. C., Ratto, G. M., Bisti, S., and Cervetto, L. (1995). Effect of blocking the Na^+/K^+ ATPase on Ca^{2+} extrusion and light adaptation in mammalian retinal rods. *Biophys. J.* 69, 439–450. doi: 10.1016/S0006-3495(95)79917-9

Dietlein, L. (1977). Skylab: "A beginning," eds D. L. Johnston, Biomedical. Washington, DC: Scientific and Technical Information Office, NASA, SP-377.

Donnelly, E. H., Nemhauser, J. B., Smith, J. M., Kazzi, Z. N., Farfán, E. B., Chang, A. S., et al. (2010). Acute radiation syndrome: assessment and management. *South. Med. J.* 103, 541–546. doi: 10.1097/SMJ.0b013e3181ddd571

Drummer, C., Hesse, C., Baisch, F., Norsk, P., Elmann-Larsen, B., Gerzer, R., et al. (2000). Water and sodium balances and their relation to body mass changes in microgravity. *Eur. J. Clin. Invest.* 30, 1066–1075. doi: 10.1046/j.1365-2362.2000.00766.x

Eckberg, D. L., Halliwill, J. R., Beightol, L. A., Brown, T. E., Taylor, J. A., and Goble, R. (2010). Human vagal baroreflex mechanisms in space. *J. Physiol.* 588(Pt 7), 1129–1138. doi: 10.1113/jphysiol.2009.186650

Edgerton, V. R., McCall, G. E., Hodgson, J. A., Gotto, J., Goulet, C., Fleischmann, K., et al. (2001). Sensorimotor adaptations to microgravity in humans. *J. Exp. Biol.* 204(Pt 18), 3217–3224.

Elliott, A. R., Prisk, G. K., Guy, H. J., and West, J. B. (1994). Lung volumes during sustained microgravity on Spacelab SLS-1. *J. Appl. Physiol.* 77, 2005–2014.

Fazio, G. G., Jelley, J. V., and Charman, W. N. (1970). Generation of Cherenkov light flashes by cosmic radiation within the eyes of the Apollo astronauts. *Nature* 228, 260–264. doi: 10.1038/228260a0

Ferrara, D., Waheed, N. K., and Duker, J. S. (2015). Investigating the choriocapillaris and choroidal vasculature with new optical coherence tomography technologies. *Prog. Retin. Eye Res.* 52, 130–155. doi: 10.1016/j.preteyeres.2015.10.002

Feuerecker, M., Feuerecker, B., Matzel, S., Long, M., Strewe, C., Kaufmann, I., et al. (2013). Five days of head-down-tilt bed rest induces noninflammatory shedding of L-selectin. *J. Appl. Physiol.* 115, 235–242. doi: 10.1152/japplphysiol.00381.2013

Fishman, A. P. (1982). Endothelium: a distributed organ of diverse capabilities. *Ann. N. Y. Acad. Sci.* 401, 1–8. doi: 10.1111/j.1749-6632.1982.tb25702.x

Fritsch-Yelle, J. M., Charles, J. B., Jones, M. M., and Wood, M. L. (1996). Microgravity decreases heart rate and arterial pressure in humans. *J. Appl. Physiol.* 80, 910–904.

Fritsch-Yelle, J. M., Charles, J. B., Jones, M. M., Beightol, L. A., and Eckberg, D. L. (1994). Spaceflight alters autonomic regulation of arterial pressure in humans. *J. Appl. Physiol.* 77, 1776–1783.

Fuglesang, C., Narici, L., Picozza, P., and Sannita, W. G. (2006). Phosphenes in low earth orbit: survey responses from 59 astronauts. *Aviat. Space Environ. Med.* 77, 449–452.

Genc, K. O., Mandes, V. E., and Cavanagh, P. R. (2006). Gravity replacement during running in simulated microgravity. *Aviat. Space Environ. Med.* 77, 1117–1124.

Greenleaf, J. E., Chou, J. L., Stad, N. J., Leftheriotis, G. P., Arndt, N. F., Jackson, C. G., et al. (1999). Short-arm (1.9 m) +2.2 Gz acceleration: isotonic exercise load-O_2 uptake relationship. *Aviat. Space Environ. Med.* 70, 1173–1182.

Grigoriev, A. I., Morukov, B. V., and Vorobiev, D. V. (1994). Water and electrolyte studies during long-term missions onboard the space stations SALYUT and MIR. *Clin. Invest.* 72, 169–189. doi: 10.1007/BF00189308

Grimm, D., Bauer, J., Kossmehl, P., Shakibaei, M., Schöberger, J., Pickenhahn, H., et al. (2002). Simulated microgravity alters differentiation and increases apoptosis in human follicular thyroid carcinoma cells. *FASEB J.* 16, 604–606. doi: 10.1096/fj.01-0673fje

Hargens, A. R., Bhattacharya, R., and Schneider, S. M. (2013). Space physiology VI: exercise, artificial gravity, and countermeasure development for prolonged space flight. *Eur. J. Appl. Physiol.* 113, 2183–2192. doi: 10.1007/s00421-012-2523-5

Hayreh, S. S. (2006). Orbital vascular anatomy. *Eye* 20, 1130–1144. doi: 10.1038/sj.eye.6702377

Herranz, R., Anken, R., Boonstra, J., Braun, M., Christianen, P. C. M., de Geest, M., et al. (2013). Ground-based facilities for simulation of microgravity: organism-specific recommendations for their use, and recommended terminology. *Astrobiology* 13, 1–17. doi: 10.1089/ast.2012.0876

Holguin, N., Uzer, G., Chiang, F.-P., Rubin, C., and Judex, S. (2011). Brief daily exposure to low-intensity vibration mitigates the degradation of the intervertebral disc in a frequency-specific manner. *J. Appl. Physiol.* 111, 1846–1853. doi: 10.1152/japplphysiol.00846.2011

Hughson, R. L., Shoemaker, J. K., Blaber, A. P., Arbeille, P., Greaves, D. K., Pereira-Junior, P. P., et al. (2012). Cardiovascular regulation during long-duration spaceflights to the International Space Station. *J. Appl. Physiol.* 112, 719–727. doi: 10.1152/japplphysiol.01196.2011

Ingber, D. E. (1997). Tensegrity: the architectural basis of cellular mechanotransduction. *Annu. Rev. Physiol.* 59, 575–599. doi: 10.1146/annurev.physiol.59.1.575

Jacobson, D. M. (1995). Intracranial hypertension and the syndrome of acquired hyperopia with choroidal folds. *J. Neuroophthalmol.* 15, 178–185. doi: 10.1097/00041327-199509000-00011

Katkov, V. E., and Chestukhin, V. V. (1980). Blood pressure and oxygenation in different cardiovascular compartments of a normal man during postural exposures. *Aviat. Space Environ. Med.* 51, 1234–1242.

Kennedy, A. R. (1998). The Bowman-Birk inhibitor from soybeans as an anticarcinogenic agent. *Am. J. Clin. Nutr.* 68(6 Suppl.), 1406S–1412S.

Kennedy, A. R. (2014). Biological effects of space radiation and development of effective countermeasures. *Life Sci. Space Res.* 1, 10–43. doi: 10.1016/j.lssr.2014.02.004

Kennedy, A. R., Ware, J. H., Guan, J., Donahue, J. J., Biaglow, J. E., Zhou, Z., et al. (2004). Selenomethionine protects against adverse biological effects induced by space radiation. *Free Radic. Biol. Med.* 36, 259–266. doi: 10.1016/j.freeradbiomed.2003.10.010

Kramer, L. A., Sargsyan, A. E., Hasan, K. M., Polk, J. D., and Hamilton, D. R. (2012). Orbital and intracranial effects of microgravity: findings at 3-T MR imaging. *Radiology* 263, 819–827. doi: 10.1148/radiol.12111986

Kumar, P., Shen, Q., Pivetti, C. D., Lee, E. S., Wu, M. H., and Yuan, S. Y. (2009). Molecular mechanisms of endothelial hyperpermeability: implications in inflammation. *Expert Rev. Mol. Med.* 11:e19. doi: 10.1017/S1462399409001112

Kusumbe, A. P., Ramasamy, S. K., and Adams, R. H. (2014). Coupling of angiogenesis and osteogenesis by a specific vessel subtype in bone. *Nature* 507, 323–328. doi: 10.1038/nature13145

Lambertz, D., Pérot, C., Kaspranski, R., and Goubel, F. (2001). Effects of long-term spaceflight on mechanical properties of muscles in humans. *J. Appl. Physiol.* 90, 179–188.

Lamoreaux, C. D., and Landeck, M. E. (2006). "Mechanism development, testing, and lessons learned for the advanced resistive exercise device," in *The 3rd Aerospace Mechanisms Symposium*. (Hampton, Virginia: Langley Research Center).

Le Bourg, E. (1999). A review of the effects of microgravity and of hypergravity on aging and longevity. *Exp. Gerontol.* 34, 319–336. doi: 10.1016/S0531-5565(99)00004-2

Leach, C. S., Alexander, W. C., and Johnson, P. C. (1975). *Endocrine, electrolyte, and fluid volume changes associated with Apollo missions.* NASA Johnson Space Center, Houston TX.

LeBlanc, A. D., Spector, E. R., Evans, H. J., and Sibonga, J. D. (2007). Skeletal responses to space flight and the bed rest analog: a review. *J. Musculoskelet. Neuronal Interact.* 7, 33–47.

LeBlanc, A., Schneider, V., Shackelford, L., West, S., Oganov, V., Bakulin, A., et al. (2000). Bone mineral and lean tissue loss after long duration space flight. *J. Musculoskelet. Neuronal Interact.* 1, 157–160.

Lee, S. M. C., Schneider, S. M., Boda, W. L., Watenpaugh, D. E., Macias, B. R., Meyer, R. S., et al. (2009). LBNP exercise protects aerobic capacity and sprint speed of female twins during 30 days of bed rest. *J. Appl. Physiol.* 106, 919–928. doi: 10.1152/japplphysiol.91502.2008

Limper, U., Gauger, P., Beck, P., Krainski, F., May, F., and Beck, L. E. J. (2014). Interactions of the human cardiopulmonary, hormonal and body fluid systems in parabolic flight. *Eur. J. Appl. Physiol.* 114, 1281–1295. doi: 10.1007/s00421-014-2856-3

Linnarsson, D., Hughson, R. L., Fraser, K. S., Clément, G., Karlsson, L. L., Mulder, E., et al. (2015). Effects of an artificial gravity countermeasure on orthostatic tolerance, blood volumes and aerobic power after short-term bed rest (BR-AG1). *J. Appl. Physiol.* 118, 29–35. doi: 10.1152/japplphysiol.00061.2014

Linsenmeier, R. A., and Padnick-Silver, L. (2000). Metabolic dependence of photoreceptors on the choroid in the normal and detached retina. *Invest. Ophthalmol. Vis. Sci.*, 41, 3117–3123.

Liu, Z., Wan, Y., Zhang, L., Tian, Y., Lv, K., and Li, Y., Guo, J. (2015). Alterations in the heart rate and activity rhythms of three orbital astronauts on a space mission. *Life Sci. Space Res.* 4, 62–66. doi: 10.1016/j.lssr.2015.01.001

Loehr, J. A., Lee, S. M. C., English, K. L., Sibonga, J., Smith, S. M., Spiering, B. A., et al. (2011). Musculoskeletal adaptations to training with the advanced resistive exercise device. *Med. Sci. Sports Exerc.* 43, 146–156. doi: 10.1249/MSS.0b013e3181e4f161

Ma, J., Zhang, L. F., Yu, Z. B., and Zhang, L. N. (1997). Time course and reversibility of arterial vasoreactivity changes in simulated microgravity rats. *J. Gravitation. Physiol.* 4, P45–P46.

Ma, X., Pietsch, J., Wehland, M., Schulz, H., Saar, K., Hübner, N., et al. (2014). Differential gene expression profile and altered cytokine secretion of thyroid cancer cells in space. *FASEB J.* 28, 813–835. doi: 10.1096/fj.13-243287

Mader, T. H., Gibson, C. R., Caputo, M., Hunter, N., Taylor, G., Charles, J., et al. (1993). Intraocular pressure and retinal vascular changes during transient exposure to microgravity. *Am. J. Ophthalmol.* 115, 347–350. doi: 10.1016/S0002-9394(14)73586-X

Mader, T. H., Gibson, C. R., Pass, A. F., Kramer, L. A., Lee, A. G., Fogarty, J., et al. (2011). Optic disc edema, globe flattening, choroidal folds, and hyperopic shifts observed in astronauts after long-duration space flight. *Ophthalmology* 118, 2058–2069. doi: 10.1016/j.ophtha.2011.06.021

Maier, J. A. M., Cialdai, F., Monici, M., and Morbidelli, L. (2015). The impact of microgravity and hypergravity on endothelial cells. *Biomed Res. Int.* 2015:434803. doi: 10.1155/2015/434803

Mao, X. W., Pecaut, M. J., Stodieck, L. S., Ferguson, V. L., Bateman, T. A., Bouxsein, M., et al. (2013). Spaceflight environment induces mitochondrial oxidative damage in ocular tissue. *Radiat. Res.* 180, 340–350. doi: 10.1667/RR3309.1

Mariotti, M., and Maier, J. A. M. (2008). Human micro- and macrovascular endothelial cells exposed to simulated microgravity upregulate hsp70. *Microgravity Sci. Technol.* 21, 141–144. doi: 10.1007/s12217-008-9066-8

McAulay, I. R. (1971). Cosmic ray flashes in the eye. *Nature* 232, 421–422. doi: 10.1038/232421a0

McMahon, D. G., Iuvone, P. M., and Tosini, G. (2014). Circadian organization of the mammalian retina: from gene regulation to physiology and diseases. *Prog. Retin. Eye Res.* 39, 58–76. doi: 10.1016/j.preteyeres.2013.12.001

Meck, J. V., Waters, W. W., Ziegler, M. G., deBlock, H. F., Mills, P. J., Robertson, D., et al. (2004). Mechanisms of postspaceflight orthostatic hypotension: low alpha1-adrenergic receptor responses before flight and central autonomic dysregulation postflight. *Am. J. Physiol. Heart Circ. Physiol.* 286, H1486–H1495. doi: 10.1152/ajpheart.00740.2003

Michel, E. L., Rummel, J. A., and Sawin, C. F. (2007). Skylab experiment M-171 "Metabolic Activity"–results of the first manned mission. *Acta Astronaut.* 2, 351–365.

Monahan-Earley, R., Dvorak, A. M., and Aird, W. C. (2013). Evolutionary origins of the blood vascular system and endothelium. *J. Thromb. Haemost.* 11 (Suppl. 1), 46–66. doi: 10.1111/jth.12253

Montecino-Rodriguez, E., Berent-Maoz, B., and Dorshkind, K. (2013). Causes, consequences, and reversal of immune system aging. *J. Clin. Invest.* 3, 958–965. doi: 10.1172/JCI64096

Moore, A. D., Lee, S. M. C., Stenger, M. B., and Platts, S. H. (2010). Cardiovascular exercise in the U.S. space program: past, present and future. *Acta Astronaut.* 66, 974–988. doi: 10.1016/j.actaastro.2009.10.009

Morrison, A. R., Yarovinsky, T. O., Young, B. D., Moraes, F., Ross, T. D., Ceneri, N., et al. (2014). Chemokine-coupled β2 integrin-induced macrophage Rac2-Myosin IIA interaction regulates VEGF-A mRNA stability and arteriogenesis. *J. Exp. Med.* 211, 1957–1968. doi: 10.1084/jem.20132130

Moss, M. L. (1977). A functional analysis of fusion of the tibia and fibula in the rat and mouse. *Acta Anat.* 97, 321–332. doi: 10.1159/000144749

Mulder, E., Frings-Meuthen, P., von der Wiesche, M., Clément, G., Linnarsson, D., Paloski, W. H., et al. (2014). Study protocol, implementation, and verification of a short versatile upright exercise regime during 5 days of bed rest. *J. Musculoskelet. Neuronal Interact.* 14, 111–123.

Narici, L., Paci, M., Brunetti, V., Rinaldi, A., Sannita, W. G., and De Martino, A. (2012). Bovine rod rhodopsin. 1. Bleaching by luminescence *in vitro* by recombination of radicals from polyunsaturated fatty acids. *Free Radic. Biol. Med.* 53, 482–487. doi: 10.1016/j.freeradbiomed.2012.05.030

Narici, L., Paci, M., Brunetti, V., Rinaldi, A., Sannita, W. G., Carozzo, S., et al. (2013). Bovine rod rhodopsin: 2. Bleaching *in vitro* upon 12C ions irradiation as source of effects as light flash for patients and for humans in space. *Int. J. Radiat. biol.* 89, 765–769. doi: 10.3109/09553002.2013.800245

Navasiolava, N. M., Custaud, M.-A., Tomilovskaya, E. S., Larina, I. M., Mano, T., Gauquelin-Koch, G., et al. (2011). Long-term dry immersion: review and prospects. *Eur. J. Appl. Physiol.* 111, 1235–1260. doi: 10.1007/s00421-010-1750-x

Nelson, E. S., Mulugeta, L., and Myers, J. G. (2014). Microgravity-induced fluid shift and ophthalmic changes. *Life* 4, 621–665. doi: 10.3390/life4040621

Oakley, R., and Tharakan, B. (2014). Vascular Hyperpermeability and aging. *Aging Dis.* 5, 114–125. doi: 10.14336/AD.2014.0500114

Parazynski, S. E., Hargens, A. R., Tucker, B., Aratow, M., Styf, J., and Crenshaw, A. (1991). Transcapillary fluid shifts in tissues of the head and neck during and after simulated microgravity. *J. Appl. Physiol.* 71, 2469–2475.

Parver, L. M. (1991). Temperature modulating action of choroidal blood flow. *Eye* 5 (Pt 2), 181–185. doi: 10.1038/eye.1991.32

Parver, L. M., Auker, C., and Carpenter, D. O. (1980). Choroidal blood flow as a heat dissipating mechanism in the macula. *Am. J. Ophthalmol.* 89, 641–646. doi: 10.1016/0002-9394(80)90280-9

Pavy-Le Traon, A., Heer, M., Narici, M. V., Rittweger, J., and Vernikos, J. (2007). From space to Earth: advances in human physiology from 20 years of bed rest studies (1986–2006). *Eur. J. Appl. Physiol.* 101, 143–194. doi: 10.1007/s00421-007-0474-z

Pietramaggiori, G., Liu, P., Scherer, S. S., Kaipainen, A., Prsa, M. J., Mayer, H., et al. (2007). Tensile forces stimulate vascular remodeling and epidermal cell proliferation in living skin. *Ann. Surg.* 246, 896–902. doi: 10.1097/SLA.0b013e3180caa47f

Pietsch, J., Ma, X., Wehland, M., Aleshcheva, G., Schwarzwälder, A., Segerer, J., et al. (2013). Spheroid formation of human thyroid cancer cells in an automated culturing system during the Shenzhou-8 Space mission. *Biomaterials* 34, 7694–7705. doi: 10.1016/j.biomaterials.2013.06.054

Pinsky, L. S., Osborne, W. Z., Bailey, J. V., Benson, R. E., and Thompson, L. F. (1974). Light flashes observed by astronauts on apollo 11 through apollo 17. *Science* 183, 957–959. doi: 10.1126/science.183.4128.957

Prisk, G. K. (2000). Microgravity and the lung. *J. Appl. Physiol.* 89, 385–396.

Prisk, G. K. (2014). Microgravity and the respiratory system. *Eur. Respir. J.* 43, 1459–1471. doi: 10.1183/09031936.00001414

Prisk, G. K., Fine, J. M., Cooper, T. K., and West, J. B. (2006). Vital capacity, respiratory muscle strength, and pulmonary gas exchange during long-duration exposure to microgravity. *J. Appl. Physiol.* 101, 439–447. doi: 10.1152/japplphysiol.01419.2005

Purdy, R. E., Duckles, S. P., Krause, D. N., Rubera, K. M., and Sara, D. (1998). Effect of simulated microgravity on vascular contractility. *J. Appl. Physiol.* 85, 1307–1315.

Rittweger, J., Bareille, M.-P., Clément, G., Linnarsson, D., Paloski, W. H., and Wuyts, F., Angerer, O. (2015). Short-arm centrifugation as a partially effective musculoskeletal countermeasure during 5-day head-down tilt bed rest–results from the BRAG1 study. *Eur. J. Appl. Physiol.* 115, 1233–1244. doi: 10.1007/s00421-015-3120-1

Riva, C. E., Hero, M., Titze, P., and Petrig, B. (1997a). Autoregulation of human optic nerve head blood flow in response to acute changes in ocular perfusion pressure. *Graefes Arch. Clin. Exp. Ophthalmol.* 235, 618–626. doi: 10.1007/BF00946937

Riva, C. E., Sinclair, S. H., and Grunwald, J. E. (1981). Autoregulation of retinal circulation in response to decrease of perfusion pressure. *Invest. Ophthalmol. Vis. Sci.* 21(1 Pt 1), 34–38.

Riva, C. E., Titze, P., Hero, M., and Petrig, B. L. (1997b). Effect of acute decreases of perfusion pressure on choroidal blood flow in humans. *Invest. Ophthalmol. Vis. Sci.* 38, 1752–1760.

Rodent Research (2016). *Rodent Research Contributes to Osteoporosis Treatments*. Spinoff.

Romero-Weaver, A. L., Lin, L., Carabe-Fernandez, A., and Kennedy, A. R. (2014). Effects of solar particle event-like proton radiation and/or simulated microgravity on circulating mouse blood cells. *Gravit. Space Res.* 2, 42–53. doi: 10.1667/RR3173.1

Romero-Weaver, A. L., Wan, X. S., Diffenderfer, E. S., Lin, L., and Kennedy, A. R. (2013). Kinetics of neutrophils in mice exposed to radiation and/or granulocyte colony-stimulating factor treatment. *Radiat. Res.* 180, 177–188. doi: 10.1667/RR3055.1

Rubin, C., Turner, A. S., Müller, R., Mittra, E., McLeod, K., Lin, W., et al. (2002). Quantity and quality of trabecular bone in the femur are enhanced by a strongly anabolic, noninvasive mechanical intervention. *J. Bone Miner. Res.* 17, 349–357. doi: 10.1359/jbmr.2002.17.2.349

Sandler, H., and Vernikos, J. (1986). *Inactivity: Physiological Effects*. New York, NY: Academic Press.

Sawant, D. A., Tharakan, B., Adekanbi, A., Hunter, F. A., Smythe, W. R., and Childs, E. W. (2011). Inhibition of VE-cadherin proteasomal degradation attenuates microvascular hyperpermeability. *Microcirculation* 18, 46–55. doi: 10.1111/j.1549-8719.2010.00067.x

Sawin, C. F., Nicogossian, A. E., Rummel, J. A., and Michel, E. L. (1976). Pulmonary function evaluation during the Skylab and Apollo-Soyuz missions. *Aviat. Space Environ. Med.* 47, 168–172.

Schrage, W. G., Woodman, C. R., and Laughlin, M. H. (2000). Hindlimb unweighting alters endothelium-dependent vasodilation and ecNOS expression in soleus arterioles. *J. Appl. Physiol.* 89, 1483–1490. doi: 10.1113/JP270279

Shi, F., Wang, Y.-C., Zhao, T.-Z., Zhang, S., Du, T.-Y., Yang, C.-B., et al. (2012). Effects of simulated microgravity on human umbilical vein endothelial cell angiogenesis and role of the PI3K-Akt-eNOS signal pathway. *PLoS ONE* 7:e40365. doi: 10.1371/journal.pone.0040365

Shinojima, A., Iwasaki, K.-I., Aoki, K., Ogawa, Y., Yanagida, R., and Yuzawa, M. (2012). Subfoveal choroidal thickness and foveal retinal thickness during head-down tilt. *Aviat. Space Environ. Med.* 83, 388–393. doi: 10.3357/ASEM.3191.2012

Shulzhenko, E., and Vil-Vilyams, I. (1975). Simulation of the human body deconditioning with the method of "dry" immersion. *Xth K.E. Tziolkovski readings*, 39–47.

Siamwala, J. H., Majumder, S., Tamilarasan, K. P., Muley, A., Reddy, S. H., Kolluru, G. K., et al. (2010). Simulated microgravity promotes nitric oxide-supported angiogenesis via the iNOS-cGMP-PKG pathway in macrovascular endothelial cells. *FEBS Lett.* 584, 3415–3423. doi: 10.1016/j.febslet.2010.06.039

Simanonok, K. E., and Charles, J. B. (1994). Space sickness and fluid shifts: a hypothesis. *J. Clin. Pharmacol.* 34, 652–663. doi: 10.1002/j.1552-4604.1994.tb02020.x

SkinSuit (2015). *Revealing the Identity of SkinSuit Man*. Andreas Mogensen's iriss blog.

Smith, S. M., Wastney, M. E., Morukov, B. V., Larina, I. M., Nyquist, L. E., Abrams, S. A., et al. (1999). Calcium metabolism before, during, and after a 3-mo spaceflight: kinetic and biochemical changes. *Am. J. Physiol.* 277(1 Pt 2), R1–R10.

Smith, S. M., Wastney, M. E., O'Brien, K. O., Morukov, B. V., Larina, I. M., Abrams, S. A., et al. (2005). Bone markers, calcium metabolism, and calcium kinetics during extended-duration space flight on the mir space station. *J. Bone Miner. Res.* 20, 208–218. doi: 10.1359/JBMR.041105

Stein, T. P. (2013). Weight, muscle and bone loss during space flight: another perspective. *Eur. J. Appl. Physiol.* 113, 2171–2181. doi: 10.1007/s00421-012-2548-9

Taibbi, G., Cromwell, R. L., Kapoor, K. G., Godley, B. F., and Vizzeri, G. (2013). The effect of microgravity on ocular structures and visual function: a review. *Surv. Ophthalmol.* 58, 155–163. doi: 10.1016/j.survophthal.2012.04.002

Tatebayashi, K., Doi, M., and Kawai, Y. (2002). Changes of intracranial pressure during head-down tilt in anesthetized and conscious rabbits. *J. Gravit. Physiol.* 9, P101–P102.

Taylor, C. R., Hanna, M., Behnke, B. J., Stabley, J. N., McCullough, D. J., Davis, R. T., et al. (2013). Spaceflight-induced alterations in cerebral artery vasoconstrictor, mechanical, and structural properties: implications for elevated cerebral perfusion and intracranial pressure. *FASEB J* 27, 2282–2292. doi: 10.1096/fj.12-222687

Trappe, S., Costill, D., Gallagher, P., Creer, A., Peters, J. R., Evans, H., et al. (2009). Exercise in space: human skeletal muscle after 6 months aboard the International Space Station. *J. Appl. Physiol.* 106, 1159–1168. doi: 10.1152/japplphysiol.91578.2008

Vasil'eva, T. V., Raskidaĭlo, A. S., Arutcheva, A. A., Okropiridze, G. G., Petrakov, A. A., Urazgil'deev, Z. I., et al. (1993). Antibacterial activity and clinical effectiveness of the new antiseptic miramistin. *Antibiot. Khimioter.* 38, 61–63.

Venturoli, D., Semino, P., Negrini, D., and Miserocchi, G. (1998). Respiratory mechanics after 180 days space mission (EUROMIR'95). *Acta Astronaut. 42*, 185–204. doi: 10.1016/S0094-5765(98)00116-7

Verheyden, B., Liu, J., Beckers, F., and Aubert, A. E. (2009). Adaptation of heart rate and blood pressure to short and long duration space missions. *Respir. Physiol. Neurobiol.* 169(Suppl.), S13–S16. doi: 10.1016/j.resp.2009.03.008

Verheyden, B., Liu, J., Beckers, F., and Aubert, A. E. (2010). Operational point of neural cardiovascular regulation in humans up to 6 months in space. *J. Appl. Physiol.* 108, 646–654. doi: 10.1152/japplphysiol.00883.2009

Vernikos, J., and Schneider, V. S. (2010). Space, gravity and the physiology of aging: parallel or convergent disciplines? A mini-review. *Gerontology* 56, 157–166. doi: 10.1159/000252852

Vernikos, J., Hosie, R., and Glenn, J. (2004). *The G-Connection: Harness Gravity and Reverse Aging*. iUniverse Inc.

Wambi, C., Sanzari, J., Wan, X. S., Nuth, M., Davis, J., Ko, Y.-H., et al. (2008). Dietary antioxidants protect hematopoietic cells and improve animal survival after total-body irradiation. *Radiat. Res.* 169, 384–396. doi: 10.1667/RR1204.1

Wang, S., Birol, G., Budzynski, E., Flynn, R., and Linsenmeier, R. A. (2010). Metabolic responses to light in monkey photoreceptors. *Curr. Eye Res.* 35, 510–518. doi: 10.3109/02713681003597255

Wantier, M., Estenne, M., Verbanck, S., Prisk, G. K., and Paiva, M. (1998). Chest wall mechanics in sustained microgravity. *J. Appl. Physiol.* 84, 2060–2065.

Warnke, E., Pietsch, J., Wehland, M., Bauer, J., Infanger, M., Görög, M., et al. (2014). Spheroid formation of human thyroid cancer cells under simulated microgravity: a possible role of CTGF and CAV1. *Cell Commun. Signal.* 12:32. doi: 10.1186/1478-811X-12-32

Weinert, B., and Timiras, P. (2003). Invited review: theories of aging. *J. Appl. Physiol.* 95, 1706–1716. doi: 10.1152/japplphysiol.00288.2003

Widrick, J. J., Knuth, S. T., Norenberg, K. M., Romatowski, J. G., Bain, J. L., Riley, D. A., et al. (1999). Effect of a 17 day spaceflight on contractile properties of human soleus muscle fibres. *J. Physiol.* 516 (Pt 3), 915–930. doi: 10.1111/j.1469-7793.1999.0915u.x

Xianyun, S., Jianhe, C., and Jingrui, M. (1997). Changes of circulation endothelial cell count in simulated weightlessness rabbit. *Chin. J. Microcirc.* 7, 8–9.

Yamaguchi, H., Uchihori, Y., Yasuda, N., Takada, M., and Kitamura, H. (2005). Estimation of yields of OH radicals in water irradiated by ionizing radiation. *J. Radiat. Res.* 46, 333–341. doi: 10.1269/jrr.46.333

Ye, X., Wang, Y., and Nathans, J. (2010). The Norrin/Frizzled4 signaling pathway in retinal vascular development and disease. *Trends Mol. Med.* 16, 417–425. doi: 10.1016/j.molmed.2010.07.003

Zhang, L. F. (2001). Vascular adaptation to microgravity: what have we learned? *J. Appl. Physiol.* 91, 2415–2430.

Zhang, L. N., Zhang, L. F., and Ma, J. (2001). Simulated microgravity enhances vasoconstrictor responsiveness of rat basilar artery. *J. Appl. Physiol.* 90, 2296–2305.

Zvejniece, L., Svalbe, B., Veinberg, G., Grinberga, S., Vorona, M., Kalvinsh, I., et al. (2011). Investigation into stereoselective pharmacological activity of phenotropil. *Basic Clin. Pharmacol. Toxicol.* 109, 407–412. doi: 10.1111/j.1742-7843.2011.00742.x

Zwart, S. R., Gibson, C. R., Mader, T. H., Ericson, K., Ploutz-Snyder, R., Heer, M., et al. (2012). Vision changes after spaceflight are related to alterations in folate- and vitamin B-12-dependent one-carbon metabolism. *J. Nutr.* 142, 427–431. doi: 10.3945/jn.111.154245

Conflict of Interest Statement: The authors declare that the research was conducted in the absence of any commercial or financial relationships that could be construed as a potential conflict of interest.

frontiers in Physiology

ORIGINAL RESEARCH
published: 16 February 2016
doi: 10.3389/fphys.2016.00042

Fluoxetine Protection in Decompression Sickness in Mice is Enhanced by Blocking TREK-1 Potassium Channel with the "spadin" Antidepressant

Nicolas Vallée[1], Kate Lambrechts[1,2], Sébastien De Maistre[3], Perrine Royal[1], Jean Mazella[4], Marc Borsotto[4], Catherine Heurteaux[4], Jacques Abraini[1,5,6], Jean-Jacques Risso[1] and Jean-Eric Blatteau[1]*

[1] Institut de Recherche Biomédicale des Armées, Equipe Résidante de Recherche Subaquatique Opérationnelle, Toulon, France, [2] UFR STAPS, Laboratoire Motricité Humaine Education Sport Santé, Université du Sud Toulon Var, La Garde, France, [3] Hôpital d'Instruction des Armées, Service de Médecine Hyperbare et Expertise Plongée, Toulon, France, [4] Centre National de la Recherche Scientifique and Université de Nice Sophia Antipolis, Institut de Pharmacologie Moléculaire et Cellulaire, UMR 7275, Valbonne, France, [5] Département d'Anesthésiologie, Université Laval, Québec, QC, Canada, [6] Faculté de Médecine, Université de Caen Normandie, Caen, France

OPEN ACCESS

Edited by:
Antonio L'Abbate, Scuola Superiore Sant'Anna, Italy

Reviewed by:
Angelo Gemignani, Consiglio Nazionale delle Ricerche, Italy
Paul Kenneth Witting, The University of Sydney, Australia

***Correspondence:**
Nicolas Vallée
nicolas.vallee5@hotmail.fr

Specialty section:
This article was submitted to Integrative Physiology, a section of the journal Frontiers in Physiology

Received: *27 August 2015*
Accepted: *29 January 2016*
Published: *16 February 2016*

Citation:
Vallée N, Lambrechts K, De Maistre S, Royal P, Mazella J, Borsotto M, Heurteaux C, Abraini J, Risso J-J and Blatteau J-E (2016) Fluoxetine Protection in Decompression Sickness in Mice is Enhanced by Blocking TREK-1 Potassium Channel with the "spadin" Antidepressant. Front. Physiol. 7:42. doi: 10.3389/fphys.2016.00042

In mice, disseminated coagulation, inflammation, and ischemia induce neurological damage that can lead to death. These symptoms result from circulating bubbles generated by a pathogenic decompression. Acute fluoxetine treatment or the presence of the TREK-1 potassium channel increases the survival rate when mice are subjected to an experimental dive/decompression protocol. This is a paradox because fluoxetine is a blocker of TREK-1 channels. First, we studied the effects of an acute dose of fluoxetine (50 mg/kg) in wild-type (WT) and TREK-1 deficient mice (knockout homozygous KO and heterozygous HET). Then, we combined the same fluoxetine treatment with a 5-day treatment protocol with spadin, in order to specifically block TREK-1 activity (KO-like mice). KO and KO-like mice were regarded as antidepressed models. In total, 167 mice (45 WT_{cont} 46 WT_{flux} 30 HET_{flux} and 46 KO_{flux}) constituting the flux-pool and 113 supplementary mice (27 KO-like 24 WT_{flux2} 24 $KO\text{-like}_{flux}$ 21 WT_{cont2} 17 $WT_{no\ dive}$) constituting the spad-pool were included in this study. Only 7% of KO-TREK-1 treated with fluoxetine (KO_{flux}) and 4% of mice treated with both spadin and fluoxetine ($KO\text{-like}_{flux}$) died from decompression sickness (DCS) symptoms. These values are much lower than those of WT control (62%) or KO-like mice (41%). After the decompression protocol, mice showed significant consumption of their circulating platelets and leukocytes. Spadin antidepressed mice were more likely to exhibit DCS. Nevertheless, mice which had both blocked TREK-1 channels and fluoxetine treatment were better protected against DCS. We conclude that the protective effect of such an acute dose of fluoxetine is enhanced when TREK-1 is inhibited. We confirmed that antidepressed models may have worse DCS outcomes, but concomitant fluoxetine treatment not only decreased DCS severity but increased the survival rate.

Keywords: bubble, decompression sickness, diapedesis, kcnk2, TREK-1, diving, depression, capillary leak

INTRODUCTION

In this study, fluoxetine and the new antidepressant spadin were used to find a treatment strategy against decompression sickness.

Circulating bubbles cause cell damage (Vallee et al., 2013), prothrombotic phenomena, ischemia, and diapedesis (Dutka et al., 1989; Zamboni et al., 1989, 1992, 1993; Dal Palu and Zamboni, 1990; Helps and Gorman, 1991). This inflammation can spread systemically and may degenerate into a vicious cycle, ending in multiple organ failure (Jacey et al., 1976; DeGirolami and Zivin, 1982; Ersson et al., 1998). Spinal cord and brain neurological damage underlie the most serious symptoms of decompression sickness (DCS; Gempp et al., 2008). These symptoms result from circulating bubbles generated by a pathogenic decompression, following a dive for example. Even after standard treatment with hyperbaric oxygen, 20–30% of victims suffer from sequelae after a neurological DCS (Blatteau et al., 2011). We aimed to establish a potential treatment strategy using an animal model of DCS.

Fluoxetine, the active compound in the antidepressant Prozac™, prevents the reuptake of serotonin (5-hydroxytryptamine, 5-HT) by inhibiting serotonin transporters (SERT) located in neurons, platelets (Lesch et al., 1993), and leukocytes (Faraj et al., 1994; Lima and Urbina, 2002; Yang et al., 2007). SERT increases the concentration of circulating serotonin (Brenner et al., 2007). When used in a single high dose, fluoxetine is also believed to mediate neuroprotection (Pariente et al., 2001; Chollet et al., 2011; Taguchi et al., 2012) by inhibiting NMDA-R (Vizi et al., 2013), regulating inflammatory effects (Kubera et al., 2001; Jin et al., 2009; Lim et al., 2009) and algesia (Kostadinov et al., 2014). We have previously demonstrated that WT mice treated with fluoxetine are more resistant to DCS and that fluoxetine inhibits the inflammatory process by reducing the level of circulating IL-6, a pro-inflammatory cytokine (Blatteau et al., 2012).

TREK-1, the product of the *kcnk2* gene, regulates cell excitability and prevents neuron death by inhibiting NMDA-dependent glutamatergic excitotoxicity induced by ischemia (Franks and Honore, 2004; Heurteaux et al., 2004; Buckler and Honore, 2005; Honore, 2007; Dedman et al., 2009). The mechanosensitive TREK-1 channel (Franks and Honore, 2004) is activated by a mechanical deformation of the cellular membrane, for example by a deformation induced by air depression (Heurteaux et al., 2004). Additionally, in mice, decompression-induced desaturation also activates TREK-1. Consequently, KO ("KO" is used in the mean of "TREK-$1^{-/-}$ mice") mice are more sensitive to DCS than WT (TREK-$1^{+/+}$) mice (Vallee et al., 2012). TREK channel activity is also under the control of several different mechanisms acting either on channel trafficking and surface density or directly on gating properties (Noel et al., 2011). Furthermore, KO mice display a depression-resistant phenotype, similar to chronic fluoxetine-treated mice (Heurteaux et al., 2006).

We have shown that the opening of TREK-1 channels is protective in DCS, suggesting that TREK-1 channel activity limits ischemia-induced glutamatergic toxicity (Vallee et al., 2012). The TREK-1 channel is directly inhibited by fluoxetine (Heurteaux et al., 2006; Bogdan et al., 2011; Sandoz et al., 2011) and by spadin, a new antidepressant that internalizes the channel after a 5-days treatment and consequently abolish channel activity (Mazella et al., 2010; Moha Ou Maati et al., 2011), so the question arises as to whether acute fluoxetine treatment could be significantly more efficient when the TREK-1 channel is impaired: we suggest if less fluoxetine can link to TREK-1, the fluoxetine anti-inflammatory effect should be enhanced in a dose-dependent manner, although the neuroprotection afford by the TREK-1 activity could be loss. Conversely, we wondered whether mice pre-treated with an anti-depressant drug, that impairs TREK-1 activity, would be sensitized to DCS.

In this study, we wanted to obtain a better understanding of the protection afforded by fluoxetine in our DCS model. We aimed to block the fluoxetine binding on TREK-1, and therefore to promote other fluoxetine pathways, resulting in a better efficiency for the inhibition of the NMDA-R or the regulation of interleukin releases for example (**Figure 2**).

Before the exposure to the pathogenic decompression, we gave an acute dose of fluoxetine on wild-type (WT: TREK-$1^{+/+}$) mice and on mice to whom TREK-1 disappeared from the membrane surface. We therefore used TREK-1 knockout (KO: TREK-$1^{-/-}$) and heterozygous (HET: TREK-$1^{+/-}$) mice, or 5 days of treatment with spadin resulting in KO-like (TREK-$1^{-/-like}$) mice, to inhibit TREK-1 channel activity. KO and KO-like mice were considered the antidepressed models. We obviously did not use chronic fluoxetine (more than 21 days are necessary) on WT mice to obtain an antidepressive state, followed by an acute dose of fluoxetine; while of interest, this would not allow us to reach a conclusion.

MATERIALS AND METHODS

Animals and Ethical Statement

All procedures involving experimental animals were in line with European Union rules (Directive 2010/63/EU) and French law (Decree 2013/118). The ethics committee of the Institut de Recherche Biomédicale des Armées approved this study. According to our animal care committee, a scoring system inspired by the Swiss veterinary guidelines was implemented to ensure the welfare of animals. A dedicated observer scored (from 0 to 3) the stress or pain relating to some criteria for each animal, and then completed a sheet (Supplementary Data). Pain of degree 3 (very painful) in one case or a total score of 12 in the table were the ethical endpoints. On this sheet, the most commonly found were: vocalizing, aggression or withdrawn behavior, reduction in exploratory behavior, licking, closed eyes, tears, bubbles in the eyes, high respiratory rate, runny nose, fur bristling, labored breathing, convulsions, paralysis, difficulty moving, and problems with the fore or rear limbs (classified as motor disorders). In this study, no score reached 12 and there was no need to cull the animal based on these criteria. Actually, mice displaying degree 3 convulsions died very rapidly. At the end of the experiment, mice were anesthetized first with halothane (5% in oxygen, Halothane, Belamont, France) in order to gain time and to minimize stress, and then with an intraperitoneal injection

of a mixture of 16 mg/kg xylazine (Rompum® 2%, Bayer Pharma) and 100 mg/kg ketamine (Imalgène® 1000, Laboratoire Rhône). Our investigator (NV) is associated with agreement number 83.6 delivered by the Health and Safety Directorate of our department, as stated in the French rules R.214-93, R-214-99, and R.214-102. Mice were housed in an accredited animal care facility. Mice kept were in group cages both during rest and during the experiments and maintained on a regular day (6:00 a.m.–6:00 p.m.)/night (12 h) cycle. Food (*AO3, UAR*) and water were provided *ad libitum* and the temperature was kept at $22 \pm 1°C$.

In TREK-$1^{-/-}$ mice, the gene encoding the TREK-1 channel was knocked out by Cre-Lox recombination (Heurteaux et al., 2004). The comparator animals were analogous C57Bl/6 mice (Charles River Laboratory, Arbresle, France). In order to preclude phenotypic variation between the different strains (Sato et al., 2006), crosses were made every 11 generations. Wild-type (WT, TREK-$1^{+/+}$) heterozygous (HET, TREK-$1^{+/-}$) and knockout (KO, TREK-$1^{-/-}$) mice were produced for this study. To avoid fluctuations due to female hormonal cycles, only males were used in this study.

Flux-Pool

In total, 167 mice (6–9 week-old) constituting the flux-pool were exposed to compressed air to induce DCS. The mice were randomly divided into four groups and numbered (**Figure 1**): 46 for the wild-type group treated with fluoxetine (WT_{flux}), 30 for the heterozygous group treated with fluoxetine (HET_{flux}), 46 for the knockout group treated with fluoxetine (KO_{flux}), and 45 wild-type controls (WT_{cont}).

Fluoxetine (50 mg/kg) was administered by gavage to experimental animals as an oral solution (Prozac™ 20 mg/5 ml, oral solution bottle of fluoxetine hydrochloride, Lilly Laboratories, France) 18 h before hyperbaric exposure, while the wild type control group (WT_{cont}) received a similar saccharine fluoxetine-free solution (7.4 g/kg). This high dose of fluoxetine was determined on the basis of previous results from a mouse model of ischemia (Jin et al., 2009; Blatteau et al., 2012; Taguchi et al., 2012).

Spad-Pool

In total, 113 mice (strain C57Black/6, 6–9 weeks of age, Harlan laboratories, Gannat, France) constituted the spad-pool and were used to replicate the experiment performed with the flux-pool, but substituting TREK-1 KO mice with spadin-induced KO mice (KO-like mice). To generate KO-like mice, mice were treated for 5 days at 9:00 a.m. with intraperitoneal injections of spadin (100 µg/Kg) in a bolus of 100 µL of NaCl 0.9%. The mixture for the acute fluoxetine treatment (50 mg/kg; 1.5 mg per mouse) was obtained from 20 mg capsules (fluoxetine hydrochloride Prozac™, Lilly Laboratories, France) diluted in 300 µL of a solution of NaCl 9% and gum arabic 5%. It was injected intraperitoneally 18 h before the end of the hyperbaric exposure (p.m. 5:00).

The first group (WT_{cont2}, $n = 21$), for control, received the equivalent 5 days of treatment (100 µL per day of NaCl 0.9%, i.p.) plus the vehicle (300 µL of NaCl 0.9% with gum arabic 5%) corresponding to the acute dose of fluoxetine. A second group (KO-like = $WT_{spadin\ 5d}$, $n = 27$) received a daily dose of spadin for 5 days plus the vehicle of the acute fluoxetine treatment. A third group (WT_{flux2}, $n = 24$) received an acute i.p. injection of fluoxetine plus the analogous 5 days-treatment without spadin. A fourth group (KO-$like_{flux}$ = $WT_{flux+spadin\ 5d}$, $n = 24$) received 5 days of treatment with spadin and the acute dose of fluoxetine. A fifth group ($WT_{no\ dive}$, $n = 17$) not submitted to the hyperbaric protocol received the same injections as WT_{cont2} mice. Batches were mixed for the hyperbaric protocol.

Hyperbaric Procedure

Hyperbaric Exposure Began at 12:30 p.m.

Each mouse was weighed 30 min before the dive. Samples of 20 mice (10 per cage) from the flux-pool or batches of 6–8 mice from the spad-pool were subjected to the hyperbaric protocol in a 200-l tank fitted with three observation ports. The mice were free to move around the cage.

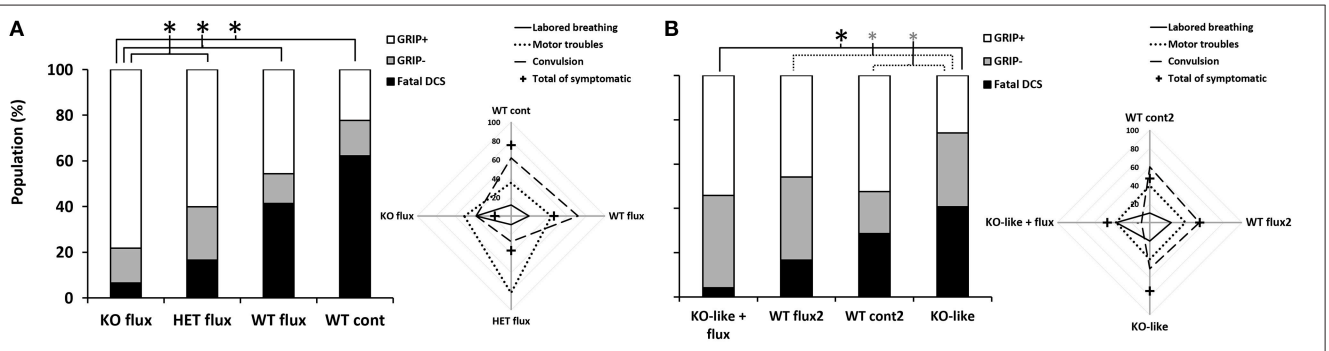

FIGURE 1 | Symptoms in different groups of mice 30 min after pathogenic decompression as a function of genotype or drug treatment or both. (A) The flux-pool. **(B)** The spad-pool. Histogram: black blocks represent the percent of mice that died following the dive (Fatal DCS); gray represents mice that failed at least one grip test (sensory motor test for forelimbs) (Grip−); white represents the proportion of mice that passed both grip tests (Grip+). Radar Chart: percentage of mice displaying a type of symptom in a population; cross represents the total (in percent) of Grip− mice, considering that a mouse can present several symptoms at the same time. WT, wild-type; KO, knockout; HET, heterozygous; KO-like, mice treated for 5 days with spadin. Flux, fluoxetine; cont and cont2, control (no active molecules). Black * denotes $p < 0.05$ between groups. Gray * denotes $p < 0.10$ (trend) between groups.

The compression protocol involved two ramps of pressure increase, first at 0.1 atm/min up to 1 atm, followed by 1 atm/min up to 9 atm; 9 atm corresponds to the pressure where animals were kept for 45 min before decompression. The decompression rate was 60 atm/min up to the surface. Compression and decompression were automatically controlled by a computer linked to an analog/digital converter (NIUSB-6211, National Instrument, USA) with two solenoid valves (Belino LR24A-SR, Switzerland) and a pressure transmitter (Pressure Transmitter 8314, Burket Fluid Control System, Germany). The software was programmed on a DasyLab (DasyLab National Instrument, USA) by our engineer. The software also controlled the temperature and oxygen rate. Compressed air was generated using a diving compressor (Mini Verticus III, Bauer Comp, Germany) coupled to a 100-l tank at 300 bars. The oxygen analyzer was based on a MicroFuel electrochemical cell (G18007 Teledyne Electronic Technologies/Analytical Instruments, USA). The temperature inside the tank was monitored using a platinum-resistance temperature probe (Pt 100, Eurotherm, France).

Water vapor and CO_2 produced by the animals were captured with soda lime (<300 ppm captured by the soda lime) and seccagel (relative humidity: 40–60%). Gases were mixed by an electric fan. The day-night cycle was respected throughout.

Behavioral and Clinical Observations

At the end of the decompression time, mice were observed for 30 min. All signs were recorded together with their time of onset: labored breathing, convulsions or death. Paralysis, difficulty moving and problems with the fore or rear limbs were classified as motor deficits.

The grip test, a motor/sensory test adapted from Hall et al. (Hall, 1985), was used to quantify forelimb involvement 15 and 30 min after the end of decompression. The mouse was placed in the middle of a 60 cm-long cord suspended at a height of 40 cm hanging from its fore paws and each performance was timed with a stop-watch, over a test duration of 30 s. Mice which escaped by climbing up and then walking along the cord corresponded to the highest score of 30 s. Mice which failed at least one test were considered as symptomatic (Grip−). The results of this behavioral test were used to define DCS and distinguished the following groups: dead (fatal DCS), mice that failed at least one grip test (Grip−) and mice that passed the grip test (Grip+).

Anesthesia and Sacrifice

All mice were anaesthetized 30 min after surfacing (after grip tests) first with halothane (5% in oxygen, Halothane, Belamont, France) in order to gain time and to minimize stress, and then by intraperitoneal injection of a mixture of 16 mg/kg xylazine (Rompum® 2%, Bayer Pharma) and 100 mg/kg ketamine (Imalgène® 1000, Laboratoire Rhône). Mice in the spad-pool were kept for heart blood sampling for biochemistry and then sacrificed by injecting pentobarbital (200 mg/kg ip, Sanofi Santé, France).

Blood Tests

Blood tests were carried out using an automatic analyzer (ABCvet, SCIL Animal care company, France) on samples taken before the dive and again 30 min afterwards. The second test values were corrected according to the hematocrit variation. Leukocytes, erythrocytes, hematocrit, platelets and Mean Platelet Volume (MPV) were analyzed in 20 µl samples taken from the tip of the tail and diluted in the same volume of 2 mM EDTA (Sigma, France).

Blood biochemistry [Na^+, K^+, Ca^{2+}, creatinine kinase, glucose, blood urea nitrogen (BUN), creatinine, transaminase, bilirubin, albumin, globulin, total proteins] was conducted with automatic analyzers (Vetscan VS2, Abaxis Veterinary Company, France; Reflovet Plus SCIL Animal Care Company, France; and Accutrend Plus, Roche Diagnostic, USA) on lithium heparin (Sigma, France) blood samples from the heart. Hemolytic samples were rejected.

Genotyping

For first part of the study (flux-pool), DNA for PCR was extracted from cells from the tip of the tail (5 mm) after overnight digestion at 56°C with protease K (200 µg/ml) (Promega, Charbonnière, France) freshly added in a buffer solution containing 100 mM Tris (pH 8.5), 200 mM NaCl, 5 mM EDTA, and 0.2% SDS. The protease K was then heat-inactivated (95°C for 5–10 min). The lysate was diluted 20-fold in ultrapure water before amplification.

PCR was carried out on 5 µl of lysate added to 20 µl of the reaction mixture. For negative controls, water was substituted for the lysate. The reaction mixture contained a pair of primers (10 pM/µl) [1–2] or [1–3] with an amplification mixture (GoTaq® Green Master Mix 2X, Promega France). DNA primers (MWG-Opéron Biotech, France) corresponding to the loci of interest in the *kcnk2* gene (Primers #1 [5′ GGT GCC AGG TAT GAA TAG AG 3′]; Primers #2 [5′ TTC TGA GCA GCA GAC TTG G 3′]; Primers #3 [5′ GTG TGA CTG GGA ATA AGA GG 3′]) were used with the following thermocycler (MultiGene Gradient, Labnet International, USA) settings: initialization step 94°C/3 min>> [denaturation step 94°C/25 s >> annealing step 61°C/25 s >> elongation step 72°C/35 s] for 35 cycles.

Amplified DNA sequences were resolved by electrophoresis (Biorad Generator, Powerpac 200; 90 V 45 min) on buffered 1.2% Tris acetate EDTA agar gels supplemented with BET for UV detection (Geneflash, Syngene Bioimaging). PCR-detected bands at both 680 bp [1–2] and 1870 bp [1–3] characterize the homozygous wild-type (WT, TREK-$1^{+/+}$), and a single band at 650 bp [1–3] characterizes the homozygous knock-out (KO, TREK-$1^{-/-}$). A pair of bands characterizes heterozygous mice (HET, TREK-$1^{-/+}$).

Statistical Analyses

Individual blood cell count data were calculated as the percentage change from baseline (the measurement before hyperbaric exposure). Numerical data points are expressed as mean and standard deviation. A contingency table was used for independence and association tests coupled with the χ^2 significance test. Different groups were compared using the Mann-Whitney (MW) test and matched comparisons within groups were analyzed using the Wilcoxon (W) test. Multiple comparisons were performed using the Kruskal-Wallis test

followed by the Bonferroni-Dunn *post-hoc* test. The significance threshold was 95% with an α-risk of 5%.

RESULTS

Flux-pool: 167 mice (91 WT, 30 HET, and 46 KO) were subjected to the hyperbaric protocol to induce DCS. In these groups, mouse weights were similar [$weight_{WTcont}$: mean = 24.0 ± 2.3 g (range: 19.4–29.3 g); $weight_{WTflux}$: mean = 24.2 ± 0.6 g (range: 23.7–25.1 g); $weight_{HETflux}$: mean = 24.5 ± 2.4 g (range: 20.4–29.4 g); $weight_{KOflux}$: mean = 24.4 ± 2.1 g (range: 20.8–30.6 g)] ($KW_{WTcont/WTflux/HETflux/KOflux}$: $n = 45/46/30/46$, $\alpha = 0.05$, $p = 0.657$).

Spad-pool: 113 mice were used in this pool. Spadin was used to generate TREK-1 KO-like mice. Again, mouse weights were similar [weight $_{KOlike}$: mean = 27.4 ± 2.2 g (range: 23.0–31.5 g); weight $_{WTflux}$: mean = 28.2 ± 2.7 g (range: 23.7–34.4 g); weight $_{KO\text{-}like\ flux}$: mean = 28.7 ± 2.0 g (range: 25.1–33.0 g) weight $_{WTcont2}$: mean = 27.2 ± 2.1 g (range: 23.1–31.3 g); weight $_{WTno\ dive:}$ mean = 27.2 ± 1.9 g (range: 24.9–32.6 g)] ($KW_{KO\text{-}like/WTflux,/KO\text{-}like\ flux/WTcont2/WTno\ dive,}$ $n = 27/24/24/21/17$, $p = 0.121$). These weights were significantly higher than those of the flux-pool ($KW_{Allgroups}$, $n = 27/24/24/21/17/45/46/30/46$, $p < 0.0001$), which may increase susceptibility to DCS.

Hence, in order to avoid confusion, results of both pools, i.e., flux and spad, are presented separately.

Clinical Observations

Compared to WT mice, the KO or KO-like mice showed no abnormal behavioral or phenotypic signs. All groups displayed a similar range of DCS symptoms (**Figure 1**).

Most of the mice were prostrate, suggesting that they were in physiological distress. Symptoms of DCS or death occurred after returning to the surface. Mice died from convulsions (on the outer edge of the radar map, **Figure 1**) and/or respiratory distress. Mice essentially displayed neurological symptoms with varying degrees of severity with motor and locomotor impairments (paraplegia, paraparesis) and, in some cases, convulsions. We also observed fewer convulsions and slightly more labored breathing in KO-$like_{flux}$ (**Figure 1B** Radar chart). The opposite trend was found for WT_{cont2} (Contingency table, $\chi^2_{KO\text{-}like/WTflux2/KO\text{-}like\ flux/WTcont2/WTno\ dive} = 63.175$ vs. 21.026, $p < 0.0001$).

In the flux-pool, DCS symptoms generally occurred at 5.8 ± 3.5 min on average after the end of the dive. When mice succumbed to DCS, it occurred rapidly, i.e., 6.1 ± 3.1 min on average. There was no significant difference for the onset of first symptoms or death latency, regardless of the group ($KW_{WTcont/WTflux/HETflux/KOflux}$: $p = 0.399$, $p = 0.390$, respectively).

In the spad-pool, first DCS symptoms generally occurred at 6.2 ± 3.4 min on average after the end of the dive. When mice succumbed from DCS, it occurred more rapidly, at 2.1 ± 4.5 min on average. There was no significant difference in the onset of first symptoms or death, regardless of the treatment ($KW_{KO\text{-}like/WTflux2/KO\text{-}like\ flux/WTcont2/WTno\ dive}$: $p = 0.620$, $p = 0.550$, respectively).

Lethal DCS, Grip−, Grip+ Status

KO_{flux} and KO-$like_{flux}$ mice were less susceptible to the hyperbaric protocol than other groups. Fewer KO-like mice succeeded in the grip tests (**Figure 1** histograms).

Analysis of the different clinical status of DCS showed a significant difference between the WTcont group and WTflux, HETflux, and KOflux groups ($KW_{WTcont/WTflux/HETflux/KOflux}$: $n = 45/46/30/46$, $\alpha = 0.05$, $p < 0.0001$) (**Figure 1**; **Table 1**). Only 7% of KO_{flux} mice died as a consequence of DCS. Additionally, KOflux mice presented a better success rate in both their grip tests (Contingency table, $\chi^2_{WTcont/WTflux/HETflux/KOflux} = 39.194$ vs. 16.919, $n = 45/46/30/46$, $\alpha = 0.05$, $p < 0.0001$).

In the spad-pool, analysis of the different DCS statuses showed a significant difference between the different groups ($KW_{KO\text{-}like/WTflux2/KO\text{-}like\ flux/WTcont2/WTno\ dive}$: $p < 0.0001$). Interestingly, a significant difference appeared between the KO-like group and the KO-$like_{flux}$ group. The main difference corresponded to the number of animals that died from DCS, i.e., 41 and 4% for the KO-like group and KO-$like_{flux}$ group, respectively (**Figure 1**; **Table 1**). Surprisingly, the number of mice that died was lower in the KO-$like_{flux}$ group than in the WT_{flux2} group, i.e., 4 and 17% respectively (**Figure 1**; **Table 1**). The success rate in both grip tests (Grip+) was lower for the KO-like group (**Figure 1**; **Table 1**; Contingency table, $\chi^2_{KO\text{-}like/WTflux2/KO\text{-}like\ flux/WTcont2/WTno\ dive} = 14.496$ vs. 15.507, $p = 0.070$).

Mice that Failed the Grip Test (Grip−)

Survivors underwent two grip tests (**Figure 1**; **Table 1**). While results of grip tests were different according to the treatment group, no treatment seems to better promote recovery or worsen the physical state of mice once symptoms become manifest.

TABLE 1 | Clinical status after a dive.

Populations		Clinical status after the hyperbaric exposure		
		Grip+(%)	Grip−(%)	Lethal DCS(%)
Flux-pool	WT cont	22	16	62
	WT flux	46	13	41
	HET flux	60	23	17
	KO flux	78	15	7
Spad-pool	WT cont2	52	19	29
	KO-like	26	33	41
	KO-like flux	54	42	4
	WT flux 2	46	38	17

Survivors underwent two grip tests. Grip tests, i.e., motor/sensory tests, were used to quantify forelimb involvement 15 and 30 min after the end of decompression. Mice which failed at least one test were considered to be symptomatic (Grip−). The results of this behavioral test were used to define DCS and distinguish the following groups: dead (Lethal DCS), mice that failed at least one grip test (Grip−) and mice that passed both grip tests (Grip+).

We previously suggested that the absence of TREK-1 channel activity could limit recovery after DCS (Vallee et al., 2012), but our present data are not in accord with such a hypothesis. For example, a large number of KO_{flux} mice passed both grip tests, but without an improvement between both tests, whereas KO-like$_{flux}$ mice not only passed both grip tests, but improved their scores between test 1 and test 2.

In more detail and with regard to the timed performance in the grip tests, WT_{flux} mice improved their mean time spent suspended from the cord (W_{WTflux}: $n = 6, \alpha = 0.05, p = 0.034$) in the second test carried out 15 min later (16.8 ± 2.1s vs. maximal time 30.0 ± 0.0 s). In the spad-pool study, better performances were observed in the second grip tests for the KO-like population ($W_{KO\text{-}like}$: $p = 0.014$, 4.1 ± 5.8 s vs. 16.0 ± 11.2 s) and the KO-like$_{flux}$ population ($W_{KO\text{-}like\ flux}$: $p = 0.014$, 11.5 ± 8.9 s vs. 22.2 ± 11.1 s).

Significant differences were observed between populations in both grip tests (first test, $KW_{WTcont/WTflux/HETflux/KOflux}$: $n = 7/6/7/7$, $\alpha = 0.05$, $p = 0.048$ and second test, KW $_{WTcont/WTflux/KOflux}$: $n = 7/6/7/7$, $\alpha = 0.05$, $p = 0.039$): the WT_{cont} group did not perform as well as mice treated with fluoxetine (first test: MW $_{WTcont/KOflux}$: $n = 7/7$, $p = 0.054$, MW $_{WTcont/WTflux}$: $n = 7/6$, $p = 0.002$; second test: MW $_{WTcont/WTflux}$: $n = 7/6$, $p < 0.0001$). WT_{flux} mice performed better in the second grip test than HET_{flux} mice ($MW_{HETflux/WTflux}$: $n = 7/7$, $p < 0.009$). With regard to timed performance in the grip tests of the spad-pool, no significant differences were observed between populations, either in the first (KW: $p = 0.190$) or second grip test (KW: $p = 0.453$), or in their delta performance (KW: $p = 0.193$).

Full Blood Counts

Erythrocyte Counts

To a small extent, a decrease in red cell counts, usually though diapedesis, can be observed after a dive and can be attributed to the decompression protocol (**Table 2**). Overall, we cannot link this decrease to an effect of treatment or to mouse genotype.

In the flux-pool, differences in erythrocyte counts could be attributed to the treatment before the dive (KW: $p < 0.0001$): WT_{cont} mice displayed lower erythrocyte counts than both WT_{flux} ($p < 0.001$) and KO_{flux} ($p < 0.003$) mice. HET_{flux} mice also presented lower erythrocyte counts than KO_{flux} mice ($p = 0.01$). Globally, erythrocyte counts decreased on average after the dive, to a small extent (W: $p = 0.003$, mean $= -0.4 \pm 7.9$), with lower counts in Grip− mice (KW $p = 0.017$). These differences can therefore be related to treatments given to the mice (KW $p < 0.0001$: WT_{cont} and WT_{flux} presented lower erythrocyte counts than KO_{flux}), but there were no variations in their consumption rate (KW $p = 0.382$) after the dive. This suggests that the red cell count decrease was due to the decompression, even when basal levels were different according to treatment.

In the spad-pool, no effect on erythrocyte counts could be attributed to the sole effects of treatments before the dive (KW: $p = 0.999$), or afterwards (KW: $p = 0.392$), or in its variation between before and after the dive (KW: $p = 0.172$). Following the dive, a significant decrease in erythrocyte counts (W $p < 0.001$, mean $= -8.6 \pm 10.1$) was observed after the decompression protocol in all survivors, but the variation was not linked to the clinical state after the dive (Grip+ vs. Grip−: MW $p = 0.299$: Grip+: mean $= -7.3 \pm 9.4\%$; Grip−: mean $= -10.2 \pm 11.0\%$).

Platelet Counts

Globally, platelet loss occurs following a dive that can be linked to the physical state of mice. Platelet consumption seemed to be more related to the clinical state of the mice than to their treatment or their genetic status (**Table 2**). Platelet consumption increased with the severity of DCS. This drop in platelet counts was attributed to clotting activity following exposure of the collagen under bubble-damaged endothelial cells in blood vessels (Persson et al., 1978; Haller et al., 1987; Thorsen et al., 1987; Nossum et al., 1999) or to direct interactions between bubbles and platelets (Hallenbeck et al., 1973; Warren et al., 1973; Giry et al., 1977).

TABLE 2 | Variation (%) in erythrocyte, leukocyte, and platelet counts before and after decompression.

Correction according to the hematocrit variation	Part of the study	Variation in blood cell counts between before and after the hyperbaric exposure (%)		
		Grip+	Grip−	All survivors
Hematocrit	1-Flux-pool	−14.4 ± 19.2	−4.5 ± 25.3	−12.6 ± 21.6*
	2-Spad-pool	+29.9 ± 51.8	+31.0 ± 48.3	+25.2 ± 43.8*
Erythrocytes	1-Flux-pool	−0.6 ± 8.9	0.2 ± 1.8#	−0.4 ± 7.9*
	2-Spad-pool	−7.3 ± 9.4	−10.2 ± 11.0	−8.6 ± 10.1*
Leukocytes	1-Flux-pool	−6.6 ± 66.6	+12.1 ± 80.8	−2.4 ± 69.7*
	2-Spad-pool	−29.0 ± 51.7	−25.4 ± 74.7	−27.4 ± 62.8*
Platelets	1-Flux-pool	+9.2 ± 33.1	−13.6 ± 29.2#	+4.5 ± 33.5
	2-Spad-pool	−26.1 ± 23.8	−41.2 ± 29.3	−32.7 ± 27.0*

*The column on the right shows the averaged count carried out for all survivors (Grip+ and Grip−). Grip− mice were considered to be symptomatic. Grip+ mice were considered to be asymptomatic. *Denotes a significant difference within all the survivors between pre- and post-decompression counts. #Denotes a significant difference between Grip+ and Grip− mice.*

In more detail, and with regards to the first part of the study, some differences in platelet counts could be attributed to the treatments before the dive (KW: $p < 0.001$): WT_{cont} displayed lower platelet counts than both HET_{flux} ($p = 0.004$) and KO_{flux} ($p < 0.001$). WT_{flux} also presented lower platelet counts than HET_{flux} ($p = 0.004$) and KO_{flux} ($p < 0.001$).

Following the dive, no significant decrease in platelet counts (mean = +4.5 ± 33.5%) was recorded when all survivors were considered (W $p = 0.728$). Nonetheless, Grip− mice tended to exhibit higher consumption of platelets than Grip+ mice (KW, $p = 0.005$; Grip+: mean = +9.2 ± 33.1%; Grip−: mean = −13.6 ± 29.2%). No link could be established between platelet consumption and treatments (KW, $p = 0.076$). This suggests that platelet consumption, attributed to clotting activity, is mainly due to the clinical state induced by decompression rather than to treatment or genotype.

In the spad-pool, the absence of a difference in platelet counts could be attributed to the treatment effects before the dive (KW: $p = 0.209$), and levels before the dive had no consequences on the clinical state after the dive (KW: $p = 0.735$).

Thirty minutes after the dive ended, a significant decrease in platelet counts (−21.2 ± 26.5%) was recorded in all survivors (MW: $p < 0.0001$). Platelet consumption was independent of the nature of the treatment (KW: $p = 0.132$). Grip+ mice had more circulating platelets (KW, $p = 0.042$) and tended to have a lower consumption (in proportion) of their platelets than Grip− mice (KW, $p = 0.069$; Grip+: mean = −26.1 ± 23.8%; Grip−: mean = −41.2 ± 29.3%). Actually, Grip− platelets had a greater volume than that of Grip+ mice ($p = 0.0014$), confirming that old platelets (with a lower normal volume) had been used in the aggregation process.

Leukocyte Counts

Globally, there was a loss of leukocyte following the dive (**Table 2**) that was usually attributed to diapedesis (Dutka et al., 1989; Zamboni et al., 1989, 1992, 1993; Dal Palu and Zamboni, 1990; Helps and Gorman, 1991). Neither treatment seemed to influence leukocyte movement greatly, or the clinical state.

In the flux-pool, differences in leukocyte counts could be attributed to the treatments before the dive (KW: $p = 0.001$), as WT_{cont} displayed lower leukocyte counts than both HET_{flux} ($p = 0.010$) and KO_{flux} ($p < 0.005$). These differences influenced their clinical state after the dive (KW: $p = 0.004$). Therefore, mice that died after the dive-decompression protocol (Lethal DCS mice) had lower leukocyte counts before the dive than Grip+ mice (4.3 ± 1.2 vs. $5.3 \pm 1.6 \times 2.10^3/\mu l$).

After the dive, in all survivors, leukocyte counts decreased by 2.4 ± 7.9% (W: $p = 0.003$). These differences in counts or variation between the different groups were not significant with regard to genotype or treatment (KW: $p = 0.129$ and $p = 0.342$), or clinical status after the dive, i.e., Grip+, Grip−, or Lethal (KW $p = 0.870$ and $p = 0.416$).

In the spad-pool, differences in leukocyte counts could be attributed to the 5 days of spadin treatment (KW, $p = 0.008$). KO-like mice displayed higher leukocyte counts than $KO\text{-like}_{flux}$ mice ($p = 0.016$), WT_{flux2} mice ($p = 0.007$) or $WT_{no\ dive}$ mice (a trend, $p = 0.096$). Differences observed before the dive possibly influenced the clinical state after the dive (KW: $p = 0.022$). Here again, Lethal DCS mice had higher leukocyte counts than Grip+ mice (6.3 ± 1.7 vs. $5.0 \pm 2.0 \times 02.10^3/\mu l$, $p = 0.032$). Nonetheless, this is the opposite result to what has just been proposed for the flux-pool study, what must invalidate the hypothesis.

Following the dive, a significant decrease in leukocyte counts (W: $p < 0.0001$, mean = −27.4 ± 62.8%) was recorded in all survivors. Nonetheless, there was no difference in the consumption of leukocytes between Grip+ and Grip− mice (KW: $p = 0.8930$: Grip+: mean = −29.0 ± 51.7%; Grip−: mean = −25.4 ± 74.7%). Leukocyte recruitment was independent of the nature the treatment (KW: $p = 0.905$).

Finally, fluoxetine administered orally before the dive tended to increase the number of circulating leukocytes, compared to control mice. When injected i.p., fluoxetine reduced leukocyte counts. In fact, intraperitoneal injection of fluoxetine induces irritation and leukocyte adhesion in the abdominal cavity (Herr et al., 2014). This effect was not counteracted by the 5 days of spadin treatment, while the latter, when given alone i.p., tended to increase leukocyte counts. Finally, however, this prestimulation was equal in all groups for the spad-pool and controlled by the administration of the vehicle in the same way as fluoxetine administration. These paradoxical effects on leukocyte counts before the dive did not influence the (high) survival rate of the KO_{flux} and the $KO\text{-like}_{flux}$ mice.

As already described (Pontier et al., 2008; Blatteau et al., 2012; Vallee et al., 2012), the leukocyte counts dropped after decompression in all survivors, and leukocyte recruitment was independent of the type of treatment.

Blood Biochemistry

Following the dive, blood biochemistry was assessed on samples from heart punctures. Compared to $WT_{no\ dive}$, sodium (KW: $p = 0.007$; *post-hoc* $p = 0.019$ $p = 0.01$), potassium (KW: $p = 0.022$; *post-hoc* $p = 0.006$ $p = 0.004$), globulin (KW: $p = 0.01$; *post-hoc* $p = 0.008$ $p = 0.001$), and transaminase (KW: $p = 0.001$; *post-hoc* $p = 0.002$ $p < 0.0001$) were found at increased levels in mice subjected to the hyperbaric protocol, regardless of the clinical state (Grip+ or Grip−) (**Table 3**). Grip− mice had higher levels of creatinine kinase (KW $p = 0.062$; *post-hoc* $p = 0.019$). The BUN level was lower in the Grip+ groupthan in the $WT_{no\text{-}dive}$ group (KW $p = 0.041$; *post-hoc* $p = 0.016$). The albumin level was lower in the Grip+ and the Grip− groups than in the $WT_{no\text{-}dive}$ group (KW: $p < 0.001$; *post-hoc* $p = 0.002$ $p < 0.0001$). Triglyceride levels were higher in Grip− than in Grip+ mice (KW $p = 0.005$; *post-hoc* $p = 0.01$). Overall, the dive induced a hemoconcentration regarding sodium potassium and AST levels. This could be due to a capillary leak consider low albumin levels (in contrast to high globulin levels). Cell destructions and/or liver shouting could also be engaged, especially when taking into account high triglycerides levels then recorded in Grip−. Increase in creatinine kinase also suggested muscle or heart straining when DCS was stated.

Blood sample analyses from two mice, punctured just before they died (Lethal DCS) showed (i) higher levels of sodium (KW $p = 0.007$; *post-hoc* $p = 0.001$), potassium (KW $p = 0.022$; *post-hoc* $p = 0.028$) or creatinine kinase (KW $p = 0.062$; *post-hoc* $p =$

TABLE 3 | Blood biochemistry analysis according to clinical status after the decompression protocol.

Effect of clinical status on:	KW	*Post-hoc* test	
Total bilirubin	0.004	Lethal DCS < $WT_{no\ dive}$	$p = 0.002$
		Lethal DCS < Grip+	$p < 0.0001$
		Lethal DCS < Grip−	$p = 0.002$
Na+	0.007	$WT_{no\ dive}$ < Lethal DCS	$p = 0.001$
		$WT_{no\ dive}$ < Grip+	$p = 0.019$
		$WT_{no\ dive}$ < Grip−	$p = 0.01$
		Grip+ < Lethal DCS	$p = 0.031$
		Grip− < Lethal DCS	$p = 0.006$
K+	0.022	$WT_{no\ dive}$ < Grip+	$p = 0.0006$
		$WT_{no\ dive}$ < Grip−	$p = 0.004$
		$WT_{no\ dive}$ < Lethal DCS	$p = 0.028$
BUN/Urea	0.041	$WT_{no\ dive}$ > Grip+	$p = 0.016$
AST/transaminase	0.001	$WT_{no\ dive}$ < Grip+	$p = 0.002$
		$WT_{no\ dive}$ < Grip−	$p < 0.0001$
Globulin	0.010	$WT_{no\ dive}$ < no DCS	$p = 0.008$
		$WT_{no\ dive}$ < DCS	$p = 0.001$
Lactate	0.016	Grip+ < Lethal DCS	$p = 0.010$
Creatinine kinase	0.062	$WT_{no\ dive}$ < Grip+	$p = 0.019$
Triglycerides	0.005	Lethal DCS > Grip+	$p = 0.005$
		Grip+ > Grip−	$p = 0.010$
Albumin	0.000	$WT_{no\ dive}$ > Grip+	$p = 0.002$
		$WT_{no\ dive}$ > Grip−	$p < 0.0001$

TABLE 4 | Blood biochemistry analysis depending on treatment after the decompression protocol.

Treatment effects on:	KW	*Post-hoc* test	
Albumin	0.001	$WT_{no\ dive}$ > $KO\text{-}like_{flux}$	$p = 0.001$
		$WT_{no\ dive}$ > WT_{flux2}	$p < 0.0001$
Na+	0.027	$WT_{no\ dive}$ < KO-like	$p = 0.0004$
K+	0.000	$WT_{no\ dive}$ < $KO\text{-}like_{flux}$	$p < 0.0001$
		$WT_{no\ dive}$ < WT_{flux2}	$p = 0.002$
Aspartate T/transaminase	0.000	$WT_{no\ dive}$ < $KO\text{-}like_{flux}$	$p < 0.0001$
		$WT_{no\ dive}$ < WT_{flux2}	$p < 0.0001$
Total bilirubin	0.000	KO-like < $KO\text{-}like_{flux}$	$p < 0.0001$
		KO-like < WT_{flux2}	$p < 0.0001$
		KO-like < $WT_{no\ dive}$	$p = 0.002$
Globulin	0.001	$WT_{no\ dive}$ < $KO\text{-}like_{flux}$	$p = 0.001$
		$WT_{no\ dive}$ < WT_{flux2}	$p = 0.001$
Lactate	0.014	KO-like > WT_{flux2}	$p = 0.003$
Triglycerides	0.029	KO-like > $KO\text{-}like_{flux}$	$p = 0.004$
		KO-like > WT_{flux2}	$p = 0.001$

0.064) in comparison with $WT_{no\ dive}$ mice, (ii) a higher sodium level in comparison with both the Grip− and Grip+ groups (KW $p = 0.007$; *post-hoc* $p = 0.006$ and $p = 0.031$ respectively), (iii) a higher lactate level (KW $p = 0.016$; *post-hoc* $p = 0.010$) and triglyceride concentration (KW $p = 0.005$; *post-hoc* $p = 0.005$) when compared to the Grip+ group, (iv) higher bilirubin levels than those of $WT_{no\ dive}$, Grip+ and Grip− mice (KW $p = 0.004$; *post-hoc* $p = 0.002$ $p < 0.001$ $p = 0.002$, respectively), (v) unchanged glycemia, calcium, cholesterol, creatinine, and total protein levels vs. the other groups.

When looking at the effect of the treatments *per se* on blood biochemistry after the dive (**Table 4**), we pointed out that mice treated with fluoxetine, such as $KO\text{-}like_{flux}$ and WT_{flux2} and corresponding to the best survival rates, had higher levels of potassium (hemoconcentration, cell destruction), AST (aspartate aminotransferase, liver function) and globulin (hemoconcentration), and lower levels of albumin (an indicator of capillary leak) and lactate (high levels indicate anaerobic) than those of the $WT_{no\text{-}dive}$ group.

KO-like mice, receiving spadin for 5 days, displayed the worst survival rate. In comparison with the $WT_{no\text{-}dive}$ group, they expressed very low levels of bilirubin, a toxic and hydrophobic breakdown product of red blood cells that is bound to and carried by albumin. They also had very high levels of lactate (anaerobic metabolism and possible mitochondria dysfunction), sodium and triglycerides; the origin of these high triacylglycerol levels in their blood could be due to adipocyte release, pancreatitis, autoimmune disease or nephritic syndrome.

DISCUSSION

In this study, fluoxetine should be regarded as an anti-inflammatory drug, considering that we opted for an acute, high dose of 50 mg/kg; the antidepressant effect of fluoxetine requires long-term treatment (28 days at 20 mg/kg) to induce synaptogenesis, and should not be considered in this study. In contrast, 5 days of spadin treatment was sufficient to internalize TREK-1 channels and consequently to exert antidepressant activity (Mazella et al., 2010; Moha Ou Maati et al., 2012).

Prevention of Decompression Sickness

The decompression protocol used in this study is comparable with that used in previous studies on mice of a similar weight (Berghage et al., 1979; Blatteau et al., 2012; Vallee et al., 2012). Mice in the spad-pool were heavier, which may have increased their susceptibility to DCS. Nonetheless, the protocols used in this study induced neurological DCS with motor and locomotor impairments and convulsions, suggesting damage to the spinal cord or brain.

The increase in AST (aspartate aminotransferase) may be due to fluoxetine hepatotoxicity, as fluoxetine is extensively metabolized in the liver to norfluoxetine and this is a well-known side effect (Inkielewicz-Stepniak et al., 2014). Fluoxetine may

also induce moderate lymphocyte infiltration within the portal tracts and ballooning degeneration of hepatocytes (Kwak et al., 2000). The low mortality associated with fluoxetine treatment led us to conclude that increased AST levels may have a minor effect on DCS outcomes. Nonetheless and except for Lethal DCS mice, we also observed increased concentrations of sodium and potassium ions and globulins, after the dive. These variations may be explained at least in part by hemoconcentration (increased hematocrit in the spad-pool) or by hepatocyte damage due to the presence of bubbles in the liver, as previously observed in rats (L'Abbate et al., 2010). Arguing in favor of liver dysfunction, the albumin and BUN (both synthetized by the liver) concentrations were low, but these lower concentrations could also been explained by damage to the glomerulus, as occurs in nephritic syndrome (Blann and Ahmed, 2014), or by capillary leak that may lead to edema (Clarkson et al., 1960). This albumin loss demonstrated that fluoxetine did not prevent capillary leak *per se*, a symptom of severe DCS. Finally, the blood biochemistry results indicate that damage induced by bubbles may have induced capillary leak, cell destructions and liver dysfunction. However, other blood components were not affected by the dive. Consequently, additional data will be necessary to validate or invalidate the liver dysfunction hypothesis. Dramatically, multivisceral dysfunction could be supported by changes in analyte concentrations in Lethal DCS mice, such as high levels of creatinine kinase or lactate.

This protocol also decreased erythrocyte, leukocyte and platelet counts, suggesting diapedesis, inflammation and clotting activity, as well as ischemia, the usual symptoms described for DCS. Platelet dysfunction has been described for fluoxetine (Lesch et al., 1993; Brenner et al., 2007), but this effect did not influence platelet recruitment or DCS outcomes in our study. On the other hand, TREK-1 channels are not known to affect clotting function directly, although they are activated by platelet activating factor (Maingret et al., 1999). Under these conditions, TREK-1 channels likely played a minor role in DCS outcomes.

The main result from our work is that mice with impaired TREK-1 channel function and treated with fluoxetine are more resistant to the consequences of decompression than WT mice treated with fluoxetine, and far more resistant than untreated KO or KO-like mice. Our data suggest that the presence of the TREK-1 channel may mitigate the global benefit of fluoxetine in DCS-related ischemia and inflammation. The second important result from our work is that 5 days of spadin antidepressant treatment, thereby blocking TREK-1 channel activity specifically, increased DCS susceptibility. However, when the same 5 days of spadin treatment was administered to mice treated with fluoxetine, the protective effect of fluoxetine was increased. These data indicate that the main protective effect of fluoxetine is mediated by a cellular pathway independent of TREK-1 channel activity.

Loss of Protective Activity of TREK-1

The high mortality rate of KO-like mice confirmed that the neuroprotection induced by the TREK-1 channel in WT was prevented by spadin (5 days of treatment). The importance of the TREK-1 channel in neuroprotection is well-documented for different physio-pathological processes, including hypoxia (Moha Ou Maati et al., 2011), glutamatergic excitotoxicity and neuronal death (Heurteaux et al., 2004). According to our previous and present studies (Vallee et al., 2012), mice that do not express the TREK-1 channel (KO-like or KO) are more likely to develop neurological symptoms after DCS damage to the central nervous system. This could be attributed to the stimulation of NMDA receptor activity, which exacerbated glutamate excitotoxicity, making the brain blood barrier (BBB) more permeable to leukocytes (Bittner et al., 2014). These KO mice are known to display an inflammatory phenotype and accelerated leukocyte trafficking across the BBB (Bittner et al., 2014).

This study focused on fluoxetine, which inhibited TREK-1 channel activity (Kennard et al., 2005; Sandoz et al., 2011) and thus reduced its neuroprotective effects. However, in the present work and in previous experiments on fluoxetine and DCS (Blatteau et al., 2012), we found that WT mice treated with fluoxetine were more resistant to DCS than untreated mice. These observations suggest that the positive anti-inflammatory effects of fluoxetine outweigh fluoxetine-induced TREK-1-inhibition.

Enhanced Protective Activity of Fluoxetine on TREK-1$^{-/-(like)}$ Mice

KO and KO-like mice treated with fluoxetine appeared to be the most resistant to decompression. It was recently shown that fluoxetine selectively inhibits glutamate-N2B NMDA receptors and then induces neuroprotection (Vizi et al., 2013). This property of fluoxetine could partly substitute for the loss of TREK-1-mediated neuroprotection. Another hypothesis can also be drawn. In the absence of TREK-1 channels at the cell membrane, more fluoxetine may have been available for binding to other fluoxetine targets, thereby increasing its protective effects. This hypothesis is suggested by the dose dependence of DCS in KO_{flux} HET_{flux} and WT_{flux} mice treated with fluoxetine. We previously attributed the main protective effect of fluoxetine in DCS to its anti-inflammatory properties from the observed decrease in IL-6 (Blatteau et al., 2012). Decreased IL-6 secretion was also described in TREK-1-deficient cells (Schwingshackl et al., 2012) and this could superimpose on the effect of fluoxetine to further reduce inflammation in TREK-1 deficient mice. It could constitute an efficient response to TREK-1$^{-/-}$-induced BBB damage (Bittner et al., 2013, 2014) or more hypothetically, an opportunity to cross the BBB more readily and more efficiently (**Figure 2**). Finally, fluoxetine is also known to prevent BBB disruption (Lee et al., 2014) thanks to its anti-inflammatory activity coupled with its ability to block NMDA receptors and attenuate glutamatergic excitotoxicity. Further studies will be required to confirm this hypothesis.

Should SSRI Treatment be a Contraindication for Diving?

Spadin was described as a new concept of antidepressant and it was shown that 4 days of treatment with spadin corresponds to 21–28 days of treatment with classical SSRIs (Mazella et al., 2010; Moha Ou Maati et al., 2012; Borsotto et al., 2015; Devader et al., 2015; Veyssiere et al., 2015). Spadin treatment induces TREK-1 internalization, resulting in the disappearance of the channel

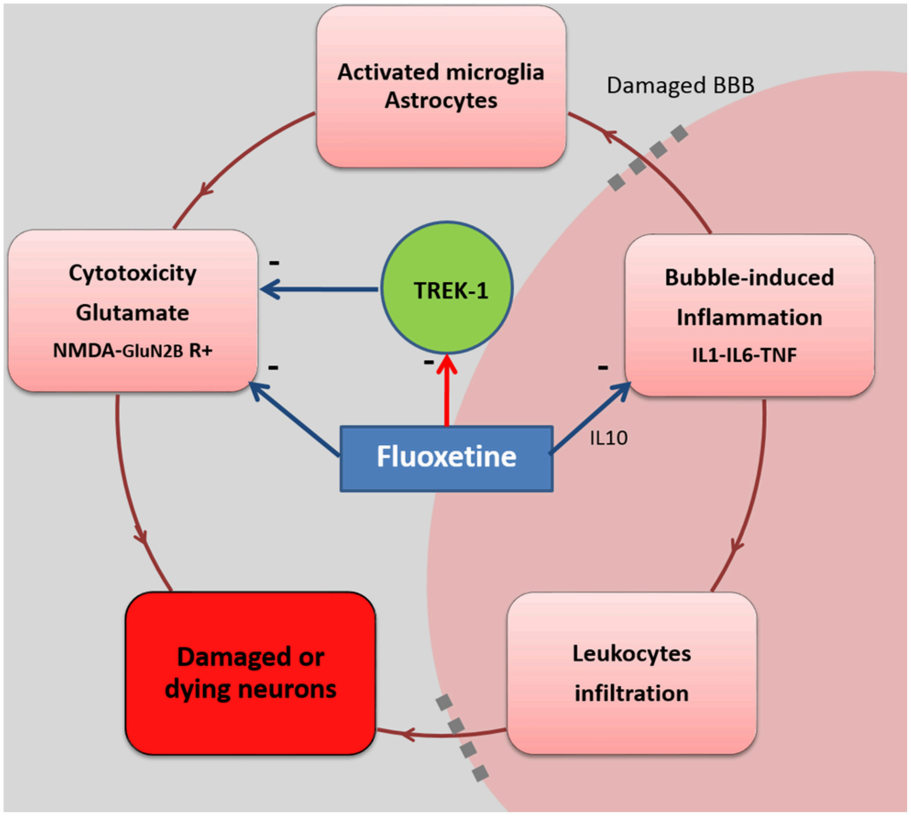

FIGURE 2 | Fluoxetine and possible interactions in a CNS-ischemia model. The circle summarizes the deleterious cascade encountered after a provocative dive, resulting from vascular bubble formation. Fluoxetine stimulates IL-10 secretion which attenuates the inflammatory response mediated by IL-1, IL-6, and TNF. This reduces leukocyte infiltration across the BBB. Fluoxetine is also known to selectively block glutamate N2B-containing NMDA receptors (non-synaptic → neurodegenerative), reducing the negative effects of excitotoxicity on neurons. However, blockade of the TREK-1 channel by an SSRI such as fluoxetine may contribute to the limitation of the protection afforded by these channels, but it may also strengthen the fluoxetine action at other sites in a dose-dependant manner.

from the plasma membrane (Mazella et al., 2010). KO mice are known for developing a depression-resistant phenotype and also for being more sensitive to ischemia (Heurteaux et al., 2006). Both KO and KO-like TREK-1 mice were more likely to succumb to DCS after dive. Therefore, we legitimately wonder whether SSRIs, in their usual indication against depression in humans, could represent a risk factor in diving, or more generally in risky sports that may induce ischemia and inflammation.

Fluoxetine, TREK-1 and Clinical Status: Weight

TREK-1 is widely expressed in central and peripheral tissues. It is highly expressed in the nervous system, digestive system, endocrine system and reproductive system, as well as in the muscular system. In the CNS, TREK-1 is expressed in both astrocytes and neurons. It should be kept in mind that fluoxetine, like spadin, could spread throughout whole body and thus could induce many interactions not anticipated in this study, even if the symptoms are mainly nervous. Moreover, it could be useful to include in further studies immuno-histological technics to confirm the infiltrating leukocyte population in the brain injury. The signaling pathways should also be of interest to assess cell viability.

CONCLUSION

We previously found that acute fluoxetine treatment affords the best protection against DCS when the TREK-1 potassium channel is impaired. We suggest that this drop in mortality may be due to decreased ischemia-induced glutamatergic toxicity, which could be due to the blockage of NMDA receptors by fluoxetine, and/or to an enhancement of the anti-inflammatory effect of fluoxetine. Following this study, exact mechanism remains to be elucidated. We also found that antidepressed mice, i.e., KO or spadin treated, showed increased susceptibility to DCS compared to WT mice. It remains to be determined whether antidepressants could be contraindicated in humans participating in risky activities such as diving that may induce ischemia, even though we found an efficient but paradoxical solution to DCS by delivering fluoxetine.

AUTHOR CONTRIBUTIONS

JB and NV: conception and design of research; JB, SM, KL, PR and NV: performed experiments; JB, KL, and NV: analyzed data; JB, KL, SM, JM, MB, CH, JA, JR, and NV: interpreted results of experiments; NV: prepared figures; JB: drafted manuscript; NV:

edited and revised manuscript; JB, KL, SM, JM, MB, CH, JA, JR, and NV: approved final version of manuscript.

FUNDING

The work should be attributed to the "Institut de Recherches Biomédicales des Armées" laboratories. It is supported by Grant No. PDH-1-SMO-2-722 from the Délégation Générale pour l'Armement of the French Army, Paris, France, and by a special Grant from "La fondation des gueules Cassées," Paris, France.

SUPPLEMENTARY MATERIAL

The Supplementary Material for this article can be found online at: http://journal.frontiersin.org/article/10.3389/fphys.2016.00042

REFERENCES

Berghage, T. E., David, T. D., and Dyson, C. V. (1979). Species differences in decompression. *Undersea Biomed. Res.* 6, 1–13.

Bittner, S., Ruck, T., Fernandez-Orth, J., and Meuth, S. G. (2014). TREK-king the blood-brain-barrier. *J. Neuroimmune Pharmacol.* 9, 293–301. doi: 10.1007/s11481-014-9530-8

Bittner, S., Ruck, T., Schuhmann, M. K., Herrmann, A. M., Moha Ou Maati, H., Bobak, N., et al. (2013). Endothelial TWIK-related potassium channel-1 (TREK1) regulates immune-cell trafficking into the CNS. *Nat. Med.* 19, 1161–1165. doi: 10.1038/nm.3303

Blann, A., and Ahmed, N. (2014). *Blood Science*: *Principles and Pathology*. Oxford, UK: John Wiley & Sons.

Blatteau, J. E., Barre, S., Pascual, A., Castagna, O., Abraini, J. H., Risso, J. J., et al. (2012). Protective effects of fluoxetine on decompression sickness in mice. *PLoS ONE* 7:e49069. doi: 10.1371/journal.pone.0049069

Blatteau, J. E., Gempp, E., Simon, O., Coulange, M., Delafosse, B., Souday, V., et al. (2011). Prognostic factors of spinal cord decompression sickness in recreational diving: retrospective and multicentric analysis of 279 cases. *Neurocrit. Care* 15, 120–127. doi: 10.1007/s12028-010-9370-1

Bogdan, R., Fitzgibbon, H., Woolverton, W. L., Bethea, C. L., Iyo, A. H., Stockmeier, C. A., et al. (2011). 5-HTTLPR genotype and gender, but not chronic fluoxetine administration, are associated with cortical TREK1 protein expression in rhesus macaques. *Neurosci. Lett.* 503, 83–86. doi: 10.1016/j.neulet.2011.08.005

Borsotto, M., Veyssiere, J., Moha Ou Maati, H., Devader, C., Mazella, J., and Heurteaux, C. (2015). Targeting two-pore domain K(+) channels TREK-1 and TASK-3 for the treatment of depression: a new therapeutic concept. *Br. J. Pharmacol.* 172, 771–784. doi: 10.1111/bph.12953

Brenner, B., Harney, J. T., Ahmed, B. A., Jeffus, B. C., Unal, R., Mehta, J. L., et al. (2007). Plasma serotonin levels and the platelet serotonin transporter. *J. Neurochem.* 102, 206–215. doi: 10.1111/j.1471-4159.2007.04542.x

Buckler, K. J., and Honore, E. (2005). The lipid-activated two-pore domain K+ channel TREK-1 is resistant to hypoxia: implication for ischaemic neuroprotection. *J. Physiol.* 562, 213–222. doi: 10.1113/jphysiol.2004.077503

Chollet, F., Tardy, J., Albucher, J. F., Thalamas, C., Berard, E., Lamy, C., et al. (2011). Fluoxetine for motor recovery after acute ischaemic stroke (FLAME): a randomised placebo-controlled trial. *Lancet Neurol.* 10, 123–130. doi: 10.1016/S1474-4422(10)70314-8

Clarkson, B., Thompson, D., Horwith, M., and Luckey, E. H. (1960). Cyclical edema and shock due to increased capillary permeability. *Trans. Assoc. Am. Physicians* 73, 272–282. doi: 10.1016/0002-9343(60)90018-8

Dal Palu, C., and Zamboni, S. (1990). [Clinical trials for primary prevention of ischemic cardiopathy. Light and darkness]. *G. Ital. Cardiol.* 20, 1044–1053.

Dedman, A., Sharif-Naeini, R., Folgering, J. H., Duprat, F., Patel, A., and Honore, E. (2009). The mechano-gated K(2P) channel TREK-1. *Eur. Biophys. J.* 38, 293–303. doi: 10.1007/s00249-008-0318-8

DeGirolami, U., and Zivin, J. A. (1982). Neuropathology of experimental spinal cord ischemia in the rabbit. *J. Neuropathol. Exp. Neurol.* 41, 129–149. doi: 10.1097/00005072-198203000-00004

Devader, C., Khayachi, A., Veyssiere, J., Moha Ou Maati, H., Roulot, M., Moreno, S., et al. (2015). *In vitro* and *in vivo* regulation of synaptogenesis by the novel antidepressant spadin. *Br. J. Pharmacol.* 172, 2604–2617. doi: 10.1111/bph.13083

Dutka, A. J., Kochanek, P. M., and Hallenbeck, J. M. (1989). Influence of granulocytopenia on canine cerebral ischemia induced by air embolism. *Stroke* 20, 390–395. doi: 10.1161/01.STR.20.3.390

Ersson, A., Linder, C., Ohlsson, K., and Ekholm, A. (1998). Cytokine response after acute hyperbaric exposure in the rat. *Undersea Hyperb. Med.* 25, 217–221.

Faraj, B. A., Olkowski, Z. L., and Jackson, R. T. (1994). Expression of a high-affinity serotonin transporter in human lymphocytes. *Int. J. Immunopharmacol.* 16, 561–567. doi: 10.1016/0192-0561(94)90107-4

Franks, N. P., and Honore, E. (2004). The TREK K2P channels and their role in general anaesthesia and neuroprotection. *Trends Pharmacol. Sci.* 25, 601–608. doi: 10.1016/j.tips.2004.09.003

Gempp, E., Blatteau, J. E., Stephant, E., Pontier, J. M., Constantin, P., and Peny, C. (2008). MRI findings and clinical outcome in 45 divers with spinal cord decompression sickness. *Aviat. Space Environ. Med.* 79, 1112–1116. doi: 10.3357/ASEM.2376.2008

Giry, P. B., Porlier, G., Eastman, D., and Radomski, M. W. (1977). Dive-induced modifications in platelet kinetics in rats. *Undersea Biomed. Res.* 4, 147–157.

Hall, E. D. (1985). High-dose glucocorticoid treatment improves neurological recovery in head-injured mice. *J. Neurosurg.* 62, 882–887. doi: 10.3171/jns.1985.62.6.0882

Hallenbeck, J. M., Bove, A. A., Moquin, R. B., and Elliott, D. H. (1973). Accerlerated coagulation of whole blood and cell-free plasma by bubbling *in vitro*. *Aerosp. Med.* 44, 712–714.

Haller, C., Sercombe, R., Verrecchia, C., Fritsch, H., Seylaz, J., and Kuschinsky, W. (1987). Effect of the muscarinic agonist carbachol on pial arteries *in vivo* after endothelial damage by air embolism. *J. Cereb. Blood Flow Metab.* 7, 605–611. doi: 10.1038/jcbfm.1987.112

Helps, S. C., and Gorman, D. F. (1991). Air embolism of the brain in rabbits pretreated with mechlorethamine. *Stroke* 22, 351–354. doi: 10.1161/01.STR.22.3.351

Herr, N., Mauler, M., Witsch, T., Stallmann, D., Schmitt, S., Mezger, J., et al. (2014). Acute fluoxetine treatment induces slow rolling of leukocytes on endothelium in mice. *PLoS ONE* 9:e88316. doi: 10.1371/journal.pone.0088316

Heurteaux, C., Guy, N., Laigle, C., Blondeau, N., Duprat, F., Mazzuca, M., et al. (2004). TREK-1, a K+ channel involved in neuroprotection and general anesthesia. *EMBO J.* 23, 2684–2695. doi: 10.1038/sj.emboj.7600234

Heurteaux, C., Lucas, G., Guy, N., El Yacoubi, M., Thummler, S., Peng, X. D., et al. (2006). Deletion of the background potassium channel TREK-1 results in a depression-resistant phenotype. *Nat. Neurosci.* 9, 1134–1141. doi: 10.1038/nn1749

Honore, E. (2007). The neuronal background K2P channels: focus on TREK1. *Nat. Rev. Neurosci.* 8, 251–261. doi: 10.1038/nrn2117

Inkielewicz-Stepniak, I., Santos-Martinez, M. J., Medina, C., and Radomski, M. W. (2014). Pharmacological and toxicological effects of co-exposure of human gingival fibroblasts to silver nanoparticles and sodium fluoride. *Int. J. Nanomedicine* 9, 1677–1687. doi: 10.2147/IJN.S59172

Jacey, M. J., Heyder, E., Williamson, R. A., and Tappan, D. V. (1976). Biochemistry and hematology at decompression sickness: a case report. *Aviat. Space Environ. Med.* 47, 657–661.

Jin, Y., Lim, C. M., Kim, S. W., Park, J. Y., Seo, J. S., Han, P. L., et al. (2009). Fluoxetine attenuates kainic acid-induced neuronal cell death in the mouse hippocampus. *Brain Res.* 1281, 108–116. doi: 10.1016/j.brainres.2009.04.053

Kennard, L. E., Chumbley, J. R., Ranatunga, K. M., Armstrong, S. J., Veale, E. L., and Mathie, A. (2005). Inhibition of the human two-pore domain

potassium channel, TREK-1, by fluoxetine and its metabolite norfluoxetine. *Br. J. Pharmacol.* 144, 821–829. doi: 10.1038/sj.bjp.0706068

Kostadinov, I. D., Delev, D. P., Murdjeva, M. A., and Kostadinova, II. (2014). Experimental study on the role of 5-HT2 serotonin receptors in the mechanism of anti-inflammatory and antihyperalgesic action of antidepressant fluoxetine. *Folia Med. (Plovdiv).* 56, 43–49. doi: 10.2478/folmed-2014-0007

Kubera, M., Lin, A. H., Kenis, G., Bosmans, E., Van Bockstaele, D., and Maes, M. (2001). Anti-Inflammatory effects of antidepressants through suppression of the interferon-gamma/interleukin-10 production ratio. *J. Clin. Psychopharmacol.* 21, 199–206. doi: 10.1097/00004714-200104000-00012

Kwak, S. D. M. Oh, H. D. M., Yeo, M., Park, M. D. S. D. M. Kim, J. D. M., Lee, J., et al. (2000). Fluoxetine-induced Acute Toxic Hepatitis. *Clin. Mol. Hepatol.* 6, 236–240. doi: 10.3350/kjhep.2000.6.2.236

L'Abbate, A., Kusmic, C., Matteucci, M., Pelosi, G., Navari, A., Pagliazzo, A., et al. (2010). Gas embolization of the liver in a rat model of rapid decompression. *Am. J. Physiol. Regul. Integr. Comp. Physiol.* 299, R673–R682. doi: 10.1152/ajpregu.00699.2009

Lee, J. Y., Lee, H. E., Kang, S. R., Choi, H. Y., Ryu, J. H., and Yune, T. Y. (2014). Fluoxetine inhibits transient global ischemia-induced hippocampal neuronal death and memory impairment by preventing blood-brain barrier disruption. *Neuropharmacology* 79, 161–171. doi: 10.1016/j.neuropharm.2013.11.011

Lesch, K. P., Wolozin, B. L., Murphy, D. L., and Reiderer, P. (1993). Primary structure of the human platelet serotonin uptake site: identity with the brain serotonin transporter. *J. Neurochem.* 60, 2319–2322. doi: 10.1111/j.1471-4159.1993.tb03522.x

Lim, C. M., Kim, S. W., Park, J. Y., Kim, C., Yoon, S. H., and Lee, J. K. (2009). Fluoxetine affords robust neuroprotection in the postischemic brain via its anti-inflammatory effect. *J. Neurosci. Res.* 87, 1037–1045. doi: 10.1002/jnr.21899

Lima, L., and Urbina, M. (2002). Serotonin transporter modulation in blood lymphocytes from patients with major depression. *Cell. Mol. Neurobiol.* 22, 797–804. doi: 10.1023/A:1021869310702

Maingret, F., Patel, A. J., Lesage, F., Lazdunski, M., and Honore, E. (1999). Mechano- or acid stimulation, two interactive modes of activation of the TREK-1 potassium channel. *J. Biol. Chem.* 274, 26691–26696. doi: 10.1074/jbc.274.38.26691

Mazella, J., Petrault, O., Lucas, G., Deval, E., Beraud-Dufour, S., Gandin, C., et al. (2010). Spadin, a sortilin-derived peptide, targeting rodent TREK-1 channels: a new concept in the antidepressant drug design. *PLoS Biol.* 8:e1000355. doi: 10.1371/journal.pbio.1000355

Moha Ou Maati, H., Peyronnet, R., Devader, C., Veyssiere, J., Labbal, F., Gandin, C., et al. (2011). A human TREK-1/HEK cell line: a highly efficient screening tool for drug development in neurological diseases. *PLoS ONE* 6:e25602. doi: 10.1371/journal.pone.0025602

Moha Ou Maati, H., Veyssiere, J., Labbal, F., Coppola, T., Gandin, C., Widmann, C., et al. (2012). Spadin as a new antidepressant: absence of TREK-1-related side effects. *Neuropharmacology* 62, 278–288. doi: 10.1016/j.neuropharm.2011.07.019

Noel, J., Sandoz, G., and Lesage, F. (2011). Molecular regulations governing TREK and TRAAK channel functions. *Channels (Austin).* 5, 402–409. doi: 10.4161/chan.5.5.16469

Nossum, V., Koteng, S., and Brubakk, A. O. (1999). Endothelial damage by bubbles in the pulmonary artery of the pig. *Undersea Hyperb. Med.* 26, 1–8.

Pariente, J., Loubinoux, I., Carel, C., Albucher, J. F., Leger, A., Manelfe, C., et al. (2001). Fluoxetine modulates motor performance and cerebral activation of patients recovering from stroke. *Ann. Neurol.* 50, 718–729. doi: 10.1002/ana.1257

Persson, L. I., Johansson, B. B., and Hansson, H. A. (1978). Ultrastructural studies on blood-brain barrier dysfunction after cerebral air embolism in the rat. *Acta Neuropathol.* 44, 53–56. doi: 10.1007/BF00691639

Pontier, J. M., Blatteau, J. E., and Vallee, N. (2008). Blood platelet count and severity of decompression sickness in rats after a provocative dive. *Aviat. Space Environ. Med.* 79, 761–764. doi: 10.3357/ASEM.2299.2008

Sandoz, G., Bell, S. C., and Isacoff, E. Y. (2011). Optical probing of a dynamic membrane interaction that regulates the TREK1 channel. *Proc. Natl. Acad. Sci. U.S.A.* 108, 2605–2610. doi: 10.1073/pnas.1015788108

Sato, Y., Seo, N., and Kobayashi, E. (2006). Genetic background differences between FVB and C57BL/6 mice affect hypnotic susceptibility to pentobarbital, ketamine and nitrous oxide, but not isoflurane. *Acta Anaesthesiol. Scand.* 50, 553–556. doi: 10.1111/j.1399-6576.2006.001002.x

Schwingshackl, A., Teng, B., Ghosh, M., West, A. N., Makena, P., Gorantla, V., et al. (2012). Regulation and function of the two-pore-domain (K2P) potassium channel Trek-1 in alveolar epithelial cells. *Am. J. Physiol. Lung Cell. Mol. Physiol.* 302, L93–L102. doi: 10.1152/ajplung.00078.2011

Taguchi, N., Nakayama, S., and Tanaka, M. (2012). Fluoxetine has neuroprotective effects after cardiac arrest and cardiopulmonary resuscitation in mouse. *Resuscitation* 83, 652–656. doi: 10.1016/j.resuscitation.2011.11.004

Thorsen, T., Dalen, H., Bjerkvig, R., and Holmsen, H. (1987). Transmission and scanning electron microscopy of N2 microbubble-activated human platelets *in vitro*. *Undersea Biomed. Res.* 14, 45–58.

Vallee, N., Gaillard, S., Peinnequin, A., Risso, J. J., and Blatteau, J. E. (2013). Evidence of cell damages caused by circulating bubbles: high level of free mitochondrial DNA in plasma of rats. *J. Appl. Physiol. (1985)* 115, 1526–1532. doi: 10.1152/japplphysiol.00025.2013

Vallee, N., Meckler, C., Risso, J. J., and Blatteau, J. E. (2012). Neuroprotective role of the TREK-1 channel in decompression sickness. *J. Appl. Physiol. (1985)* 112, 1191–1196. doi: 10.1152/japplphysiol.01100.2011

Veyssiere, J., Moha Ou Maati, H., Mazella, J., Gaudriault, G., Moreno, S., Heurteaux, C., et al. (2015). Retroinverso analogs of spadin display increased antidepressant effects. *Psychopharmacology (Berl)* 232, 561–574. doi: 10.1007/s00213-014-3683-2

Vizi, E. S., Kisfali, M., and Lorincz, T. (2013). Role of nonsynaptic GluN2B-containing NMDA receptors in excitotoxicity: evidence that fluoxetine selectively inhibits these receptors and may have neuroprotective effects. *Brain Res. Bull.* 93, 32–38. doi: 10.1016/j.brainresbull.2012.10.005

Warren, B. A., Philp, R. B., and Inwood, M. J. (1973). The ultrastructural morphology of air embolism: platelet adhesion to the interface and endothelial damage. *Br. J. Exp. Pathol.* 54, 163–172.

Yang, G. B., Qiu, C. L., Aye, P., Shao, Y., and Lackner, A. A. (2007). Expression of serotonin transporters by peripheral blood mononuclear cells of rhesus monkeys (*Macaca mulatta*). *Cell. Immunol.* 248, 69–76. doi: 10.1016/j.cellimm.2007.09.001

Zamboni, W. A., Roth, A. C., Russell, R. C., Graham, B., Suchy, H., and Kucan, J. O. (1993). Morphologic analysis of the microcirculation during reperfusion of ischemic skeletal muscle and the effect of hyperbaric oxygen. *Plast. Reconstr. Surg.* 91, 1110–1123. doi: 10.1097/00006534-199305000-00022

Zamboni, W. A., Roth, A. C., Russell, R. C., Nemiroff, P. M., Casas, L., and Smoot, E. C. (1989). The effect of acute hyperbaric oxygen therapy on axial pattern skin flap survival when administered during and after total ischemia. *J. Reconstr. Microsurg.* 5, 343–347; discussion 349–350. doi: 10.1055/s-2007-1006884

Zamboni, W. A., Roth, A. C., Russell, R. C., and Smoot, E. C. (1992). The effect of hyperbaric oxygen on reperfusion of ischemic axial skin flaps: a laser Doppler analysis. *Ann. Plast. Surg.* 28, 339–341. doi: 10.1097/00000637-199204000-00008

Conflict of Interest Statement: The authors declare that the research was conducted in the absence of any commercial or financial relationships that could be construed as a potential conflict of interest.

The Reviewer AG declares that, despite sharing a common affiliation with the Guest Associate Editor, the review process was carried out objectively and no conflict of interest exists.

frontiers in Physiology

ORIGINAL RESEARCH
published: 01 February 2016
doi: 10.3389/fphys.2016.00014

Strong Ion Regulatory Abilities Enable the Crab *Xenograpsus testudinatus* to Inhabit Highly Acidified Marine Vent Systems

*Marian Y. Hu[1,2], Ying-Jey Guh[3], Yi-Ta Shao[4], Pou-Long Kuan[5], Guan-Lin Chen[5], Jay-Ron Lee[1], Ming-Shiou Jeng[6] and Yung-Che Tseng[5]**

[1] Institute of Cellular and Organismic Biology, Academia Sinica, Taipei, Taiwan, [2] Institute of Physiology, Christian-Albrechts University Kiel, Kiel, Germany, [3] Institute of Biological Chemistry, Academia Sinica, Taipei, Taiwan, [4] Institute of Marine Biology, National Taiwan Ocean University, Keelung, Taiwan, [5] Department of Life Science, National Taiwan Normal University, Taipei, Taiwan, [6] Biodiversity Research Center, Academia Sinica, Taipei, Taiwan

Hydrothermal vent organisms have evolved physiological adaptations to cope with extreme abiotic conditions including temperature and pH. To date, acid-base regulatory abilities of vent organisms are poorly investigated, although this physiological feature is essential for survival in low pH environments. We report the acid-base regulatory mechanisms of a hydrothermal vent crab, *Xenograpsus testudinatus,* endemic to highly acidic shallow-water vent habitats with average environment pH-values ranging between 5.4 and 6.6. Within a few hours, *X. testudinatus* restores extracellular pH (pHe) in response to environmental acidification of pH 6.5 (1.78 kPa pCO_2) accompanied by an increase in blood HCO_3^- levels from 8.8 ± 0.3 to 31 ± 6 mM. Branchial Na^+/K^+-ATPase (NKA) and V-type H^+-ATPase (VHA), the major ion pumps involved in branchial acid-base regulation, showed dynamic increases in response to acidified conditions on the mRNA, protein and activity level. Immunohistochemical analyses demonstrate the presence of NKA in basolateral membranes, whereas the VHA is predominantly localized in cytoplasmic vesicles of branchial epithelial- and pillar-cells. *X. testudinatus* is closely related to other strong osmo-regulating brachyurans, which is also reflected in the phylogeny of the NKA. Accordingly, our results suggest that the evolution of strong ion regulatory abilities in brachyuran crabs that allowed the occupation of ecological niches in euryhaline, freshwater, and terrestrial habitats are probably also linked to substantial acid-base regulatory abilities. This physiological trait allowed *X. testudinatus* to successfully inhabit one of the world's most acidic marine environments.

Keywords: hydrothermal vent, V-type H^+-ATPase, Na^+/K^+-ATPase, hypercapnia, invertebrate physiology, gill, crustacean

OPEN ACCESS

Edited by:
Antonio L'Abbate, Scuola Superiore Sant'Anna, Italy

Reviewed by:
Nia M. Whiteley, Bangor University, UK
Michael B. Morris, The University of Sydney, Australia

***Correspondence:**
Yung-Che Tseng
yct@ntnu.edu.tw

Specialty section:
This article was submitted to Integrative Physiology, a section of the journal Frontiers in Physiology

Received: *01 August 2015*
Accepted: *11 January 2016*
Published: *01 February 2016*

Citation:
Hu MY, Guh Y-J, Shao Y-T, Kuan P-L, Chen G-L, Lee J-R, Jeng M-S and Tseng Y-C (2016) Strong Ion Regulatory Abilities Enable the Crab Xenograpsus testudinatus to Inhabit Highly Acidified Marine Vent Systems. Front. Physiol. 7:14. doi: 10.3389/fphys.2016.00014

INTRODUCTION

Deep sea hydrothermal vent systems support ecosystems with an enormous biomass, and reveal a rich biodiversity ranging from microbes to vertebrates (Tunnicliffe, 1992). To survive in these extreme habitats, vent associated organisms show a range of morphological and physiological adaptations to cope with challenging environmental conditions including temperature, metallic

sulfides, anoxia, hypercapnia, and low pH (Goffredi et al., 1997; Ramirez-Llodra et al., 2007). Highly acidified conditions due to the release of HCl and CO_2 are a characteristic of most seafloor vent systems including the shallow-water hydrothermal vent system of Kueishan Island (24°50′N, 121°57′E), off the coast of Taiwan (Han et al., 2014). This shallow water hydrothermal vent system has been described as one of the most acidic vents in the world, discharging water with a high content of elemental sulfur particles, having temperatures ranging between 76 and 116°C and a minimum pH of 1.52 (Chen et al., 2005; **Figure 1A**). The gas composition released by the underwater volcano is mainly CO_2 (<92%; Han et al., 2014). Even in the surrounding areas with depths between 2 and 14 m, the seawater is highly acidic ranging from pH 6.6 to 5.4 (Han et al., 2014). This challenging hydrothermal vent habitat is inhabited by *Xenograpsus testudinatus*, a crab species that is endemic to shallow-water (<200 m) vent systems (Ng et al., 2000). *X. testudinatus* is the only metazoan species found in the direct surroundings of the vents, and individuals congregate in large numbers in vent crevices with an average of 364 individuals per m^2 (**Figure 1B**). These crabs have evolved a unique feeding behavior by feeding on dead zooplankton killed by the toxic vent discharges (Jeng et al., 2004). During slack water conditions, when there are no currents, the crabs swarm out of their crevices (**Figures 1C,D**) to rapidly feed on this "marine snow" of dead zooplankton (Jeng et al., 2004).

Crustaceans are probably one of the most successful invertebrate group that occupy ecological niches in marine systems ranging from polar regions (Frederich et al., 2001) to hydrothermal vents (Joel and Haney, 2005; Dittel et al., 2008) and have radiated from seawater to freshwater and even into terrestrial habitats (Schubart et al., 1997). While those found in stenohaline marine habitats are more likely to be weak osmo-regulators or even osmo-conformers crustaceans from euryhaline or intertidal habitats are moderate to strong osmo-regulators, a physiological feature that is beneficial for adaptation to habitats with fluctuating salinities (Charmantier and Charmantier-Daures, 2001; Henry et al., 2012). The gills are the major organ involved in extracellular ion homeostasis, equipped with an efficient ion regulatory machinery that shows evolutionary conserved features comparable to the ion regulatory epithelia in cephalopods and fish (Henry et al., 2012). Similar to the situation in most vertebrate and invertebrate systems, the ubiquitous Na^+/K^+-ATPase localized in basolateral membranes creates the electro-chemical gradient that is used by secondary active transporters such as apical Na^+/H^+-exchangers or anion exchangers that can mediate ionic and pH homeostasis in crustaceans (Cameron, 1978; Heisler, 1986; Pörtner et al., 1991; Gutowska et al., 2010; Henry et al., 2012). The V-type H^+-ATPase (VHA) has also been described in gill epithelia of crustaceans, demonstrating a cytosolic or apical localization of this enzyme (Weihrauch et al., 2001; Tsai and Lin, 2007). The VHA has been shown to be involved in the acidification of intracellular organelles, and in the secretion of protons across the plasma membrane of specialized cells located in ion-regulatory epithelia (Weihrauch et al., 2002; Tresguerres et al., 2006; Hwang, 2009; Hu et al., 2014). Based on the structure of the VHA with the catalytic (V1 complex) site facing the cytoplasm, the VHA is restricted to transport protons out of the cytoplasm (Beyenbach, 2006).

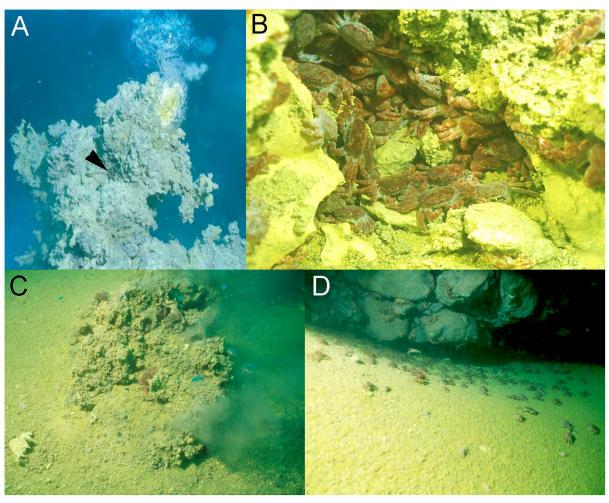

FIGURE 1 | *Xenograpsus testudinats* crabs in the hydrothermal vent habitat at Kueishan island located off Taiwan's east coast. Underwater photographs of the hydrothermal vent system at Kueishan island, showing an active chimney discharging acidic, CO_2 rich water (note the *X. testudinatus* crab in the direct vicinity of the vent opening) **(A)**. High densities of *X. testudinatus* crabs can be found in the direct surrounding of the vents hiding in sulfur-rich crevices **(B)**. Whilst feeding on zooplankton killed by the toxic discharges of the vents crabs swarm out of their shelters, and are directly exposed to highly acidic waters **(C,D)**. All images were obtained and authorized from the co-author Dr. Ming-Shiou Jeng.

In euryhaline crabs changes in environmental salinity were demonstrated to directly affect the extracellular acid-base status of these animals (Truchot, 1981, 1992). The fact that a reduction in environmental salinity induces a metabolic alkalosis while an increase in salinity leads to a metabolic acidosis demonstrated that osmo-regulation and the maintenance of acid-base homeostasis are directly linked (Whiteley et al., 2001). This connection between osmo and acid-base regulation may explain why most osmo-regulating crustaceans are relatively tolerant to environmental acid-base disturbances (Henry and Cameron, 1982; Spicer et al., 2007).

X. testudinatus is a brachyuran crab species that has a phylogenetic position close to other crab species that are characterized as strong osmo-regulators including the euryhaline crab *Eriocheir sinensis* and crabs of the genus *Hemigrapsus* spp. (Hicks, 1973; Bedford and Leader, 1977; Onken and Graszynski, 1989; Ki et al., 2009). The potential link between acid-base and osmo-regulation in many euryhaline decapod crustaceans prompted us to formulate the hypothesis that *X. testudinatus* utilizes conserved ion pumps to regulate extracellular pH. To test this hypothesis we exposed *X. testudinatus* to CO_2-induced seawater acidification (pH 6.5), and monitored changes in extracellular acid-base status as well as expression, protein concentrations and activities of the branchial Na^+/K^+-ATPase and V-type H^+-ATPase over a time course of 48 h. These results will demonstrate that evolution of strong osmo-regulatory

abilities in this phylogenetic group may represent a requisite that is accompanied by substantial acid-base regulatory abilities that allowed *X. testudinatus* to inhabit one of the most acidic marine habitats.

MATERIALS AND METHODS

Acidification Experiments

X. testudinatus with carapace width ranging between 3 to 4 cm were obtained by SCUBA divers from Kueishan Island, Taiwan (ROC) in July 2013. Crabs were collected from depth ranging between 5 and 10 m and held in recirculating natural seawater systems (500 l total volume, nitrification filter, salinity 31–32‰, temperature 28°C, constant 12 h dark:12 h light cycle) at the Institute of Cellular and Organismic Biology, Academia Sinica. Animals were fed *ad libitum* twice per day with tilapia meat. CO_2 perturbation experiments were carried our using a total of 48 animals that were distributed into six 20 l tanks (8 animals per tank). The six tanks, with three replicate tanks for each pH treatment were connected to a flow through system providing filtered (0.2 μm), natural seawater. Water was exchanged at a flow rate of ∼3 l h^{-1} to guarantee high water quality inside the test aquaria. The pH (8.0 and 6.5) in the experimental tanks was continuously adjusted by the addition of the appropriate gas mixtures using a continuous pH-stat system (pH controller, MACRO) that controlled the addition of pure CO_2 into the seawater. The experimental tanks were additionally aerated with air (O_2 saturation > 90%) to assure sufficient seawater pO_2 during the experiment. Specific seawater physicochemical conditions for the different incubations are shown in Table S1. Animals were not fed during the 48 h experimental period in order to minimize physiological artifacts caused by feeding activity. pH_{SW} was measured using a WTW 340i meter equipped with a WTW SenTix 81 electrode that was calibrated daily with Tris and AMP buffers at a salinity of 31 to monitor the experiment. Alkalinity in seawater samples was determined spectrophotometrically according to Sarazin et al. (1999). The carbonate system of seawater was calculated from A_T and pH_{SW} using the software CO2SYS (Lewis and Wallace, 1998), including the dissociation constants of Mehrbach et al. (1973) as refitted by Dickson and Millero (1987). Along the experimental duration of 48 h, extracellular acid-base parameters were measured, and gill tissue samples were collected for gene expression, protein, and enzyme analyses. Tissue and hemolymph sampling was carried out at six time points (0, 1, 4, 12, 24, and 48 h) along the time course of 48 h. At each sampling time point, one to two animals were sampled from the three experimental replicate tanks, leading to a biological replication of $n = 4$. Animals were anesthetized by cooling on ice and were killed by an incision of the frontal region of the carapace. The carapace was removed to access the branchial chamber where the gills are located. *X. testudinatus* has six gill pairs (Figures S2A,B), of which the anterior-most gill 1 (G1), is minute (length 1–2 mm); G6 is the posterior-most gill with a total length of ∼10 mm. G1–G3 are designated as anterior gills, while G4–6 are considered posterior gills. G3–G6 are similar in size while G2 is smaller (∼5 mm long). The gill formula of *X. testudinatus* is: G1,G2 podobranch, G3 and G4 arthrobranchs with a common insertion point, G5 and G6 arthrobranchs with a common insertion point. Gills from the left side were sampled for gene expression studies while those from the right side were sampled for protein and enzyme analyses. Pooled samples of posterior gills (4,5,6) were used for gene expression, activity and protein analyses. The experimental protocols for the present study were approved by the National Taiwan Normal University Institutional Animal Care and Utilization Committee (approval no.: 101005).

Extracellular Acid-Base Status

Hemolymph samples were taken from the coxa using a gas-tight Hamilton syringe. Determination of pH_e in venous hemolymph was performed in 100 μl samples using a microelectrode (WTW Mic-D) and a WTW 340 pH meter (precision ± 0.01 units) that was calibrated with Radiometer precision buffers 7 and 10 (S11M44, S11 M007). Measurements were performed inside a temperature controlled water bath adjusted to 28°C. Due to low hemolymph sample volumes for total dissolved inorganic carbon (C_T) determinations (∼100 μl) samples were diluted 1:1 with de-ionized water prior to measurements. After hemolymph sampling, the dilution and measurement of samples was carried out within less than 30 s to guarantee negligible changes in the carbonate system of hemolymph samples. C_T was determined in duplicates (100 μl each) via a Corning 965 carbon dioxide analyzer (precision ± 0.1 mmol l^{-1}; Olympic Analytical Service, England) that was calibrated using a fresh dilution series of 40, 20, 10, 5, and 2.5 mM bicarbonate in distilled water to generate a sodium bicarbonate standard curve. Carbonate system speciation (i.e., pCO_2, $[HCO_3^-]$) of hemolymph samples of *X. testudinatus* was calculated from extracellular pH (pH_e) and C_T using the Henderson–Hasselbalch equation with dissociation constants and solubility coefficients as previously described for the shore crab *Carcinus maenas* (Truchot, 1976).

Immunohistochemistry and Western Blot Analyses

For immunohistochemistry gill tissues from control animals were fixed and mounted to slides as previously described (Hu et al., 2014). The primary antibodies, a mouse monoclonal antibody α5, raised against the avian α subunit of the Na^+/K^+-ATPase (Hybridoma Bank) and a polyclonal antibody raised against part the subunit A region (SYSKYTRALDEFYDK) of the molluscan V-type-H^+-ATPase (VHA; for more detail see Hu et al., 2013) were diluted in PBS (1:100) and placed in droplets of 200 μl onto the sections, and incubated over night at 4°C inside a wet chamber. Sections were then washed (3 × 5 min) with PBS and incubated for 1 h with the secondary antibody, anti-mouse Alexa Fluor 488, or anti-rabbit Alexa Fluor 568 (Invitrogen) (dilution 1:250). After rinses in PBS (3 × 5 min), sections were examined and photographed using a fluorescence microscope (Zeiss imager A1) equipped with an appropriate filter set. Negative controls were performed several times for every antibody by omitting the primary antibody.

Immunoblotting was essentially performed as previously described (Hu et al., 2014) using 15 μL of gill crude extracts.

Proteins were fractionated by SDS-PAGE on 10% polyacrylamide gels, and transferred to PVDF membranes (Millipore), using a tank blotting system (Bio-Rad). Blots were exposed to the primary antibody (see previous section) diluted 1:250–500 and incubated at 4°C overnight. After washing with PBS-T (phosphate buffered saline containing 0.1% Tween20), blots were incubated for 2 h with horseradish conjugated goat anti-rabbit IgG antibody (diluted 1:1000–2000, at room temperature; Amersham Pharmacia Biotech). Protein signals were visualized using the enhanced chemiluminescence system (ECL, Amersham Pharmacia Biotech) and recorded using Biospectrum 600 imaging system (UVP, Upland, CA, USA). Signal intensities were calculated using the free software "Image J" (e.g., Schneider et al., 2012).

Enzyme Activity

ATPase activity was measured in crude extracts of the three posterior gills (4,5,6). The measurement is based on a coupled enzyme assay containing pyruvate kinase (PK) and lactate dehydrogenase (LDH) as previously described (Hu et al., 2014). Crude extracts were obtained by quickly homogenizing the tissue samples using a pestle followed by complete homogenization in a tissue lyzer (Qiagen) in five volumes of ice-cold imidazole buffer (Hu et al., 2014). After centrifugation for 10 min at 1000 g and 4°C, cell debris was removed and the supernatant was used as a crude extract. The reaction was started by adding 1.5 µl of the sample homogenate to the reaction buffer. The coupled to The hydrolysis of ATP reflected by the oxidation of NADH was measured photometrically at 30°C in a temperature controlled plate reader (Molecular Device, Spectra Max, M5), over a period of 15 min, with the decrease of extinction being measured at $\lambda = 339$ nm. Addition of 2 µl ouabain (5 mM final concentration) or bafilomycin (Bafilomycin A1, Sigma-Aldrich) (1 µM final concentration) to the assay was used to determine the fraction of Na^+/K^+-ATPase or H^+-ATPase activity from the total ATPase (TA) activity. The concentrations of inhibitors used in this enzyme assay are sufficient to fully inhibit the NKA (Morris et al., 1997) and VHA (Dröse and Altendorf, 1997), respectively. Six measurement replicates were performed for each sample (three with inhibitor dissolved in DMSO and three with DMSO). Enzyme activities were calculated by using the extinction coefficient for NADH of $\varepsilon = 6.31\,mM^{-1}{\cdot}cm^{-1}$ and given as micromoles of ATP consumed per gram tissue fresh mass (g_{FM}) per hour.

Preparation of mRNA

Separated gills (1–6) were homogenized in Trizol reagent (Invitrogen, Carlsbad, CA, USA) using a Tissue lyser (Quiagen). Chloroform was added to the Trizol homogenates, and total RNA was extracted from the aqueous phase and purified by addition of isopropanol. Genomic DNA contaminations were removed by DNase I (Promega, Madison, WI, USA) treatment. The mRNA for the RT-PCR was obtained using a QuickPrep Micro mRNA Purification Kit (Amersham Pharmacia, Piscataway, NJ, USA) according to the supplier protocol. Extracted mRNA concentrations were determined by spectrophotometry (ND-2000, NanoDrop Technol, Wilmington, DE), and the integrity of the mRNA was controlled by electrophoresis in RNA gels. All mRNA pellets were stored at −80°C.

Cloning of *xtNKA* Fragment

Fragments of the *X. testudinatus* Na^+/K^+-ATPase (NKA) and V-Type H^+-ATPase (VHA) genes were amplified from gill tissue by means of reverse transcription followed by PCR (RT–PCR) using primers based on highly conserved regions of the NKA and VHA from the green shore crab *C. maenas*. Reverse transcription was performed as previously described (Hu et al., 2013) and the primer pair 5′-CAGTCACTTCATCCACATCA-3′ and 5′-CACATCTCCAATAGCCAGTT-3′ resulted in a 540 bp fragment of the *NKA*. PCR fragments were separated by electrophoresis in 1.5% agarose gels. Extraction, purification, and cloning of the PCR fragments from the gel was accomplished as previously described (Hu et al., 2013). Plasmids were sequenced and sequence analysis was performed using the BLASTx program (NCBI, http://blast.ncbi.nlm.nih.gov/Blast.cgi).

Real-Time Quantitative PCR (qPCR)

The mRNA expressions of selected candidate genes were measured by qPCR using the Roche LightCycler® 480 System (Roche Applied Science, Mannheim, Germany). Primers for the Na^+/K^+-ATPase, V-type H^+-ATPase and the reference gene arginine kinase were designed using Primer Premier software (vers. 5.0; PREMIER Biosoft International, Palo Alto, CA) and are provided in Table S2. PCR reactions were performed as previously described (Hu et al., 2013, 2014) and PCR products were subjected to a melting-curve analysis. Primer efficiencies were >96% and control reactions were performed using nuclease-free water to determine background levels. Additionally, DNAse I treated RNA samples served as a control, demonstrating that no PCR product was obtained, and thus the success of the DNase I treatment. The standard curve of each gene was in a linear range with arginine kinase (AK) that served as reference gene. The expression of this reference gene has been demonstrated to be stable in the green shore crab *C. maenas* during CO_2 treatments (Fehsenfeld et al., 2011).

Statistical Analyses

Statistical analyses were performed using Sigma Stat 3.0 (Systat) software. Statistical differences between pH treatments within one time point were analyzed using a Student's *t*-test. The significance levels were set to $p < 0.05^*$ and $p < 0.01^{**}$.

RESULTS

Extracellular Acid-Base Status

Mean extracellular pH (pHe) measured in hemolymph samples along the time series of 48 h ranged between pH 7.50 ± 0.02 to 7.59 ± 0.01 in control animals (**Figure 2A**; Figure S1). In response to acidified conditions of pH 6.5, pHe dropped ($p < 0.05$) by ∼0.25 pH units compared to control animals after 1 h. pHe was partially restored after 4 h and remained stable at levels of ∼0.1 pH units below control pHe. Mean blood HCO_3^- levels were found to range from 6.4 ± 0.5 to 8.2 ± 1.1 mM in

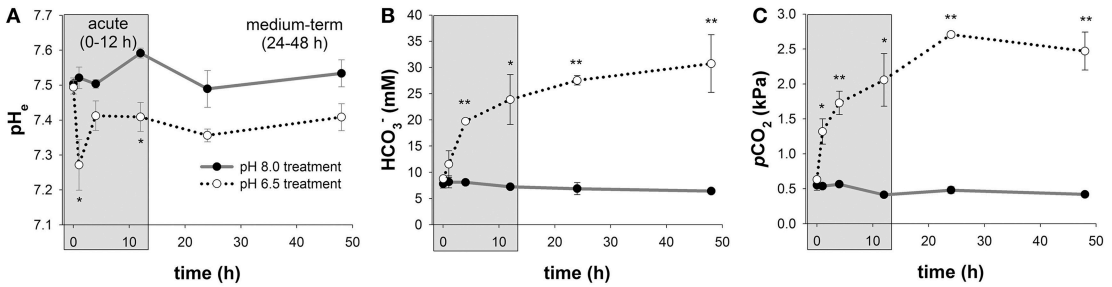

FIGURE 2 | Extracellular acid-base parameters during exposure to acidified conditions. Time series measurements of *in vivo* extracellular pH (pHe) **(A)**, hemolymph HCO_3^- levels **(B),** and pCO_2 **(C)** along the experimental period of 48 h. The exposure period is separated into a short-term (gray) and medium-term (white) acclimation period. Extracellular acid-base parameters are additionally presented in a Davenport diagram in Figure S1. Asterisks indicate significant differences between pH treatments (*$p < 0.05$ and **$p < 0.001$). Bars represent mean ± SE ($n = 4$).

control animals along the incubation period of 48 h (**Figure 2B**). In response to acidified conditions of pH 6.5, hemolymph HCO_3^- levels progressively increased from 8.8 ± 0.3 to 31 ± 6 mM during the 48 h incubation period and significant differences ($p < 0.05$ and 0.01) to control animals were observed after 4 h incubation until the end of the experiment. Hemolymph pCO_2 levels ranged from 0.41 to 0.55 kPa in control animals along the incubation period of 48 h (**Figure 2C**). In response to acidified conditions, hemolymph pCO_2 levels increased to peak values of 2.7 ± 0.3 kPa (**Figure 2C**).

Regulation of Branchial Na^+/K^+-ATPase and V-Type H^+-ATPase upon Low pH Exposure

Comparisons of routine mRNA levels of NKA and VHA did not reveal any significant differences between anterior (1–3) and posterior gills (4–6; Figure S2). In response to acidified conditions, mRNA levels of the NKA and VHA measured in the posterior gills (4,5,6) increased rapidly within 1 h by 2.3- and 11.4-fold, respectively (**Figures 3A,B**). While NKA mRNA levels returned to control levels within the acute acclimation phase of 4 h, VHA mRNA levels rapidly increased upon low pH exposure for 1 h and then decreased back to control levels within 24 h (**Figures 3A,B**). The increase in mRNA concentrations is paralleled by an increase in NKA and VHA enzyme activities (**Figures 3C,D**). Compared to control conditions where maximum NKA enzyme activities ranged from 335 ± 60 to 456 ± 9 $\mu mol_{ATP}\ h^{-1}\ g_{FM}^{-1}$, branchial NKA activities in crabs exposed to acidified conditions increased within 1 h to a maximum of 719 ± 115 $\mu mol_{ATP}\ h^{-1}\ g_{FM}^{-1}$. Along the period of 24 h, NKA activities decreased back to control levels (**Figure 3C**). Branchial VHA enzyme activities increased in response to acidified conditions with an activity peak after 12 h reaching 1.7-fold increased enzyme activities compared to control animals (**Figure 3D**). After 24 h of low pH exposure, branchial VHA activities returned back to control levels and remained slightly above control levels for the experimental period of 48 h. When comparing relative changes of NKA mRNA and activity levels along the entire experimental period a slight shift by ∼3 h in peak NKA activities can be found in comparison to mRNA levels. Moreover, while NKA mRNA levels returned to control conditions after 4 h, NKA enzyme activities remain elevated by 40% to 30% along the experimental duration of 48 h (**Figure 3E**). A more pronounced shift between peak mRNA and enzyme activity levels of ∼9 h has been observed for the branchial VHA (**Figure 3F**). After this acute phase, VHA enzyme activities decreased back to control levels after 48 h exposure to acidified conditions.

Localization of Na^+/K^+-ATPase and V-Type H^+-ATPase in Gill Epithelia

Immunohistochemical analyses demonstrate the sub-cellular localization of Na^+/K^+-ATPase and V-type H^+-ATPase in gill epithelia of posterior gills from control animals (**Figure 4A**). Using double staining, high concentrations of Na^+/K^+-ATPase were detected in basolateral membranes of the entire gill epithelium as well as in pillar cells spanning between the two epithelial layers (**Figure 4A**). V-type H^+-ATPase was predominantly located in the cytoplasm of epithelial- and pillar-cells. In contrast to the distribution of NKA in cells of the entire gill lamella, VHA immunoreactivity is only observed in single cells, predominantly pillar cells. Negative controls performed by omitting the primary antibody, did not show any signal in posterior gill lamellae, supporting the specificity of the primary antibodies used (Figure S3). Western blot analyses demonstrate specific immunoreactivity of antibodies with proteins including Na^+/K^+-ATPase (≈110 kDa) and V-type H^+-ATPase (≈70 kDa; **Figure 4B**). Western blot analyses of posterior gills of pH 8.0 and 6.5 treated crabs demonstrates increased NKA as well as VHA protein concentrations in low pH treated animals during the acute low pH acclimation phase (**Figure 4C**). NKA protein concentrations in the acute acclimation phase (12 h) are 1.4-fold higher whereas VHA protein concentrations of posterior gills are increased by 3-fold in low pH treated animals compared to pH 8.0 acclimated animals.

DISCUSSION

Acid-Base Regulation in the Vent Crab *Xenograpsus testudinatus*

Substantial acid-base regulatory abilities are a characteristic of many active marine organisms including fish, cephalopods, and

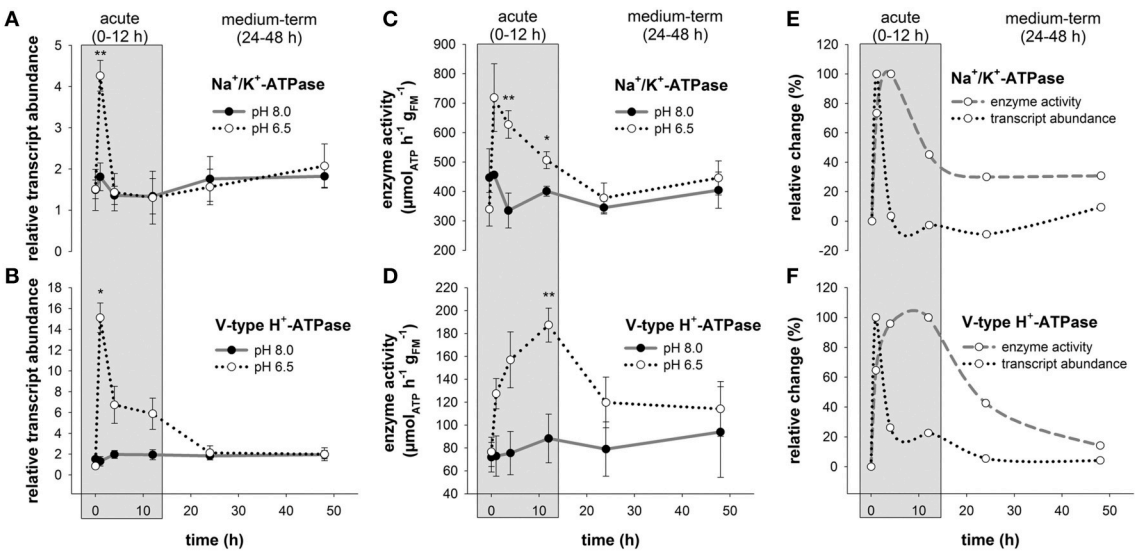

FIGURE 3 | Branchial Na^+/K^+-ATPase and V-type H^+-ATPase transcript abundance and enzyme activities during acclimation to acidified conditions. Relative changes in Na^+/K^+-ATPase (NKA) **(A)** and V-type H^+-ATPase (VHA) **(B)** transcript levels under control and acidified conditions. Transcript levels were normalized to arginine kinase (AK) as an internal control. NKA **(C)** and VHA **(D)** enzyme activities in control and low pH treated animals along the experimental period of 48 h. Combined presentation of relative changes in NKA **(E)** and VHA **(F)** mRNA levels and enzyme activities normalized to control animals. The exposure period is separated into a short-term (gray) and medium-term (white) acclimation period. Asterisks indicate significant differences between pH treatments (*$p < 0.05$ and **$p < 0.001$). Bars represent mean ± SE ($n = 3$–4).

crustaceans (Cameron, 1978; Heisler, 1986; Pörtner et al., 1991; Melzner et al., 2009; Gutowska et al., 2010; Henry et al., 2012). In these taxa, buffering of extracellular pH (pHe) is associated with an increase in blood HCO_3^- levels, which is a conserved and efficient mechanism to counter respiratory acidosis (Heisler, 1986; Pörtner et al., 1991; Gutowska et al., 2010; Henry et al., 2012). The present work demonstrates powerful extracellular acid-base regulatory abilities of *X. testudinatus* that are beneficial for this species to inhabit highly acidic hydrothermal vent habitats over long time scales. The hyperbolic increase in blood HCO_3^- levels of *X. testudinatus* in response to acidified conditions is in general accordance with findings for other strong acid-base regulators (Heisler, 1986). For example, most teleosts can rapidly and fully compensate pHe during moderate to strong hypercapnia, accompanied by an increase in blood [HCO_3^-] in excess of 20 to 30 mM (Larsen et al., 1997; Perry et al., 2010). While cephalopods were characterized to have moderate acid-base regulatory abilities (Gutowska et al., 2010; Hu et al., 2014), most brachyuran crabs were described to be moderate to strong acid-base regulators (Cameron, 1978; Truchot, 1984; Pane and Barry, 2007; Spicer et al., 2007). Detailed investigations of extracellular acid-base parameters during hypercapnic exposure in crustaceans are restricted to a few species, including the European shore crab, *C. maenas* (Truchot, 1984), the blue crab, *Callinectes sapidus* (Cameron, 1978), *Cancer magister*, *Chionoecetes tanneri* (Pane and Barry, 2007), and the velvet swimming crab, *Necora puber* (Spicer et al., 2007). All species showed an initial depression of extracellular pH over the course of 4 h, which was partially restored over the next 24–48 h through an active accumulation of hemolymph HCO_3^-. Such a marked acidosis in the acute acclimation phase (0–12 h) was not observed in *X. testudinatus* exposed to pH 6.5 (1.78 kPa pCO_2), a level greatly in excess of those experimental conditions under which *C. maenas* (0.57 kPa CO_2; ≈pH 7.2), *C. sapidus* (1.0 kPa CO_2; pH 7.08), *C. magister* and *C. tanneri* (1.0 kPa CO_2; pH 7.08) were examined. As gills were demonstrated to be the major site for ion and acid-base regulation in decapod crustaceans, (Henry et al., 2012) the following paragraph focuses on the branchial mechanisms that mediate extracellular acid-base balance in the hydrothermal vent crab *X. testudinatus*.

Branchial Acid-Base Regulatory Mechanisms

Immunohistochemical analyses demonstrate the presence of Na^+/K^+-ATPase and V-type H^+-ATPase in branchial epithelia of the hydrothermal vent crab *X. testudinatus*. These primary active ion-transporters are key players for intra- and extra-cellular regulation of ion and pH homeostasis in all animals (Emery et al., 1998; Tresguerres et al., 2005; Colina et al., 2007; Horng et al., 2009). The ubiquitous NKA located in basolateral membranes creates an electrochemical gradient that fuels secondary active transporters. For example, blocking of NKA in perfused gills of the crab *Neohelice granulata* inhibited HCO_3^- secretion and H^+ reabsorption indicating a central role in fueling secondary active transport mechanisms relevant for acid-base regulation (Tresguerres et al., 2008).

The sub cellular localization of VHA in branchial epithelia of marine organisms seems to be less conserved compared to the NKA. For example, in most teleosts, the VHA is located in apical membranes where it is believed to mediate the direct secretion

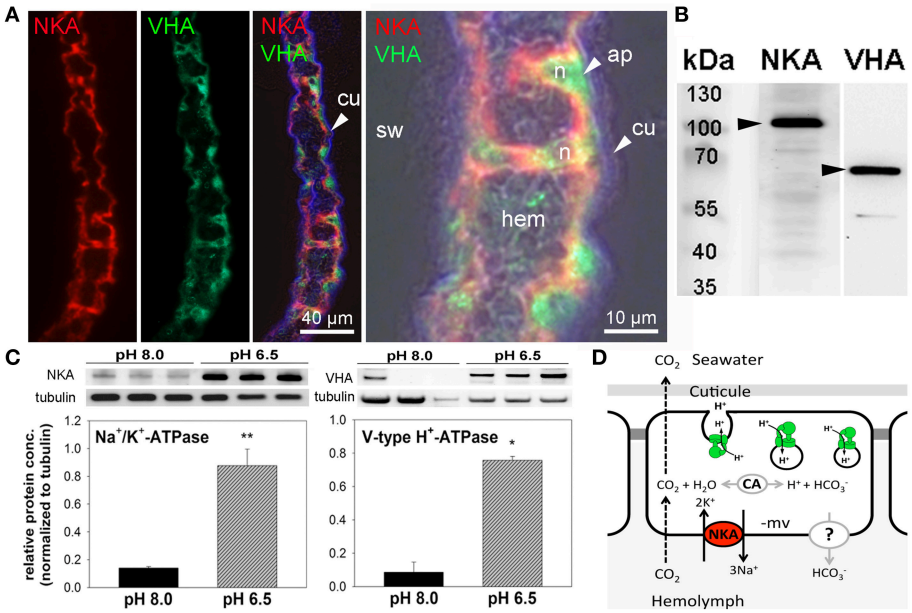

FIGURE 4 | Immuno-histochemical localization of Na^+/K^+-ATPase and V-type H^+-ATPase in branchial epithelia. Positive Na^+/K^+-ATPase (NKA) (red) immunoreactivity in basolateral membranes of the 5th gill pair of a control (pH 8) animal **(A)**. Positive immunoreactivity of the V-type H^+-ATPase (VHA) (green) antibody is mainly located in the cytoplasm of single epithelial as well as pillar cells. Background fluorescence (blue), showing the lining of the cuticule along the gill lamellae. Larger magnification of one branchial lamella demonstrating the sub cellular localization of the NKA and VHA including a bright field overlay to visualize the histology of this tissue **(A)**. Western blot analyses using gill homogenates, indicating specific immunoreactivity of the different antibodies with proteins in the predicted size range **(B)**. Determination of NKA and VHA protein concentrations normalized to tubulin in posterior gills after 12 h exposure to pH 8.0 and 6.5 conditions (*$p < 0.05$; **$p < 0.01$) **(C)**. Hypothetical model of acid-base regulation in epithelial cells of posterior gills in *X. testudinatus* **(D)**. NKA located in basolateral membranes energizes the import of bicarbonate via a putative basolateral HCO_3^- transporter. CO_2 diffuses across membranes along concentration gradients. Intracellular carbonic anhydrase (CAc) facilitates the formation of HCO_3^- and protons. Based on the findings of the present work it is speculated that cytoplasmic VHA is involved in the acidification of vesicles and protons are exocytosed across the apical membrane. Cu, cuticula; hem, hemolymph; sw, sea water; n, nucleus; ap, apical.

of protons (Horng et al., 2007; Tsai and Lin, 2007; Hwang et al., 2011). However, in marine species like the teleost, *Oryzias latipes* (Lin et al., 2012) and the squid *Sepioteuthis lessoniana* the VHA is located in basolateral membranes of ion-regulatory epithelia where it is involved in acid-base regulatory processes as well (Hu et al., 2013). In most crustaceans, the VHA has been demonstrated to be localized in apical membranes and/or in the cytoplasm of branchial epithelial cells (Weihrauch et al., 2001; Tsai and Lin, 2007). The strong cytosolic but weak apical abundance of the VHA in branchial cells of *X. testudinatus* is in accordance with observations made on other marine and intertidal brachyuran crabs including Ocypodid crabs, *Uca laceta,* and *Macrophthalmus* spp. as well as the brachyuran crabs, *Hemigrapsus sanguineus, H. penicillatus, Perisesarma bidens*, and *Chiromantes dehaani* (Tsai and Lin, 2007). The cytoplasmic localization of the VHA has been hypothesized to be involved in the trapping of NH_4^+ within acidified vesicles and subsequent exocytosis across the apical membrane (Weihrauch et al., 2002). As secretion of NH_4^+ also results in a net export of protons, it is likely that excretion of nitrogenous waste products and acid-base regulation are linked processes.

Gene expression analyses and enzyme activity measurements in the present study indicate that branchial NKA and VHA are important players of acid-base regulation that mediate bicarbonate accumulation as well as H^+ secretion in this hydrothermal vent species. In fish, cephalopods and crustaceans, the compensation of an extracellular acidosis by an accumulation of HCO_3^- is always associated with a significant net export of protons (Heisler, 1984, 1986; Cameron, 1986). As HCO_3^- formation through the hydration of CO_2 is always associated with the generation of H^+, H^+ export pathways represent an essential feature in animals that compensate an extracellular acidosis. These observations are in line with the results of the present study, demonstrating that environmental acidification stimulates expression levels of branchial VHA that is involved in the secretion of proton equivalents. Moreover, basolateral NKA has been hypothesized to energize HCO_3^- transport in crustacean branchial epithelia (Tresguerres et al., 2008). In this context a Na^+/HCO_3^- co-transporter (NBC) located in basolateral membranes has been proposed for the branchial epithelium of *Neohelice granulate* based on pharmacological observations (Tresguerres et al., 2008). Other studies suggested that basolateral anion exchangers are involved in the HCO_3^- re-absorption in crustacean gills (Freire et al., 2008; Harms et al., 2014). Although the existence, function and cellular localization of HCO_3^- transporters from the SLC 4 family are not confirmed for *X. testudinatus*, this work strongly suggests that active HCO_3^- re-absorption significantly contributes to

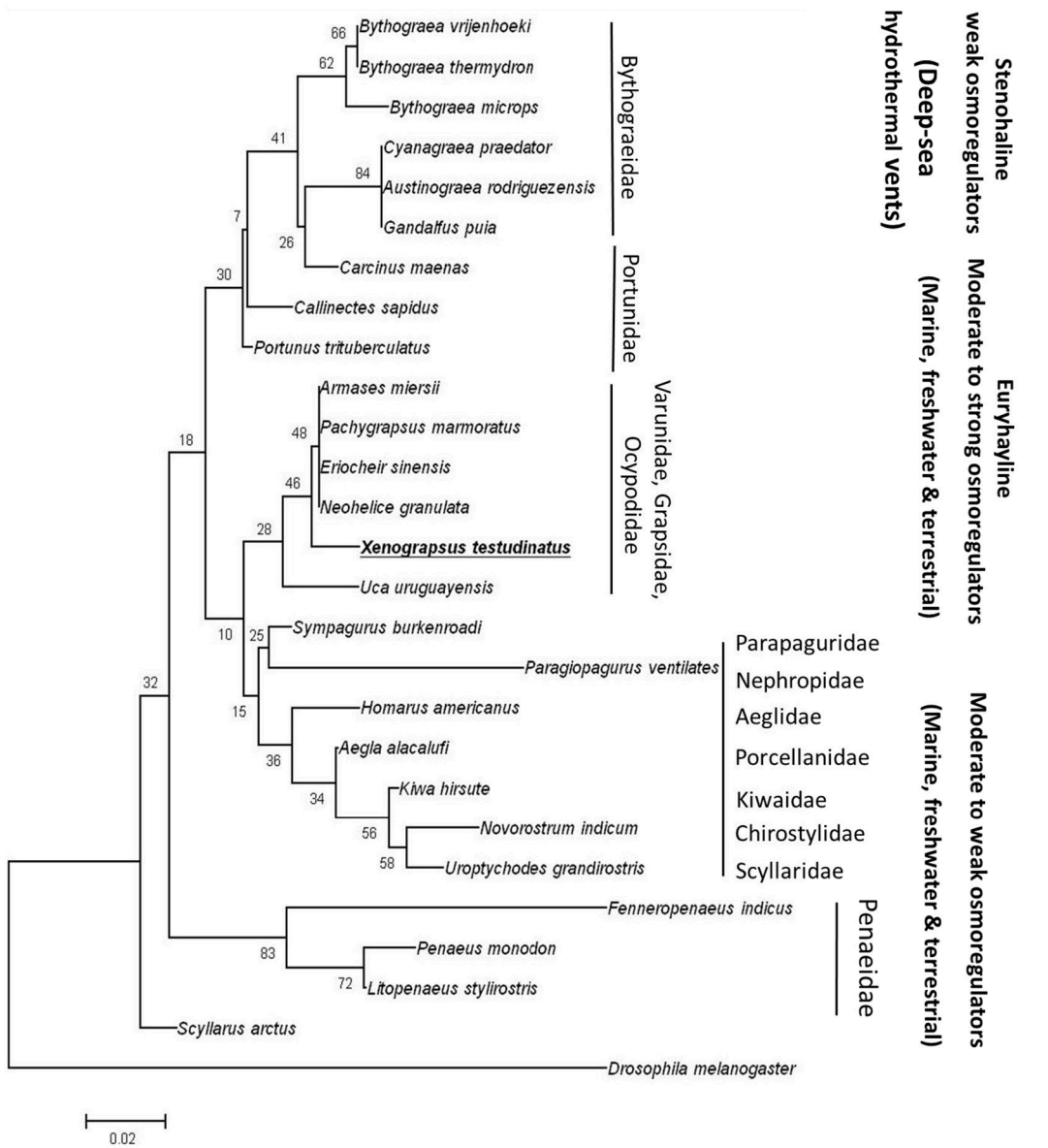

FIGURE 5 | The phylogeny of crustacean Na^+/K^+-ATPases. Routed phylogenetic tree of deduced Na^+/K^+-ATPase amino acid sequences from different decapods crustaceans. Numbers indicate bootstrap values and accession numbers for the sequences are provided along with species names. Information regarding the habitat and osmoregulatory abilities of the different species is included in the phylogenetic tree.

extracellular pH homeostasis during environmental acidification. Active HCO_3^- transport mechanism can be considered essential for the HCO_3^- buffering since dissolution of the carapace has been demonstrated to represent only a minor contribution to extracellular HCO_3^- accumulation in crustaceans (Cameron, 1985). According to this information, we propose a first model for acid-base regulatory mechanisms in gill epithelia of the hydrothermal vent crab, *X. testudinatus* (**Figure 4D**). The NKA energizes HCO_3^- uptake via a currently not identified basolateral HCO_3^- transporter and cytosolic carbonic anhydrase (CA). Based

on a study by Weihrauch et al. (2002) we hypothesize that also in *X. testudinatus* cytoplasmic VHA is involved in countering an acidosis by pumping H^+ ions into vesicles that exocytose protons or proton equivalents (e.g., NH_4^+) across the apical membrane. Accordingly, during vesicle fusion at the apical membrane a certain fraction of the cellular VHA must be temporarily transferred to the apical plasma membrane as well. In order to support this hypothesis of vesicular proton excretion in this species future studies will compare the subcellular distribution of VHA-rich vesicles between control and low pH acclimated animals.

Based on the findings of the present work this model suggests that NKA seems to be involved in acid-base compensatory mechanisms by fueling additional secondary active ion-transporters. The electroneutral transport of acid-base equivalents (e.g., HCO_3^- and H^+) *via* anion and cation exchangers is directly connected to the transport of counter ions (e.g., Na^+ and Cl^-) that supports the link between acid-base and osmoregulation found in marine euryhaline decapod crustaceans (Truchot, 1981; Whiteley et al., 2001). Accordingly it is very likely that *X. testudinatus* utilizes Na^+- and Cl^--dependent acid-base regulatory pathways via Na^+/H^+-exchangers (NHEs), and maybe also NBCs or anion exchangers that are fueled by the NKA. Using *X. testudinatus* as a model for a strong acid-base regulating crustacean further studies regarding the functional expression, enzyme abundance and subcellular localization of these secondary active transporters will provide important insights to the mechanistic connection between acid-base and osmotic regulation in decapod crustaceans.

Interestingly, the increase of the NKA and VHA on the mRNA level is only visible in the acute low pH acclimation phase, whereas enzyme activities increase with a short delay and stay elevated until the time point of 24 h. This observation reflects the time gap between mRNA expression and translation into the functional protein, which is in general accordance with findings in other eukaryotes as well as prokaryotes (Marsh et al., 2000; Glanemann et al., 2003). Although NKA and VHA enzyme activities return back to control levels after 24 h, blood HCO_3^- levels remain increased after 48 h in the low pH treatment. This suggests, that initial accumulation of HCO_3^- and the associated secretion of H^+ are reflected in the up regulation of NKA and VHA mRNA and activity levels. However, after 24 h the pHe compensation process is completed and routine NKA and VHA activity levels are probably sufficient to maintain increased hemolymph HCO_3^- levels to protect pHe homeostasis. This energy saving strategy of stabilizing hemolymph pH over long exposure times can be regarded as a key adaptation of *X. testudinatus* to occupy an ecological niche in a highly acidified hydrothermal vent habitat.

CONCLUSION

Strong acid-base regulatory abilities of *X. testudinatus* can be regarded an essential feature of this species to successfully inhabit a highly acidic hydrothermal vent environment. Functional and histological results of the present study demonstrated that extracellular acid-base regulatory mechanisms in *X. testudinatus* rely on a conserved set of ion pumps that are also found in other brachyuran crabs. In accordance to phylogenetic analyses based on mitochondrial genomes (Ki et al., 2009) and morphological systematics (Ng et al., 2000), amino acid sequence comparisons of the NKA demonstrate that *X. testudinatus* is closely related to other varunid and grapsid species including *E. sinensis* and *Pachygrapsus marmoratus* which are characterized as powerful osmo-regulators (Gross, 1961; Onken, 1999; **Figure 5**). NKA homologies also confirm molecular systematics demonstrating that deep-sea hydrothermal vent crabs of the genus *Bythograea* spp. (Mateos et al., 2012) constitute an own phylogenetic group within the crustacea (**Figure 5**). Despite having weak osmo-regulating abilities, *Bythograea thermydron* (Martinez et al., 2001) may be able to increase ATPase activities to increase H^+ efflux rates to protect from strong pH fluctuations that are a characteristic of deep-sea vent habitats (Von Damm, 1995; Tivey, 2004). However, additional studies addressing the mechanistic basis of extracellular pH regulation in crustaceans from deep-sea vent systems will be needed to support this hypothesis. Such comparative studies between deep-sea and shallow-water hydrothermal vent crabs will provide a basis for new and exciting research regarding the evolution of pH regulatory systems in crustaceans that have the ability to occupy ecological niches in highly acidic hydrothermal vent habitats.

AUTHOR CONTRIBUTIONS

MH and YT designed and conducted experiment, analyzed the data, and compiled the main manuscript. MH conducted immunohistochemical experiments and evaluate enzyme activities. YS and MJ collected and acquired the animals and photos from open filed. YG and YT carried out the molecular cloning and expression studies. PK, GC, and JL conducted CO_2 perturbation experiments, physiological measurements, and sample preparation. All authors reviewed and approved the manuscript.

ACKNOWLEDGMENTS

This study was financially supported by the grants to YT. YT from the Ministry of Science and Technology, Taiwan, Republic of China (MOST 104-2321-B-003-001), Alexander von Humbold/National Science Council (Taiwan) grant (NSC 102-2911-I-001-002-2), and a Cluster of Excellence "The future ocean" grant (CP1409) awarded to MH. We gratefully thank Mr. H. T. Lee (assistant in marine station of Institute of Cellular and Organismic Biology, Academia Sinica) for his assistance to maintain experimental systems.

SUPPLEMENTARY MATERIAL

The Supplementary Material for this article can be found online at: http://journal.frontiersin.org/article/10.3389/fphys.2016.00014

REFERENCES

Beyenbach, (2006). The V-type H^+ ATPase: molecular structure and function, physiological roles and regulation. *J. Exp. Biol.* 209, 577–589. doi: 10.1242/jeb.02014

Bedford, J. J., and Leader, J. P. (1977). The composition of the hemolymph and muscle tissue of the shore crab, Hemigrapsus edwardsii, exposed to different salinities. *Comp. Biochem. Physiol. A Physiol.* 57A, 341–345. doi: 10.1016/0300-9629(77)90203-1

Cameron, J. N. (1978). Effects of hypercapnia on blood acid-base status, NaCl fluxes and trans-gill potential in freshwater blue crabs, *Callinectes sapidus*. *J. Comp. Physiol. B* 123, 137–141. doi: 10.1007/BF00687841

Cameron, J. N. (1985). Compensation of hypercapnic acidosis in the aquatic blue crab, *Callinectes sapidus*: the predominance of external sea water over carapace carbonate as the proton sink. *J. Exp. Biol.* 114, 197–206.

Cameron, J. N. (1986). *Acid-base Regulation in Animals*. Amsterdam: Elsevier Biomedical Press.

Charmantier, G., and Charmantier-Daures, M. (2001). Ontogeny of osmoregulation in crustaceans: the embryonic phase. *Am. Zool* 41, 1078–1089. doi: 10.1093/icb/41.5.1078

Chen, C-T. A., Wang, B. J., Huang, J., Lou, J., Kuo, F., and Tu, Y. (2005). Investigation into extremely acidic hydrothermal fluids off Kueishan Tao, Taiwan, China. *Acta Oceanol. Sin.* 24, 125–133.

Colina, C., Rosenthal, J. J. C., DeGiorgis, J. A., Srikumar, D., Iruku, N., and Holmgren, M. (2007). Structural basis of Na^+/K^+-ATPase adaptation to marine environments. *Nat. Struct. Mol. Biol.* 14, 427–431. doi: 10.1038/nsmb1237

Dickson, A., and Millero, F. (1987). A comparison of the equilibrium constants for the dissociation of carbonic acid in seawater media. *Deep Sea Res. A* 34, 1733–1743. doi: 10.1016/0198-0149(87)90021-5

Dittel, A. I., Perovich, G., and Epifanio, C. E. (2008). Biology of the vent crab *Bythograea thermydron*: a brief review. *J. Shellfish Res.* 27, 63–77. doi: 10.2983/0730-8000(2008)27[63:BOTVCB]2.0.CO;2

Dröse, S., and Altendorf, K. (1997). Bafilomycins and concanamycins as inhibitors of V-ATPases and P-ATPases. *J. Exp. Biol.* 200, 1–8.

Emery, A. M., Billingsley, P. F., Ready, P. D., and Djamgoz, M. B. A. (1998). Insect Na^+/K^+-ATPase. *J. Insect. Physiol.* 44, 197–209. doi: 10.1016/S0022-1910(97)00168-6

Fehsenfeld, S., Kiko, R., Appelhans, Y., Towle, D. W., Zimmer, M., and Melzner, F. (2011). Effects of elevated seawater pCO_2 on gene expression patterns in the gills of the green crab, *Carcinus maenas*. *BMC Genomics* 12:488. doi: 10.1186/1471-2164-12-488

Frederich, M., Sartoris, F., and Pörtner, H.-O. (2001). Distribution patterns of decapod crustaceans in polar areas: a result of magnesium regulation? *Polar Biol.* 24, 719–723. doi: 10.1007/s003000100270

Freire, C. A., Onken, H., and McNamara, J. C. (2008). A structure-function analysis of ion transport in crustacean gills and excretory organs. *Comp. Biochem. Physiol. A Mol. Integr. Physiol.* 151, 272–304. doi: 10.1016/j.cbpa.2007.05.008

Glanemann, C., Loos, A., Gorret, N., Willis, L. B., O'Brien, X. M., Lessard, P. A., et al. (2003). Disparity between changes in mRNA abundance and enzyme activity in *Corynebacterium glutamicum*: implications for DNA microarray analysis. *Appl. Microbiol. Biotechnol.* 61, 61–68. doi: 10.1007/s00253-002-1191-5

Goffredi, S., Childress, J., Desaulniers, N., Lallier, L. R., and Hammond, D. (1997). Inorganic carbon acquisition by the hydrothermal vent tubeworm *Riftia pachyptila* depends upon high P-CO_2 and upon proton-equivalent ion transport by the worm. *J. Exp. Biol.* 200, 883–896.

Gross, W. J. (1961). Osmotic tolerance and regulation in crabs from a hypersaline lagoon. *Biol. Bull.* 121, 290–301. doi: 10.2307/1539433

Gutowska, M. A., Melzner, F., Langenbuch, M., Bock, C., Claireaux, G., and Pörtner, H. O. (2010). Acid-base regulatory ability of the cephalopod (*Sepia officinalis*) in response to environmental hypercapnia. *J. Comp. Physiol. B* 180, 323–335. doi: 10.1007/s00360-009-0412-y

Han, C., Ye, Y., Pan, Y., Qin, H., Wu, G., and Chen C.-T. A. (2014). Spatial distribution pattern of seafloor hydrothermal vents to the southeastern Kueishan Tao offshore Taiwan Island. *Acta Oceanol. Sin.* 33, 37–44. doi: 10.1007/s13131-014-0405-x

Harms, L., Frickenhaus, S., Schiffer, M., Mark, F. C., Storch, D., Held, C., et al. (2014). Gene expression profiling in gills of the great spider crab *Hyas araneus* in response to ocean acidification and warming. *BMC Genomics* 15:789. doi: 10.1186/1471-2164-15-789

Heisler, N. (1984). *Acid-Base Regulation in Fishes*. Amsterdam: Academic Press.

Heisler, N. (1986). *Acid-base Regulation in Animals*. Amsterdam: Elsevier Biomedical Press.

Henry, R. P., and Cameron, J. N. (1982). Acid-base balance in *Callinectes sapidus* during acclimation from high to low salinity. *J. Exp. Biol.* 101, 255–264.

Henry, R. P., Lucu, C., Onken, H., and Weihrauch, D. (2012). Multiple functions of the crustacean gill: osmotic/ionic reglation, acid-base balance, ammonia excretion, and bioaccumulation of toxic metals. *Front Physiol* 3:431. doi: 10.3389/fphys.2012.00431

Hicks, G. F. R. (1973). Combined effects of temperature and salinity on *Hemigrapsus edwardsi* (Hilgendorf) and *H. crenulatus* (Milne Edwards) from Wellington Harbour, New Zealand. *J. Exp. Mar. Biol. Ecol.* 13, 1–14. doi: 10.1016/0022-0981(73)90042-7

Horng, J.-L., Lin, L.-Y., Huang, C.-J., Katoh, F., Kaneko, T., and Hwang P.-P. (2007). Knockdown of V-ATPase subunit A (*atp6v1a*) impairs acid secretion and ion balance in zebrafish (*Danio rerio*). *Am. J. Physiol. Regul. Integr. Comp. Physiol.* 292, R2068–R2076. doi: 10.1152/ajpregu.00578.2006

Horng, J. L., Lin, L. Y., and Hwang, P. P. (2009). Functional regulation of H^+-ATPase-rich cells in zebrafish embryos acclimated to an acidic environment. *Am. J. Physiol. Cell Physiol.* 296, c682–c692. doi: 10.1152/ajpcell.00576.2008

Hu, M. Y., Guh, Y.-J., Stumpp, M., Lee, J.-R., Chen, R.-D., Sung, P.-H., et al. (2014). Branchial NH_4^+-dependent acid-base transport mechanisms and energy metabolism of squid (*Sepioteuthis lessoniana*) affected by seawater acidification. *Front. Zool.* 11:55. doi: 10.1186/s12983-014-0055-z

Hu, M. Y., Lee, J.-R., Lin, L.-Y., Shih, T.-H., Stumpp, M., Lee, M.-F., et al. (2013). Development in a naturally acidified environment: Na^+/H^+-exchanger 3-based proton secretion leads to CO_2 tolerance in cephalopod embryos. *Front. Zool.* 10:51. doi: 10.1186/1742-9994-10-51

Hwang, P. P. (2009). Ion uptake and acid secretion in zebrafish (*Danio rerio*). *J. Exp. Biol.* 212, 1745–1752. doi: 10.1242/jeb.026054

Hwang, P. P., Lee, T. H., and Lin, L. Y. (2011). Ion regulation in fish gills: recent progress in the cellular and molecular mechanisms. *Am. J. Physiol. Regul. Integr. Comp. Physiol.* 301, R28–R47. doi: 10.1152/ajpregu.00047.2011

Jeng, M. S., Ng, N. K., and Ng, P. K. L. (2004). Feeding behaviour: hydrothermal vent crabs feast on sea "snow." *Nature* 432:969. doi: 10.1038/432969a

Joel, W. M., and Haney, T. A. (2005). Decapod crustaceans from hydrothermal vents and cold seeps: a review through 2005. *Zool. J. Linn. Soc.* 145, 445–522. doi: 10.1111/j.1096-3642.2005.00178.x

Ki, J.-S., Dahms, H.-U., Hwang, J.-S., and Lee, J.-S. (2009). The complete mitogenome of the hydrothermal vent crab *Xenograpsus testudinatus* (Decapoda, Brachyura) and comparison with brachyuran crabs. *Comp. Biochem. Physiol. D Geonomics Proteomics* 4, 290–299. doi: 10.1016/j.cbd.2009.07.002

Larsen, B. K., Pörtner, H.-O., and Jensen, F. B. (1997). Extra- and intracellular acid-base balance and ionic regulation in cod (*Gadus morhua*) during combined and isolated exposures to hypercapnia and copper. *Mar. Biol.* 128, 337–346. doi: 10.1007/s002270050099

Lewis, E., and Wallace, D. W. R. (1998). *Program Developed for CO_2 System Calculations*. Oak Ridge, TN: Oak Ridge National Laboratory. ORNL/CDIAC-105.

Lin, C.-C., Lin, L.-Y., Hsu, H.-H., Thermes, V., Prunet, P., Horng, J.-L., et al. (2012). Acid secretion by mitochondrion-rich cells of medaka (*Oryzias latipes*) acclimated to acidic freshwater. *Am. J. Physiol. Integr. Comp. Physiol.* 15, R283–R291. doi: 10.1152/ajpregu.00483.2011

Marsh, A. G., Leong, P. K. K., and Manahan, T. (2000). Gene expression and enzyme activities of the sodium pump during sea urchin development: implications for indices of physiological state. *Biol. Bull.* 199, 100–107. doi: 10.2307/1542869

Martinez, A.-S., Toullec, J.-Y., Shillito, B., Charmantier-Daures, M., and Charmantier, G. (2001). Hydromineral regulation in the hydrothermal vent crab Bythograea thermydron. *Biol. Bull.* 201, 167–174. doi: 10.2307/1543331

Mateos, M., Hurtado, L. A., Santamaria, C. A., Leignel, V., and Guinot, D. (2012). Molecular systematics of the deep-sea hydrothermal vent endemic brachyuran

family Bythograeidae: a comparison of three Bayesian species tree methods. *PLoS ONE* 7:e32066. doi: 10.1371/journal.pone.0032066

Mehrbach, C., Culberso, C., Hawley, J., and Pytkowic, R. (1973). Measurement of apparent dissociation constants of carbonic acid in seawter at atmospheric pressure. *Limnol. Oceanogr.* 18, 897–907. doi: 10.4319/lo.1973.18.6.0897

Melzner, F., Gutowska, M. A., Langenbuch, M., Dupont, S., Lucassen, M., Thorndyke, M. C., et al. (2009). Physiological basis for high CO_2 tolerance in marine ectothermic animals: pre-adaptation through lifestyle and ontogeny? *Biogeosciences* 6, 2313–2331. doi: 10.5194/bg-6-2313-2009

Morris, J. F., Ismail-Beigi, F., Butler V. P. Jr., Gati, I., and Lichtstein, D. (1997). Ouabain-sensitive Na+, K(+)-ATPase activity in toad brain. *Comp. Biochem. Physiol. A Physiol.* 118, 599–606. doi: 10.1016/S0300-9629(96)00465-3

Ng, N. K., Huang, J., and Ho, P.-H. (2000). Description of a new species of hydrothermal crab, *Xenograpsus testudinatus* (Crustacea: Decapoda: Brachyura: Grapsidae) from Taiwan. *Natl. Taiwan Mus. Publ. Ser.* 10, 191–199.

Onken, H. (1999). Active NaCl absorption across split lamellae of posterior gills of Chinese crabs (*Eriocheir sinensis*) adapted to different salinities. *Comp. Biochem. Physiol. A Mol. Integr. Physiol.* 123, 377–384. doi: 10.1016/S1095-6433(99)00078-1

Onken, H., and Graszynski, K. (1989). Active Cl^- absorption by the Chinese crab *Eriocheir sinensis* gill epithelium measured by potential difference. *J. Comp. Physiol. B* 159, 21–28. doi: 10.1007/BF00692679

Pane, E. F., and Barry, J. P. (2007). Extracellular acid-base regulation during short-term hypercapnia is effective in a shallow-water crab, but ineffective in a deep-sea crab. *Mar. Ecol. Prog. Ser.* 334, 1–9. doi: 10.3354/meps334001

Perry, S. F., Braun, M. H., Genz, J., Vulesevic, B., Taylor, J., Grosell, M., et al. (2010). Acid-base regulation in the plainfin midshipman (*Porichthys notatus*): an aglomerular marine teleost. *J. Comp. Physiol. B* 180, 1213–1225. doi: 10.1007/s00360-010-0492-8

Pörtner, H.-O., Webber, D. M., Boutilier, R. G., and O'Dor, R. K. (1991). Acid-base regulation in exercising squid (*Illex illecebrosus*, *Loligo pealei*). *Am. J. Physiol. Regul. Integr. Comp. Physiol.* 261, R239–R246.

Ramirez-Llodra, A., Shank, T. M., and German, C. R. (2007). Biodiversity and biogeography of hydrothermal vent species. *Oceanography* 20, 30–41. doi: 10.5670/oceanog.2007.78

Sarazin, G., Michard, G., and Prevot, F. (1999). A rapid and accurate spectroscopic method for alkalinity measurements in seawater samples. *Water Res.* 33, 290–294. doi: 10.1016/S0043-1354(98)00168-7

Schneider, C. A., Rasband, W. S., and Eliceiri, K. W. (2012). NIH Image to ImageJ: 25 years of image analysis. *Nat. Methods* 9, 671–675. doi: 10.1038/nmeth.2089

Schubart, C. D., Diesel, R., and Hedges, S. B. (1997). Rapid evolution to terrestrial life in Jamaican crabs. *Nature* 393, 363–365. doi: 10.1038/30724

Spicer, J. I., Raffo, A., and Widdicombe, S. (2007). Influence of CO_2-related seawater acidification on extracellular acid-base balance in the velvet swimming crab *Necora puber*. *Mar. Biol.* 151, 1117–1125. doi: 10.1007/s00227-006-0551-6

Tivey, M. K. (2004). *Subseafloor Biosphere at Mid-ocean Ridges*. Dublin: American Geophysical Union.

Tresguerres, M., Katoh, F., Fenton, H., Jasinska, E., and Goss, G. G. (2005). Regulation of branchial V-H^+-ATPase, Na^+/K^+-ATPase and NHE2 in response to acid and base infusions in the Pacific spiny dogfish (*Squalus acanthias*). *J. Exp. Biol.* 208, 345–354. doi: 10.1242/jeb.01382

Tresguerres, M., Parks, S. K., Katoh, F., and Goss, G. G. (2006). Microtubule-dependent relocation of branchial V-H^+-ATPase to the basolateral membrane in the Pacific spiny dogfish (*Squalus acanthias*): a role in base secretion. *J. Exp. Biol.* 209, 599–609. doi: 10.1242/jeb.02059

Tresguerres, M., Parks, S. K., Sabatini, S. E., Goss, G. G., and Luquet, C. M. (2008). Regulation of ion transport by pH and [HCO3-] in isolated gills of the crab *Neohelice* (Chasmagnathus) *granulata*. *Am. J. Physiol. Regul. Integr. Comp. Physiol.* 294, R1033–R1043. doi: 10.1152/ajpregu.00516.2007

Truchot, J. P. (1976). Carbon dioxide combining properties of the blood of the shore crab *Carcinus maenas* (L.): carbon dioxide solubility coefficient and carbonic acid- dissociation constants. *J. Exp. Biol.* 64, 45–57.

Truchot, J. P. (1981). The effect of water salinity and acid-base status on the blood balance in the euryhaline crab, *Carcinus maenas* (L.). *Comp. Biochem. Physiol.* 68, 555–561. doi: 10.1016/0300-9629(81)90361-3

Truchot, J. P. (1984). Water carbonate alkalinity as a determinant of hemolymph acid-base balance in the shore crab, *Carcinus maenas* - a study at two different ambient pCO_2 and O_2 levels. *J. Comp. Physiol.* 154, 601–606. doi: 10.1007/BF00684414

Truchot, J. P. (1992). Acid-base changes on transfer between sea water and freshwater in the Chinese crab, *Eriocheir sinensis*. *Respir. Physiol.* 87, 419–427. doi: 10.1016/0034-5687(92)90022-O

Tsai, J.-R., and Lin, H.-C. (2007). V-type H^+-ATPase and Na^+,K^+-ATPase in the gills of 13 euryhaline crabs during salinity acclimation. *J. Exp. Biol.* 210, 620–627. doi: 10.1242/jeb.02684

Tunnicliffe, V. (1992). Hydrothermal-vent communities of the deep sea. *Am. Sci.* 80, 336–349.

Von Damm, K. L. (1995). *Physical, Chemical, Biological, and Geological Interactions within Seafloow Hydrothermal Systems*. Washington, DC: American Geophysical Union.

Weihrauch, D., Ziegler, A., Siebers, D., and Towle, D. W. (2001). Molecular characterization of V-type H(+)-ATPase (B-subunit) in gills of euryhaline crabs and its physiological role in osmoregulatory ion uptake. *J. Exp. Biol.* 204, 25–37.

Weihrauch, D., Ziegler, A., Siebers, D., and Towle, D. W. (2002). Active ammonia excretion across the gills of the green shore crab *Carcinus maenas*: participation of Na^+/K^+-ATPase, V-type H^+-ATPase and functional microtubules *J. Exp. Biol.* 205, 2765–2775.

Whiteley, N. M., Scott, J. L., Breeze, S. J., and McCann, L. (2001). Effects of water salinity on acid-base balance in decapod crustaceans. *J. Exp. Biol.* 204, 1003–1011.

Conflict of Interest Statement: The authors declare that the research was conducted in the absence of any commercial or financial relationships that could be construed as a potential conflict of interest.

frontiers in Physiology

ORIGINAL RESEARCH
published: 10 May 2017
doi: 10.3389/fphys.2017.00291

Double Knockdown of PHD1 and Keap1 Attenuated Hypoxia-Induced Injuries in Hepatocytes

*Jing Liu, Yiping Li, Lei Liu, Zhi Wang, Chuanbing Shi, Zhengyuan Cheng, Xiaoyi Zhang, Fengan Ding and Ping Sheng Chen**

Department of Pathology and Pathophysiology, School of Medicine, Southeast University, Nanjing, China

Background and Aims: Hypoxia and oxidative stress contribute toward liver fibrosis. In this experiment, we used small hairpin RNA (shRNA) to interfere with the intracellular oxygen sensor—prolyl hydroxylase 1 (PHD1) and the intracellular oxidative stress sensor—kelch-like ECH associated protein 1 (Keap1) in the hypoxic hepatocytes in order to investigate the function of PHD1and Keap1.

Methods: We first established the CCl_4-induced liver fibrosis model, subsequently, the levels of the PHD1, hypoxia-inducible factor-1α (HIF-1α), hypoxia-inducible factor-2α (HIF-2α), Keap1, and nuclear factor-erythroid 2 p45-related factor 2 (Nrf2) were detected in liver tissues. Simultaneously, AML12 cells co-transfected with PHD1 and Keap1shRNAs were constructed *in vitro*, then the intracellular oxidative stress, the proportion of cells undergoing apoptosis, and cell viability were measured. The expression of pro-fibrogenic molecules were analyzed via quantitative real-time polymerase chain reaction (qRT-PCR) and western blot. The level of alpha-1 type I collagen (COL1A1) was determined using an enzyme-linked immunosorbent assay (ELISA). Finally, serum-free "conditioned medium" (CM) from the supernatant of hypoxic AML12 hepatocytes was used to culture rat hepatic stellate cells (HSC-T6), and the levels of fibrosis-related molecules, apoptosis, and cell proliferation were determined.

Results: The marker of hypoxia—HIF-1α and HIF-2α in the livers with fibrosis were upregulated, however, the increase in PHD1 expression was not statistically significant in comparison to the control group. Sign of oxidative stress—Keap1 was increased, while the expression of Nrf2, one of the Keap1 main downstream molecules, was reduced in the hepatocytes. And *in vitro*, the double-knockdown of PHD1 and Keap1 in AML12 hepatocytes presented with decreased hypoxia-induced oxidative stress and apoptosis, furthermore, these hypoxic AML12 cells showed the increased cell viability and the doweregulated expression of pro-fibrogenic molecules. In addition, HSC-T6 cells cultured in the hypoxic double-knockdown CM demonstrated the downregulation of fibrosis-related molecules, diminished cell proliferation, and enhanced apoptosis.

Conclusions: Our study demonstrated that double-knockdown of PHD1 and Keap1 attenuated hypoxia and oxidative stress induced injury in the hepatocytes, and subsequently inhibited HSC activation, which offers a novel therapeutic strategy in the prophylaxis and treatment of liver fibrosis.

Keywords: liver fibrosis, hepatocytes, PHD1, Keap1, hypoxia, oxidative stress

OPEN ACCESS

Edited by:
Maria Giovanna Trivella, Consiglio Nazionale Delle Ricerche (CNR), Italy

Reviewed by:
Katja Breitkopf-Heinlein, Heidelberg University, Germany
Antonella Cecchettini, University of Pisa, Italy

****Correspondence:***
Ping Sheng Chen
101006524bingli@sina.cn

Specialty section:
This article was submitted to Integrative Physiology, a section of the journal Frontiers in Physiology

Received: *22 October 2016*
Accepted: *21 April 2017*
Published: *10 May 2017*

Citation:
Liu J, Li Y, Liu L, Wang Z, Shi C, Cheng Z, Zhang X, Ding F and Chen PS (2017) Double Knockdown of PHD1 and Keap1 Attenuated Hypoxia-Induced Injuries in Hepatocytes. Front. Physiol. 8:291. doi: 10.3389/fphys.2017.00291

INTRODUCTION

Liver fibrosis is a pathological process caused by numerous chronic liver damages—such as viral hepatitis, alchoholic hepatitis, and drug induced hepatotoxicity (Begriche et al., 2011). As a highly active metabolic organ, the liver is particularly prone to hypoxic environments and the damages caused by it (Nakanishi et al., 1995). A convincing body of evidence suggest that hypoxia plays an important role in the pathogenesis of liver fibrosis (Cannito et al., 2014).

Cellular hypoxia leads to activation of hypoxia-inducible factors (HIF), which is crucial for the survival of an asphyxiated/ischemic hepatocyte. In normoxia, HIF-1α and HIF-2α are first hydroxylated by prolyl hydroxylase (PHD) and then degraded by proteasomes (Kamura et al., 2000). Whereas during hypoxic condition, HIF-1α and HIF-2α accumulate and get translocated to the nuclei, thereby activating the genes responsible for limiting hypoxia-induced injury and cell death. Recently, Nimker et al. reported that the pharmaceutical inhibition of PHDs with ethyl 3, 4-dihydroxy benzoate (EDHB) protects myoblasts against hypoxia-induced oxidative damage by upregulating HIFs (Nimker et al., 2015). However, non-specific inhibition of PHDs also induces the activation of HIFs but at the cost of adverse effects such as steatosis (Minamishima et al., 2009; Rankin et al., 2009). PHD has three isoforms—PHD1, PHD2, and PHD3, each of these has numerous functions. Selective loss of PHD1, but not those of PHD2 or PHD3 could induce hypoxia tolerance in the skeletal muscle and liver cells via reprogramming of basal oxygen metabolism without inducing angiogenesis and erythrocytosis (Aragones et al., 2008; Schneider et al., 2010). Therefore, the specific inhibition of PHD1 could serve as a potential therapeutic strategy against hypoxia during liver fibrosis.

In recent years, many studies have demonstrated that oxidative stress also contributes to the pathogenesis of liver fibrosis (Ghatak et al., 2011; Mormone et al., 2012; Yang et al., 2013).The nuclear factor-erythroid 2-related factor 2 (Nrf2) has been suggested to be involved in this process. Under normal condition, Nrf2 exists in the cytoplasm where it binds to kelch-like ECH associated protein 1 (Keap1), thereby hastening the Nrf2 ubiquitination and degradation (Kang et al., 2004). During oxidative stress, Nrf2 evades Keap1 and translocates to the nucleus, where it activates antioxidant genes. Chen et al. has also demonstrated that glycyrrhetinic acid could ameliorate chronic liver fibrosis via upregulation of Nrf2 (Chen et al., 2013). Additonally, Tanaka et al. also reported that Nrf2-null mice had an increased susceptibility to liver injury (Tanaka et al., 2012). Keap1 serves to negatively regulate Nrf2 (Miyata et al., 2011), for example, Keap1-knockdown mice are less vulnerable to oxidative liver injuries during obstructive cholestasis mediated by enhanced expression of Nrf2 (Okada et al., 2009). Thus, Keap1 may be an efficient therapeutic target for relieving oxidative stress injury during liver fibrosis.

It has been reported that many cell types are involved in the pathogenesis of liver fibrosis, activated hepatic stellate cells (HSCs) play a central role in liver fibrogenesis. It is worth noting that injuried hepatocytes are considered to be the primary activator of HSCs (Nieto et al., 2002), and hepatocytes are the major parenchymal cells that account for more than 70% of all liver cells (Bogdanos et al., 2013). Furthermore, hepatocytes are highly susceptible to hypoxic injury and the drugs induced toxicity, therefore we chose hepatocytes as a therapeutic target in an attempt to ameliorate liver fibrosis. Hypoxic hepatocytes are known to generate excessive amount of reactive oxygen species (ROS) which exert oxidative stress on the liver. Moreover, such oxidative stress can further exacerbate the hypoxia in the hepatocytes, and the subsequent re-oxygenation following hypoxia leads to additional oxidative stress (Miyata et al., 2011). Therefore, the ideal therapy for liver fibrosis could be the alleviation of hypoxia along with the oxidative stress, however, no such related studies have been done so far.

RNA interference (RNAi) is a method that uses a small complementary double-stranded RNA (dsRNA) molecule to silence a target gene (Inoue et al., 2006). Considering the short half-life and high cost of current small interfering RNA (siRNA) vectors, they are not suitable for many *in vivo* studies. In contrast, short hairpin RNA (shRNA) is widely used due to its enhanced stability and transfer efficiency. Accordingly, for the present study we used shRNAs to simultaneously knockdown the expressions of PHD1 and Keap1 in the hepatocytes with the aim of exploring therapeutic target for liver fibrosis.

MATERIALS AND METHODS

Animals and Treatment

Six-week-old male Sprague-Dawley rats (250 ± 30 g) were purchased from the Animal Center of Yangzhou University (Yangzhou, China). All animals were housed in the animal experimental center of Southeast University under constant temperature (22°C) and humidity (55 ± 5%) in a controlled room with a 12–12 h light-dark cycle, where the diet and water were available *ad libitum*. The rats were acclimatized under these conditions for at least 1 week prior to experiments. All animals were randomly divided into two groups: a treatment group ($n = 10$) which received 1.5 ml/kg body weight carbon tetrachloride (CCl_4; 40% CCl_4 in olive oil) via intraperitoneal injection twice a week for eight weeks and a normal control group ($n = 10$) which received a saline injection in parallel. This study was carried out in accordance with the recommendations of the European Council Directive of the 24th November 1986 (86/609/EEC). All procedures were approved by the Animal Research Ethics Committee at the Medical School of the Southeast University (Nanjing, China).

Histology and Immunohistochemistry

Excised livers were fixed in 10% neutral-buffered formalin, embedded in paraffin, and cut into sections of 5 μm thickness. Slides were then deparaffinized with dimethylbenzene, dehydrated with graded ethanol, and stained with hematoxylin and eosin (H&E) and Masson dyes to evaluate the degree of liver fibrosis.

For immunohistochemical probing, liver slides were initially boiled in a pressure cooker containing a citric acid buffer (pH 6.0) to retrieve antigens. Then the slides were blocked with 5% BSA and incubated with primary antibodies (**Table 1**) overnight at 4°C, and with a goat anti-rabbit biotinylated secondary antibody for 20 min at 37°C. Immunolabels were detected with 3, 3-Diaminobenzidine (DAB), after which the nuclei were counterstained with hematoxylin. Slides were inspected under a fluorescence microscope at 200× magnification. For quantification analysis, the percentage of positive area for immunohistochemistry was determined using ImageJ software.

Cell Cultures and Hypoxia Treatment

AML12 (alpha mouse liver 12 cells) and HSC-T6 (rat hepatic stellate cells) were purchased from the Shanghai Institute of Biochemistry and Cell Biology. Cells were cultured in DMEM-F12 (Hyclone, USA) supplemented with 10% heat-inactivated fetal bovine serum (Bioind, Israel), and were maintained in a humidified atmosphere with 5% CO_2 at 37°C. For hypoxic exposure, AML12 cells were incubated in a tri-gas incubator (Thermo, America) of 1% O_2, 5% CO_2, and 94% N_2. Serum-free "conditioned medium" (CM) was obtained from the supernatant of AML12 cells to eliminate the influence of serum cytokines. HSC-T6 cells were cultured in CM and the cells cultured in DMEM were used as control.

TABLE 1 | The antibody for immunohistochemistry and western blot.

Antibody	Manufacturer	Cat. No.
HIF-1α	Abcam	ab179483
HIF-2α	Abcam	ab179825
PHD1	Abcam	ab108980
Nrf2	Abcam	ab137550
Keap1	Proteintech	10503-2-AP
α-SMA	Proteintech	14395-1-AP
COL1A1	Bioworld	BS60771-25
TGF-β1	Bioworld	BS1361
VEGF-A	Proteintech	19003-1-AP
IGF-1	Bioworld	BS2909
GAPDH	Bioworld	AP0063

RNA Isolation and Quantitative Real-Time Polymerase Chain Reaction

Total RNA was extracted from cells with Trizol reagent (TaKaRa, Japan). Then, 1 μg RNA was added to a 20 μl reaction volume for cDNA reverse transcription using the Prime Script™ RT reagent Kit with gDNA Eraser (TaKaRa, Japan), and quantitative real-time polymerase chain reaction (qRT-PCR) was performed using the BR® Premix Ex Taq™ (TaKaRa, Japan) in a Step One Plus real-time PCR system (Applied Biosystems, USA). Gene expression was quantified according to the $2^{-\Delta\Delta Ct}$ method. All PCR primers are listed in **Table 2**.

Protein Extraction and Western Blot

Cells were lysed with RIPA buffer (Beyotime, China) containing a Protease Inhibitor Cocktail (Roche, Germany) and then centrifuged at 12,000 × g for 15 min at 4°C. Equal amounts of protein were separated via gel electrophoresis and transferred to a PVDF membrane (Millipore Corp, USA). Membranes were blocked with 5% skimmed milk for 1 h at 37°C and incubated with primary antibodies (**Table 1**) overnight at 4°C and then with corresponding secondary antibodies for 1 h at 37°C. The blotting signal was visualized using enhanced chemiluminescence reagent (HaiGene, China). Final protein levels were normalized to that of GAPDH.

TABLE 2 | Primer sequences for quantitative PCR.

Specie	Genes	Forward sequence (5′–3′)	Reverse sequence (5′–3′)
Mouse	Keap1	TGCCCCTGTGGTCAAAGTG	AGTCCTTGGAGTCTAGCCGAG
	Nrf2	TCTTGGAGTAAGTCGAGAAGTGT	GTTGAAACTGAGCGAAAAAGGC
	PHD1	AGTCCTTGGAGTCTAGCCGAG	GGTTCGGTTACCGTCCTGC
	HIF-1α	GATGACGGCGACATGGTTTAC	CTCACTGGGCCATTTCTGTGT
	HIF-2α	TCCTTCGGACACATAAGCTCC	GACAGAAAGATCATGTCACCGT
	COL1A1	GCTCCTCTTAGGGGCCACT	CCACGTCTCACCATTGGGG
	VEGF-A	GCACATAGAGAGAATGAGCTTCC	CTCCGCTCTGAACAAGGCT
	TGF-β1	CTCCCGTGGCTTCTAGTGC	GCCTTAGTTTGGACAGGATCTG
	IGF-1	CACCCTGTGACCTCAGTCAA	CAAGGGTTCTGATGTTGCAC
	GAPDH	TGGCCTTCCGTGTTCCTAC	GAGTTGCTGTTGAAGTCGCA
Rat	COL1A1	GTACATCAGCCCAAACCCCA	CAGGATCGGAACCTTCGCTT
	α-SMA	GGAGATGGCGTGACTCACAA	CGCTCAGCAGTAGTCACGAA
	TGF-β1	AGGGCTACCATGCCAACTTC	CCACGTAGTAGACGATGGGC
	VEGF-A	CGGGCCTCTGAAACCATGAA	GCTTTCTGCTCCCCTTCTGT
	IGF-1	CAGTTCGTGTGTGGACCAAG	TCAGCGGAGCACAGTACATC
	GAPDH	GAAGGGCTCATGACCACAGT	GGATGCAGGGATGATGTTCT

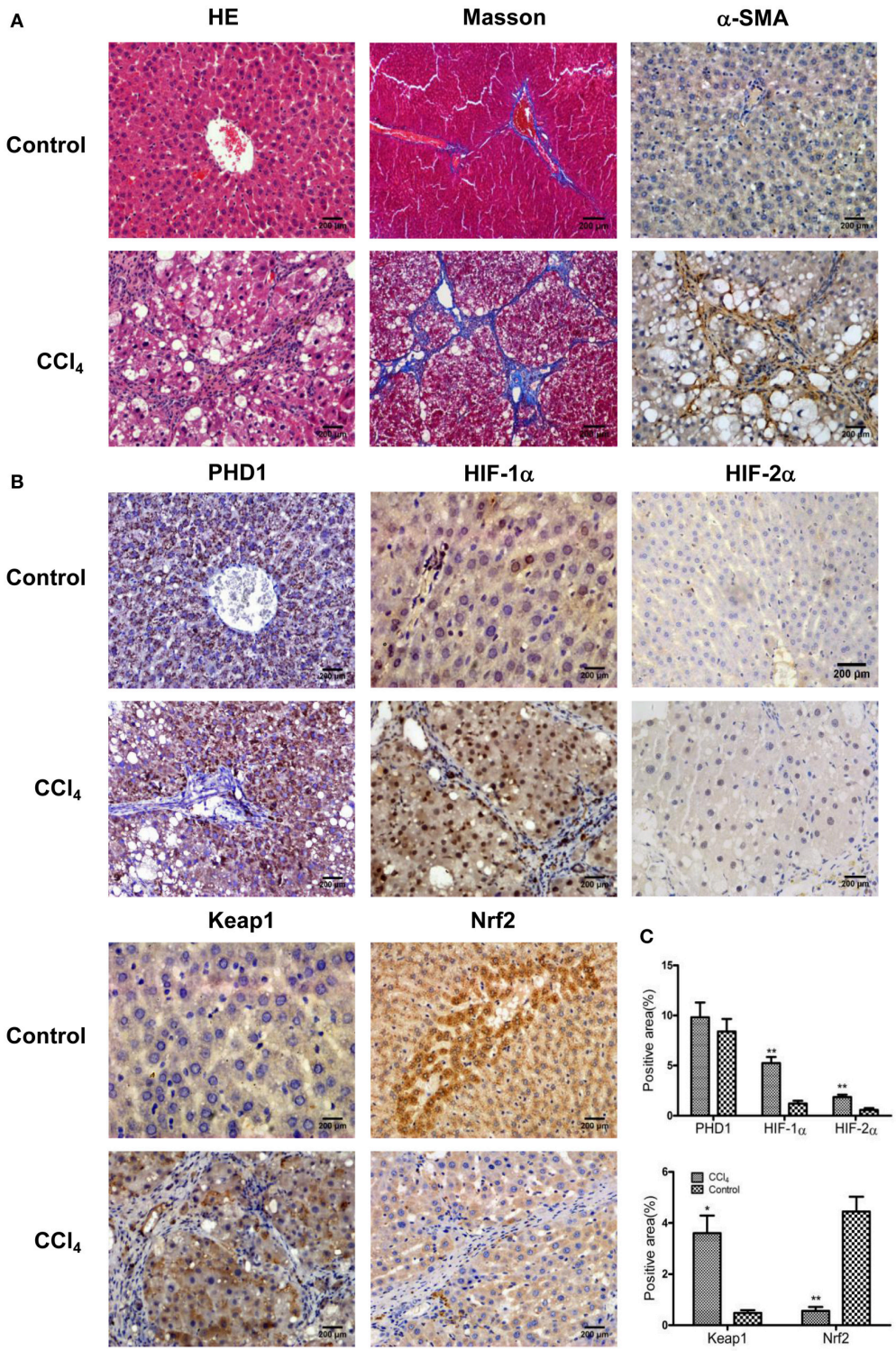

FIGURE 1 | CCl_4 upregulated the expression of Keap1, HIF-1α, and HIF-2α but decreased Nrf2 in the liver tissues. Hepatic morphology as evaluated by H&E and Masson staining **(A)**. The expression of α-SMA **(A)**, PHD1, HIF-1α, HIF-2α, Keap1, and Nrf2 **(B)** were measured by immunohistochemical staining. The percentage of positive area were quantified **(C)**. The scale bar represents 200 μm. $^{*}p < 0.05$, $^{**}p < 0.01$ vs. control.

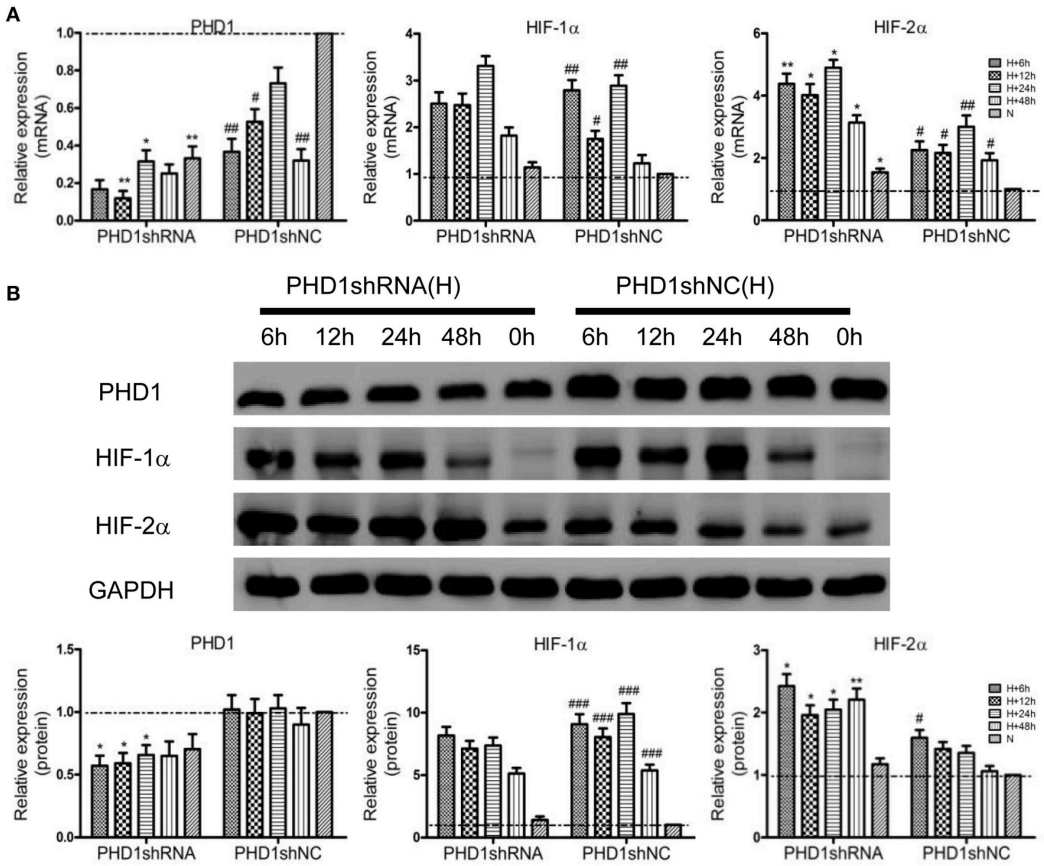

FIGURE 2 | PHD1shRNA upregulated the expression of HIFs in hypoxic AML12 cells at various time interval between 0–48 h. (A) mRNAs and **(B)** proteins levels of PHD1, HIF-1α and HIF-2α were measured by qRT-PCR and western blot, and GAPDH was used as the internal standard, $n = 3$. $^{*}p < 0.05$, $^{**}p < 0.01$ vs. shNC at equivalent time interval, $^{\#}p < 0.05$, $^{\#\#}p < 0.01$, $^{\#\#\#}p < 0.001$ vs. shNC under normoxia. N, normoxia; H, hypoxia.

Malondialdehyde (MDA), Reduced Glutathione (GSH) Levels, and Lactate Dehydrogenase (LDH) Activity Assay

MDA and GSH levels were detected in total cell lysates via commercial assay kits (Jian Cheng Bioengineering Institute, China). All levels are expressed as μmol/g protein. For detection of LDH activity, supernatants were collected and analyzed with the LDH assay kit (Jian Cheng Bioengineering Institute, China). LDH activity is expressed as U/L.

Enzyme-Linked Immunosorbent Assay for Collagen Secretion

The level of alpha-1 type I collagen (COL1A1) in the supernatants of AML12 cells was determined using a commercial enzyme-linked immunosorbent assay (ELISA) kit (Hengyuan Biology, China) according to the manufacturer's protocol. The optical density was measured at a wavelength of 450 nm.

Cell Viability Assay

Cellular viability was measured using the cell counting kit-8 (CCK-8) assay (Dojindo, Japan) following the manufacturer's protocol. Absorbance (OD value) was measured at 450 nm using an enzyme-linked immunosorbent assay reader (Thermo Fisher Scientific).

Apoptosis Assay

Cells undergoing apoptosis were stained with the Annexin-V/PI stain (Ebscience, America). For cells that were transfected with plasmids with green and red fluorescence, PI was replaced by DAPI to label apoptosis. A Flow cytometer (Becton Dickinson, USA) was used to quantify apoptotic cells.

Statistical Analysis

Results are expressed as mean ± SEM. One-way ANOVA and the Student's *t*-test were used to evaluate any variations in outcomes between different groups. A p-value < 0.05 was considered as statistically significant.

RESULTS

Hypoxia and Oxidative Stress in the Rats with Liver Fibrosis

To understand the microenvironment in the fibrotic liver tissues, we established CCl_4-induced liver fibrosis rat model. H&E staining showed that CCl_4 exposure resulted in severe damage

of the liver cells, including hepatocytes necrosis, inflammatory cells infiltration, steatosis, and fibrosis connective tissues proliferation. However, the control group presented normal histological morphology (**Figure 1A**). Masson's trichrome staining imparts a blue color to collagen against the red background of other structures. According to the microscopic examination, CCl_4 treatment resulted in an increased collagen deposition around the portal area and formation of septal fibrosis (**Figure 1A**). Furthermore, immunohistochemical staining demonstrated an increased expression of α-smooth muscle actin (α-SMA, a marker of HSC activation, which plays a critical role in liver fibrogenesis) in fibrous septae (**Figure 1A**). These results indicated that the CCl_4-induced liver fibrosis was conducted successfully. Sitmultaneously, we found the upregulation of HIF-1α and HIF-2α (markers of hypoxia), and Keap1 (an intracellular oxidative stress sensor) in hepatocytes in response to CCl_4 treatment (**Figures 1B,C**). However, Nrf2, one of the main downstream molecules of Keap1, was downregulated, while PHD1 showed no obvious change (**Figures 1B,C**).

Effects of PHD1shRNA on HIF Levels in the Hypoxic AML12 Cells

To clarify the function of PHD1 during hypoxia-induced liver injuries, PHD1shRNA was applied to transfect the AML12 cells, then the cells were exposed to hypoxia for 0, 6, 12, 24, and 48 h, the expression of PHD1, HIF-1α and HIF-2α mRNAs and proteins were measured. As shown in **Figure 2A**, PHD1mRNA expression was reduced in hypoxic shNC (negative control) cells compared to that in normoxic shNC cells. Introduction of PHD1shRNA inhibited 60–80% of PHD1 mRNA expression, achieving optimum gene silencing at 12 h of hypoxia. However, PHD1 protein level was invariably reduced by ∼50% regardless of the duration of hypoxia (**Figure 2B**). Under normoxic condition, the expression of HIF-1α and HIF-2α mRNAs (**Figure 2A**) and proteins (**Figure 2B**) were in low expression, and upon exposed to hypoxia, these expression were upregulated. Furthermore, PHD1 silencing further increased the expression of HIF-2α but not that of HIF-1α at both the mRNA and protein levels.

Effects of Keap1shRNA on Nrf2 Level in the Hypoxic AML12 Cells

To clarify the effect of Keap1shRNA, the AML12 cells were transfected with Keap1shRNA and were administrated with hypoxia for 0, 6, 12, 24, and 48 h, then the expression of Keap1 and Nrf2 at the mRNA and protein levels was determined. An 84% reduction in Keap1 mRNA (**Figure 3A**) and 50% reduction in Keap1 protein (**Figure 3B**) levels were observed at 12 h of hypoxia in the cells silenced with Keap1shRNA. As expected, Nrf2 mRNA and protein levels were increased in the hypoxic shNC cells compared to that in the normoxic shNC cells, and the expression of Nrf2 mRNA and protein were further increased in hypoxic cells treated with Keap1shRNA, which peaked at 12 h of hypoxia (**Figures 3A,B**).

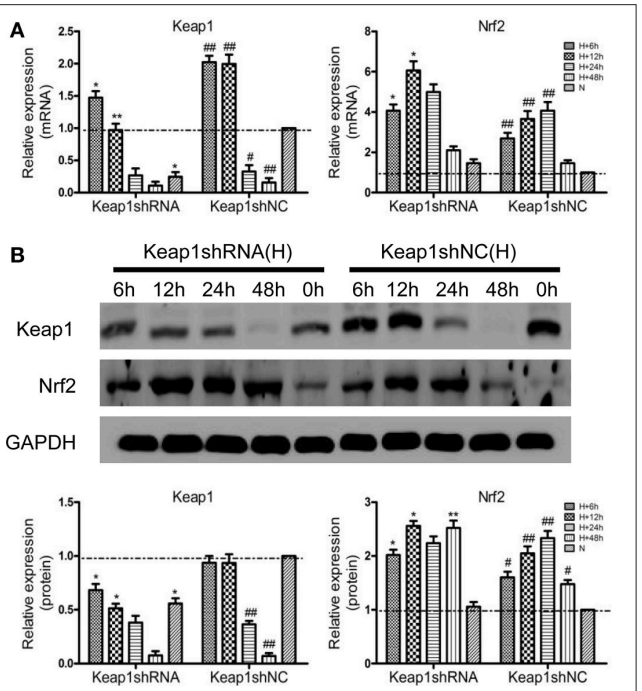

FIGURE 3 | Keap1shRNA upregulated the expression of Nrf2 in hypoxic AML12 cells at various time interval between 0–48 h. (A) mRNAs and **(B)** proteins levels of Keap1 and Nrf2 were assayed by qRT-PCR and western blot, and GAPDH was used as the internal standard, $n = 3$. $^{*}p < 0.05$, $^{**}p < 0.01$ vs. shNC at equivalent time interval, $^{\#}p < 0.05$, $^{\#\#}p < 0.01$ vs. shNC under normoxia. N, normoxia; H, hypoxia.

Effects of PHD1 and Keap1shRNAs on Oxidative Stress in the Hypoxic AML12 Cells

Since hypoxia led to an increase in oxidative stress, we next studied how molecular markers of oxidative stress—MDA and GSH (important lipid peroxidation and endogenous antioxidant marker, respectively) were regulated. The AML12 hepatocytes were co-transfected with PHD1 and Keap1shRNAs, and then were cultured for 12 h under hypoxia. When cells exposed to hypoxia, a dramatic enhancement of MDA was observed, but the treatment of single knockdown of PHD1 or Keap1 suppressed the increase, furthermore, the double knockdown group was more effective in reducing the hypoxia-induced MDA elevation (**Figure 4A**). However, no significant differences in the levels of MDA and GSH between gene knockdown cells and control cells during normoxia (**Figure 4A**), The intracellular GSH concentration presented the inverse correlation with the MDA level (**Figure 4A**).

Effects of PHD1 and Keap1shRNAs on AML12 Cells Viability during Hypoxia

To understand the effects of PHD1 and Keap1 molecules on cell biological behavior, the Annexin V-APC/DAPI double staining was used to analyze cell apoptosis. The results were presented as the sum of the percentage of early apoptotic

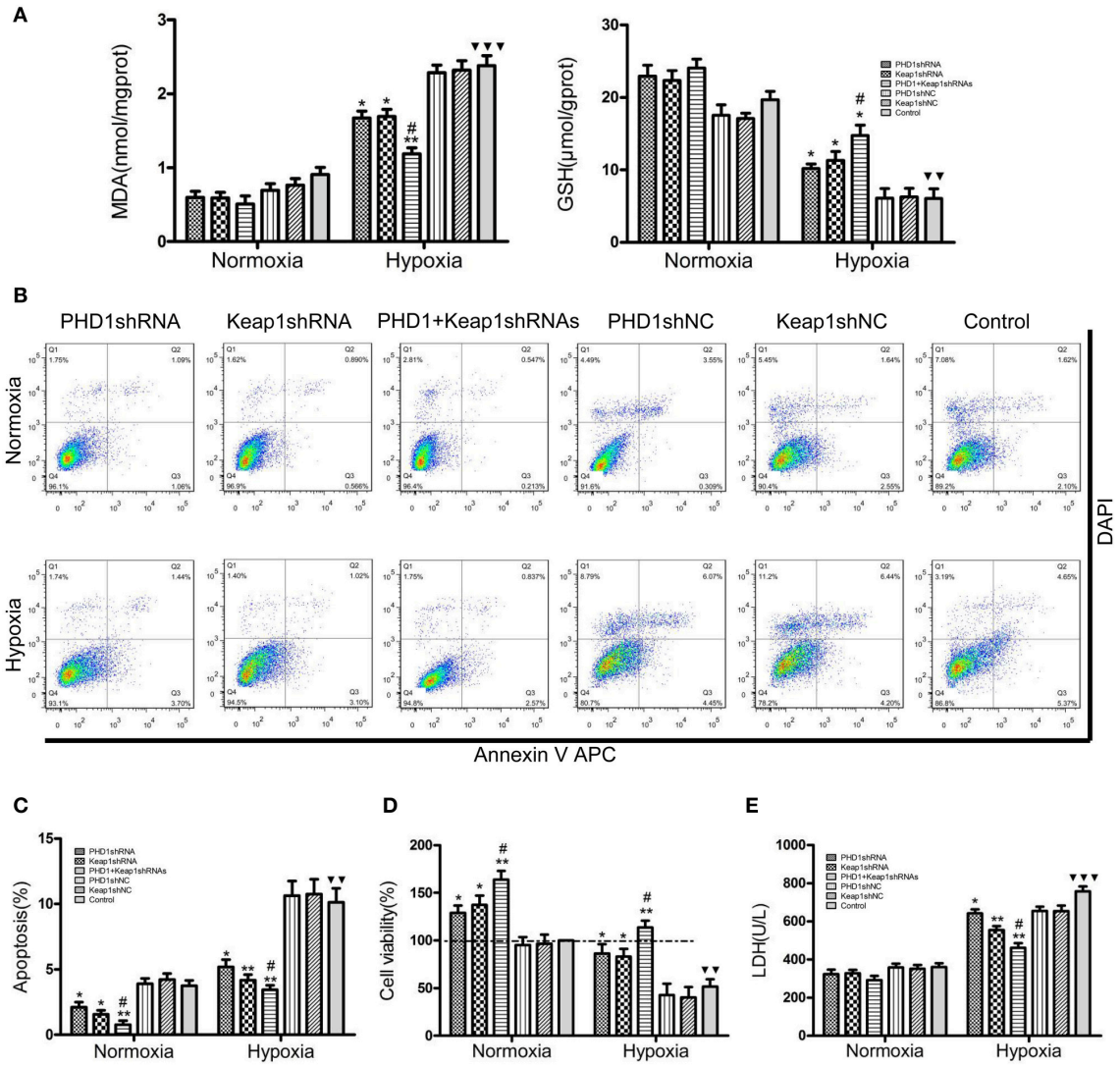

FIGURE 4 | Co-transfection of PHD1 and Keap1shRNAs inhibited oxidative stress and increased cell viability during hypoxia. Co-transfected AML12 cells were exposed to hypoxia for 12 h, and **(A)** intracellular MDA and GSH levels, **(B,C)** Annexin V-APC/DAPI double-stained cells undergoing apoptosis, **(D)** cell viability and **(E)** LDH levels were assessed. Data are expressed as mean ± SEM, $n = 3$. $^{*}p < 0.05$, $^{**}p < 0.01$ vs. respective normoxic and hypoxic control, $^{\#}p < 0.05$ vs. respective single-knockdown normoxic and hypoxic control, $^{\blacktriangledown\blacktriangledown}p < 0.01$, $^{\blacktriangledown\blacktriangledown\blacktriangledown}p < 0.001$ vs. normoxic control.

cells and late apoptotic cells. In **Figures 4B,C**, during hypoxia, the percentage of apoptotic cells in the single PHD1shRNA (6.49 ± 0.50%) or Keap1shRNA (5.86 ± 0.45%) treatment group were notably lower than in the hypoxic control group (10.14 ± 0.79%). Moreover, the apoptotic rate was further reduced in the double-knockdown group (4.63 ± 0.36%). A similar trend among treatment and control groups were also observed during normoxia.

Next, the cell viability was examined using the CCK-8 assay. The data in **Figure 4D** indicated that hypoxia evidently reduced cell viability, however, co-treatment with PHD1 and Keap1 shRNAs led to an increase in cell viability compared to single shRNA transfection. Cellular membrane integrity was analyzed by detecting LDH release. As shown in **Figure 4E**, LDH release in different hypoxia groups fluctuated with a similar tendency as MDA levels. During normoxia, we found no significant difference in LDH levels between the gene silencing and normoxic control groups. In hypoxia, PHD1shRNA or Keap1shRNA treatment group led to a decrease in LDH release, furthermore, the LDH level of the co-transfected group was lower than that of the single groups.

Effects of PHD1 and Keap1shRNAs on the Expression of Pro-fibrogenic Molecules in the Hypoxic AML12 Cells

To clarify the function of PHD1 and Keap1 during fibrogenesis, the expression of some pro-fibrogenic molecules including

COL1A1, transforming growth factor-β1 (TGF-β1), vascular endothelial growth factor-A (VEGF-A), and insulin-like growth factor 1 (IGF-1) was evaluated by qRT-PCR and western blot in the hypoxic AML12 cells. Upon exposure to hypoxia, mRNAs (**Figure 5A**) as well as proteins (**Figures 5B,C**) levels of COL1A1, TGF-β1, VEGF, and IGF-1 were upregulated, but the changes in TGF-β1 and IGF-1 proteins were not statistically significant.

During hypoxia, single knockdown of PHD1 or Keap1 induced the downregulation of mRNAs (**Figure 5A**) and proteins (**Figures 5B,C**) levels of COL1A1, TGF- β1, VEGF-A, and IGF-1 compared to the control. More interestingly, the decrease was further enhanced when PHD1 and Keap1shRNAs were simultaneously introduced. To know whether the release of COL1A1 levels were affected by PHD1 and Keap1shRNAs, an ELISA assay was performed using the AML12 cells culture supernatants. The results showed that the levels of COL1A1 in the supernatants had the same trend of reduction as those in the cell lysates (**Figure 5D**).

Effects of PHD1 and Keap1shRNAs-Treated Hypoxic AML12 Cells on the Expression of Fibrosis-Related Molecules in HSCs

Considering the complex intrahepatic microenvironment, especially the complicated relationship between hepatocytes and HSCs, HSC-T6 cells were cultured in double-knockdown CM to better simulate the *in vivo* local environment, and then the corresponding fibrosis-related molecules were examined at the mRNAs and proteins levels. During hypoxia CM, COL1A1, α-SMA, TGF-β1, VEGF-A, and IGF-1 mRNAs (**Figure 6A**) and proteins (**Figure 6B**) in hypoxic single-knockdown CM were lower than those in the hypoxic control CM, and were further decreased in double-knockdown CM. However, no significant difference in these mRNAs and proteins expression was observed between the PHD1 or Keap1shNC CM and the control CM group.

Effects of PHD1 and Keap1shRNAs-Treated Hypoxic AML12 Cells on Apoptosis and Proliferation of in HSCs

Since double-knockdown CM deregulated the expression of fibrosis-related molecules in HSCs, we next detected how the apoptosis of HSCs was regulated using Annexin V-APC/PI double staining. Apoptosis was increased in hypoxic single-knockdown CM, moreover, the apoptotic rate was further enhanced in both normoxic and hypoxic double-knockdown CM (**Figures 7A–C**). However, there was no significant difference between the knockdown

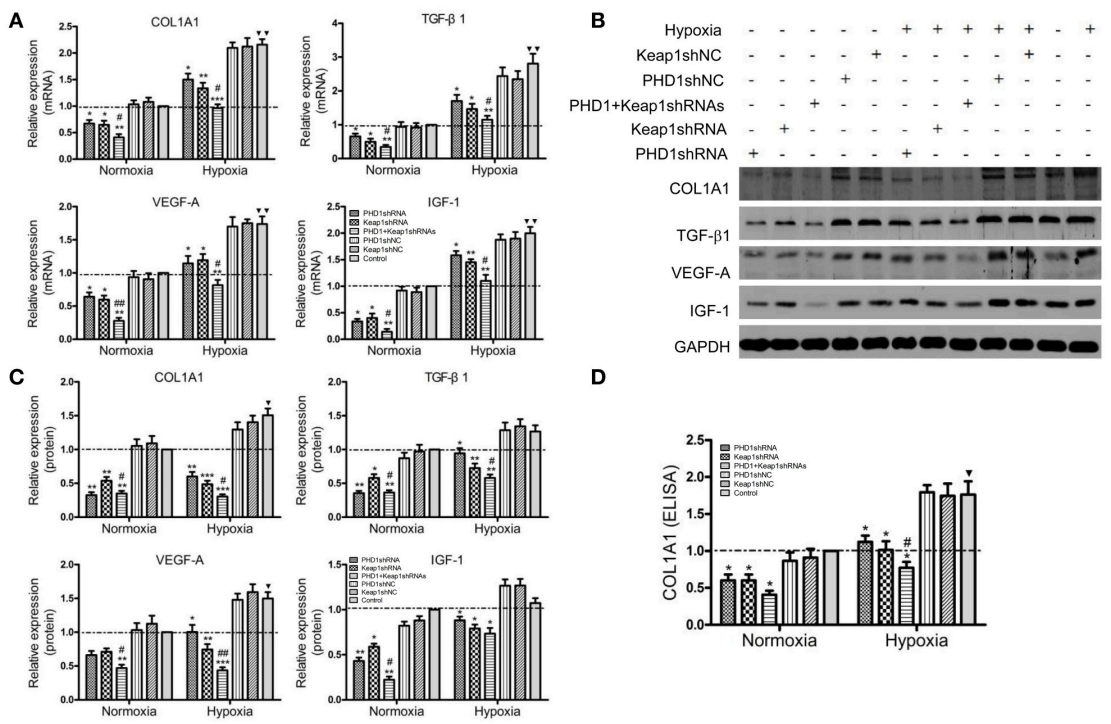

FIGURE 5 | Co-transfection of PHD1 and Keap1shRNAs inhibited expressions of pro-fibrogenic molecules during hypoxia. AML12 cells were co-transfected with PHD1 and Keap1 shRNAs, and then exposed to hypoxia for 12 h. **(A)** mRNAs and **(B,C)** proteins levels of COL1A1, TGF-β1, VEGF-A, and IGF-1 were detected by qRT-PCR and western blot. **(D)** COL1A1 level was measured by ELISA. GAPDH was used as the internal standard, $n = 3$. $^{*}p < 0.05$, $^{**}p < 0.01$, $^{***}p < 0.001$ vs. respective normoxic and hypoxic control, $^{\#}p < 0.05$, $^{\#\#}p < 0.01$ vs. respective single-knockdown normoxic and hypoxic control, $^{\blacktriangledown}p < 0.05$, $^{\blacktriangledown\blacktriangledown}p < 0.01$ vs. normoxic control.

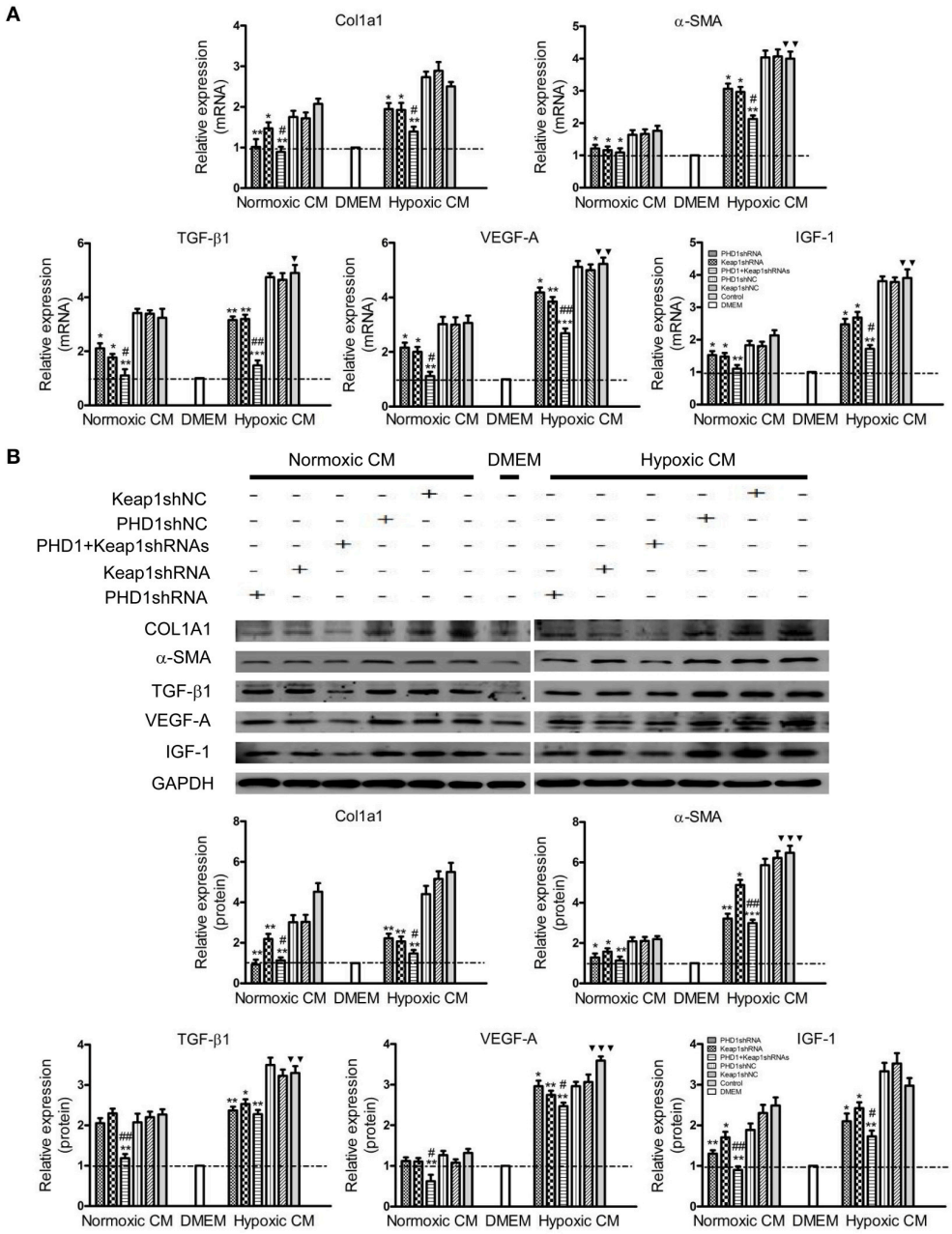

FIGURE 6 | Effects of PHD1 and Keap1shRNAs-treated hypoxic AML12 cells on the expression of fibrosis-related molecules. HSC-T6 cells were cultured in CM obtained from the supernatant of hypoxic PHD1 and/or Keap1 knockdown AML12 cells. **(A)** mRNAs and **(B)** proteins levels of COL1A1, α-SMA, TGF-β1, VEGF-A, and IGF-1 were measured via qRT-PCR and western blot. GAPDH was used as the internal standard, $n = 3$. $^{*}p < 0.05$, $^{**}p < 0.01$, $^{***}p < 0.001$ vs. respective normoxic and hypoxic control CM, $^{\#}p < 0.05$, $^{\#\#}p < 0.01$ vs. respective normoxic and hypoxic single-knockdown CM, $^{\blacktriangledown}p < 0.05$, $^{\blacktriangledown\blacktriangledown}p < 0.01$, $^{\blacktriangledown\blacktriangledown\blacktriangledown}p < 0.001$ vs. normoxic control CM.

CM groups and control CM group in normoxic CM. In addition, **Figure 7D** showed that cells cultured in CM enhanced cell viability compared with cells in DMEM, and the effect was enhanced in hypoxic CM. However, the cell proliferation of the HSC-T6 cells was reduced when cultured in single-transfected CM and was further weakened in the co-transfected CM.

DISCUSSION

In this study, we first successfully established a model of liver fibrosis induced by CCl_4, which is a suitable model for exploring the underlying mechanisms involved in liver fibrosis (Brattin et al., 1985; Lee and Friedman, 2011). By analyzing the liver tissues from model animals with fibrosis, we observed that the

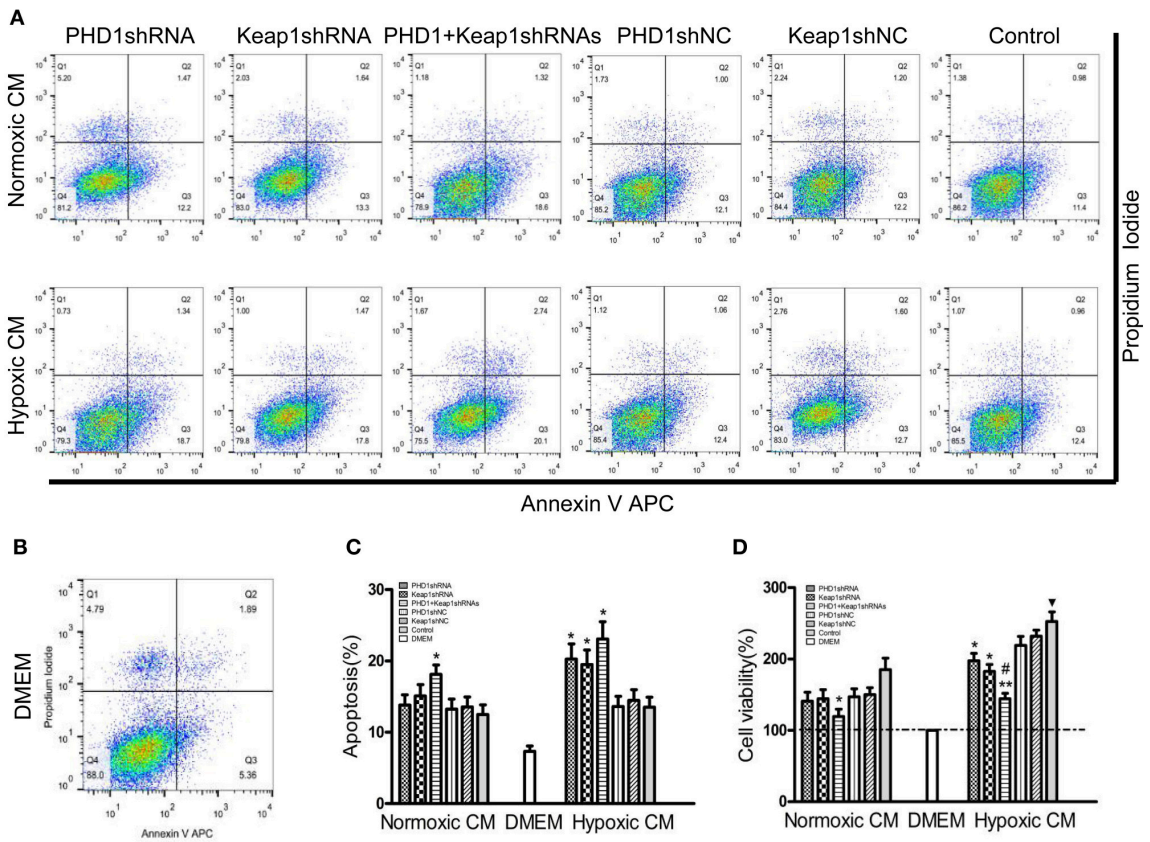

FIGURE 7 | Effects of PHD1 and Keap1shRNAs-treated hypoxic AML12 cells on the apoptosis and proliferation of HSCs. HSC-T6 cells were cultured in the CM obtained from the supernatant of hypoxic PHD1 and/or Keap1 AML12 cells. **(A–C)** AnnexinV-APC/PI double-stained cells undergoing apoptosis. **(D)** Cell viability was assessed by CCK-8 assay. Data are expressed as mean ± SEM, $n = 3$. $^{*}p < 0.05$, $^{**}p < 0.01$ vs. respective normoxic and hypoxic control CM, $^{\#}p < 0.05$ vs. respective normoxic and hypoxic single-knockdown CM, $^{\blacktriangledown}p < 0.05$ vs. normoxic control CM.

molecules related to hypoxia (HIF-1α, HIF-2α) and oxidative stress (Keap1) were increased in hepatocytes, which provided a valid theoretical basis for the *in vitro* research.

Next, to elucidate the underlying mechanisms we chose hepatocytes as the primary target. To simulate the hypoxia *in vitro*, we used 1% oxygen (normoxia with ∼20% oxygen) in the incubators similar to Fingas' study (Fingas et al., 2011). In the hepatocytes, we observed that hypoxia only leads to a decrease in PHD1mRNA but not that of its protein expression, which implied that hypoxia controls the expression of PHD1 only at the transcript level. PHD1 is not only sensitive to oxygen concentration but also vulnerable to ROS generation (Kaelin and Ratcliffe, 2008). Our results also showed that knockdown of PHD1 increased the expression of both HIF-2α mRNA and protein in the hepatocytes, but had no effect on HIF-1α level. These findings were consistent with the previous studies reporting HIF-2α as a major downstream mediator of PHD1 during hypoxia tolerance (Aragones et al., 2008; Schneider et al., 2010) and HIF-1α may be regulated by the PHD2 pathway (Takeda et al., 2007). Furthermore, we found that Keap1shRNA could efficiently suppress Keap1 expression and enhance Nrf2 expression, which suggest that Keap1 negatively regulates Nrf2. Therefore, knockdown of Keap1 is vital for promoting Nrf2-mediated cytoprotection.

Until now, most anti-fibrotic approach researches are focused on either alleviating hypoxia or oxidative stress alone, however, a single treatment have showed an unsatisfactory result with a more side-effects (Halliwell, 2013; Kim and Yang, 2015; Biswas, 2016). Considering the interrelation between hypoxia and oxidative stress, in this experiment we used shRNAs to simultaneously knockdown the expressions of both PHD1 and Keap1 so that one sided dominance of either factor was eliminated. Our data suggest that optimal interference of PHD1 or Keap1 was achieved at 12 h in hypoxic condition, therefore the co-transfected cells were cultured in 1% hypoxia up to this time point. We found that loss of PHD1 or Keap1 reduced oxidative stress by activating GSH and by subsequent inhibition of MDA. Schneider et al. reported that knockdown of PHD1 in the hepatocytes led to reduced oxidative stress (Schneider et al., 2010), and inhibition of Keap1 in the hepatocytes improved the resistance against oxidative stress by upregulating Nrf2 (Miyata et al., 2011), which are also inline with our findings and further supported our data. Importantly, our results indicated that

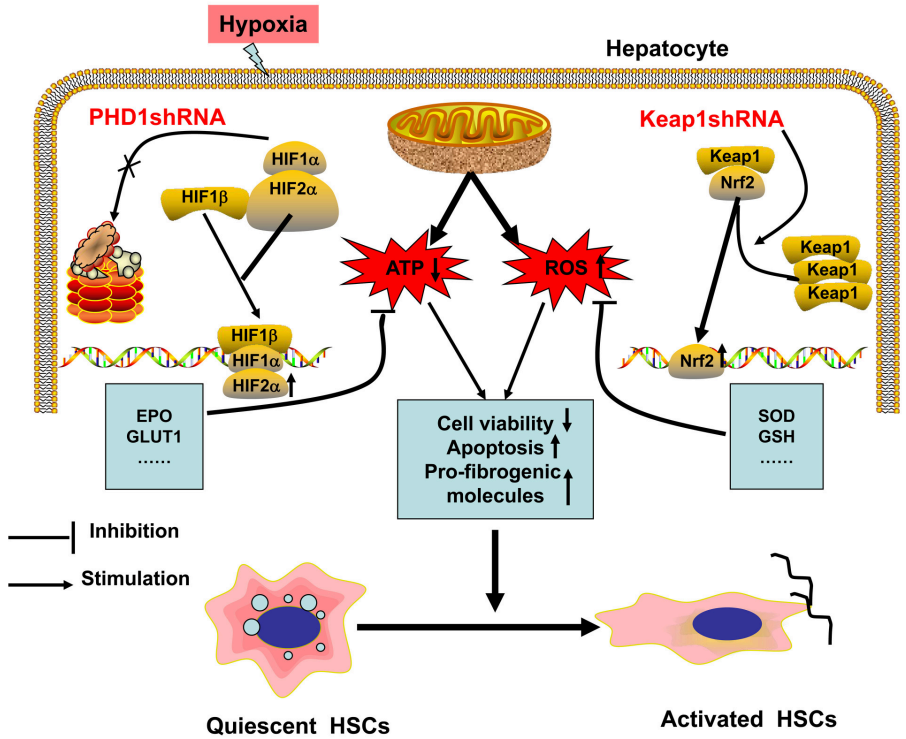

FIGURE 8 | Regulation model of hepatocytes and HSCs in response to hypoxia. When hepatocytes are exposed to hypoxia, mitochondrial ATP production decreases while ROS generation increases, which result in HSCs activation. PHD1shRNA and Keap1shRNA mainly facilitate the translocation of HIF-2α and Nrf2 into the nuclei respectively, where the activation of cytoprotective genes reduce hepatocytes injury and weaken the generation of pro-fibrogenic molecules, which finally inhibit the activation of HSCs.

combined interference of PHD1 and Keap1 had a synergistic effect on the inhibition of oxidative stress.

Previous studies have shown that apoptosis was involved in the pathogenesis of hepatic fibrosis (Hamdy and El-Demerdash, 2012; Klein et al., 2012). In the study, we observed that apoptosis was decreased in the PHD1-knockdown hypoxic hepatocytes, and the anti-apoptotic effect observed was independent of the HIF signal pathway, which may be associated with the activation of NF-κB (Fitzpatrick et al., 2016). Meanwhile, Hamdy et al. reported that Nrf2 inhibited apoptosis via activation of the anti-apoptotic Bcl-2 protein (Hamdy and El-Demerdash, 2012), and we also demonstrated that knockdown of Keap1 could inhibit the apoptosis of hepatocytes. Furthermore, combined knockdown of PHD1 and Keap1 led to stronger anti-apoptotic effects and improved viability of hepatocytes during hypoxia. Indeed, the hypoxia tolerance in the PHD1-knockdown hepatocytes is mainly as the result of the subsequent decrease in glucose oxidation and oxygen consumption.(Aragones et al., 2008; Schneider et al., 2010).

It is well known that cytokines play central roles in liver fibrosis by regulating inflammatary mediators toward various injuries (Marra, 2002). VEGF contributes to the process of liver fibrosis by promoting angiogenesis and activating HSCs (Yoshiji et al., 2003), TGF-β1 plays a critical role in inducing the epithelial-mesenchymal transition of hepatocytes and thereby promoting collagen synthesis (Gressner and Weiskirchen, 2006; Kaimori et al., 2007), and IGF-1 also stimulates collagen synthesis and HSCs proliferation (Scharf et al., 1998). Ma et al. proposed that both HIF-1α and HIF-2α acted as positive regulators of VEGF (Ma et al., 2014), moreover the changes in TGF-β1 expression was in HIF dependent manner (Qu et al., 2015). However, our data indicated that the levels of the pro-fibrogenic molecules—COL1A1, TGF-β1, VEGF-A, and IGF-1 were downregulated in PHD1 knockdown cells during hypoxia, and this may be because TGF-β1 and VEGF-A may also be under regulation of ROS besides HIF (Kuroki et al., 1996; Jobling et al., 2006). In addition, we found that the knockdown of Keap1 could inhibit the expression of pro-fibrogenic molecules. Furthermore, concomitant knockdown of both PHD1 and Keap1 synergistically reduced the expression of pro-fibrogenic molecules, thereby inhibiting the progression of fibrosis, however, the specific mechanism is still unclear.

Hypoxic hepatocytes are capable of promoting the expression of TGF-β1 and VEGF-A, which further activates HSCs (Qu et al., 2015). In addition, hepatocytes undergoing apoptosis and oxidative stress which in turn activates HSCs (Zhan et al., 2006; Subhadip et al., 2011), Therefore, considering the complex intrahepatic microenvironment and the interaction between hepatocytes and HSCs (Ayako et al., 2004), we used CM from the

supernatant of hypoxic hepatocytes to culture HSCs. Our data showed that double-knockdown CM from hepatocytes could suppress the HSCs activation and prevent the progression of fibrosis. Alternatively, prompting apoptosis of activated HSCs may also be an alternative approach to resolve fibrosis (Iredale, 2001). It is worthly noted that double-knockdown CM could induce an increased apoptosis of HSCs, thereby inhibiting their proliferation.

The possible mechanism of hypoxia-induced hepatocytes injury are illustrated in **Figure 8**. Hypoxia is the initiator of this process, and can induce oxidative stress, which decreases the cellular acitivity, enhances apoptosis, promotes expression of pro-fibrogenic molecules, and hence activates HSC. In our study, we have demonstrated that single-knockdown of PHD1 or Keap1 could alleviate hepatocellular hypoxic injury by upregulating the expression of HIF-2α and Nrf2 respectively, which then inhibits the HSC activation (**Figure 8**), moreover, double-knockdown of PHD1 and Keap1 could synergistically enhance this effect. Collectively, these findings will provide new targets for developing new effective clinical drugs to treat liver fibrosis. However, further studies are needed to confirm our hypothesis *in vivo*.

AUTHOR CONTRIBUTIONS

Conceived and designed the experiments: JL, YL, and PC; Performed the experiments: JL, LL, ZW, CS, ZC, XZ, and FD; Analyzed the data and wrote the paper: JL and YL; Revised the paper: YL and PC.

FUNDING

This work was financially supported by the National Nature Science Foundation of China (No 81370868), the Fundamental Research Funds for the Central Universities and the Scientific Research Innovation Program for Graduate Students of Jiangsu Province, China (No KYLX16_0298), and (No KYZZ15_0062).

REFERENCES

Aragones, J., Schneider, M., Van Geyte, K., Fraisl, P., Dresselaers, T., Mazzone, M., et al. (2008). Deficiency or inhibition of oxygen sensor Phd1 induces hypoxia tolerance by reprogramming basal metabolism. *Nat. Genet.* 40, 170–180. doi: 10.1038/ng.2007.62

Ayako, M., Ian, M., Philip, W. S., Paul, A. H., Beth, L. M., Michael, N. T. et al. (2004). Role of hepatic stellate cell/hepatocyte interaction and activation of hepatic stellate cells in the early phase of liver regeneration in the rat. *J. Hepatol.* 40, 910–916. doi: 10.1016/j.jhep.2004.02.005

Begriche, K., Massart, J., Robin, M. A., Borgne-Sanchez, A., and Fromenty, B. (2011). Drug-induced toxicity on mitochondria and lipid metabolism: mechanistic diversity and deleterious consequences for the liver. *J. Hepatol.* 54, 773–794. doi: 10.1016/j.jhep.2010.11.006

Biswas, S. K. (2016). Does the interdependence between oxidative stress and inflmm ation explain the antioxidant paradox? *Oxid. Med. Cell Longev.* 2016:5698931. doi: 10.1155/2016/5698931

Bogdanos, D. P., Gao, B., and Gershwin, M. E. (2013). Liver immunology. *Compr. Physiol.* 3, 567–598. doi: 10.1002/cphy.c120011

Brattin, W. J., Glende, E. A. Jr., and Recknagel, R. O. (1985). Pathological mechanisms in carbon tetrachloride hepatotoxicity. *J. Free Radic. Biol. Med.* 1, 27–38. doi: 10.1016/0748-5514(85)90026-1

Cannito, S., Paternostro, C., Busletta, C., Bocca, C., Colombatto, S., Miglietta, A., et al. (2014). Hypoxia, hypoxia-inducible factors and fibrogenesis in chronic liver diseases. *Histol. Histopathol.* 29, 33–44. doi: 10.14670/HH-29.33

Chen, S., Zou, L., Li, L., and Wu, T. (2013). The protective effect of glycyrrhetinic acid on carbon tetrachloride-induced chronic liver fibrosis in mice via upregulation of Nrf2. *PLoS ONE* 8:e53662. doi: 10.1371/journal.pone.0053662

Fingas, C. D., Bronk, S. F., Werneburg, N. W., Mott, J. L., Guicciardi, M. E., Cazanave, S. C., et al. (2011). Myofibroblast-derived PDGF-BB promotes Hedgehog survival signaling in cholangiocarcinoma cells. *Hepatology* 54, 2076–2088. doi: 10.1002/hep.24588

Fitzpatrick, S. F., Fabian, Z., Schaible, B., Lenihan, C. R., Schwarzl, T., Rodriguez, J., et al. (2016). Prolyl hydroxylase-1 regulates hepatocyte apoptosis in an NF-κB -dependent manner. *Biochem. Biophys. Res. Commun.* 474, 579–586. doi: 10.1016/j.bbrc.2016.04.085

Ghatak, S., Biswas, A., Dhali, G. K., Chowdhury, A., Boyer, J. L., and Santra, A. (2011). Oxidative stress and hepatic stellate cell activation are key events in arsenic induced liver fibrosis in mice. *Toxicol. Appl. Pharmacol.* 251, 59–69. doi: 10.1016/j.taap.2010.11.016

Gressner, A. M., and Weiskirchen, R. (2006). Modern pathogenetic concepts of liver fibrosis suggest stellate cells and TGF-β as major players and therapeutic targets. *J. Cell. Mol. Med.* 10, 76–99. doi: 10.1111/j.1582-4934.2006.tb00292.x

Halliwell, B. (2013). The antioxidant paradox: less paradoxical now? *Br. J. Clin. Pharmacol.* 75, 637–644. doi: 10.1111/j.1365-2125.2012.04272.x

Hamdy, N., and El-Demerdash, E. (2012). New therapeutic aspect for carvedilol: antifibrotic effects of carvedilol in chronic carbon tetrachloride-induced liver damage. *Toxicol. Appl. Pharmacol.* 261, 292–299. doi: 10.1016/j.taap.2012.04.012

Inoue, A., Sawata, S. Y., and Taira, K. (2006). Molecular design and delivery of siRNA. *J. Drug. Target.* 14, 448–455. doi: 10.1080/10611860600845397

Iredale, J. P. (2001). Hepatic stellate cell behavior during resolution of liver injury. *Semin. Liver Dis.* 21, 427–436. doi: 10.1055/s-2001-17557

Jobling, M. F., Mott, J. D., Finnegan, M. T., Jurukovski, V., Erickson, A. C., Walian, P. J., et al. (2006). Isoform-specific activation of latent transforming growth factor β (LTGF-β) by reactive oxygen species. *Radiat. Res.* 166, 839–848. doi: 10.1667/RR0695.1

Kaelin, W. G. Jr., and Ratcliffe, P. J. (2008). Oxygen sensing by metazoans: the central role of the HIF hydroxylase pathway. *Mol. Cell.* 30, 393–402. doi: 10.1016/j.molcel.2008.04.009

Kaimori, A., Potter, J., Kaimori, J. Y., Wang, C., Mezey, E., and Koteish, A. (2007). Transforming growth factor-β1 induces an epithelial-to-mesenchymal transition state in mouse hepatocytes *in vitro*. *J. Biol. Chem.* 282, 22089–22101. doi: 10.1074/jbc.M700998200

Kamura, T., Sato, S., Iwai, K., Czyzyk-Krzeska, M., Conaway, R. C., and Conaway, J. W. (2000). Activation of HIF1α ubiquitination by a reconstituted von Hippel-Lindau (VHL) tumor suppressor complex. *Proc. Natl. Acad. Sci. U.S.A.* 97, 10430–10435. doi: 10.1073/pnas.190332597

Kang, M. I., Kobayashi, A., Wakabayashi, N., Kim, S. G., and Yamamoto, M. (2004). Scaffolding of Keap1 to the actin cytoskeleton controls the function of Nrf2 as key regulator of cytoprotective phase 2 genes. *Proc. Natl. Acad. Sci. U.S.A.* 101, 2046–2051. doi: 10.1073/pnas.0308347100

Kim, S. Y. and Yang, E. G. (2015). Recent advances in developing inhibitors for hypoxiainducible factor prolyl hydroxylases and their therapeutic implications. *Molecules* 19, 20551–20568. doi: 10.3390/molecules201119717

Klein, S., Klosel, J., Schierwagen, R., Korner, C., Granzow, M., Huss, S., et al. (2012). Atorvastatin inhibits proliferation and apoptosis, but induces senescence in hepatic myofibroblasts and thereby attenuates hepatic fibrosis in rats. *Lab. Invest.* 92, 1440–1450. doi: 10.1038/labinvest.2012.106

Kuroki, M., Voest, E. E., Amano, S., Beerepoot, L. V., Takashima, S., Tolentino, M., et al. (1996). Reactive oxygen intermediates increase vascular endothelial

growth factor expression *in vitro* and *in vivo*. *J. Clin. Invest.* 98, 1667–1675. doi: 10.1172/JCI118962

Lee, U. E., and Friedman, S. L. (2011). Mechanisms of hepatic fibrogenesis. *Best. Pract. Res. Clin. Gastroenterol.* 25, 195–206. doi: 10.1016/j.bpg.2011.02.005

Ma, L., Li, G., Zhu, H., Dong, X., Zhao, D., Jiang, X., et al. (2014). 2-Methoxyestradiol synergizes with sorafenib to suppress hepatocellular carcinoma by simultaneously dysregulating hypoxia-inducible factor-1 and -2. *Cancer Lett.* 355, 96–105. doi: 10.1016/j.canlet.2014.09.011

Marra, F. (2002). Chemokines in liver inflammation and fibrosis. *Front. Biosci.* 7, d1899–d1914. doi: 10.2741/a887

Minamishima, Y. A., Moslehi, J., Padera, R. F., Bronson, R. T., Liao, R., and Kaelin, W. G. Jr. (2009). A feedback loop involving the Phd3 prolyl hydroxylase tunes the mammalian hypoxic response *in vivo*. *Mol. Cell. Biol.* 29, 5729–5741. doi: 10.1128/MCB.00331-09

Miyata, T., Takizawa, S., and Van Ypersele De Strihou, C. (2011). Hypoxia. 1. Intracellular sensors for oxygen and oxidative stress: novel therapeutic targets. *Am. J. Physiol. Cell. Physiol.* 300, C226–C231. doi: 10.1152/ajpcell.00430.2010

Mormone, E., Lu, Y., Ge, X., Fiel, M. I., and Nieto, N. (2012). Fibromodulin, an oxidative stress-sensitive proteoglycan, regulates the fibrogenic response to liver injury in mice. *Gastroenterology* 142, 612–621.e5. doi: 10.1053/j.gastro.2011.11.029

Nakanishi, K., Tajima, F., Nakamura, A., Yagura, S., Ookawara, T., Yamashita, H., etal. (1995). Effects of hypobaric hypoxia on antioxidant enzymes in rats. *J. Physiol.* 489 (Pt 3), 869–876. doi: 10.1113/jphysiol.1995.sp021099

Nieto, N., Friedman, S. L., and Cederbaum, A. I. (2002). Cytochrome P450 2E1-derived reactive oxygen species mediate paracrine stimulation of collagen I protein synthesis by hepatic stellate cells. *J. Biol. Chem.* 277, 9853–9864. doi: 10.1074/jbc.M110506200

Nimker, C., Kaur, G., Revo, A., Chaudhary, P., and Bansal, A. (2015). Ethyl 3,4-dihydroxy benzoate, a unique preconditioning agent for alleviating hypoxia-mediated oxidative damage in L6 myoblasts cells. *J. Physiol. Sci.* 65, 77–87. doi: 10.1007/s12576-014-0348-1

Okada, K., Shoda, J., Taguchi, K., Maher, J. M., Ishizaki, K., Inoue, Y., et al. (2009). Nrf2 counteracts cholestatic liver injury via stimulation of hepatic defense systems. *Biochem. Biophys. Res. Commun.* 389, 431–436. doi: 10.1016/j.bbrc.2009.08.156

Qu, K., Yan, Z., Wu, Y., Chen, Y., Qu, P., Xu, X., et al. (2015). Transarterial chemoembolization aggravated peritumoral fibrosis via hypoxia-inducible factor-1α dependent pathway in hepatocellular carcinoma. *J. Gastroenterol. Hepatol.* 30, 925–932. doi: 10.1111/jgh.12873

Rankin, E. B., Rha, J., Selak, M. A., Unger, T. L., Keith, B., Liu, Q., et al. (2009). Hypoxia-inducible factor 2 regulates hepatic lipid metabolism. *Mol. Cell. Biol.* 29, 4527–4538. doi: 10.1128/MCB.00200-09

Scharf, J. G., Knittel, T., Dombrowski, F., Muller, L., Saile, B., Braulke, T., et al. (1998). Characterization of the IGF axis components in isolated rat hepatic stellate cells. *Hepatology* 27, 1275–1284. doi: 10.1002/hep.510270513

Schneider, M., Van Geyte, K., Fraisl, P., Kiss, J., Aragones, J., Mazzone, M., et al. (2010). Loss or silencing of the PHD1 prolyl hydroxylase protects livers of mice against ischemia/reperfusion injury. *Gastroenterology* 138, 1143–1154.e1-2. doi: 10.1053/j.gastro.2009.09.057

Subhadip, G., Ayan, B., Gopal, K. D., Abhijit, C., James, L. B., and Amal, S. (2011). Oxidative stress and hepatic stellate cell activation are key events in arsenic induced liver fibrosis in mice. *Toxicol. Appl. Pharm.* 251, 59–69 doi: 10.1016/j.taap.2010.11.016

Takeda, K., Cowan, A., and Fong, G. H. (2007). Essential role for prolyl hydroxylase domain protein 2 in oxygen homeostasis of the adult vascular system. *Circulation* 116, 774–781. doi: 10.1161/CIRCULATIONAHA.107.701516

Tanaka, Y., Ikeda, T., Yamamoto, K., Ogawa, H., and Kamisako, T. (2012). Dysregulated expression of fatty acid oxidation enzymes and iron-regulatory genes in livers of Nrf2-null mice. *J. Gastroenterol. Hepatol.* 27, 1711–1717. doi: 10.1111/j.1440-1746.2012.07180.x

Yang, J. J., Tao, H., Huang, C., and Li, J. (2013). Nuclear erythroid 2-related factor 2: a novel potential therapeutic target for liver fibrosis. *Food. Chem. Toxicol.* 59, 421–427. doi: 10.1016/j.fct.2013.06.018

Yoshiji, H., Kuriyama, S., Yoshii, J., Ikenaka, Y., Noguchi, R., Hicklin, D. J., et al. (2003). Vascular endothelial growth factor and receptor interaction is a prerequisite for murine hepatic fibrogenesis. *Gut* 52, 1347–1354. doi: 10.1136/gut.52.9.1347

Zhan, S. S., Jiang, J. X., Wu, J., Halsted, C., Friedman, S. L., Zern, M. A., et al. (2006). Phagocytosis of apoptotic bodies by hepatic stellate cells induces NADPH oxidase and is associated with liver fibrosis *in vivo*. *Hepatology* 43, 435–443. doi: 10.1002/hep.21093

Conflict of Interest Statement: The authors declare that the research was conducted in the absence of any commercial or financial relationships that could be construed as a potential conflict of interest.

frontiers in Physiology

ORIGINAL RESEARCH
published: 04 April 2017
doi: 10.3389/fphys.2017.00201

Neurosensory and Cognitive Modifications in Europe's Toughest RandoRaid Competition: the Transpyrénéa Extreme Study

Alessandro Tonacci[1], Simona Mrakic-Sposta[2], Kristian Ujka[1], Francesco Sansone[1], Alice Ferrisi[3], Guido Giardini[4], Raffaele Conte[1] and Lorenza Pratali[1]**

[1] Institute of Clinical Physiology, National Research Council (IFC-CNR), Pisa, Italy, [2] Institute of Bioimaging and Molecular Physiology, National Research Council, Segrate, Italy, [3] Department of Psychology, University of Torino, Torino, Italy, [4] Mountain Medicine Center, Valle d'Aosta Regional Hospital Umberto Parini, Aosta, Italy

Introduction: Given the wide proliferation of ultra-long endurance races, it is important to understand the physiological response of the athletes to improve their safety. We evaluated the cognitive and neurosensory effects on ultra-endurance athletes during the Transpyrénéa (866 Km, 65,000 m positive slope), held on the French Pyrenees.

Materials and Methods: 40 athletes were enrolled (age 43.8 ± 8.8 years; 36 males). Olfactory and cognitive tests were performed before the race (T0, $n = 40$), at 166 kms (T1, $n = 28$), at 418 kms (T2, $n = 20$), and after the race (T3, 866 kms, $n = 13$). The effect of dehydration and sleep deprivation on cognitive features were also studied.

Results: Olfactory function decreased during the race (T0: 24.9 ± 4.3 vs. T3: 22.8 ± 3.5, z = -2.678, $p = 0.007$), language fluency increased (T0: 10.8 ± 2.9; T1: 11.4 ± 2.7; T2: 12.9 ± 2.8; T3: 12.9 ± 3.0; $\chi^2 = 11.132$, $p = 0.011$ for combined samples), whereas the Trail Making Test did not show any changes between pre- and post-race (T0 vs. T3 $p = 0.697$ for TMT-A, $p = 0.977$ for TMT-B). The mean aggregate sleeping time was 9.3 ± 5.4 h at T1, 22.4 ± 10.0 h at T2, 29.5 ± 20.5 h at T3, with a correlation with olfactory function ($r = 0.644$, $p = 0.018$), while Total Body Water (TBW) was not correlated with olfactory or cognitive scores.

Conclusion: Physical activity and sleep restriction in ultra-endurance could transiently affect olfactory function, while verbal fluency improved, demonstrating a dissimilar mechanism of activation/deactivation in different cortical areas. Body water loss was uncorrelated to cognition. Further studies should clarify whether cognitive and sensory deficits occur even in absence of sleep restriction.

Keywords: cognition, extreme physiology, neurosensory assessment, olfaction, smell

OPEN ACCESS

Edited by:
Enrico Capobianco, University of Miami, USA

Reviewed by:
Jie Liu, Tangdu Hospital, Fourth Military Medical University, China
Rimoldi Stefano, University Hospital Bern, Switzerland

****Correspondence:***
Alessandro Tonacci
atonacci@ifc.cnr.it
Lorenza Pratali
lorenza@ifc.cnr.it

Specialty section:
This article was submitted to Integrative Physiology, a section of the journal Frontiers in Physiology

Received: *28 November 2016*
Accepted: *20 March 2017*
Published: *04 April 2017*

Citation:
Tonacci A, Mrakic-Sposta S, Ujka K, Sansone F, Ferrisi A, Giardini G, Conte R and Pratali L (2017) Neurosensory and Cognitive Modifications in Europe's Toughest RandoRaid Competition: the Transpyrénéa Extreme Study. Front. Physiol. 8:201. doi: 10.3389/fphys.2017.00201

INTRODUCTION

RandoRaids are competitions that can be considered a mix between the so-called "Chemin Solidaires," the "Grandes Randonnées" and the Non-Stop Raid Nature, often conducted in semi-self-sufficiency and run for extremely long distances. Differently from ultra-trail marathons, RandoRaids are largely conducted in independence by the raiders, and cover longer distances.

Often completed in times that are somewhat similar to the ultra-trail marathon [the minimum average speed to complete the Tor des Géants ultra-trail (330 Km) is 2.2 km/h, while this value is set to 2.165 km/h for the Transpyrénéa RandoRaid (866 Km)], it is reasonable to think that effects on the health status of competitors would be similar to those experienced by the ultra-trailers. To date, various evidence for significant effects on physical (Vitiello et al., 2013) and cognitive functions (Tomporowski, 2002; Cona et al., 2015; Hurdiel et al., 2015; Tonacci et al., 2016) of ultra-trailers has already been observed, mainly caused by a mix of high altitude exposure (Yan, 2014), environmental conditions (Lefferts et al., 2016; Taylor et al., 2016)—including cold, heat and hypoxia—muscular fatigue, dehydration (Cian et al., 2000), and sleep deprivation (Davis et al., 2014; Fullagar et al., 2015).

According to Hurdiel et al. (2015), ultra-trailers experience a wide range of symptoms, ranging from response lags to cognitive tasks to serious symptoms such as visual hallucinations, regardless of rest duration, and time in race. In addition, neurosensory features appear to be affected by a mix of strenuous physical effort and sleep restriction/deprivation, as demonstrated in a recent study held during the Tor des Géants ultra-trail (Tonacci et al., 2016).

Cognitive reserve also turns out to be linked to physical performances, as demonstrated by Cona et al. (2015), which found the correlation between ultra-trailers' physical performances and their neurocognitive functioning, including superior inhibitory control for motor response and for processing of irrelevant information (i.e., emotional stimuli). Such findings are somehow in line with results achieved by Del Percio et al. (2009), which hypothesized a mechanism of neural efficiency ruling the performances of elite athletes also in different sport activities.

However, the cognitive abilities of athletes performing ultra-long distances—and RandoRaids in particular—are not well-explored in scientific literature, and thus present an interesting challenge to be investigated by studies conducted in naturalistic settings.

In particular, focusing on cognitive and neurosensory features, such domains are normally studied via exhaustive tests that take time to administer, so are unsuitable for longitudinal administration during the execution of a competition. However, thanks to surrogate biomarkers and quick-to-administer testing methods, it is possible to retrieve interesting information regarding the cognitive and sensory status of an athlete, even during a strenuous competition such as an ultra-long RandoRaid. The aim of our study was to evaluate the cognitive and neurosensory effects on ultra-endurance RandoRaid athletes during the Transpyrénéa race.

Abbreviations: BMI, Body Mass Index; COWAT, Controlled Oral Word Association Test; CPs, Checkpoints; LBs, Life bases; NTST, Normalized total sleep time; PET, Positron Emission Tomography; SD, Standard Deviation; SPECT, Single-Photon Emission Computed Tomography; SPSS, Statistical Package for Social Science; TBW, Total Body Water; TMT, Trail Making Test; TST, Total sleep time.

MATERIALS AND METHODS

The Transpyrénéa first took place in the summer of 2016 on the French side of the Pyrenees, covering an overall distance of 866 km with 65,000 meters of positive slope throughout the race. The race started near the Mediterranean Sea, in Le Perthus, and ended in Hendaye, on the Atlantic Ocean, following the Grande Randonnée path called GR10. The maximum time to complete the race was set to 400 h, with 22 checkpoints (CPs) and three life bases (LBs, 166, 418, 678 km) along the path.

Subjects

A total of 40 athletes (36 males, mean age: 43.8 ± 8.8 years) participated as volunteers in this study (**Table 1**). Exclusion criteria were the presence of conditions possibly affecting smell (neurodegeneration, history of head trauma, endocrine disorders, flu, and/or nasal problems), use of medications or unwillingness to give informed consent.

This information was retrieved through a structured questionnaire administered to all participants prior to the race. The questionnaire also included questions on hypertension, hypercholesterolemia, diabetes, and smoking, as well as on physical activity.

The study was approved by the institutional Ethics Committee of the Aosta Valley Hospital (n. 895; 31/8/2015) and followed the guidelines of the Helsinki Declaration. All volunteers were informed regarding the design and purposes of the study and gave written informed consent.

Experimental Overview

Four testing sessions were planned for the study. The first session, "Baseline" (T0), took place in Le Perthus (km 0, altitude 420 m above sea level) 1 or 2 days before the race depending on the availability of the athletes. After the first quarter of the race, a second session was held at the LB in Mérens-les-Vals (T1, km 166, altitude 1,060 m above sea level), while at halfway a third session was managed at the LB in Bagnères-de-Luchon (T2, km 418, altitude 640 m above sea level). At the end of the race, in Hendaye (T3, km 866, altitude 0 m above sea level), athletes were evaluated for the fourth time, within an hour of their arrival and concluding any physical effort. All the subjects enrolled were assessed within an hour of concluding the race.

Neurosensory Evaluation: Olfactory Assessment

Olfactory assessment was performed by a simple, reliable odor identification task, Sniffin' Sticks (Burghart Medizintechnik GmbH, Wedel, Germany), already shown to be employable in a naturalistic setting including the ultra-trail marathons (Tonacci et al., 2016).

The test administration was simple: each odor, contained within a felt-tip pen, was placed nearby the nostrils of the volunteer for 3s. The athlete was asked to identify each of the odors presented within a set of four answers each (the correct one and three confounders). In this study, both the "Blue," traditional version of the test (Haehner et al., 2009), and the "Purple Identification Plus" extension (Sorokowska et al., 2015) were employed, so that the number of odors presented to the athletes

TABLE 1 | Study population.

Number of subjects	40
Age (years, mean ± SD)	43.8 ± 8.8
Male gender, n (%)	36 (90)
Height (cm, mean ± SD)	176.1 ± 7.4
Smoking habit, n current/n former smokers (%)	2/4 (5/10)
Diabetes, n (%)	1 (2.5)
Hypertension, n (%)	3 (7.5)
Training, years (mean ± SD)	19.6 ± 15.5
Weekly training (h/week, mean ± SD)	11.5 ± 6.7

was 32, with the test score, ranging from 0 to 32, indicating the overall number of correct answers given.

Cognitive Assessment: Language Control and Executive Function Evaluation

Language assessment was performed in all testing sessions via a shortened version of the Controlled Oral Word Association Test (COWAT; Benton and Hamsher, 1989), chosen for its simple and quick administration, extremely compliant with the time requirements of the athletes undergoing this strenuous competition. Specifically, the COWAT is a verbal fluency test considered to be a measure of executive function. It requires participants to say as many words they can think of which begin with a particular letter of the alphabet, administered within a time limit of 30 s.

A computerized version of the Trail Making Test (TMT) was administered at T0 and at race completion (T3). Intermediate sessions were not included for TMT, as they were time-consuming for the race management of athletes. This cognitive test was performed in its entirety, consisting of two parts, namely TMT-A and TMT-B. Specifically, the first part (TMT-A) assesses cognitive processing speed, attention and sequencing abilities, whereas the second part (TMT-B) is mainly related to executive functions (Bowie and Harvey, 2006). TMT-A requested participants to connect circles labeled with numbers 1–25 in ascending order. In TMT-B, participants should alternate between numbers (from 1 to 13) and letters (from A to L) in an ascending order (i.e., 1-A-2-B and so on).

To ensure full comprehension of the test instructions, participants were provided with computer-based instructions and short test trials.

In this study, the total time needed to complete each of the two tests, their sum and the ratio between TMT-B and TMT-A, known to be an accurate measure of executive functions (Hester et al., 2005), were calculated.

Body Composition Analysis

Several indices related to body composition, including body weight, body mass index (BMI) and total body water (TBW), were measured using the bioelectrical impedance analysis (Tanita SC-331S Body Composition Analyzer; Tanita Inc., ArlingtonHeights, IL, USA). The subjects evaluated had no drink or food restrictions during the race.

Sleep Management Assessment

The number of hours of waking/sleep were asked of each participant with a structured questionnaire. A total sleep time (TST) was then calculated, together with a normalized total sleep time (NTST), as the ratio between TST and race duration, this latter parameter extracted from the official timing of the competition.

Statistical Analysis

Statistical analysis was performed using SPSS17 software (SPSS Inc., Chicago, IL, USA). As a first step, we applied the Shapiro-Wilk test to check for the normality of the variables considered. Since the variables had a non-normal distribution, we employed a non-parametrical multivariate repeated measures analysis of variance (Friedman's test). For *post-hoc* analysis, the Wilcoxon signed-rank test for paired samples was carried out to compare olfaction in the different phases of the competition. Spearman's rank test was used for correlations, in particular concerning olfaction, cognitive parameters, sleep, body composition and race variables (race duration, kms walked, and so forth).

RESULTS

Of the 40 athletes initially enrolled, 28 subjects (25 males; age 43.5 ± 8.5 years) reached Mérens-les-Vals (after an average of 60.0 ± 21.3 h) and were re-evaluated. Twenty of them (17 males, age 44.8 ± 8.7 years) successfully reached Bagnères-de-Luchon after 185.9 ± 23.7 h and were re-assessed, while 13 (11 males; age 43.8 ± 7.6 years) completed the competition in 363.3 ± 33.1 h (**Table 2**).

All the athletes entering the life bases for testing decided to undergo both the olfactory and cognitive assessments. The mean time for the complete test battery administration was 9.5 ± 3.5 min at T0, 7.5 ± 2.3 min at T1 and T2, 9.5 ± 2.4 min at T3.

Olfactory Evaluation

The olfactory performances throughout the race are displayed in **Figure 1**. A slight, non-significant trend toward a decrease in odor identification ability was seen during the race ($p = 0.108$, $\chi^2 = 6.082$ for combined samples). Conversely, the differences between T0 and T1 (z = -2.539, $p = 0.011$), as well as between T0 and T3 ($z = -2.678$, $p = 0.007$) were largely significant, whereas between T1 and T2 ($z = -0.096$, $p = 0.924$) and between T2 and T3 ($z = -0.851$, $p = 0.395$) no particular trend was noticed.

Olfactory function was somehow age-dependent ($r = -0.300$, $p = 0.063$ at T0), but independent from gender (possibly due to the low number of female subjects composing the experimental sample) or training habits. Furthermore, olfactory identification ability at T0 was not an early marker of good success in the race, with no significant differences between finishers and non-finishers ($z = -0.784$, $p = 0.449$) in this task.

Cognitive Assessment

The shortened COWAT test for verbal fluency displayed an increase in the overall score throughout the race ($p = 0.011$, $\chi^2 = 11.132$ for combined samples, **Figure 2**), with trends near significance between T0 and T1 (z = -1.627, $p = 0.104$) and between T1 and T2 ($z = -1.663$, $p = 0.096$) and significance

TABLE 2 | Characteristics of the study population throughout the race (*: significant between T0 vs. T1, °: significant between T0 vs. T3; §: significant for combined samples, at $p < 0.05$).

Variable	T0	T1	T2	T3
Number of subjects	40	28	20	13
Age (years, mean ± SD)	43.8 ± 8.8	43.5 ± 8.5	44.8 ± 8.7	43.8 ± 7.6
Male gender, n (%)	36 (90)	25 (89.2)	17 (85)	11 (84.6)
COMPETITION STATISTICS				
Hours walked (mean ± SD)	0.0 ± 0.0	60.0 ± 21.3	185.9 ± 23.7	363.3 ± 33.1
BODY COMPOSITION ANALYSIS				
Weight (kg, mean ± SD)	72.6 ± 10.9	70.6 ± 9.5	70.3 ± 8.9	68.1 ± 9.8
BMI (kg/m^2, mean ± SD)	23.3 ± 2.6	22.6 ± 2.4	22.9 ± 1.8	21.3 ± 1.6
Fat mass (kg, mean ± SD)	5.4 ± 3.5	3.7 ± 2.2	2.9 ± 2.6	2.3 ± 0.9
Total body water (kg, mean ± SD)	49.2 ± 7.2	49.0 ± 6.4	49.6 ± 5.7	46.2 ± 7.0
SLEEP ANALYSIS				
Total sleep time (hours, mean , SD)	0.0 ± 0.0	9.3 ± 5.4	22.4 ± 10.0	29.5 ± 20.5
Normalized total sleep time (% of the total race time, mean)	0.0	14.9	13.6	9.6
Olfactory identification score (mean ± SD)	24.9 ± 4.3*°	23.3 ± 3.9*	22.6 ± 3.7	22.8 ± 3.5°
Shortened COWAT score (mean ± SD)	10.8 ± 2.9°§	11.4 ± 2.7§	12.9 ± 2.8§	12.9 ± 3.0°§
TMT-A (ms, mean ± SD)	57120.5 ± 36539.0			54540.1 ± 12294.6
TMT-B (ms, mean ± SD)	62676.2 ± 25749.9			62488.6 ± 19303.6
TMT-B/A (ratio, mean ± SD)	1.199 ± 0.450			1.138 ± 0.183

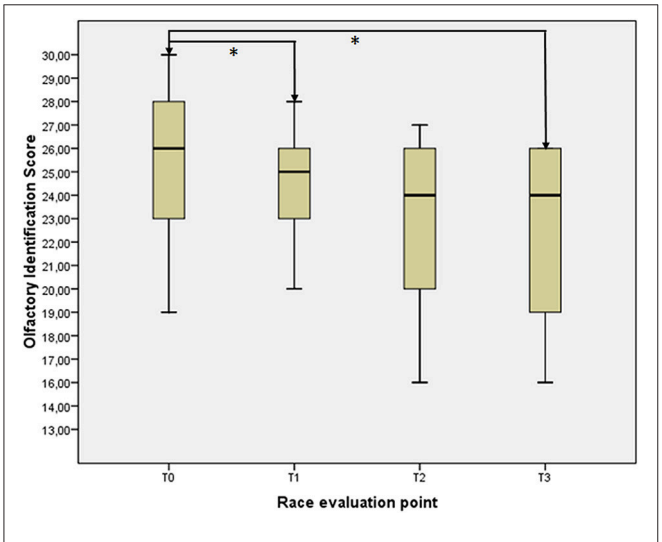

FIGURE 1 | Olfactory performances throughout the race.

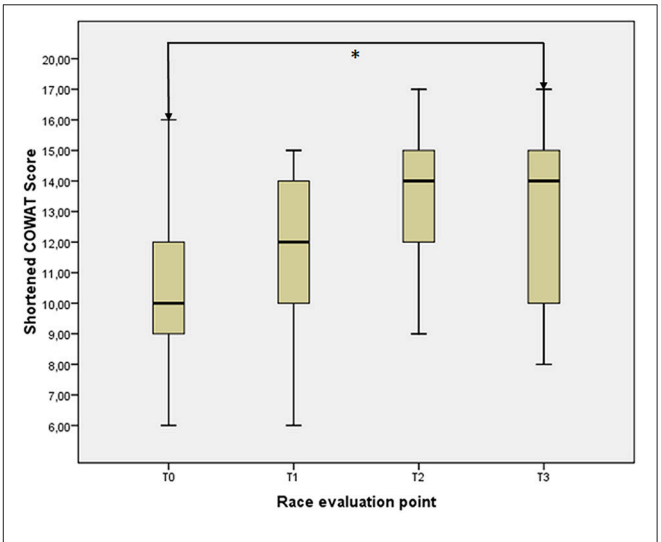

FIGURE 2 | Shortened COWAT test scores throughout the race.

reached when comparing scores at T0 and T3 ($z = -2.742$, $p = 0.006$). On the other hand, no particular difference was seen between T2 and T3 ($z = -0.212$, $p = 0.832$).

Concerning the TMT test, no differences were seen between the two testing sessions (at T0 and T3), with scores at TMT-A ($z = -0.114$, $p = 0.910$), TMT-B ($z = -0.341$, $p = 0.733$) and TMT-B/A ratio ($z = 0.000$, $p = 1.000$) that were superimposable between the two evaluation points.

Correlation between Olfaction and Cognition

A slight correlation was seen between olfactory identification score at T0 and TMT-A score at the same evaluation point ($r = -0.388$, $p = 0.015$), suggesting a possible link between the two domains studied (**Figure 3**). No significant correlation was otherwise found between olfactory function and language fluency.

Not very surprisingly, at T3 language fluency and TMT-B/A ratio were largely correlated ($r = -0.799$, $p = 0.002$), unlike what occurred at T0, where only a small, non-significant trend relating the two variables was observed ($r = -0.241$, $p = 0.164$).

Correlation between Olfaction, Cognition, and Sleep Management

A clear, significant Correlation was found between olfactory decrease throughout the race (between T3 and T0) and both TST

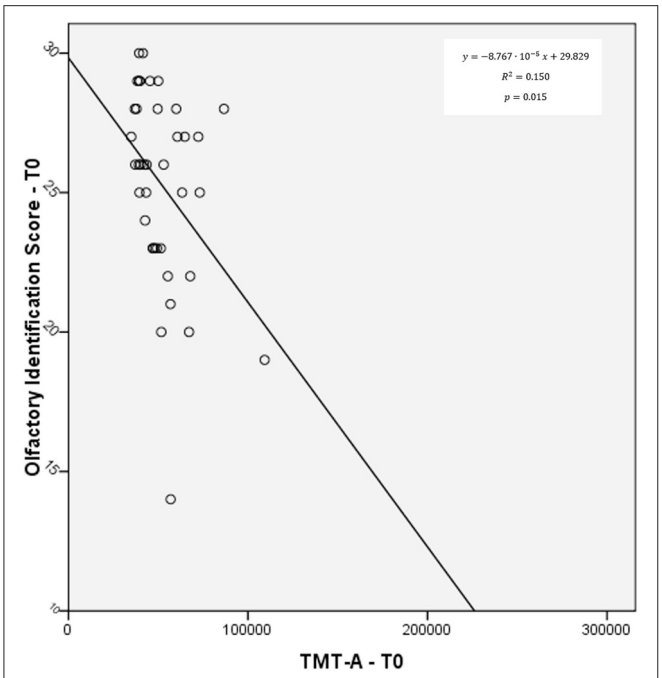

FIGURE 3 | Correlation between olfactory identification and TMT-A at T0.

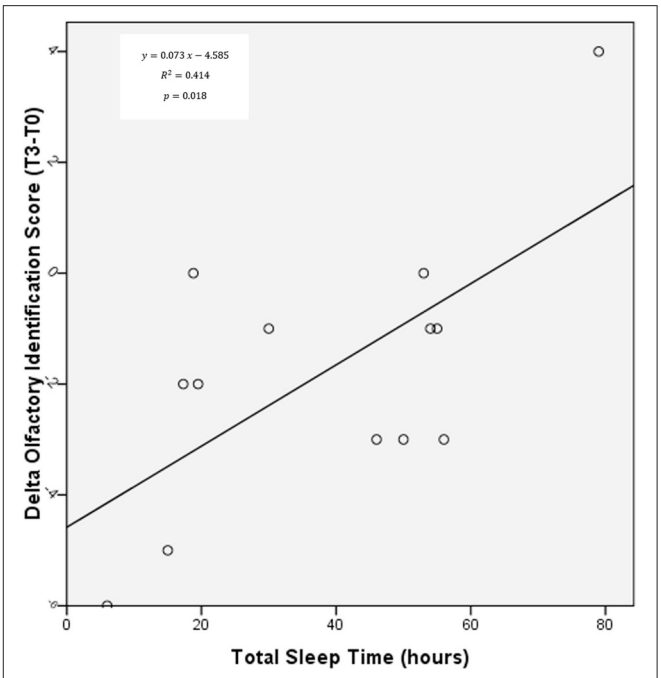

FIGURE 4 | Correlation between olfactory identification delta (calculated between T3 and T0) and TST.

($r = 0.644$, $p = 0.018$, **Figure 4**) and NTST ($r = 0.639$, $p = 0.025$), proving that longer sleep times are more likely to produce smaller decrements in olfactory function during an extreme effort like the Transpyrénéa RandoRaid. No correlations were otherwise seen between TST or NTST and cognitive variables.

Correlation between Olfaction, Cognition, and Body Composition

No significant correlations were found between olfactory or other cognitive scores nor their deltas with body composition variables (body weight, BMI, TBW, and their deltas) at any time.

DISCUSSION

This study investigated olfactory and cognitive modifications occurring during the first-ever edition of the toughest RandoRaid competition in Europe, Transpyrénéa, organized in the French Pyrenees in summer 2016. The study is a completion of a research previously published about the Tor des Géants® mountain ultra-trail marathon (Borghini et al., 2015; Mrakic-Sposta et al., 2015; Tonacci et al., 2016), adding to the referenced studies a deeper insight into cognition and the use of minimally obtrusive methods, shown to be employable in a naturalistic setting, in a completely different competition. In fact, Transpyrénéa is a much longer competition (866 vs. 330 kms) than the previous one, and therefore requires a dissimilar race management concerning sleep/wake cycles, feeding and so forth. Furthermore, environmental conditions and altimetry profiles are not comparable between the two races, thus representing completely different models to be studied.

Focusing in particular on the cognitive and sensory effects that a similar effort could have on athletes' health, several variables should be taken into account. At first, the effort itself should be considered, since prolonged strenuous physical activity could possibly bring on consequences for health, and specifically cognition and sensoriality, in athletes (Tonacci et al., 2016). Second, mechanisms of sleep deprivation or even sleep restriction are likely to deeply impact, possibly in a transient way, the cognitive and sensory features of a person (Fullagar et al., 2015). Such effects seem to be more dramatic when sleep deprivation is combined with a massive physical effort, as occurs in these events (Davis et al., 2014; Hurdiel et al., 2015), also carrying on serious symptoms, including visual hallucination, possibly impacting the safety of athletes.

Third, feeding and all mechanisms of dehydration and missed/unbalanced supply of nutrients (Murray et al., 2009) that could occur in a similar event could possibly be related to a short-term cognitive deficiency. Fourth, altitude (Yan, 2014), hypoxia, heat and cold stress, known to be both task- and severity-dependent, are probably linked to the cognitive and sensory status of an athlete (Ruffini et al., 2015; Taylor et al., 2016) and are experienced by RandoRaid and ultra-trail athletes competing in a race like the Transpyrénéa.

Therefore, this study employed olfactory testing, a minimally obtrusive, quick, user-friendly surrogate of overall cognitive function and a reliable method for assessing a specific sensory domain, along with specific cognitive testing methods to assess the cognition states of 40 athletes competing in the Transpyrénéa.

Four testing sessions were set up, at the departure (T0), after 166 (T1) and 418 kms (T2) and at the finish line (T3). To avoid particular annoyance for the athletes, a complete testing battery was administered at T0 and T3, whereas at T1 and T2 only olfactory testing and COWAT testing for verbal fluency were performed, with the computer version of TMT performed by athletes only at T0 and T3.

Olfaction—at pre-race assessment slightly related to the age of athletes, as already demonstrated (Kobal et al., 2000)—was seen as slightly decreased throughout the race, similarly to that which occurred in athletes at the Tor des Géants® (Tonacci et al., 2016), where a mix of strenuous physical effort and sleep restriction/deprivation negatively affected the olfactory function. Among the possible causes of the abovementioned sensory-cognitive detriment, sleep deprivation (or sleep restriction) was seen to be correlated with the "delta" of olfactory decrease between pre-race and post-race assessment. On the other hand, no particular effects for body composition variables were seen on cognitive domains, probably masked by other, predominant contributions, similarly to what reported during the Tor des Géants (Tonacci et al., 2016). This particular comparison was rarely performed among athletes, even though it was demonstrated that exercise-induced dehydration severely affects cognitive function (Cian et al., 2000). The findings reported by Cian et al. (2000) were referring, however, to dehydrated athletes, while none of our athletes had experienced dehydration as showed by the TBW composition.

Another cognitive domain, language fluency, was otherwise clearly improved during the race, with a similar—and opposite—dynamic when compared to olfaction. Interestingly, the cognitive domains studied with TMT—in particular those more related to the TMT-B score—and not different from each other between pre- and post-race assessment, were correlated with the COWAT score at the post-race assessment.

This different response detected with olfactory and cognitive testing is probably related to a differential activation of several cortical areas in response to stimuli. In fact, it could be stated that during the physical effort of the Transpyrénéa race, some cortical areas are more largely activated by the tasks required of the athlete in order to succeed in the competition, due to the so-called "neural efficiency" hypothesis (Vernon, 1993; Del Percio et al., 2009; Nakata et al., 2010).

This theory is based on psychometric considerations, and was strengthened by several neuroimaging studies using both ionizing radiation- (PET, SPECT) and non-ionizing radiation (fMRI)-based methods. Such research found that the subjects scoring highest on tests such as intelligence quotient, word fluency, spatial skills, and working memory show weaker fronto-parietal activation during cognitive tasks (Haier et al., 1988, 1992, 2004; Parks et al., 1988; Charlot et al., 1992; Rypma and D'Esposito, 1999; Rypma et al., 2002, 2005; Ruff et al., 2003).

Indeed, it is well-known that the cortical structures involved in olfactory identification processing (piriform and entorhinal cortex, amygdala, orbitofrontal cortex, anterior olfactory nucleus) are quite different when compared to the cortical structures called upon by COWAT for language fluency and execution (prefrontal cortex, caudate and subthalamic nuclei) and from the structures involved in tasks such as processing speed and attention (TMT-A) or visuomotor tracking, sequencing and cognitive flexibility (TMT-B).

During ultra-trail marathons or similar competitions, the athlete is called upon to process a number of stimuli that arise from the peculiarities of the race. It can be stated that ability in executing tasks, attention and visuomotor tracking is crucial for the good outcome of several sports activities (Abernethy, 1990; Ferrari and Rizzolatti, 2015), including walking, running or similar activities (Drew et al., 2008), in both good and bad visibility conditions (Durgin and Pelah, 1999). This could be the main reason why TMT and COWAT scores do not decrease throughout the race, and indeed are in some cases enhanced as seen with language fluency, whereas a cognitive pathway related to sensory stimuli, such as the olfactory path, could be somehow sacrificed for the advantage of more important cortical circuitries.

It can be hypothesized that this "double nature" of increasing the activity of some cortical parts while decreasing others that are less useful for the primary task to be accomplished (the competition in this case), could be related to some compensatory mechanisms of the brain, which occur in a wide number of disorders or sports injuries but to date have been reported in only a few studies on healthy athletes (Laurienti et al., 2002; Kudo et al., 2004). This could also be the reason why a correlation between cognitive parameters and sleep restriction was not found, contradicting some literature findings (Fullagar et al., 2015).

Limitations

The main limitation of this study is the absence of information about weather conditions for each athlete. In fact, during a similar competition, held on a route of more than 800 kms, completely different weather conditions were encountered. At the beginning of the race at Le Perthus, the temperature was quite high (around 32 °C), whereas at T1 assessment most of the athletes arrived during a thunderstorm, at night and at around 9°C temperature. However, some of our athletes encountered rainy weather at high altitude (between T1 and T2), whereas other ones were resting during the storms. Therefore, it is nearly impossible to account for the weather conditions for all the athletes, and this could be considered a limitation of this study.

Furthermore, the subjects enrolled ($n = 40$) were a subgroup of participants ($n = 242$ starters) and not necessarily a "representative sample" of the overall athlete population, despite being age- and gender-matched with the overall population participating.

Finally, the bioelectrical impedance analysis for evaluating TBW could be considered in some instances to be a further methodological limitation of the current investigation.

Conclusions

Summarizing, to the best of our knowledge, this is the first study investigating cognitive and neurosensory features in ultra-trailers performing a competition of more than 800 kms. Here, the bout of "psychocognitive stress" experienced by athletes during a strenuous competition such as the Transpyrénéa, where a massive physical effort is combined with sleep restriction (or

for some periods, sleep deprivation), could transiently affect the overall cognitive balance of athletes. Since athletes are mainly required to enhance their attention, visuospatial processing and executive processing overall in order to safely conclude the competition, some other portions of the human cortex could be less stimulated, thus decreasing their activity. This process could occur in areas supervising olfactory processing, decreasing the ability of the subjects to correctly identify odors. According to previous evidence (see Tonacci et al., 2016 for an example), this deficit is probably temporary, with a normal olfactory function that would probably be restored in a few days or weeks, possibly depending on the athlete him/herself.

Future work is required to study similar domains on shorter trails, not massively impacted by sleep deprivation issues, and on competitions with a different altimetry profile, to evaluate the effect of high altitude, cold stress and in some instances hypoxia, on such variables. Furthermore, the cortical activity of the different brain areas mentioned in this work could be an interesting object of study for research involving ultra-trail marathons and similar competitions.

ETHICS STATEMENT

The study protocol was approved by the institutional Ethics Committee of the Aosta Valley Hospital (n. 895; 31/8/2015) and followed the guidelines of the Helsinki Declaration. All volunteers were informed regarding the design and purposes of the study and gave written informed consent.

AUTHOR CONTRIBUTIONS

AT contributed substantially to the conception and design of the work, participated in data acquisition and analysis, as well as in the interpretation of results, drafted the work and approved its version to be submitted. SM contributed substantially to the conception and design of the work, participated in data acquisition and analysis, critically revised the work and approved its version to be submitted. KU contributed substantially to the design of the work, critically revised the work and approved its version to be submitted. FS contributed substantially to the conception of the work, critically revised the work and approved its version to be submitted. AF contributed substantially to the conception and design of the work, participated in data acquisition, critically revised the work and approved its version to be submitted. GG contributed substantially to the conception of the work, critically revised the work and approved its version to be submitted. RC contributed substantially to the conception of the work, critically revised the work and approved its version to be submitted. LP contributed substantially to the conception and design of the work, participated in data acquisition and analysis, as well as in the interpretation of results, drafted and critically revised the work, and approved its version to be submitted. All the authors agree to be accountable for all aspects of the work in ensuring that questions related to the accuracy or integrity of any part of the work are appropriately investigated and resolved.

ACKNOWLEDGMENTS

The authors wish to thank the organization of the Transpyrénéa competition for the possibility of using their structures for testing and for the kind availability of all the staff members. Our heartfelt thanks also go to the Trail Running Movement (TRM) for having supported our research economically. Finally, the authors wish to thank all the volunteers (and their families) who accepted participating in this study even during (and after) this massive effort: they were the "real giants" whose contribution was essential to the success of this research.

REFERENCES

Abernethy, B. (1990). Expertise, visual search, and information pick-up in squash. *Perception* 19, 63–77. doi: 10.1068/p190063

Benton, A. L., and Hamsher, K. (1989). *Multilingual Aphasia Examination. Manual of Instructions, 2nd Edn*. Iowa City, IA: AJA Associates.

Borghini, A., Giardini, G., Tonacci, A., Mastorci, F., Mercuri, A., Mrakic Sposta, S., et al. (2015). Chronic and acute effects of endurance training on telomere length. *Mutagenesis* 30, 711–716. doi: 10.1093/mutage/gev038

Bowie, C. R., and Harvey, P. D. (2006). Administration and interpretation of the trail making test. *Nat. Protoc.* 1, 2277–2281. doi: 10.1038/nprot.2006.390

Charlot, V., Tzourio, N., Zilbovicius, M., Mazoyer, B., and Denis, M. (1992). Different mental imagery abilities result in different regional cerebral blood flow activation patterns during cognitive tasks. *Neuropsychologia* 30, 565–580. doi: 10.1016/0028-3932(92)90059-U

Cian, C., Koulmann, N., Barraud, P. A., Raphel, C., Jimenez, C., and Melin, B. (2000). Influence of variations in body hydration on cognitive function: effects of hyperhydration, heat stress, and exercise-induced dehydration. *J. Psychophysiol.* 14, 29–36. doi: 10.1027//0269-8803.14.1.29

Cona, G., Cavazzana, A., Paoli, A., Marcolin, G., Grainer, A., and Bisiacchi, P. S. (2015). It's a matter of mind! cognitive functioning predicts the athletic performance in ultra-marathon runners. *PLoS ONE* 10:e0132943. doi: 10.1371/journal.pone.0132943

Davis, G. R., Etheredge, C. E., Marcus, L., and Bellar, D. (2014). Prolonged sleep deprivation and continuous exercise: effects on melatonin, tympanic temperature, and cognitive function. *Biomed. Res. Int.* 2014:781863. doi: 10.1155/2014/781863

Del Percio, C., Babiloni, C., Bertollo, M., Marzano, N., Iacoboni, M., Infarinato, F., et al. (2009). Visuo-attentional and sensorimotor alpha rhythms are related to visuo-motor performance in athletes. *Hum. Brain Mapp.* 30, 3527–3540. doi: 10.1002/hbm.20776

Drew, T., Andujar, J. E., Lajoie, K., and Yakovenko, S. (2008). Cortical mechanisms involved in visuomotor coordination during precision walking. *Brain Res. Rev.* 57, 199–211. doi: 10.1016/j.brainresrev.2007.07.017

Durgin, F. H., and Pelah, A. (1999). Visuomotor adaptation without vision? *Exp. Brain Res.* 127, 12–18. doi: 10.1007/s002210050769

Ferrari, P. F., and Rizzolatti, G. (2015). *New Frontiers in Mirror Neurons Research*. Oxford: Oxford University Press.

Fullagar, H. H., Skorski, S., Duffield, R., Hammes, D., Coutts, A. J., and Meyer, T. (2015). Sleep and athletic performance: the effects of sleep loss on exercise performance, and physiological and cognitive responses to exercise. *Sports Med.* 45, 161–186. doi: 10.1007/s40279-014-0260-0

Haehner, A., Mayer, A. M., Landis, B. N., Pournaras, I., Lill, K., Gudziol, V., et al. (2009). High test-retest reliability of the extended version of the "Sniffin' Sticks" test. *Chem. Senses* 34, 705–711. doi: 10.1093/chemse/bjp057

Haier, R. J., Jung, R. E., Yeo, R. A., Head, K., and Alkire, M. T. (2004). Structural brain variation and general intelligence. *Neuroimage* 23, 425–433. doi: 10.1016/j.neuroimage.2004.04.025

Haier, R. J., Siegel, B. V. Jr., MacLachlan, A., Soderling, E., Lottenberg, S., and Buchsbaum, M. S. (1992). Regional glucose metabolic changes after learning a complex visuospatial/motor task: a positron emission tomographic study. *Brain Res.* 570, 134–143. doi: 10.1016/0006-8993(92)90573-R

Haier, R. J., Siegel, B. V., Nuechterlein, K. H., Hazlett, E., Wu, J. C., Paek, J., et al. (1988). Cortical glucose metabolic rate correlates of abstract reasoning and attention studied with positron emission tomography. *Intelligence* 12, 199–217. doi: 10.1016/0160-2896(88)90016-5

Hester, R. L., Kinsella, G. J., Ong, B., and McGregor, J. (2005). Demographic influences on baseline and derived scores from the trail making test in healthy older Australian adults. *Clin. Neuropsychol.* 19, 45–54. doi: 10.1080/13854040490524137

Hurdiel, R., Pezé, T., Daugherty, J., Girard, J., Poussel, M., Poletti, L., et al. (2015). Combined effects of sleep deprivation and strenuous exercise on cognitive performances during The North Face® Ultra Trail du Mont Blanc® (UTMB®). *J. Sports Sci.* 33, 670–674. doi: 10.1080/02640414.2014.960883

Kobal, G., Klimek, L., Wolfensberger, M., Gudziol, H., Temmel, A., Owen, C. M., et al. (2000). Multicenter investigation of 1,036 subjects using a standardized method for the assessment of olfactory function combining tests of odor identification, odor discrimination, and olfactory thresholds. *Eur. Arch. Otorhinolaryngol.* 257, 205–211. doi: 10.1007/s004050050223

Kudo, K., Miyazaki, M., Kimura, T., Yamanaka, K., Kadota, H., Hirashima, M., et al. (2004). Selective activation and deactivation of the human brain structures between speeded and precisely timed tapping responses to identical visual stimulus: an fMRI study. *Neuroimage* 22, 1291–1301. doi: 10.1016/j.neuroimage.2004.03.043

Laurienti, P. J., Burdette, J. H., Wallace, M. T., Yen, Y. F., Field, A. S., and Stein, B. E. (2002). Deactivation of sensory-specific cortex by cross-modal stimuli. *J. Cogn. Neurosci.* 14, 420–429. doi: 10.1162/089892902317361930

Lefferts, W. K., Babcock, M. C., Tiss, M. J., Ives, S. J., White, C. N., Brutsaert, T. D., et al. (2016). Effect of hypoxia on cerebrovascular and cognitive function during moderate intensity exercise. *Physiol. Behav.* 165, 108–118. doi: 10.1016/j.physbeh.2016.07.003

Mrakic-Sposta, S., Gussoni, M., Moretti, S., Pratali, L., Giardini, G., Tacchini, P., et al. (2015). Effects of mountain ultra-marathon running on ROS production and oxidative damage by micro-invasive analytic techniques. *PLoS ONE* 10:e0141780. doi: 10.1371/journal.pone.0141780

Murray, A. J., Knight, N. S., Cochlin, L. E., McAleese, S., Deacon, R. M., Rawlins, J. N., et al. (2009). Deterioration of physical performance and cognitive function in rats with short-term high-fat feeding. *FASEB J.* 23, 4353–4360. doi: 10.1096/fj.09-139691

Nakata, H., Yoshie, M., Miura, A., and Kudo, K. (2010). Characteristics of the athletes' brain: evidence from neurophysiology and neuroimaging. *Brain Res. Rev.* 62, 197–211. doi: 10.1016/j.brainresrev.2009.11.006

Parks, R. W., Loewenstein, D. A., Dodrill, K. L., Barker, W. W., Yoshii, F., Chang, J. Y., et al. (1988). Cerebral metabolic effects of a verbal fluency test: a PET scan study. *J. Clin. Exp. Neuropsychol.* 10, 565–575. doi: 10.1080/01688638808402795

Ruff, C. C., Knauff, M., Fangmeier, T., and Spreer, J. (2003). Reasoning and working memory: common and distinct neuronal processes. *Neuropsychologia* 41, 1241–1253. doi: 10.1016/S0028-3932(03)00016-2

Ruffini, R., Di Giulio, C., Verratti, V., Pokorski, M., Fanò-Illic, G., and Mazzatenta, A. (2015). Adaptation of olfactory threshold at high altitude. *Adv. Exp. Med. Biol.* 837, 19–22. doi: 10.1007/5584_2014_70

Rypma, B., Berger, J. S., and D'Esposito, M. (2002). The influence of working-memory demand and subject performance on prefrontal cortical activity. *J. Cogn. Neurosci.* 14, 721–731. doi: 10.1162/08989290260138627

Rypma, B., Berger, J. S., Genova, H. M., Rebbechi, D., and D'Esposito, M. (2005). Dissociating age-related changes in cognitive strategy and neural efficiency using event-related fMRI. *Cortex* 41, 582–594. doi: 10.1016/S0010-9452(08)70198-9

Rypma, B., and D'Esposito, M. (1999). The roles of prefrontal brain regions in components of working memory: effects of memory load and individual differences. *Proc. Natl. Acad. Sci. U.S.A.* 96, 6558–6563. doi: 10.1073/pnas.96.11.6558

Sorokowska, A., Albrecht, E., Haehner, A., and Hummel, T. (2015). Extended version of the "Sniffin' Sticks" identification test: test-retest reliability and validity. *J. Neurosci. Methods* 243, 111–114. doi: 10.1016/j.jneumeth.2015.01.034

Taylor, L., Watkins, S. L., Marshall, H., Dascombe, B. J., and Foster, J. (2016). The impact of different environmental conditions on cognitive function: a focused review. *Front. Physiol.* 6:372. doi: 10.3389/fphys.2015.00372

Tomporowski, P. D. (2002). Effects of acute bouts of exercise on cognition. *Acta Psychol.* 112, 297–324. doi: 10.1016/S0001-6918(02)00134-8

Tonacci, A., Billeci, L., Tartarisco, G., Mastorci, F., Borghini, A., Mrakic-Sposta, S., et al. (2016). A novel application for cognitive evaluation in mountain ultramarathons: olfactory assessment. *Wilderness Environ. Med.* 27, 131–135. doi: 10.1016/j.wem.2015.11.013

Vernon, P. A. (1993). *Biological Approaches to the Study of Human Intelligence*. Norwood, NJ: Ablex.

Vitiello, D., Rupp, T., Bussière, J. L., Robach, P., Polge, A., Millet, G. Y., et al. (2013). Myocardial damages and left and right ventricular strains after an extreme mountain ultra-long duration exercise. *Int. J. Cardiol.* 165, 391–392. doi: 10.1016/j.ijcard.2012.08.053

Yan, X. (2014). Cognitive impairments at high altitudes and adaptation. *High Alt. Med. Biol.* 15, 141–145. doi: 10.1089/ham.2014.1009

Conflict of Interest Statement: The authors declare that the research was conducted in the absence of any commercial or financial relationships that could be construed as a potential conflict of interest.

frontiers in Physiology

ORIGINAL RESEARCH
published: 25 July 2017
doi: 10.3389/fphys.2017.00527

Enhanced Right-Chamber Remodeling in Endurance Ultra-Trail Athletes Compared to Marathon Runners Detected by Standard and Speckle-Tracking Echocardiography

*Kristian Ujka[1], Luca Bastiani[1], Gennaro D'Angelo[1], Bruna Catuzzo[2], Alessandro Tonacci[1], Simona Mrakic-Sposta[3], Alessandra Vezzoli[3], Guido Giardini[2] and Lorenza Pratali[1]**

[1] Insitute of Clinical Physiology, National Research Council, Pisa, Italy, [2] Mountain Medicine Center, Ospedale Regionale Umberto Parini, Aosta, Italy, [3] Institute of Bioimaging and Molecular Physiology, National Research Council, Milan, Italy

OPEN ACCESS

Edited by:
Enrico Capobianco,
University of Miami, United States

Reviewed by:
Mónica Isa Moreira-Rodrigues,
University of Porto, Portugal
Lucia Venneri,
Royal Brompton Hospital,
United Kingdom

***Correspondence:**
Lorenza Pratali
lorenza@ifc.cnr.it

Specialty section:
This article was submitted to Integrative Physiology, a section of the journal Frontiers in Physiology

Received: 25 November 2016
Accepted: 07 July 2017
Published: 25 July 2017

Citation:
Ujka K, Bastiani L, D'Angelo G, Catuzzo B, Tonacci A, Mrakic-Sposta S, Vezzoli A, Giardini G and Pratali L (2017) Enhanced Right-Chamber Remodeling in Endurance Ultra-Trail Athletes Compared to Marathon Runners Detected by Standard and Speckle-Tracking Echocardiography. Front. Physiol. 8:527. doi: 10.3389/fphys.2017.00527

Background: Strenuous and endurance exercise training have been associated with morphological and functional heart remodeling. Two-dimensional speckle-tracking echocardiography (STE) is a novel technique that allows an accurate quantification of global myocardium deformation. Our aim was to evaluate together left and right cardiac remodeling in different long-distance running athletes: marathon runners (42 km) (M) and endurance mountain runners (>300 Km) (UT).

Methods: A total of 92 athletes (70 males, 76%) including 47 M [age 45 ± 7 years; training: 18 (9–53) years*days/week], 45 UT [age 42 ± 9, training: 30 (15–66) years*days/week] underwent conventional echocardiography and STE (Beyond Diogenes 2.0, AMID) during the agonistic season.

Results: Right ventricle (RV) end-diastolic area ($p = 0.026$), fractional area changing (FAC) ($p = 0.008$) and RV global longitudinal strain (GLS) were significantly increasedin UT athletes. Furthermore, UT showed larger right atrium (RA) volume ($p = 0.03$), reduced RA GLS and significantly increased RA global circumferential strain (GCS) compared to M. After adjustment for age, sex, and HR as covariates, UT showed a reduced RA GLS (OR 0.907; CI 0.856–0.961) and increased RV FAC (OR 1.172; CI: 1.044–1.317) compared to M.

Conclusion: Athletes enrolled in UT endurance activities showed RV and RA morphological and functional remodeling to increased preload in comparison with M runners characterized by increased RV FAC and reduced RA GLS. Follow-up studies are needed to better assess the long-term clinical impact of these modifications. 2D STE is a useful tool for investigating the deformation dynamic in different sports specialties.

Keywords: extreme physiology, endurance sports, cardiac remodeling, speckle tracking echocardiography, cardiovascular diseases

INTRODUCTION

"Athlete's heart" is now a widely acknowledged term indicating a specific phenotype of cardiac morphologic remodeling to long-term physical activity (Fagard, 2003). However, the remodeling may be different among different sports according to the type of hemodynamic (volume and/or pressure) overload (Mitchell et al., 2005). Many studies using two-dimensional (2D) echocardiography have improved our understanding of "athlete's heart." Endurance exercise is a dynamic (aerobic) exercise mainly characterized by volume overload, which induces specific remodeling characterized by left ventricle (LV) and left atrium (LA) dilation and an increased relative wall thickness (RWT) and LV mass without any systolic or diastolic dysfunction (Pelliccia et al., 1991, 2005; Pluim et al., 2000). On the other hand, right ventricle (RV) remodeling has been poorly studied in athletes, mainly due to the complex anatomy and location of the RV, which makes it difficult to study by conventional echocardiography, and to the wide heterogeneity of its function (Jurcut et al., 2010). Some studies have found RV and right atrium (RA) enlargement in elite athletes (Henriksen et al., 1996; Erol and Karakelleoglu, 2002). While in recent years participation in endurance sports has increased, several concerns have been raised about the harmful effects these sports may have on cardiac morphology and function and the risk of cardiac arrhythmias (Calvo et al., 2012; La Gerche et al., 2015).

2-D speckle-tracking echocardiography (STE) is a novel, non-invasive echocardiographic technique that allows an accurate quantification of global myocardium deformation along the three-dimensional (3D) geometrical axis (Teske et al., 2007; Mondillo et al., 2011). STE is a valuable tool for pathophysiological assessment, but still has very limited clinical applications even in patients with cardiovascular disease. Recent studies using STE have improved our understanding of the functional adaption of "athlete's heart." Although there is disagreement as to whether athletes have higher LV strain compared to controls, many studies agree that decreased LV strain in athletes is an early sign of LV dysfunction typically found in patients with hypertensive or hypertrophic cardiomyopathy (Richand et al., 2007; Cappelli et al., 2010; D'Ascenzi et al., 2016). Few authors have studied RV and RA strain in athletes but results are controversial. While some authors showed that RV longitudinal strain was greater in athletes compared to controls (Pagourelias et al., 2013; Esposito et al., 2014), others found reduced RV longitudinal strain in athletes (Teske et al., 2009b). Regarding RA, 2D STE studies showed RA remodeling in elite athletes characterized by increased RA volume, reduced RA strain, and better diastolic function compared to controls (D'Ascenzi et al., 2013; Pagourelias et al., 2013). Controversial results may be due to the lack of standardization among the different STE software algorithms and to the fact that athlete's heart remodeling depends on the type and intensity of training (D'Ascenzi et al., 2016).

The aim of this study was to assess the morphological and functional remodeling of athlete's heart in different long-term intensive endurance athletes (ultra-trail endurance runners and marathon runners), using standard 2D echocardiography and STE.

Abbreviations: 2D, Two-Dimension; LV, Left Ventricle; LA, Left Atrium; RWT, Relative Wall Thickness; RV, Right Ventricle; RA, Right Atrium; STE, Speckle-Tracking Echocardiography; 3D, Three-Dimensional; UT, Ultra-Trail; M, Marathon; BP, Blood Pressure; HR, Heart Rate; SpO_2, Oxygen Saturation; BMI, Body Mass Index; ASE, American Society of Echocardiography; EAE, European Association of Echocardiography; LVMI, LV Mass Index; EF, Ejection Fraction; CO, Cardiac Output; TAPSE, Tricuspid Annular Plane Systolic Excursion; E, Early mitral/tricuspid velocity; A, Atrial mitral/tricuspid velocity; e', Early diastolic velocity; a', Atrial diastolic velocity; sPAP, Systolic Pulmonary Artery Pressure; GLS, Global Longitudinal Strain; GCS, Global Circumferential Strain; GRS, Global Radial Strain; EDA, End Diastolic Area; ESA, End Systolic Area; FAC, Fraction Area Changing; OR, Odds Ratio; ICC, Intraclass Correlation Coefficient.

METHODS

Study Population

Our study population was made of 45 ultra-endurance athletes specialized in ultra-trail running (UT) (>300 km) and 47 marathon runners (42 km) (M) recruited using local advertising. Inclusion criteria were: age 18–65, previous participation in competitive sports of their category, apparent good health status and written informed consent. Exclusion criteria were: known cardiovascular or pulmonary disease or symptoms and absence of informed consent.

The study protocol was approved by the institutional Ethics Committee of the Aosta Valley Hospital (n.895; 31/8/2015) and followed the guidelines of the Helsinki Declaration. All volunteers were informed regarding the design and purposes of the study and gave written informed consent.

Subjects were studied at rest in a quiet, temperature-controlled room. Medical history was collected with particular attention to the assessment of traditional cardiovascular risk factors. Brachial blood pressure (BP) and heart rate (HR) were measured at rest with subject in supine position using an automatic BP monitoring system, while oxygen saturation (SpO_2) was measured using a portable pulsoximeter (Pulse-oximeter Model Tuff-Sat, Datex-Ohmeda, General Electric Healthcare Clinical System, Helsinki, Finland). Three measurements were taken within a 3-min interval and averaged. Body weight, body mass index (BMI), and total body water were measured using the bioelectrical impedance analysis (TanitaSC-331S Body Composition Analyzer; Tanita Inc., Arlington Heights, IL, USA). Training time, expressed as years of training*days of training per week was also assessed and expressed as double product (Training Time = years of training*days/week) while training intensity was estimated as km run per week (km/week).

Standard 2D Echocardiography

Standard 2D echocardiography was performed using a portable echo machine with a 2.5–3.5 MHz cardiac probe (Vivid I, General Electric Healthcare Clinical System). Right and left ventricle function was assessed according to American Society of Echocardiography (ASE) and European Association of Cardiovascular Imaging (EACVI) guidelines for chamber quantification (Lang et al., 2015). Interventricular septum and posterior wall thickness and LV end-diastolic diameter were

measured in parasternal long-axis view and RWT and LV mass index (LVMI) were calculated according to guidelines (Lang et al., 2015). LV end-systolic and end-diastolic volumes were measured in the apical four-chamber view and ejection fraction (EF) was calculated by the modified biplane Simpson's method (Lang et al., 2015). Cardiac Output (CO) was measured multiplying LV outflow tract time-velocity integral, measured using pulse wave Doppler, by its cross-sectional area and heart rate. Right ventricle basal and middle diameters were measured in apical four-chamber view to assess any right ventricle dilation typically found in athletes. RV systolic function was assessed using tricuspid annular plane systolic excursion (TAPSE) measured with caliper in M-mode echocardiography according to ASE+EACVI guidelines for RV function (Rudski et al., 2010).

LV and RV diastolic function were assessed in four-chamber view using pulsed Doppler. Mitral and tricuspid early (E) and atrial (A) velocities were measured using pulsed Doppler and mitral and tricuspid E/A ratio was calculated. Tissue Doppler imaging was measured from the four-chamber view using pulsed-wave Doppler for both mitral and tricuspid annulus. Early (e') and atrial (a') diastolic velocities were measured at the lateral and septal borders of the mitral annulus and at the tricuspid lateral annulus. The ratio between mitral and tricuspid E velocity and e' (E/e') and e'/a' ratio was then calculated (Nagueh et al., 2009; Rudski et al., 2010). Systolic pulmonary artery pressure (sPAP) was estimated from the peak velocity of the tricuspid regurgitation jet by continuous flow Doppler and the systolic RA pressure estimated from the inferior vena cava diameter and its respiratory excursion (0–15 mmHg) using the formula: $sPAP = 4V^2 + RA\ pressure$ (Yock and Popp, 1984).

All 2D echocardiography parameters obtained from the UT and M were compared to normal values according the current recommendations of ASE+EACVI (Lang et al., 2015).

2-D Speckle-Tracking Echocardiography

STE was performed from an apical four-chamber view using a narrow-sector gray scale images for all four chambers, with temporal resolution of 60–90 frames/s. Gain, compression, and dynamic range were optimized to enhance myocardial definition with standardized depth, frequency, and insonation angle for all athletes. 2D strain analysis was performed offline by the same expert sonographer (G.D.), not blinded to the group allocation, using semi-automatic strain software (Beyond Diogenes 2.0, AMID). After a region of interest was manually traced along the endocardial border in end-systole and end-diastole, the software automatically calculated the chamber's volume and global strain along the three axes (longitudinal, radial, and circumferential). LV strain was measured in the apical in the four-chamber view. LV end-systolic and end-diastolic volume and global longitudinal (GLS), radial (GRS), and circumferential (GCS) strain were automatically calculated from the software (Supplementary Figure 1). LA and RA endocardial border was manually traced in four-chamber view and the end-systolic volume and strain along the three axes were calculated. End-systolic (ESA), end-diastolic area (EDA), fractional area changing (FAC), and global RV strain were also measured from an apical four-chamber image focused on the right ventricle.

Statistical Analysis

Statistical analysis was performed using SPSS software version 21.0 for Windows (IBM Corp., Armonk, NY, USA). Continuous variables were expressed as mean ± standard deviation for normally distributed variables and in median and percentiles for non-normally distributed variables, while categorical data were expressed in percentages. *T*-test for independent samples was used to assess differences between means for normally distributed variables while Mann-Whitney Test was used for non-normally distributed variables. Normal distribution was tested using Kolmogorov-Smirnov test. Categorical variables were analyzed using χ^2 test and Fisher's exact test when appropriate. Multiple regression models were made to adjust strain parameters with standard echocardiographic parameters. With the aim of evaluating strain outcomes between the different groups studied (M and UT), a binary logistic regression model with backward step-wise elimination was performed. We defined as dependent variable the group UT (1 = UT; 0 = M). Results are reported as odds ratio (OR) with a 95% confidence interval (adjusted for sex, age, and heart rate). Intra-observer reproducibility was assessed using the intraclass correlation coefficient (ICC). The Posteriori Power Analysis was based on the difference of means of several cardiac indexes (between groups). The Power Analysis for RV GCS with 45 subjects for UT Group and 47 subjects for M Group was 0.82. For RV GLS with 45 subjects for UT Group and 47 subjects for M Group, respectively, the estimated power for a two-sample means test was above 0.60 (0.61).

RESULTS

Demographic and clinical characteristics of the study population are shown in **Table 1**. The groups were comparable for age, sex, and BMI and body surface area. No significant difference in HR or BP was found between the UT and M. The prevalence of diabetes, dyslipidemia and obesity was low and with no difference between groups. Training intensity (Km/week) was not significantly different, while training time (day/week*year) was significantly higher in UT.

2-D Doppler Echocardiography

Standard echocardiography was successfully performed in all subjects (100% feasibility). The main 2D and Doppler parameters are shown in **Table 2**. In Supplementary Table 1 the 2D Doppler echocardiogram parameters were compared to normal values according to American Society of Echocardiography and European association of Cardiovascular Imaging (Lang et al., 2015). The study of LV diastolic function showed a higher mitral E/A ratio and mean e' velocity and a lower of E/e' ratio in UT runners compared to M that can be linked to a reduced LV filling pressure. However, both groups presented normal mitral inflow pattern and normal diastolic function (Supplementary Table 1). RV diameters, RV FAC and TAPSE were significantly increased in UT (**Figure 1**). RV diastolic function was normal in both groups (Supplementary Table 1). However, tricuspid E/A

TABLE 1 | Demographic and clinical characteristics of the study population.

	UT ($n = 45$)	M ($n = 47$)	*P*-value*
Age (years)	42 ± 9	45 ± 8	0.15*
Men (%)	84.4	65.3	0.57§
SBP (mmHg)	133 ± 13	130 ± 19	0.32*
DBP (mmHg)	77 ± 10	77 ± 10	0.83*
Heart Rate (bpm)	55.6 ± 6.9	54.1 ± 7.6	0.86*
BSA (m^2)	1.84 ± 0.16	1.84 ± 0.21	0.88*
BMI (kg/m^2)	22.7 ± 2.4	22.8 ± 2.3	0.79*
TI (km/week)	66.5 ± 39.1	51.8 ± 31.2	0.078#
TT (days/week*year)	30 (15–66)	18 (9–53)	**0.03**#
Hypertension (%)	4.4	6.1	1.00§
Diabetes (%)	0	2	1.00§
Smoke (%)	0	10.2	0.06§
Dyslipidemia (%)	0	6.1	0.24§
Obesity (%)	0	0	α

*SBP, Systolic Blood Pressure; DBP, Diastolic Blood Pressure; BSA, Body surface area; BMI, Body Mass Index; TI, Training Intensity; TT, Training Time. α: χ^2 test was not performed because the variable was constant. *Parametric test (Student's t-test); #Non-parametric test (Mann-Whitney test); §, χ^2 test. Significant p-values ($p < 0.05$) are marked in bold.*

TABLE 2 | Two-dimensional echocardiography and Doppler parameters.

	UT ($n = 45$)	M ($n = 47$)	*P*-value*
RWT	0.37 ± 0.0	0.37 ± 0.04	0.71
LVMI	88.6 ± 17.7	87.5 ± 11.6	0.94
LVEDV (ml)	108 ± 28	114 ± 24	0.25
EF (%)	61.6 ± 6.5	62.6 ± 2.2	0.33
CO (l/min)	4.4 ± 1.3	4.2 ± 1.3	0.52
RV bas (mm)	36.7 ± 3.6	32.1 ± 2.7	**<0.001**
RV mid (mm)	31.9 ± 5.1	27.1 ± 2.0	**<0.001**
RV FAC (%)	43.3 ± 12.5	36.4 ± 6.5	**0.002**
TAPSE	28.0 ± 0.8	24.0 ± 0.4	**<0.001**
E	78 ± 15	78 ± 13	0.82
DT	224 ± 47	238 ± 32	0.10
E/A mitral	1.6 ± 0.5	1.4 ± 0.3	**0.04**
e' mean mitral	12.7 ± 3.2	11.1 ± 1.9	**0.003**
E/e' mitral	5.6 ± 2.9	7.2 ± 1.3	**0.001**
E/A tric	1.8 ± 0.1	1.3 ± 0.3	**<0.001**
E/e' tric	5.5 ± 0.4	4.5 ± 0.2	**0.008**
sPAP (mmHg)	28.6 ± 5.5	24.3 ± 3.7	**<0.001**
mPAP (mmHg)	19.2 ± 3.3	16.6 ± 2.2	**<0.001**
PVR	2.8 ± 1.4	2.4 ± 1.2	0.14
TPR	23.8 ± 7.7	24.6 ± 7.5	0.62
IVC (mm)	19.3 ± 5.4	14.2 ± 2.4	**<0.001**

*LVEDD, Left Ventricle End Diastolic Volume; EF, Ejection Fraction; CO, Cardiac Output; RV bas, right ventricle basal diameter; RV mid, Right Ventricle middle diameter; TAPSE, Tricuspid Annulus Plane Systolic Excursion; sPAP, Systolic Pulmonary Artery Pressure; mPAP, Mean Pulmonary Artery Pressure; PVR, Pulmonary Vascular Resistances; TPR, Total Peripheral Resistances; IVC, Inferior Vena Cava; *Parametric test (Student's t-test). Significant p-values ($p < 0.05$) are marked in bold.*

and E/e' ratio were significantly increased in UT. Moreover, UT athletes showed an increased systolic and diastolic PAP and an increased inferior vena cava diameter compared to M runners. No significant difference in LV systolic function or LV dimension was found between groups.

2-D Speckle-Tracking Echocardiography

STE of the four-chamber view was feasible in 88 out of 92 subjects (95%). Four subjects (two UT and two M) were excluded due to low acoustic window or to inappropriate image acquisition. The main STE parameters are shown in **Table 3**. RV $EDA_{(ste)}$ and RV $FAC_{(ste)}$ (**Figure 2**) were significantly increased in UT compared to M, similarly to the 2D echocardiography results. Moreover, RV GLS was significantly increased in UT (**Figure 2**). UT athletes were also characterized by increased RA volume, reduced RA GLS and an increased RA GCS compared to M runners. Inferior vena cava diameter was found to be an independent predictor of RA GLS ($\beta = 0.204$, $p = 0.04$). Binary logistic regression models were made using a backward step-wise method as shown in **Figure 3**. After being adjusted for age, sex, and HR as covariates, UT showed a reduced RA GLS (OR 0.907; CI 0.856–0.961) and increased RV FAC (OR 1.172; CI: 1.044–1.317) compared to M.

Intra-operator reproducibility for STE was tested for ten subjects, reading the same images as shown in Supplementary Table 2 (Supplementary Material). ICC ranged from 0.714 to 0.990, $p < 0.05$.

DISCUSSION

In this study we evaluated the morphological and functional characteristics of cardiac remodeling in different long-term intensive endurance athletes, UT and M using standard echocardiography and STE. UT showed no significant differences regarding LV and LA volumes or STE measurements. Regarding the right chambers, UT runners showed RV and RA remodeling compared to M runners characterized by increased RV diameters and RA volume in presence of an "enhanced" RV function as indicated by increased RV FAC, TAPSE, RV GLS, RA GCS, and reduced RA GLS. The RV dilation could represent a RV adaption to bradycardia and to the increased venous return, which is associated with increased systolic function, as reported in previous studies (Erol and Karakelleoglu, 2002; D'Andrea et al., 2013; Major et al., 2015).

Moreover, the RV diastolic function, assessed as tricuspid E/A ratio and E/e' ratio, was normal. We also found increased sPAP and mPAP in UT compared to M. The increased PAP is very frequent in athletes and has also been considered a consequence of a physiological adaption to increased venous return and not to LV dysfunction (D'Andrea et al., 2011). In fact, LV E/e', an estimation of LV filling pressure, was not increased in UT while the inferior vena cava was significantly dilated suggesting remodeling due to chronic endurance exercise.

With STE we observed an increased RV $FAC_{(ste)}$ and RV GLS in UT athletes compared to M, confirming the "enhanced" RV systolic function evaluated by 2D echocardiography in UT elite athletes. Moreover, being an UT athlete was found to be an independent significant predictor of having increased RV FAC even after adjusting for age, sex, HR, and other strain covariates compared to M. On the other hand, RV GLS was not significantly different between UT and M when adjustment was made

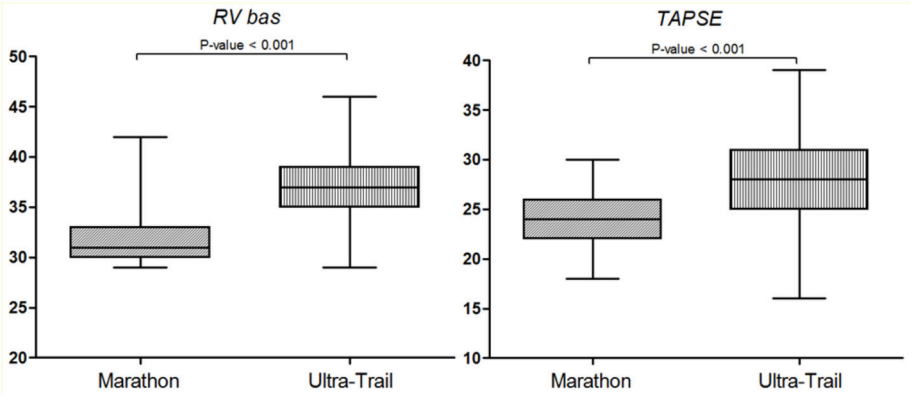

FIGURE 1 | Dot plots showing the difference between groups for RV baseline diameter and TAPSE. RV bas, Right ventricle baseline diameter; TAPSE, Tricuspid annular plane systolic excursion.

TABLE 3 | Two-dimensional speckle tracking derived parameters of the study population.

	UT ($n = 43$)	M ($n = 45$)	*P*-value*
LV $EDV_{(ste)}$	126.3 ± 20.7	117.6 ± 25.8	0.08
LV $EF_{(ste)}$	62.4 ± 3.5	63.3 ± 3.2	0.21
LV $GLS_{(ste)}$	−27.6 ± 4.2	−28.6 ± 3.4	0.25
LV GCS	−28.7 ± 4.8	−29.3 ± 4.6	0.49
LV GRS	66.6 ± 11.2	69.8 ± 8.9	0.13
RV $EDA_{(ste)}$	21.2 ± 4.6	18.8 ± 4.9	**0.026**
RV $FAC_{(ste)}$	49.2 ± 5.9	45.9 ± 5.0	**0.008**
RV GLS	−30.4 ± 4.4	−27.3 ± 4.5	**0.002**
LA $ESV_{(ste)}$	59.7 ± 15.7	59.6 ± 18	1.00
LA GLS	35.0 ± 12.2	36.5 ± 11.1	0.55
LA GCS	26.4 ± 12.5	28.7 ± 11.3	0.39
LA GRS	−32.5 ± 8.5	−34.4 ± 6.9	0.27
RA $ESV_{(ste)}$	63.9 ± 23.2	53.8 ± 17.2	**0.03**
RA GLS	31.6 ± 9.6	37.1 ± 13.5	**0.03**
RA GCS	22.2 ± 8.9	17.5 ± 6.4	**0.004**
RA GRS	−30.3 ± 2.3	−31.2 ± 7.4	0.52

*LV, Left ventricle; RV, Right Ventricle; LA, Left atrium; RA, Right Atrium; EDV, End Diastolic Volume; ESV, End Systolic Volume; EF, Ejection Fraction; GLS, Global Longitudinal Strain; GC, Global Circumferential Strain; GRS, Global Radial Strain; FAC, Fraction Area Changing; *Parametric test (Student's t-test). Significant p-values ($p < 0.05$) are marked in bold.*

for other covariates. These findings suggest an increased RV function in UT athletes, which may represent training-induced remodeling to long-lasting volume overload. In fact, although training intensity was not significantly different between groups, UT showed increased training time.

From strain analysis of RA we found an increased RA volume, a reduced RA GLS and an increased RA GCS among UT athletes. However, when adjustment was made for age, sex, HR, and strain covariates, RA volume and RA GCS were not significantly different, while RA GLS remained independently reduced in UT, suggesting decreased RA systolic contraction in this group of athletes.

In accordance with current literature (D'Andrea et al., 2015), we did not find any significant difference in LV mass, volume or function between athletes. STE-derived parameters were comparable and Tissue Doppler-derived markers of diastolic function were normal in all groups. However, UT athletes showed increased E/A ratio and reduced E/e', indicating a better diastolic function. Furthermore, no significant difference in LA dimensions of function was found between groups.

Physiological Hypothesis of "Enhanced" RV Function in UT

During acute exercise the muscles start to contract, creating compression on the veins and thus increasing the venous flow. The increased venous return to the right heart dilates the RV and RA, and according to the Starling mechanism increases the stroke volume which together with the exercise-induced tachycardia increases the cardiac output able to maintain an adequate perfusion to the muscle (Opie, 1998). Trained athletes, chronically enrolled in dynamic physical activity, undergo many hemodynamic modifications of the heart characterized by increased volume load with a constant or minimal increase of pressure load which induces a LV remodeling characterized by an increased LV mass without any significant increase in wall thickness, known as physiological hypertrophy. The LV hypertrophy is associated with a reduced HR due to parasympathetic tone predominance and an improved diastolic function. However, the remodeling due to the volume load may be even greater on the RV and RA, which has a thinner wall thickness compared to the LV (Opie, 1998; Fagard, 2003). The increased preload together with the longer diastolic filling time due to the bradycardia induce RV and RA dilation. However, despite the resting bradycardia, the athlete's heart is able to maintain cardiac output by increasing the stroke volume, which can explain the present results of RVs enlarged and with increased systolic function in UT athletes compared to M. On the other hand, the resting bradycardia increases the diastole's total duration and in association with higher preload, modifies the diastolic pattern: increasing E mitral wave (early phase of LV diastolic filling), reducing A mitral wave (atrial contribution), and thus increasing the E/A ratio, as we found in UT athletes. Furthermore, the reduced contribution of the atrial systole at rest (A mitral wave) may represent a pattern of

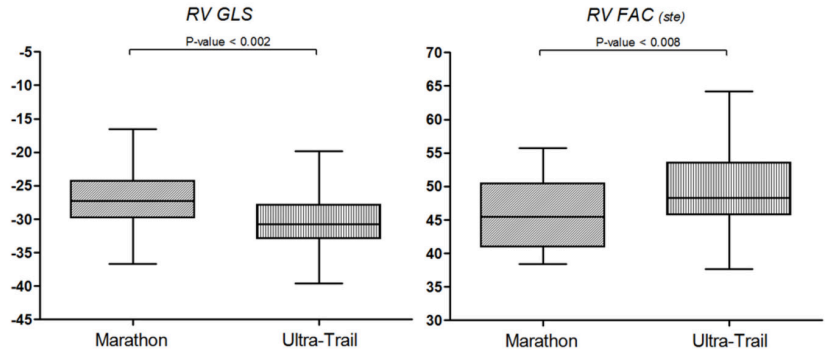

FIGURE 2 | Dot plots showing the difference between groups for RV GLS and RV FAC. RV GLS, Right ventricle global longitudinal strain; RV FAC (ste), Right ventricle fractional area changing.

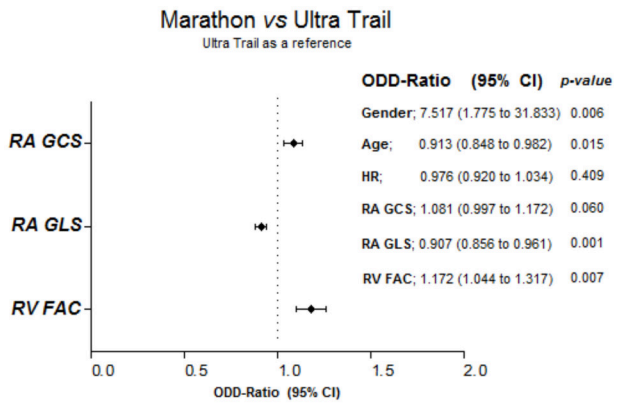

FIGURE 3 | Bimodal logistic regression models. RA, Right Atrium; RV, Right Ventricle; GLS, Global Longitudinal Strain; GCS, Global Circumferential Strain; FAC, Fraction Area Changing; HR, Heart Rate. The non-significant covariates from backward elimination were progressively removed and only the variables shown in the figure remained significant.

atrial remodeling rather than an atrial dysfunction (Opie, 1998; D'Ascenzi et al., 2013). In fact, endurance athletes showed a lower atrial contribution at rest compared to the exercise where the atrial systole contribution to ventricular filling may increase, as a reserve mechanism to afford the increased pre-load.

Comparison with Previous Studies

To understand the real significance of heart remodeling in athletes it is fundamental to differentiate physiological adaptation from inherited cardiomyopathy such as arrhythmogenic right ventricle cardiomyopathy or hypertrophic cardiomyopathy. Recently, many STE studies have focused their attention on assessing RV remodeling in endurance athletes compared to active subjects, showing contradictory results.

Teske and coauthors showed a reduced RV global and regional strain in elite athletes (training intensity 24.2 ± 5.7 h/week) and athletes (training intensity 12.5 ± 2.3 h/week) in comparison with controls, this reduction being more pronounced in athletes with marked RV dilation (Teske et al., 2009b). La Gerche et al. showed that rest RV function was reduced in 40 endurance athletes compared to non-athletes as assessed by 2D and STE, while during exercise the RV strain and strain rate increased progressively with HR without any significant difference between groups, showing no difference in RV contractile reserve (La Gerche et al., 2012). Probably, in presence of RV dysfunction in resting condition in healthy athletes, a further evaluation of RV function during exercise should be employed. Very recently, Bohm et al. studied 33 endurance athletes (including 16 elite athletes) compared with 33 healthy controls. The subjects were studied by cardiopulmonary exercise test, 2D, TDI and Strain echocardiography to assess LV and RV morphology and function, and by contrast enhanced cardiac magnetic resonance. In the final results, although the athletes showed LV and RV enlargement in presence of normal biventricular function, a pathological late enhancement was detected in only one athlete, confirming how LV and RV dilation represents physiological remodeling and is not associated with ventricular dysfunction or risk of arrhythmias (Bohm et al., 2016). The contradictory results of published studies are principally due to the fact that neither the type of athletes (kind of sports, training history, period of evaluation) studied nor the methods used were homogenous, in particular for the differences in strain software analysis. STE can be an useful tool for distinguishing between the RV physiological remodeling found in athletes and arrhythmogenic RV dysplasia (D'Ascenzi et al., 2016), but reference values for LV and RV measured should be published for healthy subjects and for athletes, a wider clinical use (D'Ascenzi et al., 2016). As matter of fact, while both of these conditions may be characterized by the RV dilation (Bauce et al., 2010), patients with arrhythmogenic RV dysplasia have been shown to have reduced RV strain compared to controls (Teske et al., 2009a).

Regarding RA, studies on atrial function in athletes are still very limited. In a recent study, D'Ascenzi et al. studied 100 athletes and 78 controls using STE found an increased RA volume and a reduced RA peak longitudinal strain in athletes compared to controls (D'Ascenzi et al., 2013). More recently, Pagourelias et al. also found increased RA volume and reduced RA early diastolic strain rate without any significant differences in RA function showing RA remodeling to volume afterload (Pagourelias et al., 2013). Our finding are in concordance with these studies regarding RA volume. In this study we found a

reduced RA GLS in UT athletes compared to M in absence of any RV diastolic dysfunction, which seem to represent physiological atrial remodeling to the increased volume load.

The literature on LV strain in athletes is also controversial. Simsek et al. found increased values of GLS in marathon athletes compared to controls (Simsek et al., 2013), while Capelli et al. found no difference in GLS between endurance athletes and controls (Cappelli et al., 2010; Caselli et al., 2015). More recently, Caselli et al. studied 200 Olympic athletes enrolled in different disciplines (including both isometric and endurance sport activities); although being normal, LV GLS was lower compared to controls, with no difference related to the sport discipline (Caselli et al., 2015). Similar results were also found from Richard et al. in professional soccer players (Richand et al., 2007). However, when compared to patients with hypertrophic cardiomyopathy, athletes had increased GLS LV strain (Richand et al., 2007; Cappelli et al., 2010; Butz et al., 2011). Thus, although there is no agreement on whether athletes have increased LV strain compared to controls, authors agree that a reduction in GLS should be considered an early marker of LV systolic dysfunction (D'Ascenzi et al., 2016).

The modifications of LA volume in athletes have been previously reported as a component of "athlete's heart" (Pelliccia et al., 2005), while its function has been neglected. In a recent study, D'Ascenzi et al. showed that LA modification in athletes goes beyond LA enlargement. In soccer players, the author found an increased mitral E/A ratio and reduced LA peak contraction strain which correlated with early diastolic annular velocity (D'Ascenzi et al., 2011). In this study, although we did not find any significant difference in LA strain between UT and M athletes, UT showed increased E/A ratio, increased early diastolic annular velocity and reduced E/e' ratio, indicating a small yet better diastolic function compared to M, confirming what was found by D'Ascenzi.

Limitations

Some limitations for this study must be stated. First, for technical reasons, strain analysis of the LV, and LA was performed only in the apical four-chamber view. Another limitation may be that the sonographer was not blinded to the group allocation which may represent an investigator bias. Finally it must be stated that our study was conducted during the agonistic season when the athletes were undergoing intense training. It would be important to assess whether the modification we found is a transitory response to the training program or a permanent remodeling phenotype of the athletes. Follow-up studies may be needed for a better understanding of the clinical impact of these results.

CONCLUSIONS

Athletes enrolled in UT endurance activities showed RV and RA morphological remodeling associated with an enhanced function in comparison with M runners, which may represent a training-induced remodeling to long-lasting volume overload. Follow-up studies are needed to better assess the long-term clinical impact of these modifications. 2D STE is a useful tool for investigating the deformation dynamic in different sport specialties.

AUTHOR CONTRIBUTIONS

KU was involved in the clinical examinations, data analysis and interpretation, writing the manuscript, and final approval of the manuscript submitted. LB was involved in the statistical analysis, final writing, and final approval of the paper. GD was involved in the data analysis and final approval of the paper. BC was involved in clinical examination and final approval of the manuscript submitted. AT was involved in the final approval of the manuscript. SM was involved in the study design, clinical examinations, and final approval of the manuscript. AV was involved in the clinical examinations and final approval of the paper. GG was involved in the study design, and final approval of the manuscript submitted. LP was involved in the study design, data analysis, and interpretation, in the drafting and final writing and approval of the paper.

ACKNOWLEDGMENTS

We would like to thank the organization of the Tor des Géants® for having allowed us to carry out the testing sessions, Col. Marco Mosso and Lt. Col. Massimo Stella for their kind hospitality at Perenni Barracks, the Military Sports Activities Department, (Courmayeur, Aosta, Italy), and Alison Frank for her competence in the English revision of the manuscript. Finally, we are indebted to the subjects for their participation and exceptional effort.

SUPPLEMENTARY MATERIAL

The Supplementary Material for this article can be found online at: http://journal.frontiersin.org/article/10.3389/fphys.2017.00527/full#supplementary-material

REFERENCES

Bauce, B., Frigo, G., Benini, G., Michieli, P., Basso, C., Folino, A. F., et al. (2010). Differences and similarities between arrhythmogenic right ventricular cardiomyopathy and athlete's heart adaptations. *Br. J. Sports Med.* 44, 148–154. doi: 10.1136/bjsm.2007.042853

Bohm, P., Schneider, G., Linneweber, L., Rentzsch, A., Kramer, N., Abdul-Khaliq, H., et al. (2016). Right and left ventricular function and mass in male elite master athletes: a controlled contrast-enhanced cardiovascular magnetic resonance study. *Circulation* 133, 1927–1935. doi: 10.1161/CIRCULATIONAHA.115.020975

Butz, T., van Buuren, F., Mellwig, K. P., Langer, C., Plehn, G., Meissner, A., et al. (2011). Two-dimensional strain analysis of the global and regional myocardial function for the differentiation of pathologic and physiologic left ventricular hypertrophy: a study in athletes and in patients with hypertrophic cardiomyopathy. *Int. J. Cardiovasc. Imaging* 27, 91–100. doi: 10.1007/s10554-010-9665-5

Calvo, N., Brugada, J., Sitges, M., and Mont, L. (2012). Atrial fibrillation and atrial flutter in athletes. *Br. J. Sports Med.* 46(Suppl. 1), i37–i43. doi: 10.1136/bjsports-2012-091171

Cappelli, F., Toncelli, L., Cappelli, B., De Luca, A., Stefani, L., Maffulli, N., et al. (2010). Adaptative or maladaptative hypertrophy, different spatial

distribution of myocardial contraction. *Clin. Physiol. Funct. Imaging* 30, 6–12. doi: 10.1111/j.1475-097X.2009.00896.x

Caselli, S., Montesanti, D., Autore, C., Di Paolo, F. M., Pisicchio, C., Squeo, M. R., et al. (2015). Patterns of left ventricular longitudinal strain and strain rate in Olympic athletes. *J. Am. Soc. Echocardiogr.* 28, 245–253. doi: 10.1016/j.echo.2014.10.010

D'Andrea, A., Bossone, E., Radmilovic, J., Caso, P., Calabro, R., Russo, M. G., et al. (2015). The role of new echocardiographic techniques in athlete's heart. *F1000Res.* 4, 289. doi: 10.12688/f1000research.6745.1

D'Andrea, A., Naeije, R., D'Alto, M., Argiento, P., Golia, E., Cocchia, R., et al. (2011). Range in pulmonary artery systolic pressure among highly trained athletes. *Chest* 139, 788–794. doi: 10.1378/chest.10-1260

D'Andrea, A., Riegler, L., Golia, E., Cocchia, R., Scarafile, R., Salerno, G., et al. (2013). Range of right heart measurements in top-level athletes: the training impact. *Int. J. Cardiol.* 164, 48–57. doi: 10.1016/j.ijcard.2011.06.058

D'Ascenzi, F., Cameli, M., Padeletti, M., Lisi, M., Zaca, V., Natali, B., et al. (2013). Characterization of right atrial function and dimension in top-level athletes: a speckle tracking study. *Int. J. Cardiovasc. Imaging* 29, 87–94. doi: 10.1007/s10554-012-0063-z

D'Ascenzi, F., Cameli, M., Zaca, V., Lisi, M., Santoro, A., Causarano, A., et al. (2011). Supernormal diastolic function and role of left atrial myocardial deformation analysis by 2D speckle tracking echocardiography in elite soccer players. *Echocardiography* 28, 320–326. doi: 10.1111/j.1540-8175.2010.01338.x

D'Ascenzi, F., Caselli, S., Solari, M., Pelliccia, A., Cameli, M., Focardi, M., et al. (2016). Novel echocardiographic techniques for the evaluation of athletes' heart: a focus on speckle-tracking echocardiography. *Eur. J. Prev. Cardiol.* 23, 437–446. doi: 10.1177/2047487315586095

Erol, M. K., and Karakelleoglu, S. (2002). Assessment of right heart function in the athlete's heart. *Heart Vessels* 16, 175–180. doi: 10.1007/s003800200018

Esposito, R., Galderisi, M., Schiano-Lomoriello, V., Santoro, A., De Palma, D., Ippolito, R., et al. (2014). Nonsymmetric myocardial contribution to supranormal right ventricular function in the athlete's heart: combined assessment by speckle tracking and real time three-dimensional echocardiography. *Echocardiography* 31, 996–1004. doi: 10.1111/echo.12499

Fagard, R. (2003). Athlete's heart. *Heart* 89, 1455–1461. doi: 10.1136/heart.89.12.1455

Henriksen, E., Landelius, J., Wesslen, L., Arnell, H., Nystrom-Rosander, C., Kangro, T., et al. (1996). Echocardiographic right and left ventricular measurements in male elite endurance athletes. *Eur. Heart J.* 17, 1121–1128. doi: 10.1093/oxfordjournals.eurheartj.a015009

Jurcut, R., Giusca, S., La Gerche, A., Vasile, S., Ginghina, C., and Voigt, J. U. (2010). The echocardiographic assessment of the right ventricle: what to do in 2010? *Eur. J. Echocardiogr.* 11, 81–96. doi: 10.1093/ejechocard/jep234

La Gerche, A., Burns, A. T., D'Hooge, J., Macisaac, A. I., Heidbuchel, H., and Prior, D. L. (2012). Exercise strain rate imaging demonstrates normal right ventricular contractile reserve and clarifies ambiguous resting measures in endurance athletes. *J. Am. Soc. Echocardiogr.* 25, 253 e251–262 e251. doi: 10.1016/j.echo.2011.11.023

La Gerche, A., Claessen, G., Dymarkowski, S., Voigt, J. U., De Buck, F., Vanhees, L., et al. (2015). Exercise-induced right ventricular dysfunction is associated with ventricular arrhythmias in endurance athletes. *Eur. Heart J.* 36, 1998–2010. doi: 10.1093/eurheartj/ehv202

Lang, R. M., Badano, L. P., Mor-Avi, V., Afilalo, J., Armstrong, A., Ernande, L., et al. (2015). Recommendations for cardiac chamber quantification by echocardiography in adults: an update from the American Society of Echocardiography and the European Association of Cardiovascular Imaging. *Eur. Heart J. Cardiovasc. Imaging* 16, 233–270. doi: 10.1093/ehjci/jev014

Major, Z., Csajagi, E., Kneffel, Z., Kovats, T., Szauder, I., Sido, Z., et al. (2015). Comparison of left and right ventricular adaptation in endurance-trained male athletes. *Acta Physiol. Hung.* 102, 23–33. doi: 10.1556/APhysiol.102.2015.1.2

Mitchell, J. H., Haskell, W., Snell, P., and Van Camp, S. P. (2005). Task force 8: classification of sports. *J. Am. Coll. Cardiol.* 45, 1364–1367. doi: 10.1016/j.jacc.2005.02.015

Mondillo, S., Galderisi, M., Mele, D., Cameli, M., Lomoriello, V. S., Zaca, V., et al. (2011). Speckle-tracking echocardiography: a new technique for assessing myocardial function. *J. Ultrasound Med.* 30, 71–83. doi: 10.7863/jum.2011.30.1.71

Nagueh, S. F., Appleton, C. P., Gillebert, T. C., Marino, P. N., Oh, J. K., Smiseth, O. A., et al. (2009). Recommendations for the evaluation of left ventricular diastolic function by echocardiography. *J. Am. Soc. Echocardiogr.* 22, 107–133. doi: 10.1016/j.echo.2008.11.023

Opie, L. H. (1998). *The Heart Physiology, from Cell to Circulation*. London: Lippincott Williams & Wilkins.

Pagourelias, E. D., Kouidi, E., Efthimiadis, G. K., Deligiannis, A., Geleris, P., and Vassilikos, V. (2013). Right atrial and ventricular adaptations to training in male Caucasian athletes: an echocardiographic study. *J. Am. Soc. Echocardiogr.* 26, 1344–1352. doi: 10.1016/j.echo.2013.07.019

Pelliccia, A., Maron, B. J., Di Paolo, F. M., Biffi, A., Quattrini, F. M., Pisicchio, C., et al. (2005). Prevalence and clinical significance of left atrial remodeling in competitive athletes. *J. Am. Coll. Cardiol.* 46, 690–696. doi: 10.1016/j.jacc.2005.04.052

Pelliccia, A., Maron, B. J., Spataro, A., Proschan, M. A., and Spirito, P. (1991). The upper limit of physiologic cardiac hypertrophy in highly trained elite athletes. *N. Engl. J. Med.* 324, 295–301. doi: 10.1056/NEJM199101313240504

Pluim, B. M., Zwinderman, A. H., van der Laarse, A., and van der Wall, E. E. (2000). The athlete's heart. a meta-analysis of cardiac structure and function. *Circulation* 101, 336–344. doi: 10.1161/01.CIR.101.3.336

Richand, V., Lafitte, S., Reant, P., Serri, K., Lafitte, M., Brette, S., et al. (2007). An ultrasound speckle tracking (two-dimensional strain) analysis of myocardial deformation in professional soccer players compared with healthy subjects and hypertrophic cardiomyopathy. *Am. J. Cardiol.* 100, 128–132. doi: 10.1016/j.amjcard.2007.02.063

Rudski, L. G., Lai, W. W., Afilalo, J., Hua, L., Handschumacher, M. D., Chandrasekaran, K., et al. (2010). Guidelines for the echocardiographic assessment of the right heart in adults: a report from the American Society of Echocardiography endorsed by the European Association of Echocardiography, a registered branch of the European Society of Cardiology, and the Canadian Society of Echocardiography. *J. Am. Soc. Echocardiogr.* 23, 685–713; quiz 786–788. doi: 10.1016/j.echo.2010.05.010

Simsek, Z., Hakan Tas, M., Degirmenci, H., Gokhan Yazici, A., Ipek, E., Duman, H., et al. (2013). Speckle tracking echocardiographic analysis of left ventricular systolic and diastolic functions of young elite athletes with eccentric and concentric type of cardiac remodeling. *Echocardiography* 30, 1202–1208. doi: 10.1111/echo.12263

Teske, A. J., Cox, M. G., De Boeck, B. W., Doevendans, P. A., Hauer, R. N., and Cramer, M. J. (2009a). Echocardiographic tissue deformation imaging quantifies abnormal regional right ventricular function in arrhythmogenic right ventricular dysplasia/cardiomyopathy. *J. Am. Soc. Echocardiogr.* 22, 920–927. doi: 10.1016/j.echo.2009.05.014

Teske, A. J., De Boeck, B. W., Melman, P. G., Sieswerda, G. T., Doevendans, P. A., and Cramer, M. J. (2007). Echocardiographic quantification of myocardial function using tissue deformation imaging, a guide to image acquisition and analysis using tissue Doppler and speckle tracking. *Cardiovasc. Ultrasound* 5:27. doi: 10.1186/1476-7120-5-27

Teske, A. J., Prakken, N. H., De Boeck, B. W., Velthuis, B. K., Martens, E. P., Doevendans, P. A., et al. (2009b). Echocardiographic tissue deformation imaging of right ventricular systolic function in endurance athletes. *Eur. Heart J.* 30, 969–977. doi: 10.1093/eurheartj/ehp040

Yock, P. G., and Popp, R. L. (1984). Noninvasive estimation of right ventricular systolic pressure by Doppler ultrasound in patients with tricuspid regurgitation. *Circulation* 70, 657–662. doi: 10.1161/01.CIR.70.4.657

Conflict of Interest Statement: The authors declare that the research was conducted in the absence of any commercial or financial relationships that could be construed as a potential conflict of interest.

frontiers in Physiology

ORIGINAL RESEARCH
published: 19 July 2016
doi: 10.3389/fphys.2016.00289

Fast Regulation of Vertical Squat Jump during Push-Off in Skilled Jumpers

Patrick Fargier[1], Raphael Massarelli[1], Tahar Rabahi[1,2], Angelo Gemignani[3] and Emile Fargier[1]*

[1] *Inter-University Laboratory on Human Movement Biology (EA 7424), Centre for Interdisciplinary Research in Sport (FED 4272), University of Lyon, University Claude Bernard Lyon 1, Villeurbanne, France,* [2] *Laboratoire de Conception, Optimisation et Modélisation des Systèmes équipe émotion-action (EA 7306), Université de Lorraine, Ile du Saulcy, Metz, France,* [3] *Dipartimento di Patologia Chirurgica, Medica, Molecolare et dell'Area Critica, Università degli Studi, Pisa, Italy*

The height of a maximum Vertical Squat Jump (VSJ) reflects the useful power produced by a jumper during the push-off phase. In turn this partly depends on the coordination of the jumper's segmental rotations at each instant. The physical system constituted by the jumper has been shown to be very sensitive to perturbations and furthermore the movement is realized in a very short time (ca. 300 ms), compared to the timing of known feedback loops. However, the dynamics of the segmental coordination and its efficiency in relation to energetics at each instant of the push-off phase still remained to be clarified. Their study was the main purpose of the present research. Eight young adult volunteers (males) performed maximal VSJ. They were skilled in jumping according to their sport activities (track and field or volleyball). A video analysis on the kinematics of the jump determined the influence of the jumpers' segments rotation on the vertical velocity and acceleration of the body mass center (MC). The efficiency in the production of useful power at the jumpers' MC level, by the rotation of the segments, was measured in consequence. The results showed a great variability in the segmental movements of the eight jumpers, but homogeneity in the overall evolution of these movements with three consecutive types of coordination in the second part of the push-off (lasting roughly 0.16 s). Further analyses gave insights on the regulation of the push-off, suggesting that very fast regulation(s) of the VSJ may be supported by: (a) the adaptation of the motor cerebral programming to the jumper's physical characteristics; (b) the control of the initial posture; and (c) the jumper's perception of the position of his MC relative to the ground reaction force, during push-off, to reduce energetic losses.

Keywords: vertical squat jump, intersegment coordination, power, motor control, explosive movement

OPEN ACCESS

Edited by:
Enrico Capobianco, University of Miami, USA

Reviewed by:
Benedito Sergio Denadai, São Paulo State University, Brazil
Sampath K. Gollapudi, Washington State University, USA

****Correspondence:***
Patrick Fargier
patrick.fargier@univ-lyon1.fr

Specialty section:
This article was submitted to Integrative Physiology, a section of the journal Frontiers in Physiology

Received: *29 February 2016*
Accepted: *27 June 2016*
Published: *19 July 2016*

Citation:
Fargier P, Massarelli R, Rabahi T, Gemignani A and Fargier E (2016) Fast Regulation of Vertical Squat Jump during Push-Off in Skilled Jumpers. Front. Physiol. 7:289. doi: 10.3389/fphys.2016.00289

INTRODUCTION

Physical activities under extreme conditions or extreme sport disciplines have increasingly interested the world of sport in recent decades. It is easily understandable that climbing Mount Everest without additional oxygen supply (e.g., West, 1983), deep diving in apnea conditions (e.g., Muth et al., 2005) or performing in ironmen's triathlon competitions (e.g., Knechtle et al., 2010) bring athletes to their physiological and psychological limits and often beyond. In several cases and

not only in sport but also in everyday life movements must be chosen and executed within a very short time under pressure and sometimes in a dangerous environment (as it may happen during automobile driving in intense traffic). The performance of physical activities possibly dangerous for body integrity strongly depends on a very accurate motor coordination, as for example in cliff diving, (e.g., Butterfield and Boyd, 2012). Sport in extreme conditions may thus lead to the study of individual psychological, physiological and biomechanical adaptations to specific constraints.

Under extreme conditions it is particularly necessary to develop the best possible coordination of bodily segments often to safely realize a good performance; possibly the best one. From this standpoint jumps have been frequently used to evaluate human physical capacities (notably from Sargent, 1921). In particular the performance of a Vertical Squat Jump (VSJ) is strictly bound to some qualities of the musculo-skeletal system that the jumper must optimally exploit to reach a maximum height of flight (Bobbert and van Soest, 2001). The height (h) of a jump is thus not only influenced by the power-generating capability of the muscles involved in the movement but also, and first of all, by the coordination of the jumper's segments during the push-off phase (e.g., Bobbert and van Soest, 2001) and by the segmental pattern of movement that is established in each individual.

In this context the pattern of movement of a given jump may be defined as the interaction of the muscular forces developed in response to the neural stimulation of the muscles with the mechanical constraints of the task (e.g., Bobbert and van Ingen Schenau, 1988). Jumpers who are experienced in VSJ develop a single pattern of movement, i.e., the way by which the rotation movements of the jumper's segments establish the vertical acceleration of the body mass center (MC). During the execution of a VSJ it has been observed that, in spite of time differences from an individual to another, the rotation of the segments implies the opening of the segmental and articular angles in a proximo-distal sequence (i.e., following the sequence trunk, thigh, leg, foot; e.g., Bobbert and van Soest, 2001). Such pattern has been considered to be the optimal sequence required to achieve a maximal jump height (Bobbert and van Soest, 2001) and it has also been found in other explosive movements, for example in the case of overarm throws (Atwater, 1979) or of counter-movement jumps (Bobbert and van Ingen Schenau, 1988). However, other patterns of movement may also be observed in VSJs, for example in elderly men where a simultaneous pattern of movement, and not a sequential proximo-distal pattern, has been reported (Haguenauer et al., 2005).

These observations regarding the establishment of a pattern of movement raise the problem of the coordination of the segmental movements and thus of the control of these movements during a push-off. An important issue, which has not yet been solved (Pinter et al., 2012). Time is a major point in the study of the motor control of a VSJ, as this is realized within ca. 300 ms. Such a time constraint places the jumper in a borderline condition to control his movements because (1) the physical system that constitutes the jumper is very sensitive to perturbation, and (2) the time of movement limits the possibilities to benefit from the known neural feedback loops (e.g., van Soest and Bobbert, 1993).

Even in the case of skilled jumpers it is probable that the pattern of the segmental and articular angles opening is not absolutely predetermined because of the intervention of different factors possibly fluctuating with time, such as muscular qualities or an exact initial posture, or the equilibrium, etc., Even the number of degrees of freedom of the brain sensorimotor system is likely to add some intra and inter-individual variability (Newell and Corcos, 1993). However, such potential variability does not interfere with the emergence of a consistent motor pattern, hence suggesting the existence of a robust process of regulation of the segment movements.

This process should be suitable for any jumper and should be revealed by the examination of the evolution of the segment coordination during the 300 ms push-off phase. This dynamics of coordination *per se*, leading to a proximo-distal pattern, remained however to be clarified and the aim of the present study was to determine such dynamics in the case of skilled jumpers. The examination of the segmental movements and of their interrelation was made in terms of kinematics but also in relation with the corresponding energetic outputs (i.e., jump efficiency) as a VSJ requires the best utilization of the produced muscular energy to reach the maximum height. This leads to the assumption that a possible regulation of the coordination should be function of this requirement.

MATERIALS AND METHODS

The study was approved by the Institutional Review Board of Claude Bernard University Lyon 1 and the participants to the experimental protocol gave their informed consent. Eight male subjects (22.75 $\pm$ 3.3 years of age, 180 $\pm$ 0.06 cm height, and 71.87 $\pm$ 6.44 kg weight) participated to the study. The subjects were students of the Faculty of Sport Sciences (STAPS) skilled in either track and field jumps or in volleyball (French regional level) and had thus a consequent experience in jumps even if not familiar with VSJ. During the experiments the subject were asked to produce maximal VSJs (**Figure 1**), while respecting the following constraints: (1) a stationary semi-squatted initial position, (2) hands kept on the hips during the jump, (3) starting the push-off phase without any initial displacement of the jumper's MC toward the ground, consequently without any countermovement. Each VSJ was video-recorded and analyzed.

Model of the Jump

The VSJ was modeled (**Figure 2**) as a planar, rigid body system represented by four segments (feet, lower legs, upper legs, and head-arms-trunk or HAT) linked by frictionless, hinge joints (e.g., Bobbert and van Soest, 2001; Babič and Lenarčič, 2007). The mass center of each segment (MCi) was found on the same vertical plane defined by a system of orthogonal axes (OX, OZ) related to the ground; the jumper's MC laid also on the same plane (**Figure 2**).

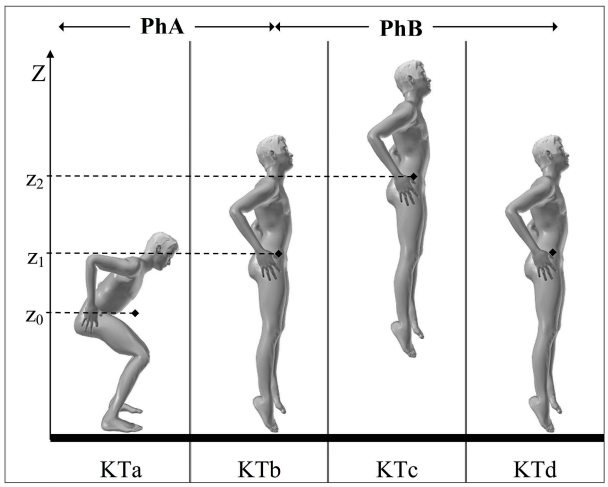

FIGURE 1 | Key times (KTa-d), phases (PhA-B), and performance (h) of a VSJ. KTa: initial position (the jumper stands still, heels on the ground, knee joint angle of ∼90°, hands on hips); KTb: take-off (end of contact between the support and the jumper); KTc: peak of the flight phase (the mass center of the jumper, MC, reaches its maximal height of flight); KTd: landing (moment at which the feet touch again the ground); PhA: push-off phase (realized without initial countermovement, it starts at t0 when the segments of the jumper begin to rotate and ends at take-off); PhB: flight phase (it starts at take-off and ends at the instant of landing). The height of the jump (h) is given by the difference between the vertical coordinate of MC (♦) at take-off (z1) and at the peak of the flight phase (z2): $h = z2 - z1$. During the push-off the coordinate of MC evolve from z0 (initial position) to z1 (instant of take-off) and then to z2 (apex of the jump).

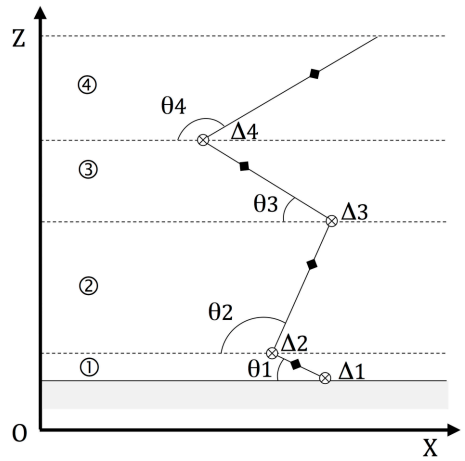

FIGURE 2 | Modeling the jump. The model consists of four segments: ①, ②, ③, and ④ (respectively feet, legs, thighs, and head-arms-trunk). Other constituent elements are: the rotation axes orthogonal to (OX, OZ) (⊗), the segmental angles θi and the segmental mass centers MCi (♦).

Data Acquisition

Before each experiment subjects were asked to execute few warm-up exercises and some VSJs to obtain a correct execution of the movement. They were subsequently asked to perform a maximum VSJs in 3 trials.

Five optical markers were placed, on the gleno-humeral joint (shoulder), the great trochanter (hip), the lateral condyle of the femur (knee), the lateral malleolus (ankle), and the fifth metatarsal (toe) (e.g., Aragón-Vargas and Gross, 1997). Subjects were filmed on the right sagittal plane with a camcorder (JVC©, GR-DVL 9200) at a distance of 7 m. The angle between the optical axis of the camcorder and the plane of movement was 90°. The video sequences have been deframed with the software Adobe Première© to obtain an image frequency of 50 Hz.

Video images were digitized using self-developed software. The coordinates for the markers were obtained from digitization of the central point of the landmarks and the coordinates, as function of time, were smoothed by using a moving average of order 1. The anthropometric values of the segments required for the analysis of the data were obtained from Winter (1990; see Supplementary Material 1 and Supplementary Figure 1). To ensure the pertinence of Winter's proportional model in the present study the measure of h (for each subject) was also obtained with a force platform (AMTI© OR6-7-2000; frequency of acquisition: 500 Hz/software BioAnalysis© see also Supplementary Material 2). This measurement was compared to that obtained from the video analysis using the anthropometric tables of Winter (1990) (see Supplementary Material 2).

Basic Characteristics of the VSJs

The most correct execution among 3 VSJs, for each subject, was chosen for analysis. The decision was made on the respect of the instructions given to execute the jump (initial stabilization of a semi-squatted position, arms akimbo during the jump, and initialization of the push-off without countermovement). This was systematically determined from the recorded videos of the jumps. As a further control, the measured *h*-values of the VSJ were compared to those obtained in other studies with skilled jumpers realizing maximal VSJs (e.g., Bobbert et al., 2008).

The heights of the jumps were measured as defined in **Figure 1** and Supplementary Material 2 and the time length of the push-off phases as in Supplementary Material 3. To confirm the measurements the VSJ height from each subject was obtained with a force platform (see Section Data Acquisition).

The pattern of movement was also determined by measuring the opening of the articular angles (β) of the hip, the knee, and the ankle (**Figure 3**). To this end the variation (varia) of a given articular angle at each instant (t) of the push-off was taken in consideration [$varia_t = (\beta_{t+1} - \beta_{t-1})/2dt$].

Dynamics of Coordination among Segments

In a maximum VSJ, the rotation of the segments during push-off must lead to the translation of the jumper's MC to a maximal, vertical and linear velocity at take-off (starting from a static initial position; e.g., Van Ingen Schenau, 1989; see also **Figure 2**).

The movements of the segments were characterized at each instant of the push-off by: (a) the effect of the angular *velocity* of a segment i on the vertical velocity of the jumper's MC, this effect being quantified by: $C_v = \dot{\theta}_i \cdot \cos\theta_i$; (b) the effect of the angular

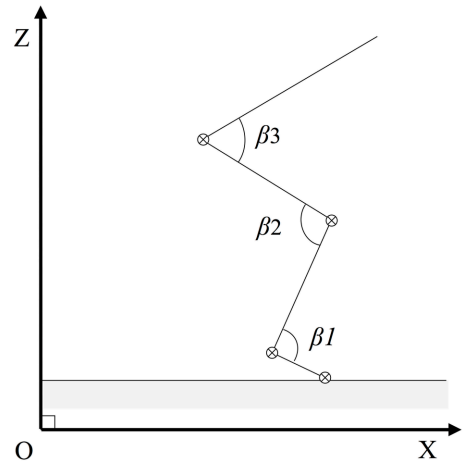

FIGURE 3 | Articular angles of the jumper. The model of the jump (see **Figure 2**) includes three rotation axis (⊗) corresponding to three articulations (hip, knee, and ankle joints) thus to three articular angles βi.

acceleration of the segments on the vertical acceleration of MC, being quantified by: $C_a = d\left(\dot{\theta}_i \cdot \cos\theta_i\right)/dt$; and (c) the *efficiency* in the production of useful power (P_u) at the jumper's MC by the rotation of the segments (Supplementary Material 1).

Concerning point (c) it should be kept in mind that the rotation of the segments may produce some "lost" power (P_l), which does not contribute to the goal of the jump (see for example: Bobbert and van Soest, 2001). On this basis the produced muscular power (P_{musc}) is the sum of P_u and P_l. This leads to the expression of the energetic efficiency of the segments rotation as the ratio (R) between useful and muscular power, i.e., $R = P_u/P_{musc}$ (see Supplementary Material 1).

Determination of Possible Segmental Coordination Types

To determine the presence of possible different coordination types the influence of the segmental movements on the vertical velocity and acceleration of MC was performed. It was found that an initial phase (T1) in the curve of the MC vertical velocity remained close to 0 m/s and was followed by a second phase (T2) in which the velocity of MC became definitely positive and increased through time. This confirmed previous observations (e.g., Bobbert and van Soest, 2001).

In the T2 phase possible early negative and later positive values of C_v (see Section Dynamics of Coordination among Segments) were searched in the curves of each segment, leading to the determination of consecutive different phases of C_v in all segments. Breaking points in the variations of the segmental C_a were searched in the curves determined by the following equation: $\left[d\left(\dot{\theta}_i \cdot \cos\theta_i\right)/dt_{(t+1)} - d\left(\dot{\theta}_i \cdot \cos\theta_i\right)/dt_{(t-1)}\right]/2dt$.

The T1 and T2 phases in C_v and the breaking points in C_a for each segment led to a possible comparison among jumpers in order to suggest the hypothetical existence of a common dynamics of coordination and, consequently, to identify three sequential segment coordination types (to be called Ty_i, Ty_{inter}, and Ty_{fin}) in each jump.

Coordination and Energetic Efficiency

The effects of the segmental rotation on the vertical velocity and acceleration of the jumper's MC led to the determination of consecutive types of coordination during push-off. The instantaneous energetic efficiency R (see Section Dynamics of Coordination among Segments and Supplementary Material 1) was calculated to search for a possible relation between R and the evolution of the coordination.

Statistical Analysis

Several statistical tools have been used according to the different aims of the study.

Basic Characteristics of the Jumps (Pattern of Movement)

The determination of the jumpers' pattern of movement (i.e., the opening of the articulations; see Section Basic Characteristics of the VSJs) was made following two steps. At first it was observed, for each articulation of a jumper, the instant at which a continuous increase above the average value of the angular variation was apparent. Then, for each segment, the test of homogeneity of Buishand (1982, 1984) was applied using the software Khronostat 1.01© to indicate a statistically significant breaking point in the curves of segmental angular velocity.

Dynamics of Coordination among Segments

The analysis of the two time periods that characterized the rise of MC during push-off (T1 and T2, see Section Determination of Possible Segmental Coordination Types) was determined by observing the instant at which the vertical velocity of the jumper's MC remained positive and increased. This was confirmed by the test of Buishand.

The presence of negative or positive C_v (in T2) was determined and the breaking points in C_a were analyzed by the test of Buishand (see Section Determination of Possible Segmental Coordination Types and Supplementary Material 1).

Coordination and Energetic Efficiency (R and a_{MCz})

The possible relation between the variation of the energetic efficiency of the segmental movements and the dynamics of the coordination of the segments during push-off was verified by the coefficient of correlation of Spearman between R and the vertical acceleration of the jumper's MC (a_{MCz}; output of the segments rotation).

RESULTS

The average jump height was 0.34 ± 0.06 m ($n = 8$) for an average push-off lasting 0.29 ± 0.02 s. Breaking points in the curves of the segmental articular angles were observed at a time instant that showed thereafter a continuous increase above the average value of the angular variation. The time instants at which

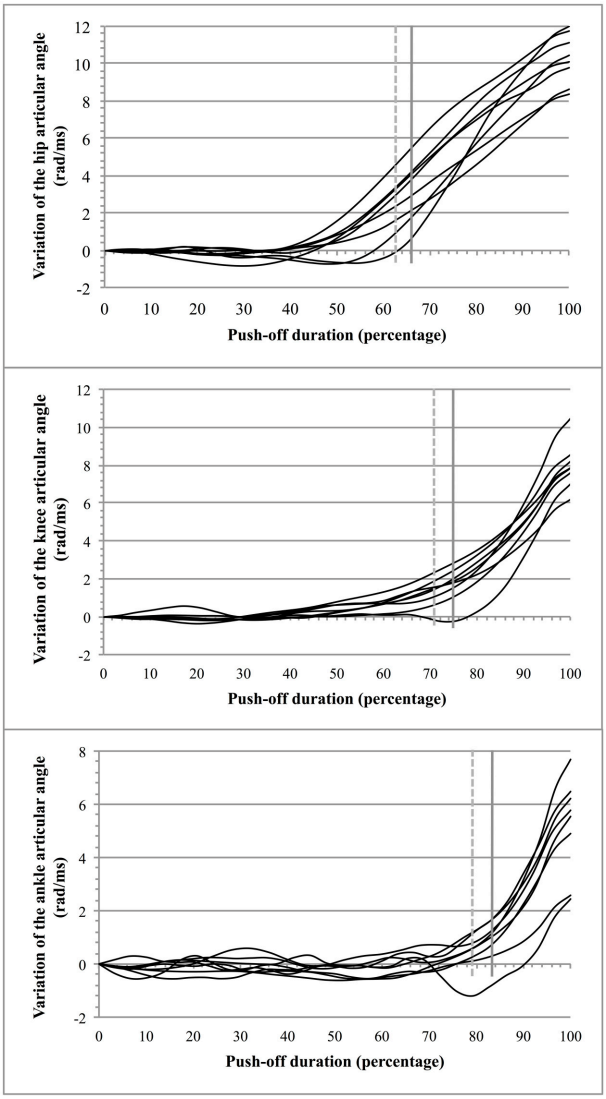

FIGURE 4 | Opening of the articular angles during push-off. For a given articular angle βi (hip, knee, and ankle): the vertical dotted gray line indicates the average breaking point obtained from the test of Buishand and the vertical full gray line indicates the average instant from which the opening of a given articular angle increases beyond the mean value of variation of the corresponding articular angle.

these breaking points appeared (**Figure 4**)[1] were found at: 66.3 ± 3% (hip), 75 ± 6% (knee), and 83.3 ± 5.1% (ankle) of the total time duration. A similar pattern of movement (**Figure 4**) was confirmed with the test of Buishand that showed quite comparable breaking points in the opening of the articulations (each breaking point of the curves was found to have a value of $p < 0.001$). The values were: 63.4 ± 3.3% for the hip, 71.7 ± 6% for the knee, and 79.2 ± 4.8% for the ankle. The two procedures (observation and test of Buishand) led to congruent results (the difference between the two procedures was of 3.4 ± 1.4%).

[1]Presented as percent of the time period of the push-off phase to normalize differences among subjects.

Consecutive Intersegment Coordination

During push-off the rotation of the segments did not immediately provide a clear and continuous rise of the jumper's MC (the movements of the segments were not sufficient for such a rise and/or tending to neutralize each other at the beginning of the push-off). As it may be seen in **Figure 4**, two periods of push-off were observed that agreed with the data of Bobbert and van Soest (2001) (each breaking point of the curves was found to have a value of $p < 0.001$): (a) an initial period (T1 = 0.13 ± 0.02 s; i.e., 43% of the total push-off time) in which the vertical velocity of the jumper's MC remained close to 0 m/s and was not durably positive; and (b) a second period (T2 = 0.16 ± 0.03 s; i.e., 57% of the total push-off time) starting at the moment at which the velocity of MC became definitely positive. The effect of the segmental rotation on the vertical displacement of MC (both velocity and acceleration) led to the determination of three consecutive coordinations during T2.

Taking as an example jumper S6 (**Figure 5**) the influence of the segment rotation on the vertical velocity of the jumper's MC presented three distinct phases (**Figure 5A**). In the initial phase of C_v (from 0 to 21% of time) 2 segments (feet and HAT) did not influence positively the vertical velocity of MC. In the following phase of C_v (from 21 to 57.9% of time, i.e., 36.9% of time) 1 segment (feet) did not positively influence the vertical velocity of MC. In the final phase of C_v (from 57.9 to 100% of time; i.e., 42.1% of time) each segment of the jumper (feet, lower legs, upper legs, and HAT) showed a positive influence. The test of Buishand showed that the effects of the segmental rotation on the vertical acceleration of MC produced statistically significant breaking points at, respectively, 52.6% of time for the lower legs ($Q = 8.73$; $p < 0.0001$), at 57.9% for the HAT segment ($Q = 8.95$; $p < 0.0001$), and at 73.6% for the feet ($Q = 6.63$; $p = 0.002$) (**Figure 5B**). None of the breaking points observed in C_a appeared during the first phase of C_v, 2 of them did so during the second phase of C_v, and 1 during the last phase of C_v (**Figure 5C**). This led to the determination of 3 *coordination types* (Ty): (a) Ty_i with 2 negative segmental C_v and no breaking point in C_a; (b) Ty_{inter} with the passage of 1 negative segmental C_v to 0 and 3 breaking points in C_a; and (c) Ty_{fin} with each segmental C_v being positive and no breaking point in C_a (**Figure 5C**).

The dynamics of the movements found in S6 was similar in the other 7 subjects even if there was a definite variability in the realization of the three coordination types (Ty_i, Ty_{inter}, and Ty_{fin}, see: Supplementary Figure 2). Thus: (a) Ty_i showed 1 or 2 negative C_v and no breaking point in C_a; (b) Ty_{inter} was characterized by a decrease in the number of negative C_v and/or several breaking points in C_a; (c) in Ty_{fin} each C_v was positive without any breaking point in C_a (see Supplementary Figure 2).

Coordination and Energetic Efficiency

When the three types of coordination (Ty_i, Ty_{inter}, and Ty_{fin}) were compared to the corresponding energy ratio R the changes of coordination type (indicated in dark gray, white, and light gray backgrounds; **Figure 6**) evolved in parallel with the improvement of R.

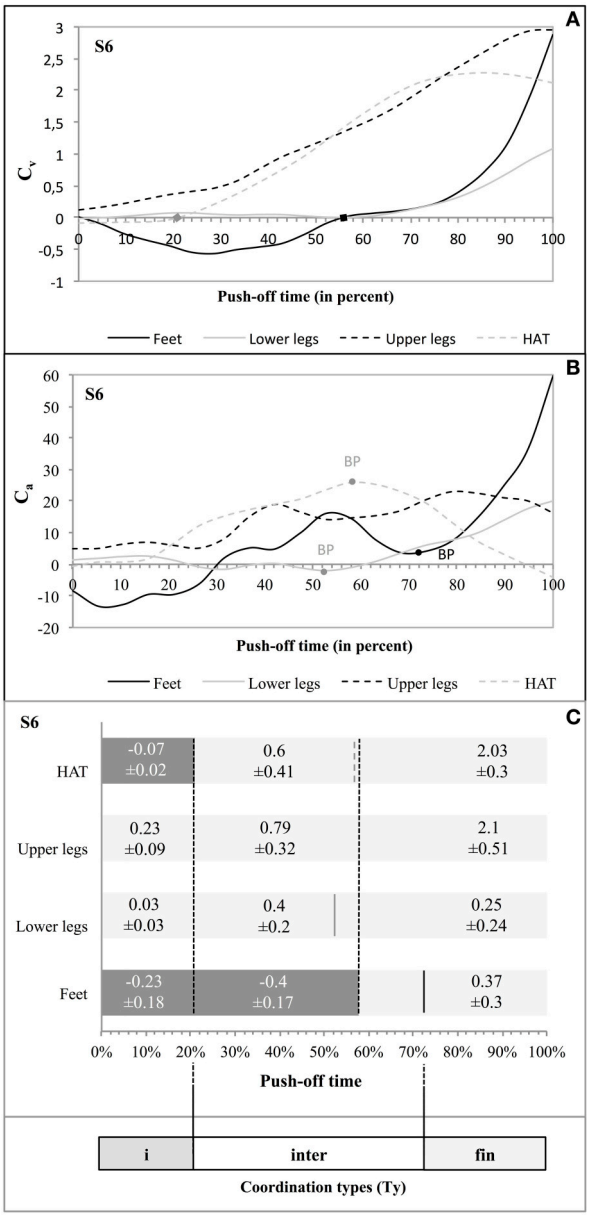

FIGURE 5 | Coordination types (Ty_i, Ty_{inter}, and Ty_{fin}) during push-off in S6. The curves C_v as function of time **(A)** show the influence of each segment of the jumper on the vertical velocity of his MC. The 2 squares on the axis of the abscissa indicate the passage from a negative C_v to a positive C_v of a given segment on the vertical velocity of MC. The curves C_a as function of time **(B)** show the influence of each segment of the jumper on the vertical acceleration of his MC; the breaking points are given when the *p*-value gives a significant probability ($p < 0.05$; see Supplementary Material 4). The bar chart **(C)** supplies the evolution of C_v as function of time for each segment. The mean values of C_v (± standard deviation) are also given. The doted vertical black lines (crossing the whole bars) indicate the phases of C_v for which these values are given. The vertical lines crossing a single bar indicate any breaking point (BP) identified by the Buishand test (full black line = BP feet; full gray line = BP lower legs; and dotted gray line = BP HAT). On this base, three consecutive types of coordination were determined, with: **(A)** Ty_i with 2 negative segmental C_v and no BP point in C_a; **(B)** Ty_{inter} with an evolution in the segmental C_v from 1 negative influence to none and 3 BP in C_a; and **(C)** Ty_{fin} during which each C_v was positive, and without any BP in C_a.

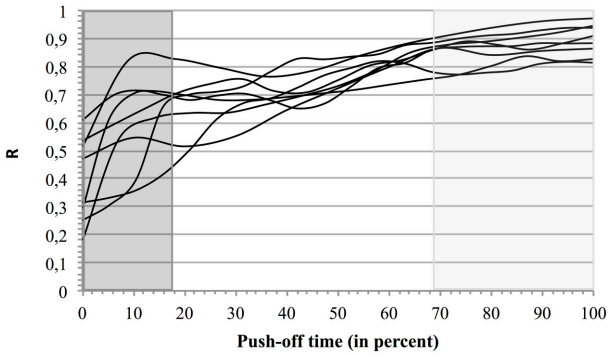

FIGURE 6 | Energetic efficiency R in 3 types of coordination. For each jumper the curves of R as function of time are presented on a background indicating the mean identified segmental coordination types (percent of the push-off time). The first type (Ty_i) is indicated by a dark gray background, the second (Ty_{inter}), by a white background, and the third one (Ty_{fin}), by a light gray background.

The coefficient of correlation of Spearman between R and the vertical acceleration of the jumper's MC (a_{MCz}) was positive for each subject with a $p \leq 0.007$ (**Table 1**).

Figure 7 illustrates this correlation in the case of S6, showing both a_{MCz} and R as function of time (regression line: $y = 0.0356x + 2.1518$).

The mean values of both instantaneous R and vertical acceleration of the jumper's MC (a_{MCz}), for each type of coordination, are given in **Table 2**.

In spite of the presence of some variability in R and a_{MCz} values, from one subject to another, the data systematically showed that the mean value of R increased from one type of coordination to the subsequent one (**Table 2**). The same trend was observed in the case of the instantaneous R and a_{MCz} (**Table 1** and **Figure 7**). For example, in S6 the mean value of R (from 0 to 1) was of 0.26 ± 0.1, then of 0.79 ± 0.07, and finally 0.91 ± 0.01; the mean value of a_{MCz} (in m/s^2) was initially 3.66 ± 1.79, then 14.38 ± 2.20, and finally 20.81 ± 1.12.

DISCUSSION

The present study concerns the dynamics of the coordination among four body segments during the push-off of a VSJ. The main hypothesis suggested the presence of a common dynamics among jumpers, even if differences in the segmental movements were probable.

Basic Characteristics of the VSJ (Push-Off Time, Height, and Pattern of Movement)

The mean value of the push-off time, lasting for 0.29 ± 0.02 s, and the mean height performance (0.34 ± 0.06 m) were in accordance with the average values already reported in the literature (e.g., Bobbert et al., 2008)[2]. The jumping

[2]The mean height performance was comparable to the literature even if such comparisons are quite difficult to make because of the different techniques used to measure jump height (Aragón-Vargas, 2000). Thus, Bobbert et al. (2008) reported

TABLE 1 | Coefficient of correlation of Spearman between R and of a_{MCz} (m/s^2).

	S1	S2	S3	S4	S5	S6	S7	S8
Rho (R; a_{MCz})	0.65	0.92	0.88	0.6	0.77	0.93	0.73	0.46
***p*-value**	0.006	<0.0001	<0.0001	0.005	0.0004	<0.0001	0.0009	0.007

The coefficient of correlation of Spearman (Rho) was calculated between R (the instantaneous energetic efficiency between useful and muscular power) and the vertical acceleration of the jumper's MC (a_{MCz}). For each subject the coefficient was positive with a p-value of at least $p \leq 0.007$.

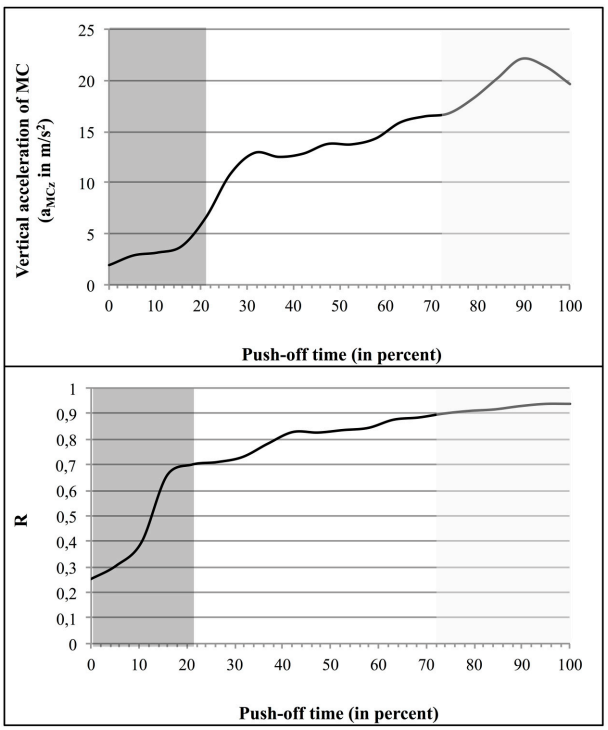

FIGURE 7 | Variation of a_{CMz} and R as function of time: example of the jumper S6. The first coordination type (Ty_i) is indicated by a dark gray background, the second (Ty_{inter}), by a white background, and the third one (Ty_{fin}), by a light gray background.

skill of the subjects volunteering in the present study was confirmed by the opening of the articular angle of the hip earlier than that of the knee or the calf (see Section Results).

Dynamics of Inter-Segmental Coordination and Motor Control

The results showed the presence of *common* characteristics in the subjects' segmental movements during the push-off (see Section Consecutive intersegment coordination and Supplementary Figure 2, Supplementary Material 4). Thus, after the initial period of the push-off (T1), during which the segmental rotations provided a low vertical velocity of MC and not always with a positive value, it followed a second period (T2) during which the vertical velocity of the MC was increased and remained positive. During T2, and considering the four segments as a whole, three consecutive coordination types were observed (see Section Consecutive Intersegment Coordination and Supplementary Figure 2, Supplementary Material 4). This dynamics of coordination led to an increase in the number of segments influencing positively the vertical velocity of MC (from 2 to 3 in Ty_i and systematically 4 in Ty_{fin}). The intermediate coordination type, Ty_{inter}, participated to this evolution and showed breaking points in the segmental contributions to the vertical acceleration of MC (Supplementary Figure 2).

This *common dynamics of coordination* may imply the intervention of a programmed control of the movement (optimized through experience) by the impulses transmitted to muscles from the central nervous system. This may happen even if the observation of a given pattern of movement does not give sufficient information to deduce a corresponding pattern of stimulation by the central nervous system (e.g., Hudson, 1986; Robertson and Fleming, 1987; Bobbert and van Soest, 2001). It has been shown, in simulation studies (e.g., Prokopow et al., 2005), that the timing of muscles stimulation in VSJ has a determining influence on the quality of the push-off. In addition the very fast sequence of the three coordination types, shown in the present work (below 0.2 s), and above all the rapid changes in the segmental influences on the vertical displacement (velocity and acceleration) of MC during the second coordination type, Ty_{inter}, may evoke the intervention of a mechanism of regulation during push-off. This support the idea of a distal modulation as it has been proposed by van Soest and Bobbert (1993) and Bobbert et al. (2013). This implies feedbacks from muscle to muscle, on the basis of an established cerebral and/or cerebellar motor program and of a relation strength-length-velocity. This might instantaneously regulate the jump by the viscoelastic properties of the muscle-tendon couple. Such modality of regulation presents the advantage to involve mechanisms of control much faster than that imputable to cerebellar circuitries in forward and inverse internal models (both kinematic and dynamic models) (e.g., Wolpert et al., 1998; Katsnelson, 2003). However, the slower motor velocity observed at the beginning of the push-off might also suggest a potential role of the neural feedback loops that would thus fade through the time of push-off.

The data shown in Supplementary Figure 2 and concerning the segmental participation to the vertical acceleration of the

that gymnasts could jump up to 0.41 ± 0.05 m, while Bobbert et al. (2006) reported a height of 0.284 m (no SD was given) in adults having performed in volleyball or gymnastics. It should be noted that in the latter studies the height of jump was defined as the difference between the height of the jumper's MC at the peak of the jump and that of the subject standing up before push-off; understandably the measure of the jump height gave higher values than that measured in the present study (**Figure 1**). These observations finally support the idea that the subjects of the present study did their best, thus producing a maximal effort.

TABLE 2 | Means values of R of a_{MCz} (m/s^2) as function of the coordination type.

Jumps	Coordination type 1 (Ty_i)		Coordination type 2 (Ty_{inter})		Coordination type 3 (Ty_{fin})	
	Mean R	Mean a_{MCz}	Mean R	Mean a_{MCz}	Mean R	Mean a_{MCz}
S1	0.70 ± 0.04	15.6 ± 2	0.78 ± 0.02	16.7 ± 0.9	0.83 ± 0.01	30.9 ± 8.1
S2	0.67 ± 0.22	14.50 ± 3.82	0.79 ± 0.03	21.70 ± 0.55	0.90 ± 0.07	25.14 ± 2.19
S3	0.49 ± 0.15	6.10 ± 2.97	0.78 ± 0.03	13.39 ± 0.51	0.79 ± 0.02	16.54 ± 1.53
S4	0.54 ± 0.21	7.89 ± 3.26	0.74 ± 0.07	13.55 ± 2.04	0.88 ± 0.005	20.73 ± 0.98
S5	0.52 ± 0.04	18.95 ± 2.5	0.77 ± 0.09	28.70 ± 1.05	0.86 ± 0.005	34.20 ± 2.72
S6	0.26 ± 0.1	3.66 ± 1.79	0.79 ± 0.07	14.38 ± 2.20	0.91 ± 0.01	20.81 ± 1.12
S7	0.59 ± 0.05	9.43 ± 2.92	0.72 ± 0.02	18.32 ± 2.10	0.85 ± 0.04	18.86 ± 1.24
S8	0.45 ± 0.23	12.83 ± 2.63	0.73 ± 0.09	15.12 ± 1.25	0.91 ± 0.02	17.07 ± 1.69

For each type of coordination (Ty_i, Ty_{inter}, and Ty_{fin}) the table presents the mean values of both energetic efficiency between useful and muscular power (R), and vertical acceleration of the jumper's MC (a_{MCz}).

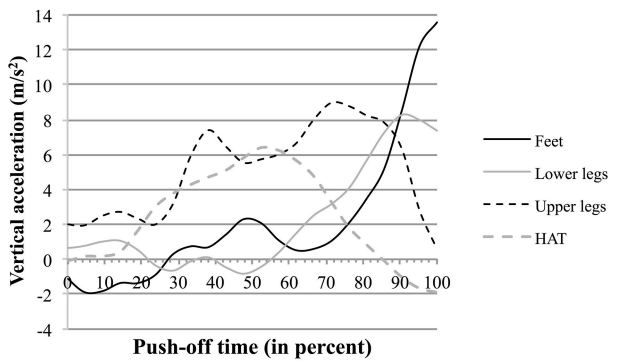

FIGURE 8 | Vertical acceleration of a jumper's segments as function of time during push-off : example of the jumper S6. The full and dotted black lines, and the full and dotted gray lines represent the curves as function of time (percent of the push-off phase time length) of the vertical acceleration of the jumper's feet, upper legs, lower legs, and HAT, respectively.

MC are compatible with such hypothesis. For example in S6 (see also **Figure 5B**) the breaking points show that the influences of the feet and of the lower legs evolve inversely to that of HAT. This is emphasized in **Figure 8** showing the curves of the vertical component of the acceleration of the jumper's segments during push-off. Thus, the vertical component of the acceleration of the lower legs segment increased ca. 50% of push-off time, while it started to decrease in HAT. Similarly the vertical component of the acceleration of the feet increased to 70% of push-off time, while it started to decrease in the upper legs segment.

Common Motor Control and Inter-Individual Variability

The possible distal regulation of the push-off, following a given pattern of neural stimulation, is compatible with the observed inter-individual variability in segmental movements (see Supplementary Figure 2) provided that a *common referential element* for the regulation is present (see in the following).

Such variability may be due to a different cerebral programming of the VSJ or may be a function of the segment geometry and/or of the muscular capacities of the jumper. It may also be suggested that the initial posture may also play a role. Initial posture is established by the instructions given to the jumper by the experimenter (**Figure 1**). However, even if it would be possible to repeatedly set up a knee angle at exactly 90°, it should not be pertinent to do so, essentially because imposing a strict initial posture might influence the performance of the individual and his/her effort intensity (e.g., Sanders and Wilson, 1992). On the other hand keeping a given posture requires a dynamic process in which the subject's MC may oscillate randomly (e.g., Gurfinkel and Shik, 1973). As a consequence the jumpers begin their push-off starting from similar but not identical postures. In the case of a VSJ achieved from an initial free position, as in the present experiments, the posture variations observed in the videos were not very important. This suggests that the push-off might be regulated at the peripheral level only (from different initial positions of the segments and different muscular stretching), and consequently that a source of intra-individual variability might contribute to inter-individual variations in the segmental movements during push-off.

The regulation of the movement during push-off must be performed as function of a reference. Such a reference may be a "referential" movement determined from the initial stimulation of the muscles (van Soest and Bobbert, 1993). It should however be considered that from an initial posture a jumper must give to his/her MC the fastest vertical velocity at the instant of take-off. This must be done by producing the greatest useful power, at each instant of the push-off, thus by maintaining the MC vertical (theoretically without fluctuations) to the point of application of the ground reaction force. Such position of the MC may thus represent a value of reference to regulate the movement (Gurfinkel, 1973; Massion, 1992).

To examine the possible fluctuations in the position of the MC, relative to such vertical, the results of the present experiments allow to determine at each instant of the push-off the angle α made by the velocity vector of

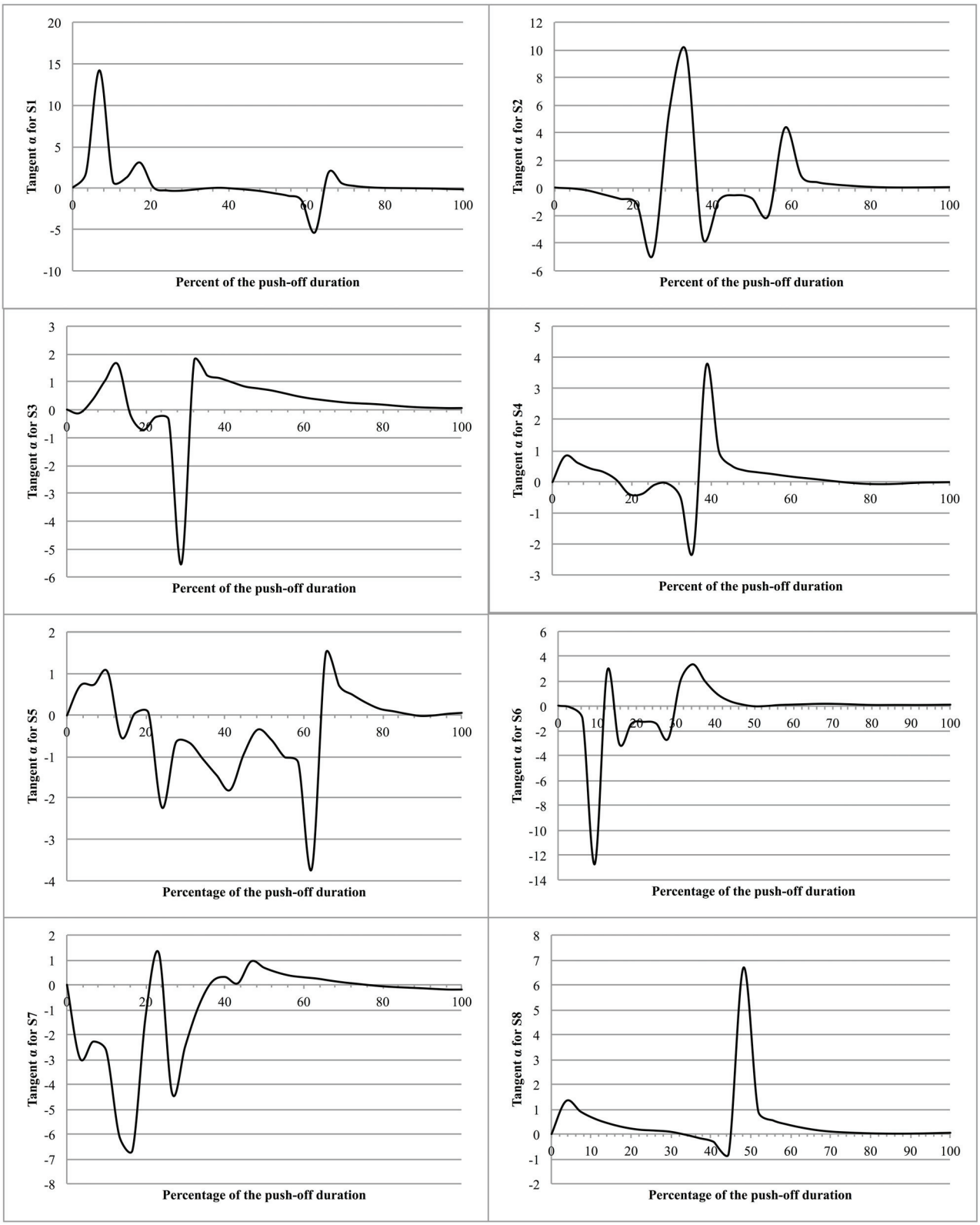

FIGURE 9 | Tangent α as function of time during push-off. The figure presents the eight jumps as function of the percent of the push-off time. The ordinate is the tangent to the α angle made by the velocity vector of the MC (V_{MC}) with the vertical passing by the point of application of the ground reaction force (tangent $\alpha = V_{MCx}/V_{MCz}$).

the MC ($\overrightarrow{V_{MC}}$) with the vertical passing by the point of application of the ground reaction force, knowing that: tang(α) = V_{MCx}/V_{MCz}. It is interesting to note that any divergence of the velocity vector to the vertical reference produces an adjustment that reduces the divergence, thus suggesting *a persistent regulation of equilibrium* during the jump (**Figure 9**).

Moreover, the evolution of the segment coordination during T2 suggests a *continuous increase of energetic efficiency* (**Tables 1, 2**), i.e., an increasing utilization of produced muscular power as useful power. This finding and the evolution of tang(α) indicate that jumpers generate an increased vertical velocity of MC while reducing the power losses by maintaining their MC vertical to the point of application of the ground reaction force. The conclusion is that the evolution of the segments rotation, from an initial posture, is function of a less energetic cost.

The ensemble of the present and published data suggests the following conclusions: (a) the push-off control is dependent upon a motor cerebral stimulation adapted to the jump and to the jumper's segments characteristics; (b) the continuous regulations of the jump may be probably related to the jumper's perception of the position of MC relative to the ground reaction force; (c) such regulations are made to reduce energetic losses; (d) the control of the initial posture is determinant in the dynamics of the segment coordination. It should be emphasized that the ensemble of the results make possible the regulation of the VSJ in a very short time, even below 10 ms[3], thus in physiologically extreme conditions of control.

AUTHOR CONTRIBUTIONS

The authorship criteria (author guidelines) were met by PF, RM, TR, AG, and EF. Conceived and designed the experiments: PF, RM, TR, AG, and EF. Performed the experiments: PF, RM, and EF. Analyzed the data: PF, RM, TR, AG, and EF. Contributed reagents/materials/analysis tools: PF, RM, TR, AG, and EF. Wrote the paper: PF, RM, and EF.

ACKNOWLEDGMENTS

Our Thanks to Drs. Karine Monteil and Pierre Legreneur for their participation to the video recordings and the digitalization of the images.

SUPPLEMENTARY MATERIAL

The Supplementary Material for this article can be found online at: http://journal.frontiersin.org/article/10.3389/fphys.2016.00289

[3]This can be deduced for example from subject S6 (Supplementary Figure 2) where the BP of the lower legs segment is at 52.6% of time duration and the BP of HAT is at 57.9% (Section Consecutive intersegment coordination), i.e., a difference of 5.3% (total time duration of 0.19 s). In real time the regulation between two segments happened in ∼0.009 s.

REFERENCES

Aragón-Vargas, L. F. (2000). Evaluation of four vertical jump tests: methodology, reliability, validity, and accuracy. *Meas. Phys. Educ. Exerc. Sci.* 4, 215–228. doi: 10.1207/S15327841MPEE0404_2

Aragón-Vargas, L. F., and Gross, M. M. (1997). Kinesiological factors in vertical jump performance: differences among individuals. *J. Appl. Biomech.* 13, 24–44.

Atwater, A. E. (1979). Biomechanics of overarm throwing movements and of throwing injuries. *Exerc. Sport Sci. Rev.* 7, 43–85. doi: 10.1249/00003677-197900070-00004

Babič, J., and Lenarčič, J., (2007). "Vertical jump: biomechanical analysis and simulation study," in *Humanoid Robots, New Developments*, ed A. C. de Pina Filho (Vienna: I-Tech Education and Publishing), 551–566.

Bobbert, M. F., Casius, L. J. R., and Kistemaker, A. (2013). Humans make near-optimal adjustments of control to initial body configuration in vertical squat jumping. *Neuroscience* 237, 232–242. doi: 10.1016/j.neuroscience.2013.01.055

Bobbert, M. F., Casius, L. J. R., Sijpkens, I. W. T., and Jaspers, R. T. (2008). Humans adjust control to initial squat depth in vertical squat jumping. *J. Appl. Physiol.* 105, 1428–1440. doi: 10.1152/japplphysiol.90571.2008

Bobbert, M. F., de Graff, W. W., Jonk, J. N., and Casius, L. R. J. (2006). Explanation of the bilateral deficit in human vertical squat jumping. *J. Appl. Physiol.* 100, 493–499. doi: 10.1152/japplphysiol.00637.2005

Bobbert, M. F., and van Ingen Schenau, G. J. (1988). Coordination in vertical jumping. *J. Biomech.* 21, 249–262. doi: 10.1016/0021-9290(88)90175-3

Bobbert, M. F., and van Soest, A. J. (2001). Why do people jump the way they do? *Exerc. Sport Sci. Rev.* 29, 95–102. doi: 10.1097/00003677-200107000-00002

Buishand, T. A. (1982). Some methods for testing the homogeneity of rainfall records. *J. Hydrol.* 58, 11–27. doi: 10.1016/0022-1694(82)90066-X

Buishand, T. A. (1984). Tests for detecting a shift in the mean of hydrological time series. *J. Hydrol.* 73, 51–69. doi: 10.1016/0022-1694(84)90032-5

Butterfield, R. J., and Boyd, K. (2012). Injuries in high diving [Abstracts of XVIIth FINA World Sports Medicine Congress]. *J. Sports Sci. Med.* 11, 780.

Gurfinkel, V. S. (1973). On two types of static disturbances in patients with local lesions of the brain. *Agressologie* 14D, 65–72.

Gurfinkel, V. S., and Shik, M. L. (1973). "The control of posture and locomotion motor control," in *Motor Control*, eds A. A. Gydikov, N. T. Tankov, and D. S. Kosarov (New York, NY: Plenum), 217–243.

Haguenauer, M., Legreneur, P., and Monteil, K. M. (2005). Vertical jumping reorganization with aging: a kinematic comparison between young and elderly men. *J. Appl. Biomech.* 21, 236–246.

Hudson, J. L. (1986). Coordination of segments in the vertical jump. *Med. Sci. Sports Exerc.* 18, 242–251. doi: 10.1249/00005768-198604000-00015

Katsnelson, A. (2003). Current approaches to the study of movement control. *PLoS Biol.* 1:e50. doi: 10.1371/journal.pbio.0000050

Knechtle, M. D., Baumann, B., Wirth, A., Knechtle, P., and Rosemann, T. (2010). Male ironman triathletes lose skeletal muscle mass. *Asia Pac. J. Clin. Nutr.* 19, 91–97. doi: 10.5167/uzh-33316

Massion, J. (1992). Movement, posture and equilibrium: interaction and coordination. *Prog. Neurobiol.* 38, 35–56. doi: 10.1016/0301-0082(92)90034-C

Muth, C.-M., Ehrmann, U., and Radermacher, P. (2005). Physiological and clinical aspects of apnea diving. *Clin. Chest Med.* 26, 381–394. doi: 10.1016/j.ccm.2005.05.007

Newell, K. M., and Corcos, D. M. (1993). "Issues in variability and motor control," in *Variability and Motor Control*, eds K. M. Newell and D. M. Corcos (Champaign, IL: Human Kinetics Publishers), 1–12.

Pinter, I. J., van Soest, A. J., Bobbert, M. F., and Smeet, J. B. J. (2012). Conclusions on motor control depend on the type of model used to represent the periphery. *Biolog. Cybern.* 116, 441–451. doi: 10.1007/s00422-012-0505-7

Prokopow, P., Hay, D., Fukashiro, S., and Himeno, R. (2005). Quantitative evaluation of the importance of coordination on jump achievements and kinematics in human vertical squat jump. *Jpn. J. Biomech. Sports Exerc.* 9, 69–82.

Robertson, D. G., and Fleming, D. (1987). Kinetics of standing broad and vertical jumping. *Can. J. Sport Sci.* 12, 19–23.

Sanders, R. H., and Wilson, B. D. (1992). Comparison of static and counter movement jumps of unconstrained movement amplitude. *Austr. J. Sci. Med. Sport* 24, 79–85.

Sargent, D. A. (1921). The physical test of a man. *Am. Phys. Educ. Rev.* 26, 188–194.

Van Ingen Schenau, G. J. (1989). From rotation to translation: constraints on multi-joint movements and the unique action of bi-articular muscles. *Hum. Mov. Sci.* 8, 301–337. doi: 10.1016/0167-9457(89)90037-7

van Soest, A. J., and Bobbert, M. F. (1993). The contribution of muscle properties in the control of explosive movements. *Biol. Cybern.* 69, 195–204. doi: 10.1007/BF00198959

West, J. B. (1983). Climbing Mt. Everest without oxygen: an analysis of maximal exercise during extreme hypoxia. *Respir. Physiol.* 52, 265–279. doi: 10.1016/0034-5687(83)90085-3

Winter, D. A. (1990). *Biomechanics and Motor Control of Human Movement*. New York, NY: Wiley & Sons.

Wolpert, D. M., Miall, R. C., and Kawato, M. (1998). Internal models in the cerebellum. *Trends Cogn. Sci.* 2, 338–347. doi: 10.1016/S1364-6613(98)01221-2

Conflict of Interest Statement: The authors declare that the research was conducted in the absence of any commercial or financial relationships that could be construed as a potential conflict of interest.

Advantages of publishing in Frontiers

OPEN ACCESS
Articles are free to read, for greatest visibility

COLLABORATIVE PEER-REVIEW
Designed to be rigorous – yet also collaborative, fair and constructive

FAST PUBLICATION
Average 85 days from submission to publication (across all journals)

COPYRIGHT TO AUTHORS
No limit to article distribution and re-use

TRANSPARENT
Editors and reviewers acknowledged by name on published articles

SUPPORT
By our Swiss-based editorial team

IMPACT METRICS
Advanced metrics track your article's impact

GLOBAL SPREAD
5'100'000+ monthly article views and downloads

LOOP RESEARCH NETWORK
Our network increases readership for your article

Frontiers
EPFL Innovation Park, Building I • 1015 Lausanne • Switzerland
Tel +41 21 510 17 00 • Fax +41 21 510 17 01 • info@frontiersin.org
www.frontiersin.org

Find us on